Functional Analysis of a Rho GTPase Activating Protein Involved in Epithelial Differentiation and Morphogenesis

Ahmed Nehad Elbediwy

Thesis submitted to University College London for the award of Doctor of Philosophy

November 2012

Department of Cell Biology

Institute of Ophthalmology

University College London

11-43 Bath Street

London

EC1V 9EL

Declaration of Work

I, Ahmed Nehad Elbediwy, hereby confirm that the work that is presented in this thesis is my own. Where information has been derived from alternate sources, I confirm that I have indicated this in the correct context within the thesis

University College London

November 2012

Abstract

Polarized epithelial cells form selective barriers between tissues and various body compartments that are essential for normal development and organ function. A mature apical junctional complex (AJC), consisting of tight junctions (TJ), adherens junctions (AJ), and desmosomes is crucial for functional polarized epithelia. Rho-GTPases are key regulatory proteins of many cellular processes, including epithelial adhesion and polarization. These small GTPases are in turn controlled spatially and temporally by guanine nucleotide exchange factors (GEFs) that promote GTP-binding, resulting in their activation; and GTPase activating proteins (GAPs) that promote GDP hydrolysis, resulting in their inactivation. In this thesis I studied a novel junction associated GAP protein known as SH3BP1 in a variety of epithelia. SH3BP1 was identified in a functional siRNA screen that was designed to identify actin regulators of epithelial polarisation and differentiation. I will show that SH3BP1 localises to the early AJC when TJ and AJ are not yet properly separated. SH3BP1 regulation is important for tight junction formation and, its depletion affects polarity and junction integrity. I will demonstrate that SH3BP1 is functionally important in epithelial cell lines from different tissues as well as in organotypic three dimensional cultures. A major part of my thesis will focus on the demonstration that SH3BP1 is a crucial EGF receptor signalling effector that guides morphological alterations and actin dynamics. Using the A431 cell line EGF signalling model, I will demonstrate SH3BP1 is required to regulate both Rac1 and Cdc42 signalling, and subsequently its role in the recruitment of junctional proteins first to dorsal ruffles and then to forming tight junctions. I will

provide evidence that SH3BP1 forms a heteromeric complex with the scaffold JACOP/paracingulin and the actin capping regulator CD2AP that has a key role in the regulation of actin dynamics. Based on my data, I will propose a new model on how a negative regulatory complex guides cytoskeletal dynamics and junction formation and, thereby, promotes epithelial differentiation.

Table of Contents

Table of Figures

Chapter 1

Chapter 3

Chapter 4

Chapter 5

Chapter 6

Table of Tables

Chapter 2

List of Abbreviations

AJ	Adherens Junctions
aPKC	Atypical protein kinase C
ATP	Adenosine triphosphate
ATPase	Adenosine triphosphate hydrolysing protein
Caco-2	Colorectal adenocarcinoma
CAR	Coxsackievirus-adenovirus receptor
CD2AP	CD2-associated Protein
Cdc42	Cell division cycle 42
CTD	Carboxy terminal domain
Dbl	Diffuse B cell Lymphoma
DH	Dbl-homologous

DLC	Deleted in Liver cancer
DMEM	Dulbecco's Modified Eagle Medium
DMSO	Dimethyl sulfoxide
DNA	Deoxyribonucleic acid
dNTP	Deoxynucleotide Triphosphate
DOCK	Dedicator of cytokinesis
DRH	Dock homology regions
E-cadherin	Epithelial cadherin
ECL	Enhanced chemiluminescence
EDTA	Ethylenediaminetetraacetic acid
EPLIN	Epithelial Protein Lost in Neoplasm
Erk	Extracellular regulated kinase

FBS	Fetal bovine serum
FRET	Fluorescence energy resonance transfer
GAP	GTPase Activating Protein
GDI	Guanine nucleotide Dissociation Inhibitor
GDP	Guanosine diphosphatase
GEF	Guanine exchange factor
GFP	Green fluorescent protein
GLISA	G-protein linked immunosorbent assay
GSK3	Glycogen synthase kinase 3
GST	Glutathione S-transferase
GTP	Guanosine triphosphatase
GTPase	Guanosine triphosphatase hydrolysing protein

GuK	Guanylate kinase
HCE	Human corneal epithelial cells
HCL	Hydrochloric acid
IgG	Immunoglobulin G
IKK	IκB kinase
IPTG	Isopropyl β-D-1-thiogalactopyranosid
JACOP	Junction-associated coiled-coil protein
JAM	Junction adhesion molecules
LB	Luria-Bertani
MDCK	Madin-Darby Canine Kidney
mDia	Mammalian diaphanous
MeOH	Methanol

MLC	Myosin II regulatory light chain
MRCK	Myotonic dystrophy related kinase
MUPP1	Multi-PDZ-domain protein 1
MYPT	Myosin phosphatase target subunit
NF-kB	Nuclear factor kappa-light-chain-enhancer of activated B-cells
NTD	Amino Terminal domain
PAGE	Polyacrylamide gel electrophoresis
PAK	p21-activated kinase
PAR	Partitioning protein
PATJ	Pals 1 associated tight junction protein
PBS	Phosphate buffered saline
PCNA	Proliferating cell antigen

PCR	Polymerase Chain Reaction
PDZ	Post synaptic density protein (PSD95), Drosophila disc large tumour suppressor (DlgA), and zonula occludens-1
PFA	Paraformaldehyde
PH	Pleckstrin Homology
PI(3,4,5)P3	Phosphatidylinositol 3,4,5-Trisphosphate
PI(3,5)P2	Phosphatidylinositol 3,4-bisphosphate
PI(3)P	Phosphatidylinositol 3-phosphate
PI(4,5)P2	Phosphatidylinositol 4,5-bisphosphate
PI(4)P	Phosphatidylinositol 4-phosphate
PI3K	Phosphatidylinositol 4,5-bisphosphate 3-kinase
PKC	Protein Kinase C

PMSF	Phenylmethylsulfonyl fluoride
Rac1	Ras-related C3 botulinum toxin substrate 1
Rho	Ras homolog
RNA	Ribonucleic acid
RNAi	Ribonucleic acid interference
ROCK	Rho-associated protein kinase
SDS	Sodium dodecyl sulphate
SH3	Src Homology 3
SH3BP1	SH3 domain binding protein 1
shRNA	Short Hairpin ribonucleic acid
siRNA	Short interfering ribonucleic acid
TCF	T- cell factor

TEM	Transmission electron microscopy
TER	Transepithelial electrical resistance
Tiam-1	T-cell lymphoma invasion and metastasis-inducing protein
TJ	Tight Junction
TNFα	Tumour necrosis factor
VASP	Vasodilator-stimulated Phosphoprotein
WASP	Wiscott-Aldrich Syndrome Protein
Wnt	Wingless and Int
ZO-1	Zonula Occludens 1
ZONAB	(ZO-1)–associated nucleic acid binding protein

Chapter 1

Introduction

Chapter 1 – Introduction

Overview

Distinct types of cells cooperate to form functional complex organisms. One such cell type is represented by epithelial cells that allow separation of compartments of different composition and form protective layers that protect organisms from the environment. Epithelila cells have distinctive cell surface domains termed apical, basal and lateral; the latter are often combined to basolateral [1]. The apical surface mediates many tissue specific functions, such as terminal digestion and nutrient uptake in the case of intestinal epithelia. The basal surface contacts the extracellular matrix (ECM), and the lateral surface, is important for the formation of cell-cell contacts between adjacent cells. The basolateral domain also mediates many homeostatic functions, such as Na^+ and K^+ exchange by Na^+K^+-ATPase. This functional cell surface polarity requires the formation of biochemically distinct cell surface domains. Intriguingly, many fundamental molecular mechanisms that are required to the polarisation of epithelial cells also mediate functional polarisation of other cell types, such as neurons, or during different types of processes that require cell reorientation and polarity, such as migration [1-6]. The formation of cell-cell contacts between adjacent epithelial cells is essential for the formation of functional epithelial sheets capable to separate compartments of different composition. Epithelial cells form distinct types of cell-cell contacts: the most prominent ones are called cell junctions. At the apical end of the lateral

membrane resides the Apical Junctional Complex (AJC), which consists of the Zonula Occludens or the Tight Junction (TJ) and the Zonula Adherens or the Adherens Junction (AJ). A second adhesive junctions, desmosomes, form epithelial junctional complex together with the AJC [6, 7]. Epithelial cells also form gap junctions that allow exchance of ions and small hydrophilic molecules between neighbouring cells. Formation of these intercellular junctions is highly regulated and is required for epithelial cells to carry out their specific physiological roles during development and homeostasis.

The formation and control of cell-cell junctions is a highly regulated process. This involves interplay between cellular signal transduction mechanisms that guide assembly and function of the cytoskeleton, or directly target specific junctional components altering their functional properties [8, 9]. An important molecular mechanism that is employed by many of these signal transduction pathways relies on molecular switches called Rho GTPases. These are small proteins that can hydrolyse guanine nucleoside triphosphate (GTP) to guanine nucleoside diphosphate (GDP) [10, 11]. GTP binding and hydrolysis represents a molecular switch mechanism: In the GTP-bound form, Rho GTPases are active and signal by binding and activating downstream effectors; GTP hydrolysis leads to a conformational switch, resulting in inactivation of the signalling activity. Activation of Rho GTPases is stimulated by guanine nucleotide exchange factors (GEFs) that catalyse the exchange of GDP by GTP; inactivation by GTP hydrolysis is promoted by GTPase Activating Proteins (GAPs). GEFs and GAPs are thus of central importance for the orchestration of Rho GTPase signalling.

My thesis focuses on the mechanisms that regulate the assembly of epithelial junctions and, in particular, how Rho GTPase signalling guides junction assembly. I will particularly focus on the molecular processes that regulate Rho GTPase activity and how they are linked to the cytoskeletal rearrangements required for assembly of the AJC and epithelial differentiation.

Cell-cell junctional complexes

Intercellular junctional complexes are complex multi-protein strucures that share a basic architectural principal: they consist of transmembrane proteins that mediate cell-cell adhesion and are linked to cytosolic protein complexes that function as cytoskeletal linkers and signalling centres that guide junction assembly and function, and trasmit signals to the cell interior to guide cell behaviour and differentiation [12]. Epithelial cells form three main junctonal complexes (Figure 1.0). I will discuss these three junctions individually, both in terms of their main structural components as well as their signalling proteins, as each one has a unique composition and specific functions.

Figure 1.0 The structural organisation epithelial cell-cell adhesion complexes.

(A) Adjacent epithelial cells adhere to one another by forming cell-cell junctional complexes. This so-called epithelial junctional complex is composed of TJs, AJs and desmosomes. TJs and AJs are connected directly to F-actin. (B) TJs are composed of transmembrane proteins, such as occludin, claudins and JAMs, bound to a cytoplasmic complex containing ZO proteins that providea link to the actin cytoskeleton. AJs are comprised of two main complexes: the E-cadherin-catenin complex and the nectin-afadin complex.

Tight junctions

TJs are located in the apical-most region of the lateral membrane [14]. They form a morpholoigical and functional border between the apical and basolateral domains of the plasma membrane, and act as semi-permeable gates between cells, regulating the flow of ions and solutes as well as passage of cells through the paracellular pathway. TJs also coordinate a range of signalling pathways, that regulate a variety of important biological mechanisms, including cell polarisation and differentiation, proliferation and migration [10, 15, 16].

In electron micrographs of ultrathin sections, TJs appear as so-called ‘kissing points’, apparent hemifusions of the outer leaflets of the plasma membrane of adjacent epithelial cells (Figure 1.1a). By freeze fracture electron microscopy, TJs appear as an arrangement of intramembrane strands, which form a mesh-like network encircling the cells at the apical end of the basolateral membrane (Figure 1.1b) [10, 16]. Because of their morphological appearance, TJs have long been regarded as hemi-fusions of neighbouring plasma membranes. However, this model, which was proposed before junctional membrane poteins had been identified, has now mostly been discarded in favour of a protein-mediated cell-cell adhesion model. Various studies have shown that TJs are composed of a number of components, including integral membrane and scaffolding proteins, as well as components of various signalling cascades and regulators of the actin cytoskeleton.

Figure 1.1 The tight junction structure by electron microscopy.

(A) Shows pneumocytes in a newborn lamb lung with the TJ indicated with arrowheads. The AJ is found below the TJ. (B) Shows a freeze fracture of a TJ. The TJ appear as a meshwork of intermembrane filaments, which encircles the cells. The strands consist of rows of 10nm diameter particles indicated by arrowheads. Scale bar 120nm.

Structural basis of tight junctions

The molecular structure of TJs shares the same principle architecture with other junctional complexes. They are composed of mutiprotein complexes formed by three types of proteins: transmembrane proteins, cytoplasmic plaque proteins such as adaptors and cytoskeletal proteins, as well as signalling proteins such as transcription factors and protein kinases [8, 10].

Integral membrane proteins are crucial for the structural integrity of the TJ. These proteins are usually classified by how many times they travers the plasma membrane. TJs contain single-pass transmembrane proteins such as JAMs and CAR [17], three-pass transmembrane proteins such as Bves [18], and four-pass transmembrane proteins such as occludin, claudins, tricellulin and MarvelD3 [17, 19]. These proteins bridge the space between adjacent cells, mediate intercellular adhesion, and form the paracellular gate. With their cytoplasmic domains, they interact with cytoplasmic plaque components, which is thought to be important for junction assembly and regulation, as well as for the regulation of signalling mechanisms that guide cell behaviour [16, 20, 21].

The cytoplasmic plaque contains multidomain proteins, such as ZO-1, ZO-2 and ZO-3, that function as scaffolding proteins. Many of these proteins have PDZ (PSD95/DlgA/ZO-1) homology domains that mediate interactions with other proteins and thereby promote junction assembly [22]. The plaque proteins serve as linkers between the transmembrane proteins and the actin cytoskeleton, and also function as adaptors for molecules involved in cell signalling [12, 21].

The last group of TJ proteins includes amongst others, tumour suppressors such as the lipid phosphatase PTEN, regulatory proteins, and transcriptional and posttranscriptional regulators such as ZONAB [23]. These TJ associated proteins are involved in the regulation of junction function (e.g. paracellular permeability), but also of cell proliferation, cell polarity and differentiation, and gene expression [16].

Integral membrane proteins

Occludin is a ~60 kDa tetraspan transmembrane protein that is the first transmembrane protein identified within TJs. Even though occludin is strongly associated with the junctional intermembrane strands, it seems that it is not essential for their assembly [15, 24]. This was demonstrated by Saitou *et al.* Using occludin deficient embryonic stem cells, which can form fully polarized epithelial cells with functional TJs [25]. However, occludin knockout mice exhibit complex gross and histological phenotypes resulting in inflammation, hyperplasia of gastric epithelia and testicular atrophy. Even though junctions can form in the absence of occludin, its depletion seems to cause moderate defects in tight junction stability [26, 27]. This may be explained by the possibility that occludin loss can be compensated for by other tetraspan proteins such as tricellulin and MarvelD3; however, depletion of MarvelD3, occludin and tricellulin together only led to a modest retardation of junction assembly [28]. As both the N-terminal and C-terminal domains of occludin interact with cytosolic plaque proteins, occludin has been linked to many

signalling pathways [24]. The C-terminal domain of occludin is crucially involved in many key interactions of occludin. This includes interactions with F-actin, ZO-1, ZO-2, ZO-3, and Transforming Growth Factor Beta (TGFβ) Type 1 Receptor [20, 29, 30]. Occludin has also been suggested to affect activation of Rho GTPases [31], Mitogen Activated Protein Kinase (MAPK) and Akt signalling pathways [32]. Occludin has also been linked to the leading edge localisation of a number of polarity complex signalling molecules, such as atypical Protein Kinase C (aPKC), Par3 and PATJ during cell migration [33].

Claudins form a family with 24 members in humans and have a molecular weight of of 18-27 kDa. They are also tetraspan transmembrane proteins and are thought to constitute the backbone of the junctional intermembrane strands [26]. Claudins were originally discovered by Tsukita and colleagues who identified claudin-1 and claudin-2 [34]. The members of the claudin family contain two extracellular loops that vary in the number of charged residues they contain. This feature of claudins is thought to be crucial for the formation and selectivity of paracellular pores that control the ionic selectivity of TJs [35]. Claudins are expressed in a tissue specific manner. For example, claudin-5 and -15 are expressed only in endothelial cells; and different claudins exhibit different expression profiles along the renal nephron, which is thought to contribute to the distinct paracellular permeability properties in different nephron segments [36].

A study by Martinez-Estrada *et al* revealed that overexpression of Snail and Slug, members of the Snail superfamily of zinc-finger transcription factors, resulted in a decrease in transepithelial electrical resistance of MDCK cells and repression of expression of claudin-1, 3, 4 and 7 [37]. These transcription

factors also repress the genes encoding occludin and E-cadherin [38, 39]. Since the Snail superfamily of transcription factors has been shown to be important in epithelial to mesenchymal transition (EMT) [40], these results suggest that repression of claudins and other junction-associated proteins is results in progression of EMT and, consequently, cancer progression. Claudin family members associate with various PDZ domain containing adaptor proteins such as ZO-1, ZO-2, ZO-3, MUPP1 and with protein kinases such as WNK4, which phosphorylates claudin-1 to regulate paracelluar ion conductance, and matrix metalloproteinase's such as matrix metalloproteinase 2 and matrix metalloproteinase 14, that are thought to regulate junctions proteolytically [41]. This suggests that different types of regulatory mechanisms target claudins to modulate paracellular ion selectivity and other permeability properties.

MarvelD3 is a 40 kDa protein recently demonstrated to be an integral membrane protein of TJs [19]. There are two known isoforms of MarvelD3. These splice variants share the same 198 amino acid N-terminal cytoplasmic domain but vary in the region containing the transmembrane domains [19]. MarvelD3 shows a distant structural similarity to occludin within the region containing the transmembrane domains, which form a MARVEL (MAL and related proteins for vesicle trafficking and membrane link) domain; however in contrast to occludin, its C-terminal domain is shorter and its N-terminal domain longer [19]. Depletion of MarvelD3 by RNA interference, resulted in no major changes in junctional integrity [19, 28]. The importance of MarvelD3 has not been fully established, as it was only recently discovered; however, it may be important in the stabilisation of cell-cell adhesion, since the protein was found to be downregulated in Snail induced EMT in human pancreatic cells [42].

Tricellulin is a~65 kDa transmembrane protein localised at the tricellular corners of epithelial cells [43]. Together with MarvelD3 and occludin, tricellulin comprises the tight junction-associated MARVEL domain subfamily. Tricellulin was shown to participate in the barrier function of TJs: depletion of tricellulin by RNA interference impaired barrier function and disorganized tricellular and bicellular TJ contacts at least in some model systems, suggesting that tricellulin is crucial in epithelial barrier formation and function [43]. Tsukita and colleagues further found that upon depletion of occludin, tricellulin levels were increased, thus further supporting the proposal that distinct junctional membrane proteins can play compensatory roles [44].

Junctional Adhesion Molecules (JAMs) are a family of about 45 kDa glycosylated transmembrane proteins that belong to the immunoglobulin superfamily [15]. JAMs are divided into two distinct groups. The first group contains JAM-A, JAM-B and JAM-C. They all have a class II PDZ binding motif located at the end of their C-terminus that can interact with adaptor molecules such as ZO-1 and Par3 [45, 46]. JAM-A has also been shown to bind a number of other proteins through its PDZ binding domain, including MUPP1, afadin/AF6 (a protein associated with nectin-based AJs), CASK and PICK1 [41]. JAM-A is involved in the formation of the TJ barrier in endothelial and epithelial cells [47, 48], and also plays an important role in apico-basal polarity in epithelia. JAM-A has also been shown to regulate epithelial morphogenesis, as MDCK cells could no longer form cysts with a defined lumen in a three dimensional morphogenesis assay when JAM-A was depleted [49]. The second group of JAMs includes the Coxsackievirus and Adenovirus receptor (CAR), ESAM and JAM-D. CAR also seems to contribute to the barrier function of TJs. Cohen *et al*

demonstrated that overexpression of CAR in epithelial cells leads to an increase in transepithelial resistance (TER) [50]. CAR also interacts with ZO-1 [17]. JAMs are involved not only in barrier function but also in leukocyte trafficking during inflammation and angiogenesis [51, 52]

Adaptor proteins

The junctional membrane proteins are anchored in a complex protein network formed by different types of adaptor proteins. They are to some extent redundant in the structural organisation of the TJ, but also participate in various signalling pathways in which they seem to fulfill functions that are more specific. Some of the most studied adaptors are ZO-1, cingulin and paracingulin/JACOP.

The adaptor protein ZO-1 is the first TJ protein discovered. ZO-1 is a 210-225 kDa protein that contains three PDZ domains, an SH3 domain, actin filament binding domain, as well as a gunylate kinase homolgy domain [53, 54]**.** Because of the latter domain, ZO-1 and proteins with a homolgous domain structure are often referred to as membrane-associated gunylate kinase homologues (MAGUKs); however, none of these proteins seems to possess kinase activity. Apart of the above mentioned membrane proteins, ZO-1 binds to multiple cytosolic proteins [29]. One such binding partner is the Y Box transcription factor ZONAB [55]. The interaction between ZO-1 and ZONAB is mediated by the SH3 domain of ZO-1 and results in cytoplasmic sequestration of the transcription factor and, hence, inhibition of its transcriptional activity. ZO-1 and ZONAB expression and localization are cell density dependent: in

confluent cells, the expression of ZO-1 is high and ZONAB low and, therefore ZONAB is sequestered at cell-cell junctions; in low confluent cells, expression of ZO-1 is low and of ZONAB high, resulting in transcriptionally active ZONAB [56]. ZO-1 can also interact with various other junctional proteins such as its close relatives ZO-2 and ZO-3, as well as other components of TJs (e.g., cingulin) and AJs (e.g., alpha-catenin, AF6/afadin) [24, 57].

Cingulin is a ~140kDa protein that contains a globular head domain, a central coiled coil domain that forms a rod and supports dimerisation, and a C-terminal tail domain. It was originally identified as it co-purified with myosin II [58]. Cingulin has been found to play an important role in RhoA signalling by recruiting the RhoA activators GEF-H1 and p114 RhoGEF to the TJ [59, 60]. As cells become more confluent, cingulin is thought to recruit and inactivate free GEF-H1 to the TJ, leading to reduced RhoA signalling in the cytoplasm and inhibition of cell proliferation. Nevertheless, at the junction itself, cingulin promotes RhoA signalling by recruiting p114RhoGEF.

Paracingulin/JACOP is a ~160 kDa protein with strong similarity to cingulin. It possesses the same domain structure as cingulin, and the region that contains the rod and tail domains shares a 39% similarity with cingulin [61]. The head domains of both proteins have been shown to interact with ZO-1 at the junction, thus providing an additional link between ZO-1 and the cytoskeleton [61, 62]. In contrast to cingulin, however, paracingulin/JACOP does not localise exclusively to TJs but can also associate with AJs. Depletion of paracingulin/JACOP results in a delay in both TJ and AJ formation, suggesting that it functions in the regulation of junction assembly [63]. Depletion of paracingulin/JACOP also resulted in lower levels of active Rac1, which could be rescued by

overexpression of the Rac1 GEF Tiam1. Tiam1 was also reported to interact with paracingulin/JACOP [63]. As seen originally with cingulin, RhoA activity is increased in paracingulin depleted cells, which is thought to reflect an inhibitory interaction with GEF-H1 [63].

Signalling proteins

The scaffolding and cytoskeletal proteins form what is known as a cytoplasmic plaque that recruits a large array of different signalling proteins [24, 56, 64]. Several of these proteins have already been mentioned as they bind to adaptor and transmembrane proteins. In principle, they can be divided according to their biological activities. For example, several protein kinases (e.g, WNK4a, CDK4) have been shown to associate with TJs and regulate paracellular permeability (e.g., WNK4a) or are part of mechanisms by which junction formation regulates proliferation (e.g., CDK4, a binging partner of ZONAB) [65]. Other examples are protein and lipid phosphatases such as PP2A and PTEN [66]. The tumour suppressor PTEN is a particularly intriguing example, as its activity at cell junctions is thought to be important for the generation and maintenance of cell polarity (see below). As already mentioned, TJs also harbour regulators of Rho GTPases (e.g, GEF-H1, p114RhoGEF), which will be discussed in more detail later.

The final class of TJ-associated signalling proteins are transcriptional and posttranscriptional regulators. The first such protein that was discovered is ZONAB, a protein, as mentioned above, which is recruited to TJs by binding to ZO-1. ZONAB can regulate gene expression transcriptionally by binding to

specific promoter binding sites as well as posttrancriptionally by binding to specific mRNAs [55, 65]. Other examples, include symplekin, a component of the polyadenylation machinery and binding partner of ZONAB; as well as the transcription factors AP-1 and C/EBP that interact with ZO-2, a protein that can itself travel to the nucleus to bind SAF-B [67].

Adherens junctions

The zonula adherens or Adherens Junctions (AJs) are a major component of the intercellular junctional complex in epithelia and endothelia. AJs perform a number of functions such as to provide mechanical strength by interconnecting cell junctions and the actin cytoskeleton, to control the initiation of cell-cell adhesion and polarisation, and to regulate several intracellular signal transduction pathways [12, 68]. The AJ consists of two main adhesive protein complexes: the cadherin/catenin and the nectin/afadin complexes [69]. Each of these two complexes is explored in more detail below.

Cadherin-catenin complex

E-cadherin is a Ca^{2+}-dependent, single-pass transmembrane glycoprotein that belongs to the classic cadherin family (N-, P- and R-cadherin being other members) of adhesion proteins and forms a complex with alpha- and beta-catenin [70]. Classical cadherins have five extracellular repeat domains known

as extracellular cadherin (EC) domains. These domains are critical in the formation of interaction points between neighbouring cells and to initiate the formation of the AJ [71]. The cytoplasmic domain of E-cadherin binds to catenins that provide a direct link to the actin cytoskeleton and nuclear functions. Thus, E-cadherin complexes are involved in actin rearrangements, endocytosis, protein degradation, intracellular signalling and gene transcription [12, 72]. Once E-cadherin forms initial extracellular contacts, the adjacent E-cadherin molecules interact and seal along the periphery of the cell and strengthens the contact between adjacent cells, thus forming the early AJ [73]. The stability of E-cadherin/catenin/actin complexes is coupled by the actin binding protein EPLIN (Epithelial Protein Lost in Neoplasm), which itself is recruited by the cadherin-catenin complex to stabilise actin filaments [74]. Other actin binding proteins that bind to the cadherin-catenin complex include ZO-1, spectrin, vinculin, alpha-actinin, vezatin and the nectin-afadin complex [75]. Structually, the cytoplasmic domain of E-cadherin contains two distinct binding domains: a Juxtamembrane Domain (JMD) that binds p120 catenin [76], and a Catenin Binding Domain (CBD) that binds beta-catenin [77].

p120 catenin belongs to a subfamily of armadillo proteins, which have important roles in the regulation of cadherin adhesion [78]. p120 catenin was first identified by Reynolds *et al* as a substrate for Src tyrosine receptor kinase [79]. The protein, along with beta-catenin, was found to be tyrosine phosphorylated in v-Src transformed cells, as well as in response to various growth factors [78, 79]. This resulted in a loss of epithelial integrity and more invasive characteristics [78]. p120 catenin was later classified as a member of the catenin family based on sequence homology to the beta-catenin armadillo

domain [12, 80]. Binding of p120 catenin with the JMD domain of E-cadherin is proposed to stabilize E-cadherin at the plasma membrane during intiation of the AJ. This was demonstrated with experiments making use of E-cadherin constructs carrying mutations in the JMD, which showed that p120 catenin upon binding to E-cadherin, increases the adhesiveness of cell-cell contacts [12].

Beta-catenin binds to the CBD domain of E-cadherin [81].This interaction is disrupted by tyrosine phosphorylation of beta-catenin at amino acids Y489 and Y654, while its binding to alpha-catenin is weakened by tyrosine phosphorylation at amino acid Y142. The kinases involved in these phosphorylation events are the tyrosine kinase Src and the EGF receptor, which phosphorylate amino acid Y654; Abl non-receptor tyrosine kinase, which phosphorylates amino acid Y489; and Fer kinase that phosphorylates amino acid Y142 [12]. It has also been suggested that BCL9-2, a transcription factor with an important role in EMT and invasion, regulates beta-catenin switching between its adhesive and transcription functionality. Phosphorylation at amino acid Y142 on beta-catenin favours BCL9-2 binding and results in shuttling of the protein to the nucleus and induction of gene transcription. This was further supported with siRNA-mediated knockdown of BCL9-2, which caused translocation of beta-catenin from the nucleus to the plasma membrane and a more epithelial-like phenotype [12].

Alpha-catenin is known to exist in two states: monomeric and homodimeric [12]. Initially it was thought that alpha-catenin provided the link between the E-cadherin/beta-catenin complex and the actin cytoskeleton. However, Yamada *et al* recently demonstrated that a simultaneous interaction between E-cadherin/beta-catenin/alpha-catenin and actin *in vitro* can not be established

[82]. It is thought that alpha-catenin allosteric switching between states only allows it to associate with either beta-catenin or actin, but not both proteins at once. Monomeric alpha-catenin binds beta-catenin, whereas in its homodimeric state it binds actin.

Nectin-afadin complex

Nectins are immunoglobulin (Ig) superfamily adhesion molecules (CAMs) that are involved in the structural integrity of cell-cell adhesion, as well as being in the regulation of a number of cellular processes including polarization, differentiation, migration, and survival [83, 84]. The nectin subfamily is comprised of four mammalian members (nectins 1-4). All nectins contain an extracellular domain comprised of three IgG-like loops and a cytoplasmic domain with a PDZ binding motif at their C-terminus [85]. The cytoplasmic domain of nectins interacts with the actin binding protein afadin/AF6 [85]. Afadin, a scaffolding protein, interacts with Ras/Rap family GTPase signalling components as well as other actin binding proteins such as alpha-catenin and ZO-1 [69]. Ikeda *et al* demonstrated that knockout of afadin had a detrimental effect on epithelial organization [86]. The formation of AJs by nectins, therefore requires afadin. Nectin-based adhesion has been proposed to be of primary importance for junction formation and is thought to trigger a complex signalling cascade that stimulates actin reorganisation and formation of stable cell junctions (Figure 1.2).

Nectin-Like Molecules (NECLs) comprise a family of five members with varying roles. They share similar domains to nectins, however, the crucial difference is that they cannot bind to afadin and are not part of the nectin-afadin complex [87].

There is also evidence for molecular crosstalk between the AJ and TJ. It has been shown that Nectin-2, the spliced form of AF6 and alpha-catenin interacts with ZO-1. JAM also binds to the PDZ domain of AF6 and forms a complex with ZO-1 [88, 89]. Another scaffolding protein which has been shown to bind both TJ and AJ components is protein interacting with C-kinase-1 (PICK-1), which binds both nectin and JAM [88]. However, it is not clear whether some of these interactions represent stable complexes or rather transition states during junction assembly, as has been demonstrated for the ZO-1/alpha-catenin interaction [90].

Figure 1.2 Nectin-induced intracellular signalling during the formation of adherens junctions.

The schematic shows the structural basis of the nectin-afadin complex and how it is involved in the regulation of signalling networks that guide cytoskeletal organisation and junction formation. Diagram adapted from [87].

Desmosomes

Desmosomes, like AJ, are an adhesive cell-cell junction located in epithelial cells [91]. Desmosomes are disc-shaped symmetrical junctions, which are made up of three main types of proteins: cadherins, catenins (armadillo proteins) and plakin [92, 93]. The cadherin family members found in desmosomes are Desmocollin (Dsc) and Desmoglein (Dsg). The Dsc and Dsg cytoplasmic domains are in contact with the armadillo signalling proteins Plakoglobin (PG) and Plakophilin (PP). These proteins form a cytoplasmic plaque that connects desmosomes to the intermediate filament cytoskeleton, thus offering structural stability to the desmosomes and thereby to the tissue as a whole [92, 94]. PG is found not only in desmosomes but also in the AJ. PG also binds to Desmoplakin (DP) a critical member of the plakin protein family that is essential for desmosomal adhesion and provides the link to the cytoskeleton via its interaction with keratin filaments [91, 95]. PP on the other hand associates with a variety of desmosomal components, including both Dsc and Dsg, PG, DP, and also directly binds to intermediate filaments [92, 95]. These interactions bring the cellular membranes into close contact to allow desmosomal cadherins to cluster and bind together via their extracellular domains and thus form stable desmosomes.

Formation of cell-cell junctions and establishment of cell polarity

Formation of cell junctions requires series of cell shape changes and, depending on the model studied, active migration to allow neighbouring cells to approach and adapt to each other, initiation of cell-cell contacts and adhesion, followed by the maturation of stable cell junctions. This apparently simple sequence of steps is mediated by complex processes, which involve the formation of different types of stable and transient protein complexes and dynamic reorganization of the cytoskeleton, that ultimately lead to the formation of polarized epithelia with mature junctional complexes.

The formation of cell junctions and epithelial polarization are closely intertwined processes, and many of the signalling proteins that regulate polarization transiently or stably associate with the junctional complex. The initial sensing of the cellular environment by the cells includes locating cells in close proximity and interactions with the extracellular matrix (ECM) [96]. Adhesion to the ECM is thought to provide a crucial spatial cue that is critical for the orientation of the apicobasal axis of polarization [96]. Cells can sense and modify the chemical composition as well as the assembly and stiffness of the ECM [97]. The importance of the ECM is shown by various studies that suggest that tumour progression and metastasis is linked to altered ECM composition and stiffness [98]. The correct adhesion of cells to the ECM is thought to be mediated primarily through the adhesion receptor family of integrins [99].

The molecular mechanisms that drive epithelial polarisation involve protein complexes that have not only been conserved through evolution but are also

important for the polarization of other cell types (e.g., neurons) and for dynamic processes that require repolarization of cells (e.g., migration). There are three main groups of polarity proteins that participate in these protein-protein interactions in a highly dynamic manner. These are the apical determinants which consist of Par3, Par6 and aPKC (atypical Protein Kinase C); and the Crumbs associated proteins consisting of a Crumbs homologue (in vertebrate epithelial, this is usually Crb3), PALS1 (Protein Associated with LIN-7, the vertebrate homologue of fly Stardust) and PATJ (PALS1 Associated Tight Junction Protein); as well as the the basolateral Scribble associated proteins that consists of Scribble (Scrib), Lgl (Lethal Giant Larvae) and Dlg (Discs large) [100, 101].

Formation of cell-cell contacts

Initiation of junction formation is mediated by the main adhesion receptors of AJs: E-Cadherin and nectins. Although many investigators favour models in which cell-cell adhesion is initiated by E-cadherin, extensive work perform by Takai's laboratory suggests that nectin-mediated cell-cell adhesion precedes E-cadherin engagement (Figure 1.2) [83, 84, 102] . According to the later model, nectin-engagement stimulates a series of signalling events, involving the tyrosine kinase src, as well as Rap and Rho GTPases, that initiate reorganization of the cytoskeleton and stimulate the formation of E-Cadherin-based cell-cell contacts. However, it is not clear how far these sequence of events is influenced by the model system or experimental conditions analyzed.

Nevertheless, formation of TJs is downstream of E-cadherin-mediated cell-cell contact formation, as blocking E-cadherin function also prevents TJ formation. It is thought that E-cadherin activation stimulates signalling pathways required for TJ formation [103, 104].

E-Cadherin-based cell-cell adhesion first appears as adjacent puncta that then start to merge and form larger plaques until continous junctional belts surround the cells [73, 76, 105]. This initial cell-cell contact recruits the main components of AJs, such as alpha- and beta-catenin, but also components of TJs, such as ZO-1; hence, they are generally referred to as promordial junctions as they neither represent mature AJs nor TJs [66].

Formation of primordial junctions is initiated by dynamic actin-driven processes that allow cells to approach each other. This was first shown by Vasioukhin *et al* studying keratinocytes and stimulating junction formation either with a calcium switch protocol (i.e., cells are plated in low calcium medium that does not support junction formation, and subsequent adhesion is initated by adding calcium, which is required for cadherin-mediated adhesion) or with a wound healing assay (i.e., monolayers or tissues are wounded, leading to cell migration to close the wound and reformation of cell junctions) [106]. They observed that formation of primordial junctions involved two rows of E-cadherin-positive punctae. From these opposing punctae, bundles of actin filaments originated, and over time sealed to form a continuous contact line [106]. The actin-rich cell protrusions formed are called filopodia, a dynamic specialization of the plasma membrane (see below). However, initation of cell-cell contacts is not always mediated by filopodia but, depending on the cell model analysed, can also be driven by waves of lamellipodia, another type of dynamic actin-

based plasma membrane specialization, that are forming and contracting until cell-cell adhesion occurs [107].

The formation of these early junctional punctae can be considered as **Stage I** in a three-stage model of junction formation [73, 106]. **Stage II** is then the formation of large E-cadherin-positive plaques that result from merging of neighbouring punctas. Simultaneously, actin filaments start to rearrange allowing the rapid spreading of E-cadherin along the contact site, a 'zippering' up of the contact site [73, 106].

Apart from the junctional proteins already mentioned, many regulators of the actin cytoskeleton and actin-binding proteins have been found to localize to early stage I and II cell-cell contacts, including Arp2/3 [108], alpha-actinin, vinculin, zyxin [109], Mena/VASP [110], and formins [109, 111]. These proteins are thought to drive formation of filopodia and lamellipodia, respectively, permitting initial cell-cell contacts, and the actin filament reorganization required for the progression from stage I to stage II.

The final stage of junction formation, **Stage III**, is the separation and maturation of primordial junctions into a mature junctional complex with distinct TJs and AJs. Junctional maturation involves the formation of a junctional actin ring and recruitment of TJ proteins such as JAM-A and components of polarity complex proteins [112]. Par3, which is recruited by JAM-A, and aPKC localize to early forming TJs, and have been shown to be important for TJ formation [113, 114]. aPKC is also required for emerging junctions to mature by stimulating maturation of TJs [115].

Cell polarization

Interactions with the ECM are thought to provide the first cue that defines the axis of polarization. Therefore, organotypic culture systems have been established in which the cells are grown in a three-dimensional (3D) ECM, permitting the analysis of the molecular mechanisms that mediate epithelial polarization and differentiation *in vitro* under conditions more similar to those *in vivo* [116]. As this experimental system offers a more physiological experimental environment than standard two-dimensional culture systems, it has been widely used to analyse the molecular mechanisms underlying epithelial polarization.

When grown in a 3D ECM composed of collagen and/or Matrigel, epithelial cells form round spherical structures known as cysts. Differentiated cysts are well organized structures consisting of a monolayer of polarized cells, joined by intercellular junctions, around a central lumen with the apical membrane lining the lumen and the lateral membrane in contact with the ECM surrounding the cysts [116]. Figure 1.3 shows the different steps during cyst formation. Cellular cyst forms due to the initial contact of E-cadherin between two adjacent cells at the lateral surface and then develop into multicellular hollow cysts (Figure 1.3) [117].

Figure 1.3 Illustration of cyst development.

(A) A single MDCK cell (B) divides to form two cells joined by a lateral surface. (C) Morula like cells compact, (D) followed by continual cell division results in cell aggregation and cytoskeletal shape changes. (E) A polarised cyst forms with a liquid filled lumen with distinctive apical, basal and lateral surfaces. Cells embedded into an extracellular matrix can form an epithelial cyst within 5-8 days. Taken from [117].

Lumen formation has been to attributed to two distinct mechanisms called hollowing and cavitation. Hollowing involves the trafficking and exocytosis of intracellular vesicles to the cell surface of opposing cells, delivering the apical determinants to form the lumen [1, 118]. This allows adjoining cells to orientate apically toward the lumen and the tissue expands in a highly polarised manner. This has been seen in kidney and vascular 3D models. Interplay between the Rho GTPase Cdc42, Par6 and aPKC is crucial for lumen formation during cystogenesis via hollowing. Enrichment of the phosphoinositide Phosphatidylinositol-4,5-biphosphate (*PtdIns(4, 5) P2*) at the apical membrane, a process that requires the lipid phosphatase and tumour suppressor PTEN, allows recruitment of Cdc42 and subsequent binding to Par6 and aPKC, promoting generation of apico-basal polarity and a single polarised lumen [1, 118].

The second molecular mechanisms known as cavitation occurs when cells proliferate and the lumen is generated by apoptosis of cells in the middle of the structure. Cells not in contact with an ECM rapidly undergo apoptosis and are cleared, giving rise to an outer epithelial layer with a central lumen [1, 118]. Cavitation is seen in 3D cultures of mammary acini and *in vivo* in mouse mammary end buds. Proapototic Bcl-2 family proteins regulate cellular apoptosis of luminal clearing, although autophagy also seems to play a role [119]. Polarity proteins aPKC and Par6 also regulate apoptosis of luminal cells during epithelial morphogenesis [1, 120].

An important landmark of polarization in epithelial is the differential distribution of phosphoinositides in the inner leaflet of the plasma membrane. In mammalian epithelial cells, two versions of phosphoinositides distinguish the

apical and basolateral domains. Phosphatidylinositol-4,5-biphosphate (*PtdIns(4, 5) P2*) is abundant in the apical membrane, while phosphatidylinositol-3,4,5-triphosphate (*PtdIns (3, 4, 5) P3)* is found exclusively in the basolateral surface and is absent in the apical surface [121, 122]. Evidence for the importance of phosphoinositides in the maintenance of membrane identity and epithelial polarization was shown by two studies by Martin-Belmonte *et al* and Gassama-Diagne *et al.*, respectively. In the study by Martin-Belmonte *et al*, exogenous *PtdIns (4, 5) P2* was added to the basolateral domain of epithelial cysts, resulting in a dramatic shrinkage of the lumen and redistribuiton of the apical markers gp135 and ezrin to basolateral surfaces, thus supporting the importance of *PtdIns (4, 5) P2* for apical identity [121]. In a separate study by Gassama-Diagne, exogenous *PtdIns (3 ,4, 5) P3* was added to the apical surface of MDCK cells and triggered the apical surface to acquire basolateral characteristics, indicating that *PtdIns (3, 4, 5) P3* is an important determinant of basolateral surface identity and that *PtdIns (4, 5) P2* and *PtdIns (3, 4, 5) P3* play complimentary roles in the formation of apico-basal polarity [121, 122]. During the apical specification process during cyst formation, PTEN accumulation at apical poles leads to the enrichment of *PtdIns (4, 5) P2*, which then stimulates the apical recruitment of the Rho GTPase Cdc42 by annexin 2, a lipid binding protein. Cdc42 signalling then stimulates apical reruitment of a Par6/aPKC complex and apical expansion [121, 123]. Interestingly, Par3, a common component of Par6/aPKC complexes, does not associate with the apical membrane but remains at the junctional complex, suggesting that its function is no longer required in the complex that stimulates apical expansion.

PTEN has also been linked to cell polarity in other experimental systems, where it seems to have a somewhat distinct function. PTEN had been shown to directly bind to Baz/Par3 *in vitro* and *in vivo*, and to colocalize with Baz/Par3 in the apical cortex of epithelia and photoreceptors in Drosophila [124, 125]. In Drosophia photoreceptor epithelial cells, this interaction stimulates recuitment of PTEN to the junctional complex leading to the preferential apical accumulation of *PtdIns (3, 4, 5)* P3 [125]. Thus, the interaction between Par polarity proteins and PTEN is important for the polarized distribution of phosphoinositides and the development of cell polarity in different systems.

The polarity complexes that guide apical specification and cell junctions are closely interconnected and several components of these complexes have been shown to interact [101]. Formation of primordial junctions stimulates the recruitment of Par3/6 and aPKC to the forming junctional complex [126]. aPKC then phosphorylates JAM-A at S285 to promote the maturation of immature cell-cell contacts [127]. In fully polarized cells, S285-phosphorylated JAM-A is localized exclusively at the TJs, and S285 phosphorylation of JAM-A is required for the development of a functional epithelial barrier as well as normal 3D cyst morphogenesis. aPKC also phosphorylates Par3, which promotes the above-described apical exclusion and junctional retention of Par3 [115, 128]. Apical aPKC/Par6 complex also promotes apical accumulation of the Crumbs polarity complex, which is thought to be required for apical expansion and delineation from the maturing junctional complex. Crumbs complex compents have also been shown to interact with TJ proteins [59]. However, the functional relevance of these interactions remains to be determined.

Rho GTPases

Rho GTPases are key components of the signalling mechanisms that guide epithelial junction formation and differentiation. They can cycle between active (GTP-bound) and inactive (GDP-bound) forms, and thus function as molecular switches [11, 129]. As mentioned above, cycling between GTP and GDP bound forms is catalyzed by intracellular proteins that stimulate the exchange of GDP by GTP - Guanine nucleotide Exchange Factors (GEFs) - or promote GTP hydrolysis - GTPase Activating Proteins (GAPs) [11, 129]. The exception are atypical Rho GTPases, which include RhoBTBs, RhoE and RhoH, that can be regulated at the expression level or by ATP hydrolyses as in the case of RhoBTB3 [130, 131]. However, I will focus my description on the main members of the Rho GTPase family - Cdc42, Rac1 and RhoA - as they have been directly linked to the regulation of epithelial junction formation and polarization. Moreover, the three GTP-binding proteins are key regulators of actin organization; hence, I will highlight in this context the type of actin-driven processes that are regulated by specific Rho GTPases [132, 133]. For efficient adhesion, cadherins and many other adhesion receptors needs to be associated with actin filaments; hence, regulation of the cytoskeleton is critical to understand epithelial junction formation, polarization and differentiation.

Cdc42

Cdc42 was first identified in *Saccharomyces cerivisiae* as a temperature sensitive mutant of the cell cycle [134]. Subsequent work in various experimental models demonstrated that Cdc42 is an evolutionarily conserved regulator of cell polarization and plays fundamental roles in the regulation of the actin cytoskeleton [135]. As described above, one of the best known epithelial functions of Cdc42 is that of a regulator of the Par3/Par6/aPKC complex. Active Cdc42, as does active Rac1, can bind to Par6, which stimulates activation of aPKC [136]. This interaction is not only important during eithelial polarization, but also regulates microtubule orientation during directed cell migration, a process that also involves another Cdc42 effector, MRCK (myotonic dystrophy kinase-related Cdc42-binding kinase), that regulates nuclear positioning by the spatial regulation of myosin II activity [137]. Apart from Par6, Cdc42 and Rac1 share several common effectors. Examples are PAKs (p21-activated protein kinases) that play important roles in the regulation of the cytoskeleton and cell shape [138, 139] . Another common binding partner is IQGAP1, a protein that can bind the GTP as well as the nucleotide-free GTPase, and links Cdc42 and Rac1 to regulation of microtubule organization and cadherin-dependent adhesion strength [140].

Cdc42 regulates fundamental processes that are driven by actin dynamics and induce membrane remodelling and cell shape changes. The quintessential example is the formation of filopodia [132, 135]. Filopodia have been described as tentacles that cells use to probe their environment. Induction and growth of filopodia requires actin polymerization [141]. Initiation of filopodia is stimulated

by the insulin-receptor substrate p53 (IRSp53). This is an I-BAR domain protein, which contains three domains: an N-terminal modified Bin-Amphiphysin-Rvs161/167 (BAR) domain, a partial Cdc42/Rac Interactive Binding domain (CRIB) domain that can indeed interact with Cdc42 and Rac1, and a C-terminal SH3 domain [142, 143]. IRSp53 interacts with various actin binding proteins such as WAVE1, WAVE2, Mena, Pro/Shank, Dia1, dynamin1, N-WASP and Eps8. N-WASP is an important binding partner in this context, as it is required for IRSp53-induced filopodia.

N-WASP is a close homologue of WASP, which is the product of the gene responsible for the Wiskott-Aldrich syndrome, and can directly link Cdc42 to actin polymerization by functioning as a nucleation promoting factor [141]. Although there are some inconsistencies between different experimental systems and laboratories, one important mechanism to initiate actin polymerization during filopodial induction relies on the Arp2/3 complex. The Arp2/3 complex utilises G-actin to initiate new barbed ends (the growing end of F-actin) on preexisting barbed ends [144]. However, it has been suggested that the classic Cdc42-N-WASP-Arp2/3- pathway for filopodia formation may not be entirely correct. A study by Snapper *et al* showed that the extension of filopodia can occur in the absence of N-WASP [145] and there is evidence that filopodia can form in an Arp2/3-independent manner [146]. Moreover, IRSp53 recruits a number of proteins to filopodia that regulate actin polymerisation and organization such as mDia1, MENA/VASP, actin-elongation-promoting protein, and EPS8 [141].

These proteins have various activities. For example, Ena/VASP family proteins were found to interact with the tips of the growing filopodia, thus preventing

capping from taking place, and, in conjunction with the formin Dia2, providing actin monomers to the tip of the developing filopodium [147, 148]. Other proteins such as EPS8 promote actin filament bunding [141].

During the addition of actin subunits to the end of protrusions during actin polymerisation, however, there comes a point when the growth of these protrusions must be terminated. This involves capping proteins binding to the barbed ends to stabilize these filaments. A good example of a capping protein is the capping protein CapZ. This capping protein, originally identified in muscle cells, is from a family of proteins that bind with a high affinity to the barbed ends of actin filaments to block their elongation [149]. This capping aspect is thought to be required for the spatio-temporal control of actin polymerisation in cells. For example depletion of CapZ has been demonstrated to induce aberrant formation of filopodia [150].

Various proteins can uncap or inhibit activity of capping proteins at barbed ends. For example, polyphosphoinositides can uncap these actin barbed ends *in vitro* [109]. There are also proteins that inhibit capping such as CD2AP, a multiple SH3 domain containing protein that is required for the formation and maintenance of slit diapragham-like junctions, a specialized type of cell-cell junctions located in the kidney glomerulus, by linking the protein nephrin to the cytoskeleton [151]. CD2AP was found to interact with various actin regulating proteins such as cortactin, CapZ and capping protein (CP).

Rac1

The Rac subfamily of Rho GTPases consist of four members: Rac1, Rac2, Rac3 and RhoG [152]. As mentioned above, Rac share several effectors with Cdc42 and have also been linked to junction formation and actin-driven membrane dynamics. However, instead of filopodia, Rac stimulates lamellipodial extensions and membrane ruffling [152]. Lamellipodia are also initiated through the activation of the Arp2/3 complex, a process that involves Rac activation of WAVE family proteins, which are nucleation promoting proteins like the Cdc42 effector N-WASP [153]. Rac also uses this actin polymerisation-driven pathway to regulate cellular movement. Rac activates WAVE, which in turn activates Arp2/3 that promotes actin polymerisation and pushes the leading edge forward [152].

Rho

There are three distinct proteins within the Rho family: RhoA, RhoB and RhoC [154]. Rho proteins have been extensively studied in cellular responses mainly through the enzyme C3 transferase. This clostridial enzyme inhibits RhoA, RhoB and RhoC by ADP-ribosylation of Asn41 within the effector binding domain of the Rho protein [155]. Of all the Rho proteins, RhoA has been studied most exensively

RhoA has been linked to a variety of actin dependent cellular processes. These include cell-cell adhesion, cell motility, platelet aggregation, contraction and

cytokinesis [156]. Ridley and Hall found direct evidence for the involvement of RhoA in the formation of stress fibres. Using a constitutively activated mutant (Val14RhoA), they found that it stimulates stress fibre formation [157]. This indicates that RhoA is a crucial player in the regulation of signal transduction pathways linking RhoA to the reorganization of the actin cytoskeleton.

GEFs, GAPs and GDIs

As mentioned previously, Rho GTPases exist either in a GDP-bound or in a GTP-bound state. Switching of states is regulated by two main classes of proteins: GEFs and GAPs (Figure 1.4). A third class of regulatory proteins are Guanine nucleotide Dissociation Inhibitors (GDIs), which regulate membrane association of the GTPases [11, 158, 159].

Figure 1.4 The Rho GTPase molecular switch.

Guanine Nucleotide Exchange factors (GEFs) are activators of Rho GTPases, while GTPase Activating Proteins (GAPs) are inactivators. GDIs sequester Rho GTPases in the cytosol. Adapted from [160].

Guanine nucleotide Dissociation Inhibitors (GDIs)

Three mammalian GDIs have been identified [161]. They are located in the cytosol, and form complexes with Rho GTPases in their inactive form. This prevents activation of the specific Rho GTPase by GEFs as well as restricting the normal translocation of the GTPase between the cytosol and membranes [154]. GDIs can also interact with active GTPases, thus preventing the GTPase from hydrolysing and interacting with downstream effectors [154].

Guanine nucleotide Exchange Factors

GEFs are regulatory proteins that stimulate the activation of Rho GTPases by catalysing the exchange of GDP by GTP. The first Rho GEF was isolated from diffuse B-Cell lymphoma. It was found to transform fibroblasts and was hence given the name Dbl [162]. At the time the functional relevance of Dbl was not known. Hart *et al* further clarified its mechanistic properties by showing that Dbl catalyzed the exchange of GDP by GTP of Cdc42 [163]. Over 70 GEFs have now been identified in the human genome and many have not yet been characterized in great detail [159]. Most of these GEFs share two homology domains with Dbl that are arranged in tandem: the Dbl Homology (DH) and the Pleckstrin Homology (PH) domain. The DH domain is the actual catalytic domain that binds to Rho GTPases in their GDP-bound form and promotes nucleotide exchange. The function of the PH domain is not the same in all GEFs and has been linked to membrane association and regulation of GEF

activity by binding to phosphoinositides, as well as to a role in GTPase selectivity by binding to DH domain interacting GTPases [164, 165]. A second group of GEFs, the Dock180 related proteins, does not contain a DH domain but harbours two Dock-Homology Regions: DHR1 and DHR2. The latter domain acts as the exchange factor domain in these proteins and DHR1 functions as a regulatory domain that binds lipids and other proteins [166].

The exchange of GDP by GTP by Rho GTPases without GEFs is slow; GEFs speed up the exchange by several orders of magnitude [159]. This is achieved by modifying the Rho GTPase nucleotide binding site by inducing a conformational change in the nucleotide binding site that reduces the affinity for GDP and leads to GDP being replaced by GTP, which in turn displaces the GTPase from the DH binding pocket during the course of the exchange reaction [159].

GTPase Activating Proteins

GAPs are negative regulators of Rho GTPase signalling and were initially identified by Garrett *et al* [167]. GAPs bind to GTP bound forms of Rho GTPases and enhance their GTPase activity. The first characterised GAP, Breakpoint cluster region protein (Bcr), was found to increase the intrinsic ability of Rac to hydrolyze GTP to GDP [168]. Since this initial description, there have been over 70 human GAPs discovered. Intriguingly, there are over three times more GAPs then there are Rho GTPases, and the numbers are similar for GEFs. Moreover, most GEFs and GAPs are not specific for a single Rho

GTPases. This vast excess in regulators has several potential explanations. Firstly, various GAPs and GEFs maybe expressed in a tissue specific manner; hence, the provide cell- and tissue-specific functions. Alternatively, GAPs or GEFs may regulate a specific pathway or process, and may function at specific subcellular sites. An example for this is provided by the two GEFs for RhoA GEF-H1 and p114RhoGEF, which both bind to the scaffold cingulin at TJs. p114RhoGEF is recruited to the forming junctional complex to form a complex with myosin II and stimulates junctional actinomyosin activity; GEF-H1 is active thoughout the cytoplasm and recruited to TJs at a later stage, where it is inactive, leading to downregulation of RhoA signalling pathways that stimulate cell proliferation [59, 60].

All GAPs contain a RhoGAP domain, which is comprised of a conserved 140-150 amino acid sequence. Rho GAP and Ras GAP domains are related in terms of structure and functionality although the homology is low [169, 170]. The GAP domain consists of 9 alpha helices and contains a highly conserved arginine residue that is critical for activity of the GAP. This arginine residue is present on a loop in the RhoGAP domain, and binding of the GAP to the Rho GTPase allows the arginine finger residue to enter the Rho GTPase active site, where it neutralises a negatively charged phosphate group to promote GTP hydrolysis [169-171].

Regulation of GAPs

Physiological regulation of Rho GTPase signalling is highly regulated; so, one would expect that GAPs are regulated as well to ensure correct termination of

Rho GTPase signalling steps. Indeed, there is evidence for the regulation of GAPs, the main mechanisms by which GAPs are regulated rely on phosphorylation, lipid binding and protein binding, and subcellular targeting.

There is increasing evidence that GAPs are regulated by kinases. p190 RhoGAP a GAP for RhoA was found to be phosphorylated and activated by the non-receptor tyrosine kinase Src, leading to decreased levels of RhoA [169]. As well as activation of GAPs by phosphorylation, inhibition of GAP activity may occur. Liu *et al* demonstrated in their study that the Cdc42 GAP TCGAP was a substrate of the src non-receptor tyrosine kinase family member Fyn. Using HEK293T cells, Fyn phosphorylated and inactivated TCGAP, thereby promoting Cdc42 signalling [172]. Similarly, the Rac1 GAP, CdGAP can be phosphorylated by the MEK-ERK pathway, resulting in inactivation of its GAP activity toward Rac1 *in vivo* and *in vitro* [173].

GAP activity can also be regulated by binding to lipid molecules. The best example of this is the Rac GAP β2-chimaerin. This GAP contains a C1 domain, which is a 50 amino acid motif known to bind phorbol ester and phosphatidylserine. The association of β2-chimaerin with phospholipids such as phosphatidylserine increases its GAP activity toward Rac in a concentration dependent manner and also stimulates recruitment of the GAP to the plasma membrane [174, 175].

GAPs can also be regulated by various protein-protein interactions. Binding of CdGAP to the endocytic scaffold and GEF intersectin, is thought to induce a conformational change on CdGAP that inhibits its GAP activity. It is thought this is due to the action of the C-terminal proline rich regions found in CdGAP that inhibits its N-terminal Rho GAP domain. Subsequently, intersectin recruits

various other proteins to the complex, which are involved in actin dynamics, such as WASP, and activates the Rho GTPase Cdc42 [169, 176].

It thus seems that the diversity of GAPs with a multitude of different protein domains enables cells to control Rho GTPase signalling in response to different types of signals and at different subcellular sites. A key domain found in a small number of GAPs is the BAR domain, which has also been linked to regulation of GAP localization and activity.

BAR domain containing GAPs

A small group of Rho GAPs contain Bin/Amphiphysin/Rvs (BAR) domains. BAR domains are found in many proteins that regulate actin remodelling and membrane dynamics (e.g., IRSp53) and have also been identified in some GAPs, one of which has been shown to associate with TJs. My work has led to the identification of two new junction-associated BAR domain-containing GAPs.

BAR domains can mediate binding to different ligands, including membranes and other proteins. Many BAR domains bind membranes in a curvature sensitive manner and can even bend membranes, which is thought to be of functional importance for the role of such proteins in membrane and actin remodelling [177-180]. Crystal structure studies of BAR domains revealed that they are composed of three anti parallel coiled coil helices that can promote homodimerisation [178, 180, 181].

BAR domains can be classified into three distinct types. The first is the classical BAR domain, which includs N-BAR domains and other lipid binding domains; N-BAR domains differ from classical BAR domains by the presence of an amphipathic helix positioned at the N-terminus of the BAR domain. This extra amphipathic helix enhances binding to liposomes [181]. The N-BAR domain causes curvature in membranes by interacting with negatively charged residues on membrane lipid head groups and remodels the membrane to adapt to the curvature presented by the N-BAR domain surface [182]. The second type is the F-BAR domain (Fes/CIP4 homology BAR), which also binds lipids, contains three pairs of conserved basic residues in its structure and is involved in membrane tubulation [181]. F-BAR domains are found in many actin regulatory proteins such as Transducer of Cdc42-dependent actin assembly (Toca-1).The third type is the I-BAR domain, which have a cigar-like shape. Positively charged residues aid in its interaction with the plasma membrane [181]. I-BAR domain of IRSp53 is thought to link it to the membrane and at the tip of filopodia [181].

Different types of BAR domains have been found in several proteins that also have a Rho GAP domain. Examples include oligophrenin-1, a protein that has been linked to mental retardation, and GRAF1, a GAP that has been linked to regulation of endocytosis and acute myologenous leukaemia [183, 184]. In some GAPs, the BAR domain has an autoinhibitory function [185]. A BAR domain GAP of particular importance for my thesis is SH3 Binding protein 1 (SH3BP1), which was originally identified by Cicchetti *et al*. who found that it binds to the SH3 domain of the non-receptor tyrosine kinase Abl *in vitro* [186].

SH3BP1 contains a N-terminal BAR, a Rho GAP, and a C-terminal SH3 binding domain. The GAP domain that has been shown to stimulate GTP hydrolysis by Rac1 and Cdc42 in vitro; and overexpressed SH3BP1 suppresses PDGF induced membrane ruffling supporting its negative role in Rac signalling [187]. Weak GAP activity toward RhoA was also reported [188]; however, the physiological relevance of this activity is not clear. It has recently been shown that regulation of Rac by SH3BP1 at the leading edge is important for cell migration [189]. Leading edge targeting seems to involve binding to the exocyst, a complex involved in plasma membrane tethering of secretory vesicles.

SH3BP1 has a similar domain structure as Rich1/Nadrin [190-192]. Rich1 was found to be an important component of TJs [193, 194]. Rich1 is recruited and inactivated at the TJ by the scaffold protein angiomotin (Amot). The polarity proteins Pals1, PATJ and Par3 were found to interact with the Amot complex, which also contains the tumour suppressor Merlin/NF2. Rich1 function is important for Cdc42 and Rac regulation, and thereby regulates apical polarization. It is not known whether other BAR domain GAPs play a role in the regulation of cell-cell junctions and epithelial polarization.

Rho GTPases and junction formation

The formation of epithelial junctions has been shown in numerous studies to be dependent on Rho GTPases. Both constitutively active and dominant negative forms of Cdc42, Rac1 and RhoA disrupts the epithelial junctional complex to varying degrees, with the CA forms of RhoA and Cdc42 having the strongest

effect on the TJ proteins occludin, ZO-1, claudin-1, claudin-2, and junctional adhesion molecule (JAM)-A [195-197].

Studies by various labs indicated that cell-cell adhesion and E-cadherin activation stimulate activation of Rac in different cell types [198-200]. Active Rac1 was found localised to the leading edge of contacting lammelipodia subsequently preceding junction formation using a biosensor in live MDCK cells; active Rac has also been localised to established cell-cell contacts in keratinocytes using a recombinant effector protein as a probe [201]. It thus seems that induction of cell-cell adhesion stimulates Rac activation in different cell types. Moreover, E-cadherin ligation using coated beads or plating cells on E-cadherin also stimulates Rac activation, indicating that E-cadherin engagement is an important driver of Rac activation [200, 202].

There are conflicting reports regarding the activation of Cdc42 by newly forming contacts. In some laboratories and cell types, Cdc42 has been shown to be activated by newly developing E-cadherin based contacts [203]. Conversley in keratinocytes, E-Cadherin engagement does not activate Cdc42 but rather leads to a decrease in total levels of active Cdc42 [204]. The reason for these different results are not clear. However, it is possible that they are due to the cell types analysed or to the conditions used, as additional cell-cell adhesion proteins can contribute to Cdc42 activation that may be expressed in different amounts in different tissues or whose engagement may be influenced by the experimental conditions. A prominent example are nectins, that, upon ligation, stimulate activation of both Cdc42 and Rac [205].

Early studies on RhoA activation suggested that E-Cadherin engagement results in a slow but steady decrease in total levels of RhoA activity (5).

However, calcium induced cell-cell adhesion in keratinocytes induces active RhoA levels, and Rho is required for E-cadherin recruitment to nascent cell-cell contacts (10). Similarly, activation of RhoA was reported at forming cell-cell contacts in MDCK and Caco-2 cells [60, 201]. Similarly to Rac and Cdc42, it thus seems that there are cell type and experimental condition dependent variations. An important contribution to the conflicting results is likely to be made by the method that is used to monitor activation. Measurements of total levels of active GTPases are very accurate but may not detect activation occuring in response of induction of adhesion if the same GTPase is inactivated concurrently at other subcellular sites. Hence, different cell types may lead to different results. It is thus clear that methods for the measurment of spatial activation of GTPases need to be employed to reach definitive conclusions.

During junction formation, the main function of RhoA seems to be myosin II activation [206]. Activated RhoA bound to Rho-associated protein kinase (ROCKs), which subsequently phosphorylated and inactivate myosin light chain phosphatase and also seemed to phosphorylate myosin light chain inself, which led to an increase in myosin II activity along the junctional complex. At least in part, this mechanism is stimulated by the recruitment of a RhoA GEF, p114RhoGEF, to forming TJs, resulting in juntional actinomyosin contraction and formation of functional TJs in intestinal and corneal epithelial cells [60]. Another GEF for RhoA, ARHGEF11, has recently also been shown to interact with ZO-1 and to regulate TJ formation in mammary epithelial cells [207]. It is currently not clear whether different epithelial cells rely on different GEFs for RhoA or whether indeed multiple RhoA GEFs are required in a given cell type.

The mechanisms that inactivate RhoA throughout the cytoplasm have also been investigated. GEF-H1, which accumulates at mature TJs, is a major activator of RhoA throughout the cytoplasm [208]. During junction assembly, it binds to cingulin, a junctional scaffold protein, resulting in junctional sequestration and

The mechanisms that inactivate RhoA throught the cytoplasm have also been investigated. GEF-H1, which accumulates at mature TJs, is a major activator of RhoA throughout the cytoplasm [208]. During junction assembly, it binds to cingulin, a junctional scaffold protein, resulting in junctional sequestration and inhibition of its GEF activity [59]. Formation of AJs also inhibit RhoA signalling. p190 RhoGAP is recruited to AJs in response to Rac activation by binding to p120 catenin, resulting in activation of its GAP activity, hence, leading to reduced RhoA signalling [209]. In contrast, a recent paper suggested that the AJ-associated Ect2, a GEF for RhoA and Cdc42, stimulates RhoA signalling at the junction and that this is required for stable AJs [210]. However, an earlier paper suggested that junctional Ect2 functions as a GEF for Cdc42, and associates and regulates the Par3/Par6/aPKC complex [211]. Another regulator of RhoA-associated with AJs is ARHGAP10, which is thought to regulate alpha-catenin recruitment [212]. However, as ARHGAP10 can also inactivate Cdc42, it is not clear whether this is due to RhoA or Cdc42 signalling. Finally, the motorized RhoA GAPs myosin 9A and 9B have been shown to associate with the AJC and regulate junction assembly [213-215]. There relative importance seems to depend on the cell type and conditions analyzed.

Junction formation as well as various other processes is also dependent on interactions of GEFs and GAPs with cytoskeletal components. For example, Ect2 is known to be important during cytokinesis. During mitosis, the dissolution

of the nuclear envelope allows the release of Ect2 and subsequently allows it to localise with microtubules and the mitotic cleavage furrow where it is believed to activate RhoA [216]. Recently, it has also been shown to promote mitotic cell rounding prior to cytokinesis [217]. GEF-H1 is another GEF that interacts with microtubules and microtubule binding inhibits its GEF function [218]. In Drosophila, the protein DRhoGEF2 seems to be related to GEF-H1 and is also regulated by microtubule binding [219].

Cdc42 and Rac1 have also both been linked to junction formation and, to some extent, seem to be able to perform similar functions. The function of both Cdc42 and Rac had originally been analyzed by the expression constitutively active and dominant-negative constructs in different types of epithelial cells and were found to regulate assembly of a functional epithelial junctional complex [195, 220-224]. Moreover, siRNA-mediated depletion of Cdc42 and genetic deletions of the Cdc42 gene have also been shown to disrupt epithelial junction formation [225, 226]. Furthermore, Rac1 becomes activated in response to initial E-cahderin ligation and, at least in some cell systems, is required for the stablization of cell junctions by promoting F-actin association and reorganization at forming junctions [227]. As Cdc42 and Rac1 share many common effectors that regulate junction assembly and dynamics (e.g., PAKs; Par3/Par6/aPKC complex), it is not as such surprising that they can regulate similar processes and might thus be the underlying reason why different epithelial cell models and/or different experimental conditions have led to different requirements for Cdc42 and Rac1 for junction formation [106, 204, 225, 226, 228].

Several GEFs for Cdc42 have been shown to associate with the AJC. As mentioned above, Ect2 had been shown to drive junctional Cdc42 activation

and stimulation of the Par3/Par6/aPKC complex [211]. The GEF Tuba was shown associate with TJs by binding to ZO-1, and its depletion resulted in a delay in the formation of junction assembly [229]. Tuba has also been shown to regulate cyst morphogeneiss by guiding mitotic spindle polarity in cyts and driving apical Cdc42 activation during lumen formation [230-232]. Similarly, the GEF ITSN2 has been demonstrated to regulate spindle polarity and cyst morphogenesis [233].

Rac activation has also been studied and best understood junctional Rac GEF is TIAM1, which stabilises AJs [234]. TIAM1 binds to Par3, resulting in the stimulation of function TJ assembly [113, 235]. Different modes of TIAM1 recruitment to junctions have been described and it has also been shown to bind to paracingulin/JACOP [63]. The GEF Trio has also been shown to be recruited to AJs and that it regulates a Rac-depenent pathway that suppresses E-cadherin transcription [236]. Rac activity at AJs is also promoted by stabilization due to a feedback loop with Ajuba, a protein that becomes activated by the Rac effector kinase PAK1 and subsequently stabilises GTP-bound Rac [237].

Junctional Cdc42 and Rac activity can also be regulated by GAPs. The best known example was mentioned above, Rich1, a GAP that is important for epithelial polarization and is recruited to TJs [193, 194]. ARHGAP12, which can also stimulate Cdc42 and Rac, has also been shown to accumulate at AJs [238]. It is downregulated by HGF signalling and prevents scattering and Rac activation if overexpressed, suggesting that it is important for the stabilization of AJs, as Rac activation can also stimulate junction dissociation [239, 240].

There is thus compelling evidence for the functional importance of the main Rho GTPases RhoA, Rac1 and Cdc42 for the assembly and regulation of AJs and TJs. While the first Rho GEFs and Rho GAPs have beed identified that are important for these functions, we are still lacking sufficiently detailed information to understand the orchestration of Rho GTPase signalling at epithelial junctions.

EGFR signalling

Many growth factors bind and stimulate transmembrane proteins with cytoplasmic tyrosine kinase domains. Stimulation of such growth factor receptors leads to dramatic changes in signalling pathways that regulate cell differentiation, morphology, cytoskeletal organization and junction formation. Many of these pathways involve Rho GTPases. The receptor for epidermal growth factor (EGFR) is of central importance in epithelial cells.

The structure of EGFR is comprised of an extracellular domain, involved in binding to EGF ligand, a membrane spanning segment, and the cytoplasmic tyrosine kinase domain [241]. Upon EGF binding, the receptor undergoes dimerization and its tyrosine kinase activity is switched on. Various tyrosine residues located on target proteins as well as the receptor itself are consequently phosphorylated. Upon activation, the receptor is internalised via endocytosis, which is not only important for signalling but also for terminating the signal once the receptor reaches late endosomes [241-243].

EGFR activation results in the stimulation of multiple signalling pathways that can lead to Rho GTPase activation. A main pathways is Ras signalling, which

leads to activation of Raf and Erk signalling. Erk can stimulate GEFs such as GEF-H1 and thereby stimulate RhoA activation [244]. EGFR also regulates phosphatidylinositol 3-kinase activation (PI3K), which activates the production of PtdIns (3, 4, 5) P3, leading to the stimulation of Akt, which leads to the stimulation of Vav2, a GEF for multiple Rho GTPases. EGFR also stimulates the activation of the tyrosine kinase src, a major upstream regulator of Rho GTPases [245].

The overall response of EGF signalling depends on the cell type and the experimental conditions. In some epithelial cells, EGF signalling induces dissolution of cell junctions and cell scattering; in other cells, EGF induces junction formation and differentiation [246-251]. Similarly, EGFR signalling is important for normal development and maintenance of the skin, but can cause cell transformation and skin cancer if deregulated [252].

Rho GTPases have been linked to both processes: EGF-induced scattering and EGF-induced junction formation. Scattering induced by increased EGF-signalling is a Rac1-dependent process and involves a recently identified effector, armus, that regulates E-cadherin degradation [253]. In another study Toca1 was activated by EGF stimulation and was shown to play an important role in actin remodelling during cell migration. Depletion of Toca1 resulted in a decrease in filopodia [254]. Toca1 in conjunction with Abelson-interacting protein 1 (Abi1) is also important for the regulation of actin nucleation, as their absence impairs localization of Arp2/3 [254]. This links to an earlier study that showed that EGF induced Cdc42 was required for the translocation of Arp2/3 to the leading edge of motile cells [254, 255]. On the other hand, in confluent cultures of the keratinocyte cell line A431, EGF induces increased levels of

active Rac1 and Cdc42; The levels of activated Cdc42 and Rac1 at the plasma membrane increased in a diffuse manner before being found present in membrane associated ruffles and lamellipodia [256]. Activity of Rac1 subsided rapidly after EGF stimulation, whereas levels of Cdc42 activity remained high [256, 257]. Interestingly, A431 cells start to form TJs if stimulated by EGF and AJs remain assembled [258]. Whether induction of TJ formation is a Rho GTPase-dependent is not known yet.

Deregulation of EGF receptor signalling is an important disease mechanism. The EGF receptor is found to be upregulated in a number of cancers. Further exploration of the genome found mutations in the EGF receptor gene in cancers such as lung [259]. Thus the EGF receptor has become a focal point for the development of cancer therapy. Upregulation of the EGF receptor is also correlated with a poor prognosis during cancer progression. EGF receptor upregulation has also been linked to polycystic kidney disease and a EGFR specific tyrosine kinase inhibitor resulted in therapeutic benefits in mice [260]. Thus, EGF is an important growth factor in health and disease, and a potential therapeutic target for different types of disease conditions.

Experimental plan

The focus of this project is on the regulation of Rho GTPases in the context of epithelial junction formation and maintenance, and, in particular, the negative regulation of these small GTP binding proteins by the GAP protein SH3BP1. This protein was chosen to study further as it was identified in siRNA based functional screen using the human epithelial colon adecarcinoma cell line Caco-2 as a regulator of epithelial junction assembly. I have analyzed the role of SH3BP1 in two types of epithelia: Caco-2 cells and A431 cells, in order to determine the function of SH3BP1 in junction formation and maturation, and to identify the molecular mechanism by which it supports epithelial differentiation.

Hypothesis

Research by various laboratories demonstrated that inactivation as well as over-stimulation of Rho GTPase signalling prevents normal formation of the AJC. Hence, proper spatial and temporal control of Rho GTPase activation and inactivation appears to be required for junction assembly. We have therefore hypothesized that specific negative regulators of Rho GTPases exist that are recruited to sites of actin-driven membrane remodelling and junction formation to ensure proper timing of Rho GTPase signalling.

Specific Aims

Aim 1 - To perform a function siRNA screen to identify negative regulators of Rho GTPases in the context of junction stability.

Aim 2 - To determine the role of SH3BP1 in early assembly and maturation of the AJC in distinct epithelial cell models.

Aim 3 - To identify interaction partners of SH3BP1 and to design a model for SH3BP1 function.

Chapter 2

Materials and Methods

Chapter 2 - Materials and Methods

All materials used are from Sigma unless otherwise stated

DNA cloning techniques

All the DNA constructs used in the project are listed in table 2.0:

Name of Plasmid	**Description**
pcDNA4/TO/Myc-His-A/B – HA Full length SH3BP1	HA tag added to N-terminus of vector using XhoI junction. Human SH3BP1. Made by PCR using an SH3BP1 EST clone (MRC Geneservice) as template and the following primers: Forward: 5’-CGCGGATCCATGCAGGACCTGCCAGGCAACGACAACAGCAC CGCCGGCCTCGAGATGATGAAGAGGCAGCTGCACCGC – 3’ Reverse:

	5’ – AAGCTCTAGATCAGTTGGTCTCTGAGGCAAGGCTC – 3’ BamHI/XbaI fragment cloned in to BamHI/XbaIpcDNA4/TO/Myc-His-A/B – HA
pcDNA4/TO/Myc-His-A/B – HA SH3BP1 BAR domain mutant	HA tag added to N-terminus of vector using XhoI junction. Human SH3BP1 BAR domain mutant. Made by PCR using an SH3BP1 EST clone (MRC Gene service) as template and the following primers: Forward: 5’ – CGCGGATCCATGCAGGACCTGCCAGGCAACGACAACAGCA CCGCCGGCCTCGAGATGATGAAGAGGCAGCTGCACCGC – 3’ Reverse: 5’ – CAAGCTCTAGACTACGAAGGGGAGTGGTCTGCTTGG – 3’ BamHI/XbaI fragment cloned in to BamHI/XbaIpcDNA4/TO/Myc-His-A/B – HA
pcDNA4/TO/Myc-His-	HA tagged Human SH3BP1 (R312) mutant. Made by single step

A/B – HA Full length SH3BP1 (R312A)	PCR mutagenesis using pcDNA4/TO/Myc-His-A/B – HA Full length SH3BP1 as A template and the following primers: Forward: GAGGGTCTCTTCGCTCTGGCTGCTGGG Reverse: CCCAGCAGCCAGAGCGAAGAGACCCTC The arginine residue was converted to an alanine residue.
pGEX-4T-3 GST SH3BP1 Full Length	Human SH3BP1 Full length. Made by PCR using pcDNATO/myc-his-A/B – HA Full length SH3BP1 as template and the following primers: Forward: GCGAATTCCATGATGAAGAGGCAGCTGCACCGCATGCG Reverse: GGCGGCCGCCTCAGTTGGTCTCTGAGGCAAGGCTCCTGGG EcoRI/NotI fragment cloned in to EcoRI/NotIpGex-4T-3.

pGEX-4T-3 GST SH3BP1 BAR domain mutant	This was made by subcloning the SH3BP1 BAR domain mutant fragment from the pcDNA4/TO/Myc-His-A/B – HA to the pGex-4T-3 GST SH3BP1 using a BamHI/XbaI Restriction digests.
pGEX-4T-3 GST SH3BP1 C-Terminal domain mutant	Human SH3BP1 C-Terminal domain mutant. Made by PCR using full length SH3BP1 as template and the following primers: Forward: GCGAATTCCCTCTTCTCAGCTGTTACCCTCCAGGACACAGTC Reverse: GGCGGCCGCCTCAGTTGGTCTCTGAGGCAAGGCTCCTGGG EcoRI/NotI fragment cloned in to EcoRI/NotIpGex-4T-3.
pCAGGSneodelEcoRI HA tag JACOP	Kindly provided by Dr Mikio Furuse, Kyoto University, Japan.
pcDNA4/TO/myc-his-A/B - HA Full length SH3BP1 siRNA resistant mutant	Human SH3BP1 siRNA resistant construct. Made by PCR using full length SH3BP1 as a template and the sequence changed from: GATGACAGCCACCCACTTC To:

	AATGACAGCAACACACTTC
pcDNA4/TO/myc-his-A/B - HA Full length SH3BP1 (R312A) siRNA resistant mutant	Human SH3BP1 siRNA resistant R312A mutant. Made by PCR using full length SH3BP1 R312A as a template and the sequence changed from: GATGACAGCCACCCACTTC To: AATGACAGCAACACACTTC

Table 2.0 List of DNA constructs used in project.

Primers used to generate the constructs are listed. Nucleotide bases highlighted in red indicate enzyme restriction sites or bases altered by site directed mutagenesis.

Polymerase chain reaction

Table 2.1 shows concentrations of individual components used for PCR reactions.

Product	**Volume**
Primers (Provided by MWG)	1µl each primer
10x Buffer with $MgCl_2$ (Roche)	5µl
dNTP mix (1.25mM each) (Promega)	8µl
Template DNA	1µl
Expand High Fidelity PCR Enzyme (Roche)	0.5µl
H_2O	29µl
10% DMSO	5µl

Table 2.1 PCR reaction constituents.

The Biometra T3 Thermocycler PCR machine (Anachem) was programmed with the following settings: Initialising step, 95^{o}C for 2 minutes; 30 cycles of denaturation at 94^{o}C for 30 seconds, annealing at 60^{o}C for 30 seconds and extension at 72^{o}C for 2 minutes; final elongation step at 72^{o}C for 10 minutes.

PCR products were run on low melt agarose gels, bands were excised and DNA purified.

DNA agarose gel electrophoresis

Preparation of 1% agarose gels was performed using either standard agarose (Invitrogen) or low melt agarose (Bioproducts Ltd) combined with either TBE for standard agarose or TAE for low melt agarose (both National Diagnostics, USA). To the dissolved agarose, Gel red at a 1 in 10,000 dilution (Biotium, USA) or ethidium bromide at 0.5 mg/ml was added to stain the DNA. A 1KB DNA marker (Invitrogen) was loaded alongside the samples, and 6x DNA loading buffer (0.25% Bromophenol blue, 0.25% Xylene cyanol FF and 30% glycerol) was added to the samples. Low melt agarose gels were run at 75mV and standard agarose gels at 120mV. The gels were imaged using a UV transilluminator-based digital imaging station (Syngene).

Low melt agarose DNA purification using silica beads

To each sample excised agarose gel slice 1ml of 6M sodium iodide was added. Samples were then placed in a water bath at 70^{o}C for 10 minutes. Once melted, 40µl of silica beads were added and resuspended by inverting the tubes. After 10 minutes, the samples were centrifuged at 10,000 rpm for 1 minute, and the supernatants were discarded. The pelleted beads were then washed three

times with 1ml of ice-cold wash buffer (50mM NaCl, 10mMTris HCL (pH 7.5), 2.5mM EDTA and 50% (v/v) ethanol) centrifuging each time for 1 minute at 10,000 rpm. After the final centrifugation, the resulting DNA pellets were suspended in 40µl of distilled water. The samples were incubated in a heating block at 70^{o}C for 10 minutes and then centrifuged for 1 minute at 10,000 rpm. The supernatants containing the purified DNA were then transferred to fresh tubes for further processing.

Low melt agarose DNA ligation procedure

After melting agarose slices at 70^{o}C, 3µl of vector (~50ng) and 7µl of DNA insert (~10 - 50ng) were mixed. For background tubes, the insert DNA was replaced with H_2O. The tubes were reincubated at 70^{o}C for 10 minutes to ensure that the agarose did not start to gel. During this time, an ice bucket was prepared containing fresh microcentrifuge tubes containing 10µl of a master ligation mix that was prepared by mixing 7 parts of distilled water, 2 parts of 10x DNA ligase buffer, and 1 part of T4 DNA ligase (NEB). Ten microlitres of the DNA mix was then added to the 10µl of ligation mix, pipetted once up and down, and placed on ice. The samples were placed in a refrigerator overnight. The next day, the samples were incubated a further 2-3 hours at ambient temperature before transformation.

TA cloning kit ligation using PCR 2.1 vector (Invitrogen)

The purified DNA inserts were first incubated with Taq polymerase by adding 1µl of 10x PCR buffer, 1µl dNTPs (1.25mM of each) and 0.2µl Taq polymerase to 8µl of the DNA sample. The tubes were then incubated at 72^{o}C for 10 minutes. A ligation mix was then prepared that contained 4µl of the above solution, 2µl H_2O, 2µl of the PCR 2.1 vector, 1µl 10x buffer and 1µl T4 DNA ligase. The ligation was allowed to proceed for 2 hours at ambient temperature and then overnight at 4^{o}C.

Transformation of ligated DNA using competent bacteria

Frozen competent DH5α *E.coli* were left to thaw on ice. Once thawed, 1.7µl 1.4M β-mercaptoethanol was added per 100µl of bacterial suspension. After 10 minutes, 100µl of bacterial suspension were added to each DNA sample to be transformed. Transformations were then incubated on ice for 30 minutes before applying a heat shock in a 42^{o}C water bath for 45 seconds. The samples were immediately placed on ice and, after 3 minutes, 1ml lysogeny broth (LB) was added to each sample. The transformed bacteria were then allowed to recover at 37^{o}C for 60 minutes before plating on LB-agar plates containing 100µg/ml ampicillin or 50µg/ml kanamycin. Plates were left overnight at 37^{o}C. When transforming TA ligation samples, IPTG (Roche; 1mM final concentration) and X-gal (40µg/ml final concentration) were added to the LB-agar plates to identify colonies harbouring a plasmid with insert by blue/white selection.

Preparation of competent *E.coli* bacteria DH5α or BL21pLysS

A colony of bacteria was grown in LB medium overnight in suspension culture. The following day, 4ml of the culture was added to 400ml of LB and incubated at 25ºC with vigorous shaking until the OD_{600} was between 0.4 and 0.6. The culture was chilled for 20 minutes on ice and spun at 4000 rpm for 10 minutes at 4ºC. The pellet was resuspended in 150ml ice-cold TB buffer (10mM Pipes-KOH pH 6.7, 15mM $CaCl_2$, 0.25M KCl and 55mM $MnCl_2$). The bacteria were pelleted again by spinning at 4ºC for 10 minutes. The supernatant was discarded and the pellet resuspended in 30ml TB. After adding 2.25ml DMSO, the suspension was left on ice for 10 minutes. Finally, 500µl aliquots of bacteria were prepared and snap frozen using liquid nitrogen. The competent bacteria were stored at -80ºC and defrosted on ice before being used for transformation.

Site-directed mutagenesis

Table 2.2 shows the concentrations of individual component used for site-directed mutagenesis reactions.

Product	**Volume**
Primers	2µl of each primer (80ng/µl)
10x Pfu Buffer (Stratagene)	5µl

dNTP mix (2mM each) (Promega)	5µl
Template DNA	2µl and 1µl
PfU enzyme (Stratagene)	1µl
H_2O	14µl
Betaine (5M)	15µl
Mgcl2 (25mM)	4µl

Table 2.2 Site-directed mutagenesis constituents.

The Biometra T3 Thermocycler PCR machine (Anachem) was programmed with the following settings: Initialising step at 95^{o}C for 2 minutes; 30 cycles of denaturation at 95^{o}C for 30 seconds, annealing at 48^{o}C for 30 seconds, and extension at 68^{o}C for 2 minutes per kB of template length; and a final elongation step at 68^{o}C for 12 minutes. After the PCR, the wild type DNA was removed from the mixture by DpnI restriction enzyme digestion (NEB; 25µl of the PCR reaction, 5µl of 10x Buffer 4, 19µl of H_2O, and 1µl of DpnI were mixed). The digestion mixtures were incubated at 37^{o}C for 1hour before inactivating DpnI by incubating at 80^{o}C for 20 minutes.As a negative control,1µl WT DNA in 24µl H_2O were used instead of the 25µl PCR mix. 4µl of the digests were transformed into competent DH5α cells.

Protein analysis

Immunoblotting techniques

Cells were washed three times with PBS before lysing the cells in 1.5x Laemmli sample buffer (3% SDS, 15% glycerol, 0.5M Tris HCL pH 6.8, 0.0015% bromophenol blue and 100mM DTT; 100μl/well of a 48-well plate) and homogenising with a 25 gauge needle (BD). Proteins were resolved by running Tris-buffered gels at a constant voltage of 25mV per gel using Hoefer Might Small twin gel systems. The transfer was performed using wet transfer systems (BioRad) at 4^{o}C and nitrocellulose membranes (LI-COR). The transfers were allowed to proceed for two to three hours, depending on the size of the proteins to be analysed. The membranes were then stained with amido black (0.1% Destain, which contained 20% methanol and 7.5% acetic acid) followed by destaining for 30 minutes. The membranes were rinsed with water and neutralised with PBS for 5 minutes. The membranes were subsequently blocked with 5% milk in PBS containing 0.1% Tween-20 for one hour. Finally, primary antibody was then added, and the membranes were incubated at ambient temperature overnight or at 4^{o}C for longer periods of time. The membranes were then washed three times for 20 minutes with PBS/0.1% Tween-20. The secondary antibody was then added in PBS/0.1% Tween-20 and incubated for two hours. Finally, the membranes were washed again three times for 20 minutes each with PBS/0.1% Tween-20, and twice for 10 minutes with PBS only. If antibodies against phosphorylation sites were used, PBS was

replaced by TBS. The immunoblots were developed either by enhanced chemiluminescence (ECL; GE Healthcare) using X-ray film, if horseradish peroxidase-conjugated antibodies were used, or with an Odyssey infrared imager (LI-COR) if fluorescently labelled antibodies were employed.

Co-immunoprecipitation (Co-IP)

Cells were seeded at 20% confluence using a 15cm plate. Cells were left for 3-5 days in order to allow them to form TJs and polarize. The day before cells were ready, immunobeads were prepared by adding 3μg of antibody to 50μl of Protein A or Protein G beads (G.E Healthcare or Generon). Once cells were 90% confluent, they were washed with cold PBS. Shortly before use cocktails of protease (PMSF, aprotinin, benzamidine, pepstatin, and leupeptin) and phosphatase inhibitors (NaF, sodium pyrophosphate, and sodium orthovanadate) were added to the extraction buffer (0.5% TX100 in PBS). Cells were harvested in extraction buffer (using 2ml per plate). Cells were scraped and sucked up using a syringe with a 23 gauge needle (BD) into a 50ml tube. Cell extracts were passed three times through a 23 gauge needle and were then incubated on ice for 15 minutes. The samples were then divided into microcentrifuge tubes and 100μl (30% w/v) inactive Sepharose beads were added to each tube (G.E Healthcare), mixed by inverting twice, and left on ice for 15 minutes, occasionally inverting the tubes. Tubes were then spun at 13,000 rpm for 10 minutes at 4^{o}C. Corresponding supernatants were then first pooled before dividing them into the tubes containing the immunobeads; an

aliquot was kept as a total input control. The tubes were incubated on an end-over-end shaker at 4^{o}C for 2 hours. Finally, the immobeads were washed twice with PBS-0.5% Triton-X100 and once with PBS before adding 50µl 1.5x Laemmli sample buffer and heated at 70^{o}C for 10 minutes.

Fusion protein expression and purification

Preparation of pGEX-4T-3 fusion proteins for use in GST pull-downs

Fusion protein constructs were made in pGEX-4T-3. The plasmids were transformed into BL21pLysS competent *E-Coli* and plated on an LB agar plate containing 50µg/µl ampicillin and 34µg/µl chloramphenicol. The next day colonies were picked and inoculated in 100ml of LB containing ampicillin and chloramphenicol. The suspension cultures were incubated overnight at 37^{o}C. The next day, the bacterial cultures was spun at 6000 rpm for 15 minutes (using 250ml centrifuge tubes), and the pellets were then resuspended in 500ml of fresh LB containing ampicillin and 0.5mM IPTG. The cultures were then incubated on a shaker for 1-2 hours at 25^{o}C. The bacteria were then pelleted at 6000 rpm for 15 minutes at 4^{o}C, and extracted with 30ml of lysis buffer (PBS, 0.5% Triton X-100, 1mM DTT) containing protease inhibitors (50µg/ml benzamidine, 1mM PMSF, 10µg/ml aprotinin, 10µg/ml pepstatin A, 10µg/ml leupeptin and 1mM DTT). The samples were then left on ice for 30 minutes

before sonicating three times for 10 seconds. The sonicated samples were then centrifuged for 10 minutes in an SS-34 rotor at 10000 rpm (using 30ml centrifuge tubes). The samples were then divided into 5ml aliquots and frozen. To test protein induction, 300µl of extracts were added to 200µl lysis buffer and 40µl glutathione beads (30% slurry). The samples were then incubated on a rotator for 2 hours. Samples were then washed with PBS/0.5% Triton-X100 followed by PBS. The washed beads were resuspended in 1.5x sample buffer (50□l) and the samples were analysed by SDS- PAGE and Coomassie staining. The gels were then imaged on the Odyssey infrared imager (LI-COR).

pGEX-4T-3 fusion protein purification

To every 30ml of bacterial extract, 2ml of 30% slurry of glutathione beads were added and placed on a rotor shaker at 4^{o}C for two hours. The samples were then loaded into purification columns (Pierce) with filters that had been pre-equilibrated with lysis buffer. The columns were then washed with lysis buffer until eluates had an OD_{280} of 0.02 or smaller. The fusion proteins were then eluted with 1.5ml 25mM reduced glutathione in 10mM Tris pH 8.0. Three elutions were performed and collected in 2 ml tubes and OD_{280} was read. In cases where the three elutions were not efficient, 2 further elutions using SDS elution buffer (0.125ml SDS 10%, 9.5ml of water and 0.5ml of Tris 1M pH 8) were performed. The samples were then dialyzed against PBS at 4^{o}C for 24 hours. The dialysis buffer was changed twice during this time. The samples

were then split into small aliquots and frozen at -20^{o}C. An aliquot was analysed by SDS-PAGE, and concentrations were assessed with a BSA standard curve.

GST pull-down

Fusion protein sample supernatants were thawed on ice, and loaded onto 40μl glutathione Sepharose beads (30% w/v) and placed on a rocker for 2 hours. Lysates were prepared with extraction buffer (0.5% TX-100 and 1x PBS) as described above for immunoprecipitation. Fusion protein loaded beads were then washed three times with lysis buffer before incubating with the cell extracts for two hours on a an end-over-end shaker. Samples were washed and analysed by SDS-PAGE as described for immunoprecipitates.

Basic tissue culture techniques

Cell culture

Caco-2 (Human Epithelial Colorectal Adenocarcinoma), A431 (epidermoid carcinoma), HCE (Human Corneal Epithelial), and MDCK (Madin-Darby canine kidney) cells were cultured in DMEM (PAA) containing 10% Foetal Bovine Serum (FBS) (PAA) (20% FBS in the case of Caco-2 cells). Penicillin/streptomycin (PAA) was added to the media that contained 10 units/ml

of penicillin and 10μg/ml of streptomycin. Depending on the experiments, cells were grown in 6, 12, 24, 48 or 96-well plates (Nunc). Cells were passaged after detaching them by incubating with 0.05% Trypsin/EDTA (PAA) for 15 minutes in the incubator. For siRNA experiments cells were transfected at 20% confluence, and for transient transfections at 60% confluence.

Stable cell lines generation techniques

Picking clones

After transfection, the cells were split into 15-cm dishes and grown in medium containing the appropriate selection antibiotics (neomycin, 1μg/ml; and puramycin, 1μg/ml;). The cells were left to grow for a few weeks until the colonies reached a size of 0.5-1cm diameter. To pick the colonies, the cells were incubated with Trypsin/EDTA solution until they began to round up. The trypsin was aspirated and the plate left in the incubator at 37^{o}C for a further 5 minutes. Individual clones were then transferred to a 48-well plate. After picking the clones, the remainder of the cells were washed off with 6ml full media and plated in a 6 well dish. This represented the pool of clones.

Immunofluorescence techniques

Fixation techniques

Methanol fixation (-20^{o}C)

Cold methanol (-20^{o}C) (Fisher Scientific) was added to cells plated on glass coverslips, and the cells were transferred to -20^{o}C for 5 minutes. The methanol was discarded and the samples were rehydrated with PBS at room temperature. The PBS was then discarded and blocking solution (PBS/1% BSA /20mM glycine/0.1% NaN_3) was added for 15 minutes. Cells were stored in blocking solution or stained immediately.

Triton X-100 (0.1%) extraction/-20^{o}C methanol fixation

Cells were cooled on ice for 1 minute. Triton X-100 (Sigma) (0.1%) in BB buffer (100mM KCl, 3mM $MgCl_2$, 1mM$CaCl_2$, 200mM Sucrose and 10mM Hepes pH 7.1) was added and incubated for 1 minute on ice. The Triton-X100 solution was discarded and a standard -20^{o}C methanol fixation was carried out as explained above.

Paraformaldehyde fixation/0.3%Triton X-100 permeablisation

Paraformaldehyde (PFA) solution (3% in PBS) was added to the cells and left for 30 minutes at room temperature. The PFA solution was discarded and PBS containing 0.3% Triton X-100 and 0.3% BSA were added. After 5 minutes, the permeabilization solution was discarded and the cells were washed twice with blocking buffer. Samples were then stored in blocking buffer until they were stained with antibodies.

Staining of cells plated on coverslips

The selected primary antibodies were diluted in blocking solution and added to the fixed cells. The primary incubation was either at room temperature for 2 hours or at 4^{o}C overnight. The cells were washed three times in PBS and the fluorescent secondary antibodies, also diluted in blocking solution were added, the samples were left in the dark for 2 hours. The cells were then washed three times with PBS, and each well was filled with 1ml of PBS to facilitate removal of coverslips for mounting. The coverslips were mounted on slides (VWR) using Prolong Gold Antifade Mountant (Invitrogen).

Transfection techniques

Transfection using Lipofectamine 2000

Cells were trypsinizedand plated so that they were ~60% confluent on the day of transfection. For cells plated in 48 well dishes, 0.3µg of DNA was added per sample in 25µl OptiMem (PAA). A separate tube was prepared for the transfection reagent comprising per well 2µl Lipofectamine transfection reagent (Invitrogen) and 23µl OptiMem. The tubes were incubated at room temperature for 5 minutes. The diluted DNA and Lipofectamine 2000 samples were then combined and left at room temperature for another 20 minutes. During this time, 200µl DMEM containing 10% FBS was added to each well. The 50µl of Lipfectamine/DNA complexes were then added to the cells. After 4 hours, the transfection mix was aspirated and replaced with 350µl DMEM/10% FBS. Cells were analysed after 24 hours at 37^{o}C.

Transfection using jetPEI

Cells were trypsinized and plated so that they were ~60% confluent on the day of transfection. For cells plated in 48 well dishes, 0.5µg of DNA was added per sample in 25µl 150mM NaCl. A separate tube designated B was prepared for the transfection reagent comprising per well 1µl jetPEI transfection reagent (Polyplus) and 25µl 150mM NaCl. Both tubes were vortexed for 10 seconds.

Tube B was then added to the DNA containing tube and this tube was vortexed for 10 seconds before being left at room temperature for 20 minutes. During this time, 250µl DMEM containing 10% FBS was added to each well. The 50µl of jetPEI/DNA complexes were then added to the cells. Cells were analysed after 24 hours at 37^{o}C.

Calcium phosphate transfection

Cells were plated the day before transfection at 60% confluence in a 6-well plate. Plasmid DNA was precipitated by adding 10µg DNA to 200µl 2x Hepes buffer pH 7.1. To this 200µl $CaCl_2$ was added drop-wise while vortexing. The precipitate was formed by leaving the tube for 30 minutes at room temperature. The 400µl solution was then added to the cells after the medium had been aspirated. The cells were then incubated at 37^{o}C for 30 minutes and 3ml of full medium was added. The next day the medium was removed and a glycerol shock was performed for 2 minutes using 12.5% glycerol in DMEM containing 10mM Hepes (pH 7.4). Each well was rinsed once with 3ml PBS and 3ml full medium were added. Cells were left to express the specified protein for 48 hours at 37^{o}C.

siRNA transfection using Interferin

Cells were plated the day before transfection so that they were 20-30% confluent. The transfections were prepared by adding 0.5μl-1μl 20μM siRNA (Dharmacon) to 50μl OptiMem for each transfection in a 48-well plate. After 5 minutes, 1μl Interferin transfection reagent (Polyplus Transfections) was added, and the mix was vortexed for 10 seconds. After 20 minutes at room temperature, 200μl DMEM/10% FBS was added and mixed gently by inverting the tubes three times. The mix was added to the cells and left for 24 hours. Fresh medium was then added and the cells were cultured for a further 48-72 hours. If larger wells were transfected, the volumes used were proportionally increased. For all experiments requiring replating (i.e., FRET and Ca-switch assays), cells were transfected with siRNAs in 6-well plates.

Culture of Caco-2 epithelial cells in 3D cultures

For 3D morphogenesis, siRNA-transfected Caco-2 cells were plated on top of a layer of growth factor-reduced Matrigel (BD Biosciences) [137, 261]. Briefly, coverslips in 48-well plates were covered with 90μl of Matrigel (9.3mg/ml) and left to polymerise for 45 minutes. Then, 10,000 cells were plated in 300μl of low glucose medium containing 2% Matrigel. After 48 hours, the medium was replaced with fresh medium containing 2% Matrigel and 0.1μg/ml cholera toxin.

After another 48 hours, the medium was carefully replaced with fresh medium/Matrigel/cholera toxin mix. The samples were then fixed 10 hours later.

3D culture fixation and staining conditions

Cells were fixed using 3% paraformaldehyde. The samples were then washed twice with PBS for 5 minutes and incubated for 30 minutes with a BSA/SDS/Triton-X100 blocking solution (1% BSA, 0.1% NaN_3, 20mM glycine, 0.1% SDS and 1% Triton-X100 in PBS) to permeabilize. Cells were stained using blocking solution and primary antibody overnight at 4^oC. Cells were washed three times with PBS and once using blocking solution. Secondary antibody staining and washes were carried out as for the primary antibody. Cells were then mounted face up, Prolong Gold was added on top of the cells that were then covered with a 22mm x 22mm square coverslip, and sealed with superglue around the edges.

Cyst Quantification

Quantification of lumen size diameter was performed using the measuring tool in Image J. Only cysts that had reached a minimal size of 30µm diameter were considered for the morphological quantification to avoid bias because of the smaller cysts.

Calcium switch assays

Cells that had been transfected with siRNAs for 24 hours in 6-well plates were trypsinised for 20 minutes in order to ensure absence of cell-cell adhesion, and pipetted once to disperse. Cells from three wells were pooled for each experiment by resuspending them in 14ml of medium. The tubes were spun at 1000 rpm for 5 minutes, and the cells were resuspended in 6ml of low calcium medium (Sigma, spinner culture medium with 2mM glutamine/1mM sodium pyruvate), penicillin/streptomycin and 5% dialysed FBS. The cells were pelleted again and resuspended in low calcium medium. This was performed twice in order to remove the calcium. To the basolateral chamber of the Transwell plates, 1.5ml of low calcium medium was added. Cells were resuspended in 2.5ml low calcium medium for four filters or 3.6ml for six glass coverslips, and 600μl of samples were plated. The cultures were then incubated at 37^{o}C for 16-24 hours. Junction formation was then induced by carefully aspirating the low calcium medium and adding calcium containing medium (0.5ml into the apical chamber and1.5ml into the basolateral chamber of Transwell cultures; 600μl per 48 well). The cultures were then incubated at 37^{o}C for 30 minutes before starting to measure transepithelial electrical resistance (TER). TER was measured with a silver/silver-chloride electrode to determine the voltage deflection induced by an AC square wave current of ± 20 μA at 12.5 Hz using an EVOM (World Precision Instruments, Sarasota, FL). After 48 hours, paracellular permeability in the apical to basolateral direction was determined using 4kD FITC-conjugated Dextran (1mg/ml) and 70kD Rhodamine B-conjugated dextran (2mg/ml) over a time period of 3 hours. Fluorescence was

then determined with a FLUOstar OPTIMA microplate reader (BMGLabTech, Offenburg, Germany). Cells were removed at the indicated timepoints and fixed.

G-LISA Rho GTPase activation assay

Rho GTPase activities were determined using the G-LISA kit from Cytoskeleton Inc. (U.S.A). All names of buffers and components refer to reagents provided by the kit. Cells were washed on ice with cold PBS and immediately lysed in lysis buffer as recommended by the manufacturers of the kit. To a 96-well plate, 10μl of sample and 300μl of precision red solution were added, and protein concentrations were determined using a plate reader. Protein concentrations were subsequently equalised by the addition of lysis buffer. For Cdc42, 0.25mg/ml was used, and for RhoA and Rac1 1mg/ml. The extracts were added to specific Rho GTPase assay wells and left at 4^{o}C on a rocker at 300 rpm. Incubation times were 15 minutes for Cdc42 and 30 minutes for Rac1. The samples were then washed twice with wash buffer and vigorously tapped onto a tissue to remove residual buffer that may cause background. To the wells 200μl of antigen presenting buffer was then added and left for 2 minutes. The samples were then washed three times with wash buffer, again removing residual buffer by tapping onto a tissue. Primary antibody was prepared and added to the wells. The plates were left at room temperature on a rocker at 300 rpm as indicated by the manufacturer's protocol. Samples were washed three times with wash buffer and vigorously patted in between each wash. The secondary HRP-conjugated antibody was added to the cells, followed again by incubating

the plate at room temperature on a rocker as indicated in the protocol. After incubation the samples were then washed three times with wash buffer, removing residual buffer each time by tapping onto a tissue. HRP bound to the wells was then measured colourimetrically using the substrates and buffers provided by the kit.

Fluorescence resonance energy transfer (FRET)

For FRET experiments, siRNA transfected cells were plated into *ibidi* 8-well chamber slides. After 48 hours, the cells were transfected with pRaichu-Cdc42 plasmid [262]. After another 24 hours, FRET signal distribution was analysed using a Leica SP2 microscope (63x/1.4 objective, 37^{o}C, in medium with 10 mM Hepes, pH 7.4) and Leica LCS FRET software using the donor recovery after acceptor bleaching protocol. Bleaching of the YFP signal was set to 30%. The shown FRET efficiency maps were then generated using the Leica LCS software by calculating the FRET efficiency according to the formula $[(D_{post}-D_{pre})/D_{post}]*100$ (D represents donor intensity). For quantification, CFP images were subtracted and mean FRET intensities were quantified with ImageJ. For each image, all cell-cell contacts were quantified and as many internal areas; averages of all cell-cell contacts and all internal areas in a field then gave one value each per imaged field, and these values were used for the final statistical analysis. Normalisations were performed by dividing mean values obtained for specific fields by the mean values obtained for the entire field imaged.

siRNA library screen

Caco-2 cells were used for the siRNA screen. The cells were seeded onto glass coverslips in 48-well plates so that they reached 20-30% confluence after 20 hours (~20,000 cells/well). Cells were seeded onto glass coverslips and the following day transfected as indicated using the standard Interferin transfection method described above. Each siRNA was transfected into cells on three coverslips in different plates. After 24 hours, the medium was replaced, and after another 48 hours in culture the cells were fixed with the methanol protocol. The cells were then processed for immunofluorescence and analysed by epifluorescence microscopy. The phenotypes were assessed qualitatively and divided into three groups according to the severity of the phenotype: strong, mild, and normal. The screen was first performed with a pool of siGenome siRNAs targeting Rho GTPases and GAPs (Dharmacon). Identified hits from the primary screen were then assayed again using chemically modified siRNAs that are thought to exhibit less off-target effects (Dharmacon).

Microscope methodology

All epifluorescent images of fixed specimens were acquired with a Leica DMIRB fluorescent microscope using a 63x/1.4 oil immersion objective fitted with a Hamamatsu C4742-95 camera and simple PCI software. Confocal images were acquired with a Zeiss LSM 700 confocal laser scanning microscope or a Leica SP2 confocal microscope using 63x/1.4 immersion oil objectives. Zeiss 518F

immersion oil was used for all objectives. Images were acquired at ambient temperature using ZEN 2009 or Leica LCS, respectively. Images were adjusted for brightness and contrast with Adobe Photoshop. Time-lapse movies of A431 cells expressing a EGFP-actin construct were recorded at 37^{o}C using a Zeiss Axiovert 200M microscope with a 40x/0.6 objective and a Hamamatsu C4742-95 camera. Movies were acquired with simple PCI software, recording images every 5 seconds.

Statistical analysis

Averages and standard deviations were calculated and provided in the graphs. Respective n values are provided in the figure legends. The indicated p values were obtained with two-tailed Student's t-test.

Antibody specificity

All secondary fluorescent antibodies were tested in the laboratory, in order to rule out non specific staining and possibility of bleed through the channels. Therefore potential for staining patterns to be non specific is unlikely.

Antibodies

Antibodies used are listed in alphabetical order in table 2.4 with the host species in which they were raised, where they were sourced from, and the dilutions/concentrations used for immunfluorescence (IF), immunoblotting (IB) and immunoprecipitation (IP). 'Poly' refers to polyclonal antibodies. Table 2.5 shows the corresponding secondary antibodies used.

Antibody	**Host Species**	**Clone number**	**Source**	**IB Dilution**	**IF Dilution**	**IP Dilution (ug)**
Alpha-tubulin	*Mouse*	*1A2*	*Matter Lab*	*1:20*	*-*	*-*
Alpha-catenin	*Rabbit*	*Poly*	*Sigma*	*1:2000*	*1:1000*	*3*
Beta-actin	*Mouse*	*AC-74*	*Sigma*	*-*	*1:2000*	*-*
Beta-catenin	*Rabbit*	*Poly*	*Sigma*	*1:2000*	*1:1000*	*3*
CapZα1	*Mouse*	*7*	*Santa Cruz*	*1:100*	*1:50*	*-*
CD2AP	*Mouse*	*B4*	*Santa Cruz*	*1:1000*	*1:200*	*3*
Cdc42	*Mouse*	*P1*	*Santa Cruz*	*1:500*	*-*	*-*
Cdc42-GTP	*Mouse*	*Mono*	New East Bioscience	-	*1:100*	*-*
Cingulin	*Rabbit*	*H-180*	*Santa Cruz*	*1:1000*	*1:500*	*-*
Cofilin	*Mouse*	*Mono*	*BD*	*1:500*	*-*	*-*

DPPIV	*Mouse*	*3/775/42*	*Matter Lab*	*-*	*1:500*	*-*
E-cadherin	*Mouse*	*Mono*	*BD*	*1:1000*	*1:500*	*3*
Erk 1/2	*Rabbit*	*Poly*	*Cell Signalling*	*1:1000*	*-*	*-*
GP73	*Rabbit*	*Poly*	*Matter Lab*	*-*	*1:500*	*-*
GST	*Rabbit*	*AH*	*Matter Lab*	*1:1000*	*-*	*-*
HA tag	*Mouse*	*Mono*	*Matter Lab*	*1:5*	*1:10*	*-*
HA tag	*Rabbit*	*4325*	*Matter Lab*	*-*	*1:500*	*-*
HA tag	*Rat*	*Mono*	*Roche*	*1:2000*	*1:1000*	*-*
JACOP	*Rabbit*	*H-188*	*Santa Cruz*	*1:1000*	*1:400*	*-*
JACOP	*Rabbit*	*Poly*	*Furuse*	*-*	*-*	*3*
Na^+K^+ Pump	*Mouse*	*Mono*	*Matter Lab*	*-*	*1:500*	*-*
Occludin	*Mouse*	Mono	*Invitrogen*	*1:2000*	*1:1000*	*3*
OPHN1	*Rabbit*	*H-100*	*Santa Cruz*	*-*	*1:200*	*-*
p120 catenin	*Mouse*	*Mono*	*BD*	*1:1000*	*1:500*	*3*
Phospho Cofilin	*Rabbit*	*Poly*	*Cell Signalling*	*1:500*	*-*	*-*
Phospho Erk 1/2	*Mouse*	*Mono*	*Cell Signalling*	*1:1000*	*-*	*-*
Rac1-GTP	*Mouse*	*Mono*	New East Bioscience	*-*	*1:100*	*-*
SH3BP1	*Goat*	*Poly*	*Everest*	*1:1000*	*1:200*	*3*

Trio	*Rabbit*	*Poly*	*Matter Lab*	*-*	*-*	*3*
ZO-1	*Mouse*	*Mono*	*Invitrogen*	*1:2000*	*1:1000*	*3*
ZO-1	*Rabbit*	*4913*	*Matter Lab*	*1:1000*	*1:300*	*3*
ZO-2	*Rabbit*	*4915*	*Matter Lab*	*1:1000*	*1:300*	*3*
ZO-3	*Rabbit*	*4917*	*Matter Lab*	*1:1000*	*1:300*	*3*

Table 2.4 List of primary antibodies used during project.

Antibody (Host species)	**Target Species**	**Source**	**IB Dilution**	**IF Dilution**
A488 (Donkey)	*Rabbit*	*Invitrogen*	*-*	*1:300*
A488 (Donkey)	*Rabbit*	*Invitrogen*	*-*	*1:300*
A488 (Donkey)	*Mouse*	*Invitrogen*	*-*	*1:300*
A555 (Donkey)	*Mouse*	*Invitrogen*	*-*	*1:300*
A555 (Donkey)	*Rabbit*	*Invitrogen*	*-*	*1:300*
A545 (Donkey)	*Goat*	*Invitrogen*	*-*	*1:300*
Horseradish peroxidase (Goat)	*Mouse*	*Jackson Immunoresearch*	*1:3000*	*-*
Horseradish peroxidase	*Rabbit*	*Jackson Immunoresearch*	*1:3000*	*-*

(Goat)				
Horseradish peroxidase (Donkey)	*Goat*	*Jackson Immunoresearch*	*1:3000*	*-*
FITC (Donkey)	*Rabbit*	*Jackson Immunoresearch*	*-*	*1:300*
FITC (Donkey)	*Mouse*	*Jackson Immunoresearch*	*-*	*1:300*
FITC (Donkey)	*Goat*	*Jackson Immunoresearch*	*-*	*1:300*
FITC (Donkey)	*Sheep*	*Jackson Immunoresearch*	*-*	*1:300*
FITC (Donkey)	*Rat*	*Jackson Immunoresearch*	*-*	*1:300*
Cy3 (Donkey)	*Mouse*	*Jackson Immunoresearch*	*-*	*1:300*
Cy3 (Donkey)	*Rabbit*	*Jackson Immunoresearch*	*-*	*1:300*
Cy3 (Donkey)	*Goat*	*Jackson Immunoresearch*	*-*	*1:300*
Cy5 (Donkey)	*Mouse*	*Jackson Immunoresearch*	*-*	*1:300*
Cy5 (Donkey)	*Rabbit*	*Jackson*	*-*	*1:300*

		Immunoresearch		
Cy5 (Donkey)	*Goat*	*Jackson Immunoresearch*	*-*	*1:300*
Infrared 680 (Donkey)	*Rabbit*	*LI-COR*	*1:10000*	*-*
Infrared 680 (Donkey)	*Mouse*	*LI-COR*	*1:10000*	*-*
Infrared 680 (Donkey)	*Goat*	*LI-COR*	*1:10000*	*-*
Infrared 800 (Donkey)	*Rabbit*	*LI-COR*	*1:10000*	*-*
Infrared 800 (Donkey)	*Mouse*	*LI-COR*	*1:10000*	*-*
Infrared 800 (Donkey)	*Goat*	*LI-COR*	*1:10000*	*-*

Table 2.5 List of secondary antibodies used during project.

siRNA Oligonucleotides

Tables 2.6-2.10 are a complete list of siRNAs used and their corresponding targets. The siRNAs were purchased from Dharmacon. The pools used comprise four individual oligonucletides used as a pool during the screen, or two distinct siRNAs in the case of SH3BP1 and CD2AP for further validation.

Gene	**Accession Number**	**Sequence**
CDC42	NM_001791	GGAGAACCAUAUACUCUUG
CDC42	NM_001791	GAUUACGACCGCUGAGUUA
CDC42	NM_001791	GAUGACCCCUCUACUAUUG
CDC42	NM_001791	CGGAAUAUGUACCGACUGU
RAC1	NM_018890	CGGCACCACUGUCCCAACA
RAC1	NM_018890	AGACGGAGCUGUAGGUAAA
RAC1	NM_018890	UAAGGAGAUUGGUGCUGUA
RAC1	NM_018890	UAAAGACACGAUCGAGAAA
RAC2	NM_002872	GAGAUGGGGCCGUGGGCAA
RAC2	NM_002872	CAGCCAAUGUGAUGGUGGA
RAC2	NM_002872	CCAAUGUGAUGGUGGACAG
RAC2	NM_002872	ACAAGGACACCAUCGAGAA
RAC3	NM_005052	AAACUGACGUCUUUCUGAU

RAC3	NM_005052	GGAGAUUGGCUCUGUGAAA
RAC3	NM_005052	ACGUGAUGGUGGACGGGAA
RAC3	NM_005052	CGAGAAUGUUCGUGCCAAG
RHOA	NM_001664	AUGGAAAGCAGGUAGAGUU
RHOA	NM_001664	GAACUAUGUGGCAGAUAUC
RHOA	NM_001664	GAAAGACAUGCUUGCUCAU
RHOA	NM_001664	GAGAUAUGGCAAACAGGAU
RHOB	NM_004040	GCAUCCAAGCCUACGACUA
RHOB	NM_004040	ACACCGACGUCAUUCUCAU
RHOB	NM_004040	CAUCCAAGCCUACGACUAC
RHOB	NM_004040	CAACUGCUGCAAGGUGCUA
RHOBTB1	NM_014836	AAAUGAAGCUGCCUGUUUA
RHOBTB1	NM_014836	GAACUUGGCUUACCAUACU
RHOBTB1	NM_014836	GGACGUGACAUUUAAAUUG
RHOBTB1	NM_014836	GAACACCCGUUAUCCUUGU
RHOBTB2	NM_015178	UGACAUGGAUUAUGAAAGG
RHOBTB2	NM_015178	GACCGUCGCUUUGCUUAUG
RHOBTB2	NM_015178	CCCGAGACGUGGUAGAUGA
RHOBTB2	NM_015178	GGACAACGCCGUGGGUAAG
RHOBTB3	NM_014899	ACAGAUGGCCGUCGAAUAU
RHOBTB3	NM_014899	GUAAUUACAUGGAAGCAAA

RHOBTB3	NM_014899	CAACCUGGCUACUUCAUUU
RHOBTB3	NM_014899	CAACGUUAAUGACAAGUUU
RHOC	NM_175744	GGAGAGAGCUGGCCAAGAU
RHOC	NM_175744	AUAAGAAGGACCUGAGGCA
RHOC	NM_175744	GGAUCAGUGCCUUUGGCUA
RHOC	NM_175744	GAGAGCUGGCCAAGAUGAA
RHOD	NM_014578	UGAACAAGCUCCGAAGAAA
RHOD	NM_014578	GAUUGGAGCCUGUGACCUA
RHOD	NM_014578	CCGAACAGCUUUGACAACA
RHOD	NM_014578	AGACGUCGCUGCUGAUGGU
RHOF	NM_019034	GGGAGAAUGUGGAGGACGU
RHOF	NM_019034	CGGCCGGGCAAGAAGACUA
RHOF	NM_019034	AGAUCGUGAUCGUGGGCGA
RHOF	NM_019034	ACGACAACGUCCUCAUCAA
RHOG	NM_001665	CUACACAACUAACGCUUUC
RHOG	NM_001665	CCAGUCCGCCGUCCUAUGA
RHOG	NM_001665	GCAACAGGAUGGUGUCAAG
RHOG	NM_001665	CGUCAUCUGUUUCUCCAUU
RHOH	NM_004310	CAAGUGGAUUGGUGAAAUU
RHOH	NM_004310	GAGUACAGCAGGUGUUUGA
RHOH	NM_004310	GCUCAGCCCUUAGCAAUCG

RHOH	NM_004310	GGCCAACCAUAACUCAUUC
RHOJ	NM_020663	AGAAACCUCUCACUUACGA
RHOJ	NM_020663	CCACUGUGUUUGACCACUA
RHOJ	NM_020663	UCGUAAACCCUGCCUCUUA
RHOJ	NM_020663	CCCGUUUGCUGUAUAUGAA
RHOQ	NM_012249	UACCGGAACUUAAGGAAUA
RHOQ	NM_012249	AGAAUAGGAUCAAGAUGUA
RHOQ	NM_012249	UAGCAAGACUGAAUGAUAU
RHOQ	NM_012249	GAACAAGGACAGAAACUAG
RHOT1	NM_018307	GAACUCAACUUCUUUCAGA
RHOT1	NM_018307	GAACCAGUAUACAGAAAUA
RHOT1	NM_018307	GAACAUAUCAGAGCUCUUU
RHOT1	NM_018307	CAGAAUACCUUGCUUAAUC
RHOT2	NM_138769	UCUCAGAGCUGUUCUACUA
RHOT2	NM_138769	ACGAAGAGCUCAACGCUUU
RHOT2	NM_138769	GGACGUGCGCAUCCUGUUA
RHOT2	NM_138769	GAGAAGAUUCGAACUAAGU
RHOU	NM_021205	GUACUGCUGUUUCGUAUGA
RHOU	NM_021205	GAACGUCAGUGAGAAAUGG
RHOU	NM_021205	CAGAGAAGAUGUCAAAGUC
RHOU	NM_021205	AAGCAGGACUCCAGAUAAA

RHOV	NM_133639	GAGGGACGAUGUCAACGUA
RHOV	NM_133639	GAAGAAACUGAAUGCCAAA
RHOV	NM_133639	GUAUUUGACUCGGCUAUUC
RHOV	NM_133639	GCUCAGCCUUGACGCAGAA
RND1	NM_014470	CGACUCGGAUGCAGUAUUA
RND1	NM_014470	GAACAGAGGGUGGAGCUUA
RND1	NM_014470	GCCAAAAGCUGUUCCAUUA
RND1	NM_014470	GAACUCAUCUCUUCUACCU
ARHN	NM_005440	GAACUACACUGCGAGCUUU
ARHN	NM_005440	GACAUUAGCCGACCAGAAA
ARHN	NM_005440	ACACAAGGAUCGAGCCAAA
ARHN	NM_005440	UCAGGGAUGUCUUCCAUGU
ARHE	NM_005168	AGAAUUACACGGCCAGUUU
ARHE	NM_005168	GAACGUGAAAUGCAAGAUA
ARHE	NM_005168	GAAAUUAUCCAGCAAAUCU
ARHE	NM_005168	UAGUAGAGCUCUCCAAUCA

Table 2.6: Primary screen (siGenome siRNAs) for Rho GTPases

Gene	Accession Number	Sequence
ABR	NM_001092	GAAGAUCUCUGCCCUCAAG
ABR	NM_001092	CAACCUGGCUACCGUGUUU
ABR	NM_001092	GAAGAGAUCUACAUUAACC
ABR	NM_001092	CAGAGGAACUCAAAGUGAA
ARHGAP1	NM_004308	GCCAAGUGCUCAAAUAUGA
ARHGAP1	NM_004308	GGAGACUGUUGCCUACUUA
ARHGAP1	NM_004308	GGCAGGAGAUGACAAGUAU
ARHGAP1	NM_004308	GAUCUGACCUUGGAUGACA
FLJ20896	NM_024605	GUGAAACACUUAACAAAUG
FLJ20896	NM_024605	GAAGUGAAGACAAUAACAA
FLJ20896	NM_024605	GGAGAAUUCUGCAGAUUGG
FLJ20896	NM_024605	GAAUAUUGUUGUGGAAAUC
ARHGAP11A	NM_014783	UACAGACUCUUAUCGAUUA
ARHGAP11A	NM_014783	GUUCGAAGAUCUCUGCGUU
ARHGAP11A	NM_014783	GGUAUCAGUUCACAUCGAU
ARHGAP11A	NM_014783	AAGCGUACAUUGCCAGUAG
ARHGAP15	NM_018460	GAAAUGAGUUCCUUCUACA
ARHGAP15	NM_018460	GAUGCAAUAUAUCGAGUUA
ARHGAP15	NM_018460	GAACCUAUAUCCAGACACA

ARHGAP15	NM_018460	GCACUGAAUUGCUAAGUCA
ARHGAP17	NM_018054	GCAGACAUGUACAACUUUA
ARHGAP17	NM_018054	AAACAGAAGUCCUUAGUGA
ARHGAP17	NM_018054	GGGAGCAGCUUGCAAGAUU
ARHGAP17	NM_018054	CUGAAGAGGUGGAAUUUAA
ARHGAP18	NM_033515	GGAAACAGAAGGCCUCUUA
ARHGAP18	NM_033515	UGACAGCGCUAUUAGAACA
ARHGAP18	NM_033515	CGAGGCAUCUAACCUUGUU
ARHGAP18	NM_033515	CCAUGCACUUAUUGAUUAA
ARHGAP20	NM_020809	GCACUCACCUGGACAACUU
ARHGAP20	NM_020809	GCUCAUUAAUCAGAGUUUA
ARHGAP20	NM_020809	GAAUUGUGCCUACUCUAAA
ARHGAP20	NM_020809	CCAUCCGGCUCAUCAGUAA
ARHGAP21	NM_020824	UAAAGAAGCUGUCAUCCUA
ARHGAP21	NM_020824	GGAGACAGCUCUUCAGUUC
ARHGAP21	NM_020824	AAAGGAAACUUCUCAGUAA
ARHGAP21	NM_020824	GUAAAUCACUUGCAUCAGA
ARHGAP22	NM_021226	CUAGGAAGCUUGACUGUUG
ARHGAP22	NM_021226	GGGAUCAGCUUUUCUACUA
ARHGAP22	NM_021226	AUUACAACCUGCUCAGAUA
ARHGAP22	NM_021226	GGGAUUUAUUUCUCUACAA

ARHGAP23	XM_290799	GAAGACGGCCCUGCCCAUA
ARHGAP23	XM_290799	GGAACGAGCCGUAUUCUGG
ARHGAP23	XM_290799	GGGAAAGCGUCAUUGGGAA
ARHGAP23	XM_290799	GAAUGGAGGCCGUGGAGGA
ARHGAP24	NM_031305	AGAACAAGCUGGAGAGUUA
ARHGAP24	NM_031305	GGAGGAUACUGUUCGUUAU
ARHGAP24	NM_031305	CGAGAGAGGAAACACAAUA
ARHGAP24	NM_031305	GGUCUUUGGUCCUAAUAUC
ARHGAP25	XM_376060	GGACUUCCACCUACGAUAA
ARHGAP25	XM_376060	GAUCAGAGACCAUGAAGUC
ARHGAP25	XM_376060	GCAGGUUCCUACAUGAAAU
ARHGAP25	XM_376060	CAAGAGCUACGAAAGGAAA
ARHGAP26	NM_015071	GAACAUGACUCAGAACUUU
ARHGAP26	NM_015071	CCAAACAGCAUCCUUAAUU
ARHGAP26	NM_015071	CAUAGGAGAUGCAGAAACA
ARHGAP26	NM_015071	GAAAGAAUCUCAGCUUCAG
LOC201176	NM_199282	CCGAGUCGCUGACCAGUUA
LOC201176	NM_199282	GAAAGCGGCUCCGGAAGAA
LOC201176	NM_199282	GGACUCCUCUGUUCGAUGG
LOC201176	NM_199282	GCACUUCCGCCAGUUCAUU
ARHGAP28	NM_001010000	GAAGCAAACACUCUGAUUA

ARHGAP28	NM_001010000	CCAUUCAACUCAACAAUCA
ARHGAP28	NM_001010000	GAAUAUAUACCUGCCUUCA
ARHGAP28	NM_001010000	GUGAAGAACUUGAUGCCAA
ARHGAP4	NM_001666	CGCAAGAGCUCCCUCAAGA
ARHGAP4	NM_001666	GCUGAGAUCUGCGUUGAAA
ARHGAP4	NM_001666	GGAGACAUGGAGAAGUUUA
ARHGAP4	NM_001666	GACAGACCAUUGAGACAGA
ARHGAP5	NM_001173	GUACGAAUUUGCAACCAUA
ARHGAP5	NM_001173	UGAAAGCGCUCGUUCCAAA
ARHGAP5	NM_001173	GAGAGCAGAUUUCCAGUUA
ARHGAP5	NM_001173	UGAGAUCACUGCUAAAUUU
ARHGAP6	NM_001174	AAACUUAGCCACCAUAUUU
ARHGAP6	NM_001174	GUACACAGCUUUCAUCAAC
ARHGAP6	NM_001174	GAAACUGGAUUCACUAGGA
ARHGAP6	NM_001174	CAUCAUCGCUGUUGUGCAA
ARHGAP8	NM_181334	ACAAGGAGUUCGAUAGGAA
ARHGAP8	NM_181334	GAUAGGAAGUACAAGAAGA
ARHGAP8	NM_181334	GCAUACAAGGAGUUCGAUA
ARHGAP8	NM_181334	CCGUGAACUUUGACGACUA
ARHGAP9	NM_032496	GAACAAUGAUGUCCUGCAA
ARHGAP9	NM_032496	GAAGAGACCGCCCUUACAA

ARHGAP9	NM_032496	GAAGGUCGGUUAGAUUUGG
ARHGAP9	NM_032496	GGGCCGAAGUUGUUUCAUG
BCR	NM_004327	GUAAAGCUCUCGGUCAAGU
BCR	NM_004327	GCAUUCCGCUGACCAUCAA
BCR	NM_004327	CAGGAGCGCUUCCGCAUGA
BCR	NM_004327	CAGAAGAAGUGUUUCAGAA
CENTD1	NM_015230	GCAAGAAGCUUUAAAUUGA
CENTD1	NM_015230	GAACCCGACUGUAGUAUUA
CENTD1	NM_015230	GAUGGAAGCAGAAGAAUUA
CENTD1	NM_015230	CAAAGAGGACUUCUAUUUA
CENTD2	NM_015242	GAGAAGGAGUGGCCUAUUA
CENTD2	NM_015242	GCAGGGAUCUUACAUCUAU
CENTD2	NM_015242	GGAGAUCACUGCCAUUGUG
CENTD2	NM_015242	ACAAGAAUCUAGAGGAGUA
CENTD3	NM_022481	GAACUUGGCUCUGCUGUUU
CENTD3	NM_022481	GGAGGAGUCUGAUGUACUU
CENTD3	NM_022481	GGAGAAAUAUAAAGAUGUG
CENTD3	NM_022481	CCAGACAGCUCCCAAAUCU
CHN1	NM_001822	GAAUAUAGACCUCCUGUUU
CHN1	NM_001822	UAUGAGAUCUCCAGAACUA
CHN1	NM_001822	CAAUUCCACUCAUUACAUA

CHN1	NM_001822	GACCUACACUUUGGCUUUA
CHN2	NM_004067	UCAAGAAAGUGUACUGUUG
CHN2	NM_004067	GAAGAGGUUUGAGUCGAUU
CHN2	NM_004067	UGAUAACACUGUACAUAGA
CHN2	NM_004067	CGAUAUAUCUGCCAAUGUC
DLC1	NM_006094	UUAAGAACCUGGAGGACUA
DLC1	NM_006094	GUACGAAAGAGGAGCGUUU
DLC1	NM_006094	UUAAAGAAGUCAAAGAGAA
DLC1	NM_006094	GCAUGUACUUAGAGGGCUU
GMIP	NM_016573	GAACUGGACUUGCGGCUCA
GMIP	NM_016573	GAACGUGACCCUUGAGAUG
GMIP	NM_016573	GAAGUGCACGGCUGAGAUA
GMIP	NM_016573	CGAGUGUCCUCAAGCGAUU
GRLF1	NM_024342	UCAGCGAGAUCCAAUGUAA
GRLF1	NM_024342	GGAGGAAUCUGUAUACAUG
GRLF1	NM_024342	GAACAGCGAUUUAAAGCAU
GRLF1	NM_024342	GAUGGGCUGUCUUUCAUUA
INPP5B	NM_005540	GAAGAGGAUUACACCUAUA
INPP5B	NM_005540	GCAUCUGCGUUGUGAAUUC
INPP5B	NM_005540	ACUUGGAGCUCUUCGUAAA
INPP5B	NM_005540	AACAGGAGCAUGCAGCUUA

MYO9A	NM_006901	GAAAGAAGCUUAGCCCUUA
MYO9A	NM_006901	GAUAAUACCUGCUGCAUAA
MYO9A	NM_006901	GAACAUACAUUACGGAUAU
MYO9A	NM_006901	GAACAAAGGCUAAGAGAAA
MYO9B	NM_004145	GAACCGAAAUGUCAAGAUU
MYO9B	NM_004145	CCAAGUACGUGAAGAUGUA
MYO9B	NM_004145	GCUCUCAGGUCGACUCUAA
MYO9B	NM_004145	GCAAAGCUCAGAAGAAGAA
NF1	NM_000267	CACCGAGUCUUACAUUUAA
NF1	NM_000267	GGAAUAAGAUGGUAGAAUA
NF1	NM_000267	GAUAGAAGCUACAGUAAUA
NF1	NM_000267	CAACAAAGCUAAUCCUUAA
OCRL	NM_000276	GAAAUUACCUCCCAAGUUG
OCRL	NM_000276	UGAAAUCCCUGAUGAGGAA
OCRL	NM_000276	UGACAUAGCUUCUAACAGU
OCRL	NM_000276	GAAAGGAUCAGUGUCGAUA
OPHN1	NM_002547	GAAAGAAUCUCAGUUACAA
OPHN1	NM_002547	GCGAGAGGCUCAAGUGUUA
OPHN1	NM_002547	GAACAUAGUGGUGGAAAUA
OPHN1	NM_002547	GCUAGUGAUUUGCUGAUUA
PLXNA1	NM_032242	GAACGUGCCUGACCUCUCA

PLXNA1	NM_032242	GCAGAUCGAUGACGACUUC
PLXNA1	NM_032242	GCAGUGAACCGCAUCUAUA
PLXNA1	NM_032242	GCACCAACCUGGCCACUGU
PLXNB1	NM_002673	GAGAGGAGCCGACUACGUA
PLXNB1	NM_002673	GCAGAGACCUCACCUUUGA
PLXNB1	NM_002673	GCAAACAUCUGAUAACAUG
PLXNB1	NM_002673	UCACAGACCUCAUGACUGA
PLXNB2	XM_371474	GCAACAAGCUGCUGUACGC
PLXNB2	XM_371474	ACCAAUACACGCAGAAGUA
PLXNB2	XM_371474	UGAACACCCUCGUGGCACU
PLXNB2	XM_371474	CGGCAGAUGGUGCAGGUCA
RACGAP1	NM_013277	CAAAUUAUCUCUGAAGUGU
RACGAP1	NM_013277	CCACAGACACCAGAUAUUA
RACGAP1	NM_013277	GAACAUCAGCUUCUCAAGA
RACGAP1	NM_013277	GUAAUCAGGUGGAUGUAGA
RALBP1	NM_006788	GAAUGUAACUAUCUUCUGA
RALBP1	NM_006788	GAUCAGCCCUACUAAGUUU
RALBP1	NM_006788	GAACGAAGAGCUGGAAAUA
RALBP1	NM_006788	GAAGGCAUCUACAGAGUAU
SH3BP1	NM_018957	GACCUGUACCACUUUGUUA
SH3BP1	NM_018957	GAUGACAGCCACCCACUUC

SH3BP1	NM_018957	CAUCGAGGCCUGCGUCAUG
SH3BP1	NM_018957	GAGCGCAGACACCCUCUUC
SRGAP1	NM_020762	CAUGAGGGCUUAGACAUUA
SRGAP1	NM_020762	UUAACGAUCUGAUUUCUUG
SRGAP1	NM_020762	GACCAGAGUAACCAUGAUA
SRGAP1	NM_020762	GCAAUACACGGGCUUCAAU
SRGAP2	XM_059095	GAGACUACCUCGGUUGAAG
SRGAP2	XM_059095	GGAAAGGACAGGCUGAGUA
SRGAP2	XM_059095	CCAAAGAAGGGCCAGAUAA
SRGAP2	XM_059095	GCGGACAGAUUGCAGUCUA
SRGAP3	NM_014850	CCAAUGAGCUCUACACAGU
SRGAP3	NM_014850	GCACGGCUCUGCACGAGUU
SRGAP3	NM_014850	GAAUAUGAAGCCCAAAUAA
SRGAP3	NM_014850	CAGAACUGCUCAUGCGUUA
STARD13	NM_052851	GAUGUGAACUUCCAAAGGA
STARD13	NM_052851	CCAAGGCACUUUCUAUUGA
STARD13	NM_052851	GGGCAACUUUCCACACUUA
STARD13	NM_052851	GAAAGUUCCCGACUACAAA
STARD8	NM_014725	GAAGAAGGACACUCCAUUU
STARD8	NM_014725	CGACGUGGCUGACCUGCUA
STARD8	NM_014725	GAACCUGCGUCAAAUGAAU

STARD8	NM_014725	GAACCCACCUUUGCCUCUA
TAGAP	NM_054114	UGAAACAGGUUGCAGAUAA
TAGAP	NM_054114	GACCAGAGCCUGUCAUUUG
TAGAP	NM_054114	ACACUAAACGCCAAUAAUA
TAGAP	NM_054114	AGAAGGACCUGAACAACAA

Table 2.7: Primary screen (siGenome siRNAs) for GTPase Activating Proteins (GAPs).

Gene	Sequence
Rho GTPases	
CDC42	CGGAAUAUGUACCGACUGU
CDC42	GCAGUCACAGUUAUGAUUG
CDC42	GAUGACCCCUCUACUAUUG
CDC42	CUGCAGGGCAAGAGGAUUA
RAC1	GUGAUUUCAUAGCGAGUUU
RAC1	GUAGUUCUCAGAUGCGUAA
RAC1	AUGAAAGUGUCACGGGUAA
RAC1	GAACUGCUAUUUCCUCUAA
RHOA	CGACAGCCCUGAUAGUUUA

RHOA	GACCAAAGAUGGAGUGAGA
RHOA	GCAGAGAUAUGGCAAACAG
RHOA	GGAAUGAUGAGCACACAAG
RHOBTB1	GAACUUGGCUUACCAUACU
RHOBTB1	GGACGUGACAUUUAAAUUG
RHOBTB1	GAACACCCGUUAUCCUUGU
RHOBTB1	GACAGACGCUUUGCAUAUG
RHOBTB3	ACAGAUGGCCGUCGAAUAU
RHOBTB3	CCGGAAAUGUCGUUGCUUA
RHOBTB3	GAAGAGUCCCACUGACAUU
RHOBTB3	CCAUGAACCUUGAUAUAGU
RHOQ	CACCUAGAAUGUAAGUUAA
RHOQ	GCAGUUGGUCCCUAAGUGA
RHOQ	GAGCGACAACUUAUAUACA
RHOQ	GUAAUAAGGUCAUAACUGC

Table 2.8: Secondary screen (on-Target plus siRNAs) for Rho GTPases.

Gene	**Sequence**
GAPS	

MYO9A	GAACAUACAUUACGGAUAU
MYO9A	CUCCAAAGGCUAAGCGCAA
MYO9A	AAACAAUGGCUUCGAGAUU
MYO9A	GCGUAUUCGUCGAGGAAAC
MYO9B	CCAAGUACGUGAAGAUGUA
MYO9B	GCUCUCAGGUCGACUCUAA
MYO9B	CAGGGAAGGUGAAAUAUCA
MYO9B	UGAAACCCUUCUAGUCGUA
OPHN1	GAAAUGGGCUUUAGGAAUA
OPHN1	CAACAUGGGAGUAAUCUUU
OPHN1	CUAGUGAUUUGCUGAUUAA
OPHN1	GUAUAUAAGCUACCAGAAA
PLXNA1	GGACAUAUGCCAUGCGGGU
PLXNA1	CAUGAUUGUGCUAGCGUUU
PLXNA1	CGUCCAAGAUCGUGCGGCU
PLXNA1	GGAAGAAGUUUGCGUCUGU
PLXNB1	GCUCAGAUUUGGCGCUGUU
PLXNB1	UCAGAGAGGAUGUGGAGUA
PLXNB1	CUGAGGUUCUGGAUCAAUA
PLXNB1	GAGAGGAGCCGACUACGUA

SH3BP1	UGGAGAUUCAGGCCGAUUA
SH3BP1	GAGGGAGAACCACGGCCAA
SH3BP1	UCCAGAAGCUCGUGUCCGA
SH3BP1	GCCCAGUCUCUUUGAGUAA
SRGAP3	GAACUGCUCAUGCGUUAUC
SRGAP3	GGACCUAUCUCUCAGCUGA
SRGAP3	CAACGCAGCUAUAAGCAAA
SRGAP3	GAGGAGAAGCAGUUCAAUA
STARD13	GGAUGAAAGUUCCCGACUA
STARD13	GUUAAUUGGAGGACCGGUA
STARD13	GCUUAUGAUGUGGCGGAUA
STARD13	GUACAGACAACCCGGUCAU
STARD8	AUCCAGAACCUGCGUCAAA
STARD8	GACAUGACGAUUUGGCAUA
STARD8	GCUUAUGGUAGUGGGCUAA
STARD8	CCACUUUCCUCCAGAUCUA

Table 2.9 Secondary screen (on-Target plus siRNAs) for GAPS.

Gene	**Sequence**

CapZα1	GAUGGGCAACAGACUAUUA
CapZα1	UGAAAGACCAUUAUUCCAA
CapZα1	CACUAACUGUUUCGAAUGA
CapZα1	UCUGUACUGUUUAUGCUAA
CD2AP	GGGCGAACUUAAUGGUAAA
CD2AP	GAGCAAAUGAAGUGUAAUA
CGNL1 (JACOP)	GCAGGGAGCUCGCAGAAAU
CGNL1 (JACOP)	CGGAGUACCUGAUUGAAUU
CGNL1 (JACOP)	CGAGUAAAGUGCUGGAUGA
CGNL1 (JACOP)	GGGAGAAAUACGACAGUUA
SH3BP1	GAUGACAGCCACCCACUUC
SH3BP1	UGGAGAUUCAGGCCGAUUA

Table 2.10 siRNAs used during SH3BP1 validation and interaction studies.

CHAPTER 3

siRNA Screen of GTPase Activating Proteins in Caco-2 cells

Chapter 3: siRNA Screen of GTPase Activating Proteins in Caco-2 Cells

Part of this chapter was published: J Cell Biol. 2012 Aug 20;198(4):677-93.

Introduction to chapter 3

TJs and AJs are crucial components of epithelial cells. They mediate cell-cell adhesion, regulate epithelial differentiation and tissue formation, and are essential for the formation of epithelial tissue barriers as they regulate paracellular diffusion. TJs also function as morphological and functional borders between apical and the basolateral cell surface domains. Rho GTPases play fundamental roles in the regulation of epithelial physiology and function. They regulate junction assembly and polarisation, but are also components of signalling pathway that originate at junctional complexes and guide epithelial behaviour, such as cell proliferation and migration. In this chapter, I will show the results of an siRNA screen designed to identify GTPase Activating Proteins (GAPs) and Rho GTPases that are important functional components of Rho signalling mechanisms that guide formation of epithelial tight and adherens junctions.

Results – Chapter 3

Identification of junctional associated negative regulators of Rho GTPases

Although different members of the Rho GTPase family have been linked to epithelial junction formation and differentiation, our knowledge is still limited to the main members Cdc42, Rac1 and RhoA, and little is known about their regulators. In the case of Rho GTPase regulators, some GEFs have been identified, but our understanding of functionally important GAPs and which Rho GTPases they regulate is still very limited. Hence, we decided to screen for functionally important Rho GTPases and Rho GAPs using a siRNA-based approach.

The human intestinal epithelial cell line Caco-2 was used as a model system, as it forms polarized monolayers with functional TJs and can be efficiently transfected with siRNAs [60]. As a positive control we first performed a siRNA transfection experiment with siRNAs targeting Cdc42, as this Rho GTPase is an evolutionarily conserved regulator of cell polarisation [263]. Transfection of siRNAs targeting Cdc42 led to spread cells and a disrupted distribution of the TJ protein ZO-1 and the AJ protein beta-catenin, and an effect on polarity with a disorganised expression of the apical marker DPPIV and the basolateral protein Na^+K^+ATPase. We also observed an effect on cytoplasmic polarity with a

scattering of the Golgi marker GP73 (Figure 3.0). Immunoblotting demonstrated that depletion of Cdc42 was indeed efficient (Figure 3.1).

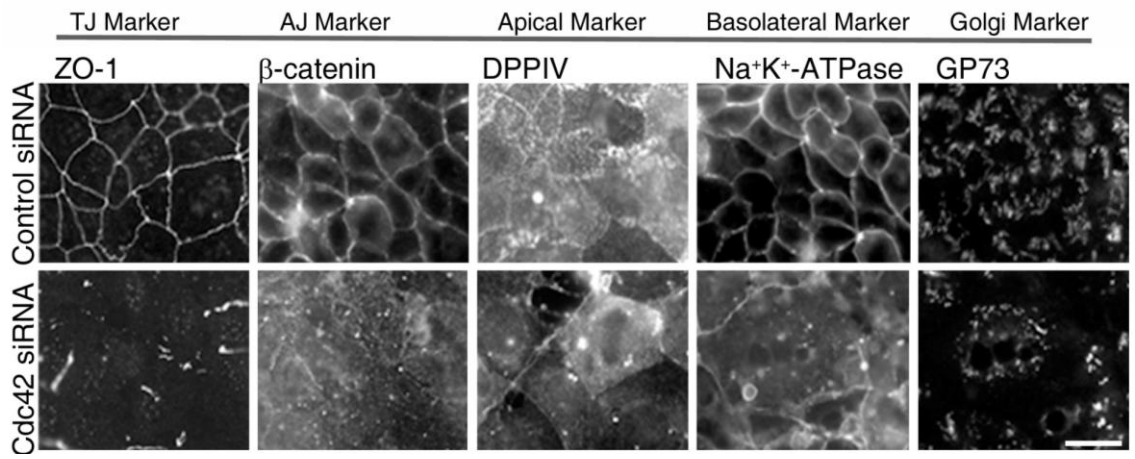

Figure 3.0 Cdc42 depletion affects polarisation and junction formation.

Caco-2 cells were transfected with either control siRNAs or a pool of Cdc42-directed siRNAs. After 72 hours, the cells were fixed with methanol. Coverslips were stained for the indicated proteins. Shown are epifluorescent images of markers for TJ (ZO-1) and AJ (beta-catenin), as well as an apical (DPPIV), a basolateral (Na+K+ ATPase) and a golgi (GP73) marker. Shown are representative images obtained during establishment of the screening assay. Comparable images were obtained during the screen. Scale bar 10μm.

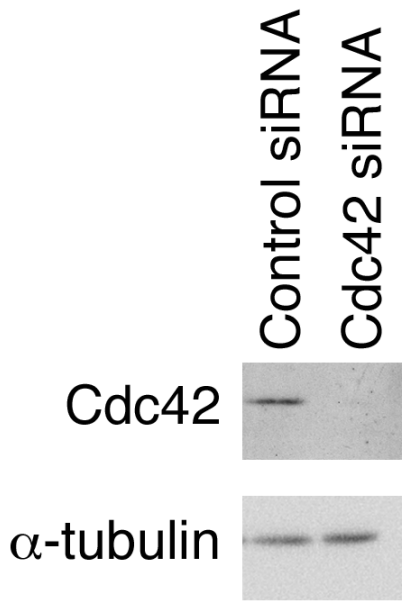

Figure 3.1 Depletion of Cdc42 in Caco-2 cells is efficient.

Whole cell lysates from Caco-2 cells transfected with either control siRNAs or a pool of Cdc42-specific siRNAs were analysed by immunoblotting for Cdc42. Alpha-tubulin was used as a loading control. This shown immunoblot is a representative of the obtained when the screening protocol was established. Depletion of proteins during the actual screen was not followed as antibodies against most proteins are not available.

We next employed a siRNA library of GAPs and Rho GTPases that contained pools of four siRNAs targeting each protein. As previously for the Cdc42 depletion test, Caco-2 cells grown on glass coverslips were transfected with siRNAs and were then fixed three days later and stained for junctional and polarisation markers to assess the effect on cell morphology, junction formation and polarisation.

The screen was performed in two rounds. In the first round (performed by K.Matter), a set of four different oligos was used in a pool for each protein. This resulted in a number of candidate proteins that might regulate junction formation and differentiation. These hits were then screened a second time (performed by C.Zihni and A.Elbediwy). For this second screen, pools of new siRNAs were employed that carried modifications to reduce off-target effects. Most of these siRNAs also targeted different sequences to the original siRNA library (see Materials and Methods).

The siRNA transfections were evaluated by epifluorescence microscopy on a qualitative level. The phenotypes of the siRNA transfections were grouped into four categories. Samples that looked like the control siRNA transfections were classed as ‘Normal’. Transfections that led to somewhat flatter and larger cells with intact junctions were considered ‘Mild’. ‘Moderate’ phenotypes were allocated to transfections that led to flattened cells and at least partially disrupted junction assembly. ‘Severe’ represents the class of siRNA transfections with the strongest phenotypes, such as the one of Cdc42.

Of all the Rho GTPases, only siRNA transfections targeting RhoA and Cdc42 were classified as hits with a severe phenotype (Figure 3.2). In fact, their

phenotypes were very similar. Surprisingly, siRNAs targeting Rac1 had no effect. Given this surprising result with Rac1, we repeated the Rac1 depletions in two separate experiments. However, still only a mild effect on the TJ marker ZO-1 was observed (Figure 3.3).

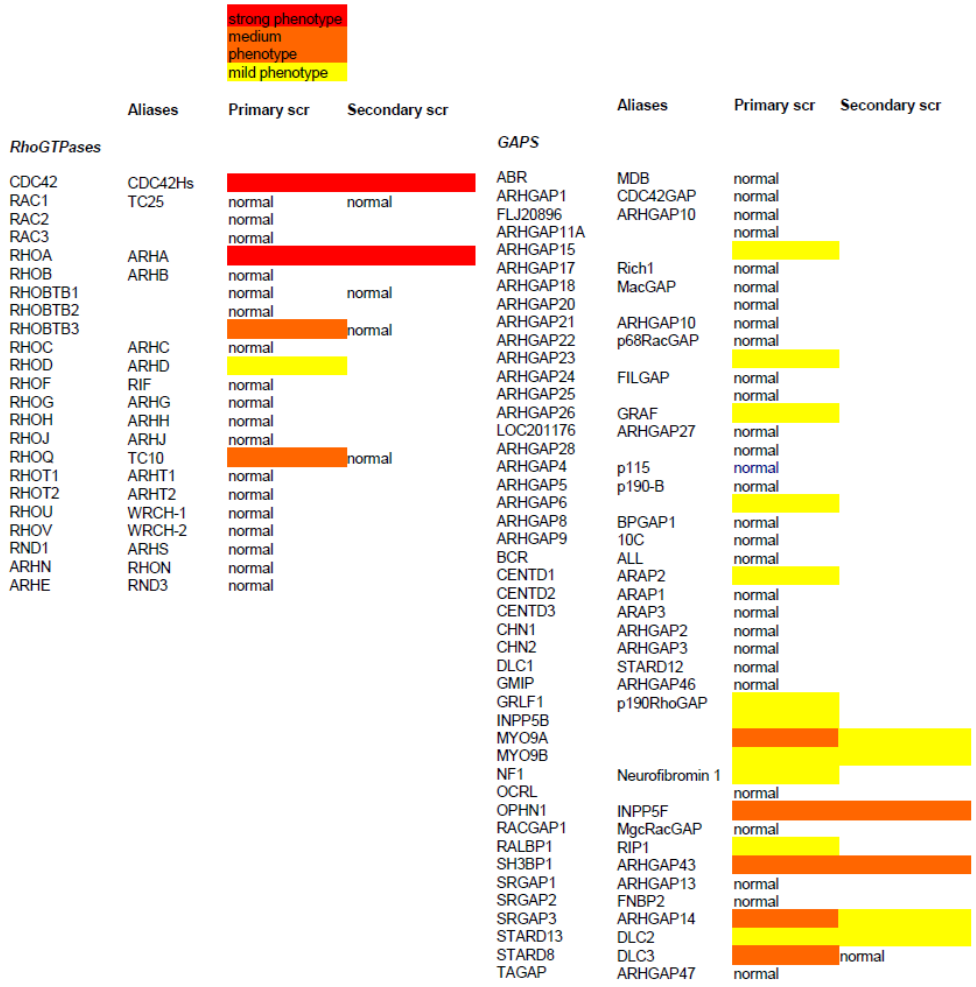

Figure 3.2 Functional siRNA screen of Rho GTPases and GAPs.

Primary screen (scr) was performed using siGENOME siRNAs for the proteins indicated. Secondary screen was peformed using more specific on target siRNAs. Colours indicate severity of phenotype. 'Normal' refers to samples that looked like control cells. Transfections that led to flatter and larger cells with intact junctions were considered 'Mild'. 'Moderate' phenotypes were allocated to transfections that led to flattened cells and at least partially disrupted junctions. 'Severe' represents the class of siRNA transfections with the strongest phenotypes, such as the one of Cdc42.

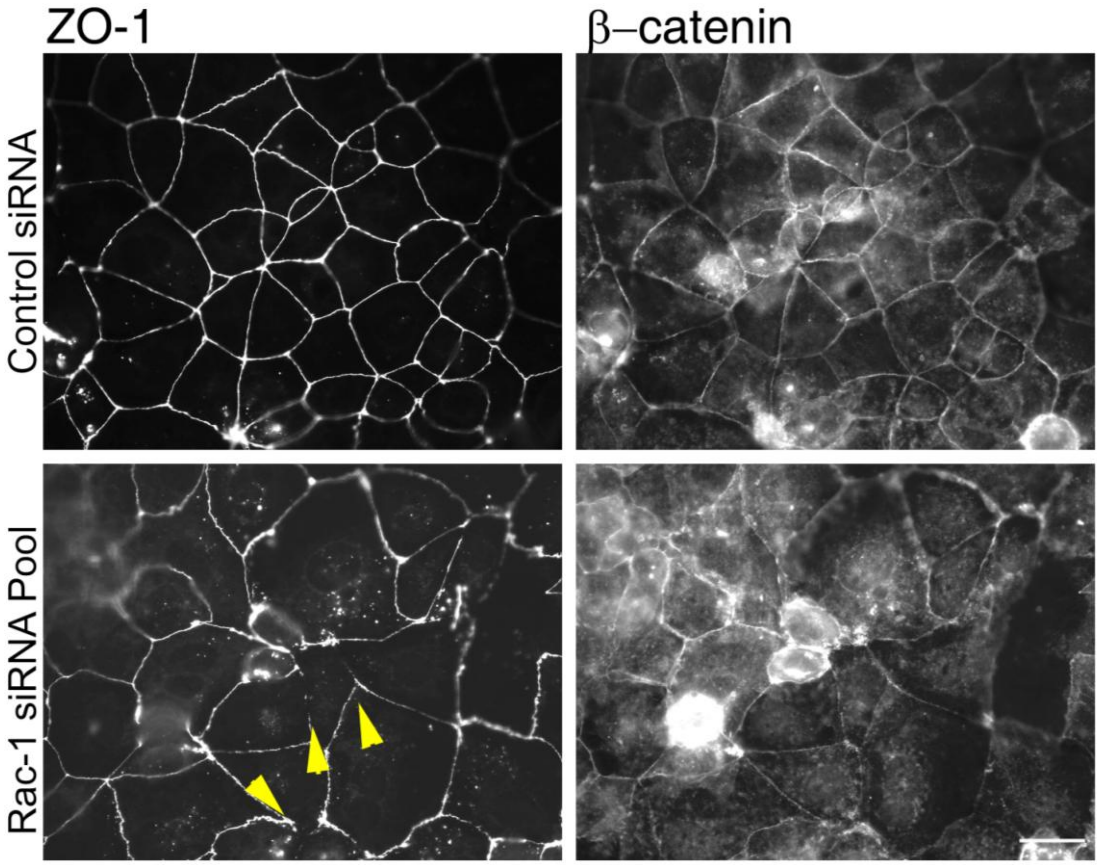

Figure 3.3 Rac1 depletion mildly affects the AJC.

Caco-2 cells were transfected with either control siRNAs or a pool of Rac1 directed siRNAs. After 72 hours, the cells were fixed with methanol. Coverslips were stained for the indicated proteins. Yellow arrows indicate areas of the TJ marker ZO-1 affected by Rac1 depletion. Shown are epiflourescent images of markers for TJ (ZO-1) and AJ (beta-catenin). Scale bar 10µm.

The GAPs with the strongest hits in the screen were the Cdc42/Rac1 GAP SH3BP1, the RhoA GAPs OPHN1 and MYO9A, and two RasGAPs that function as RhoGTPase effectors, PLXNA1 and PLXNB1 [264, 265].Depletion of these proteins led to reduced junctional staining for markers of both TJ and AJ, and a mislocalisation of polarity apical and basolateral polarity markers (Figure 3.4). The phenotypes of siRNAs targeting these proteins were all considered as moderate: they were not as severe as those of Cdc42 and RhoA depletions but considerably more striking than those of, for example, Rac1.

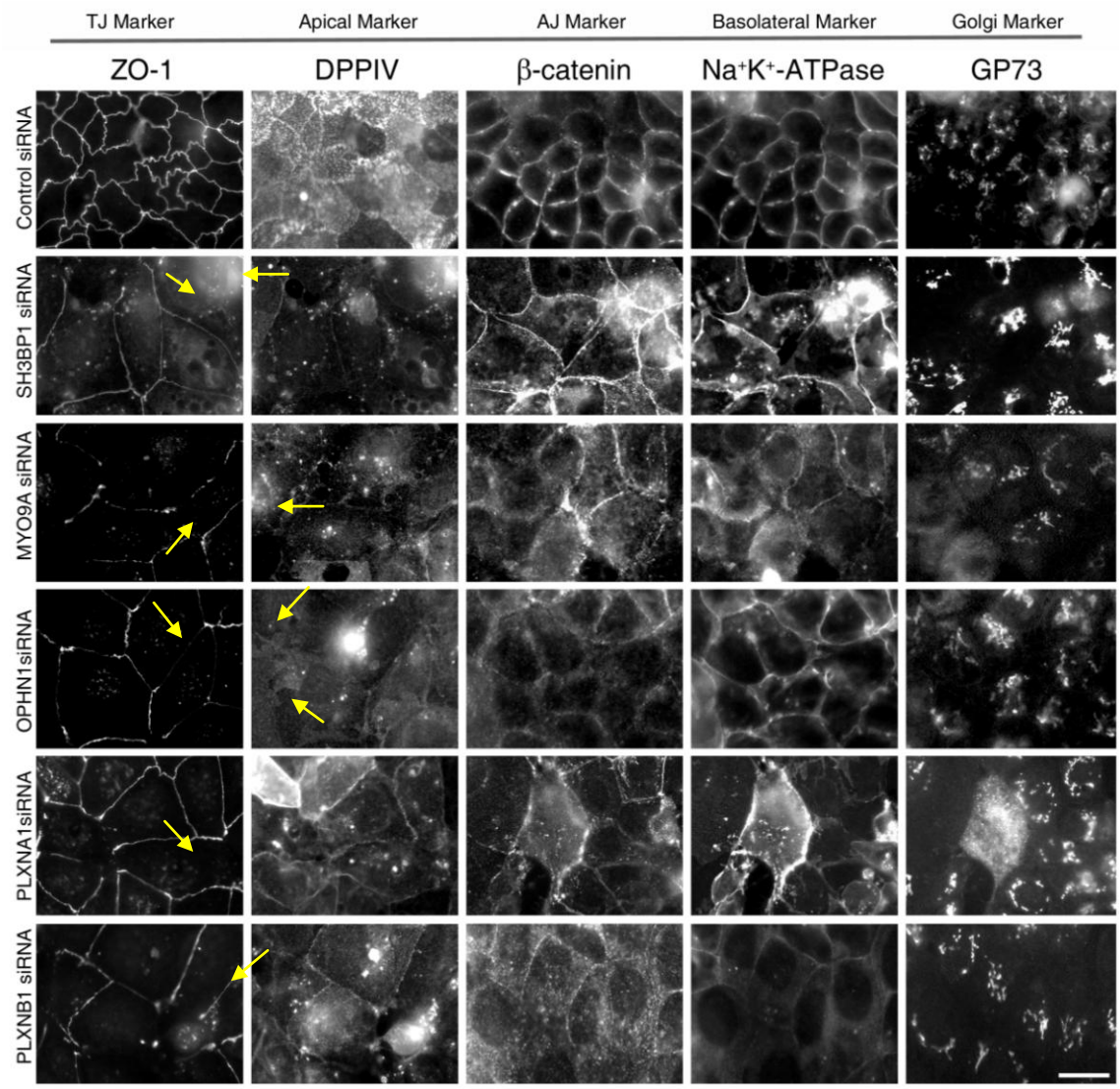

Figure 3.4 GAPs with strongest phenotypes in screen.

Caco-2 cells were transfected with either control siRNA or a pool of specific siRNAs targeting the proteins shown. The screen was performed in triplicate and carried out twice. The cells were transfected with the standard siRNA/Interferin protocol, grown for 72 hours and then fixed with methanol. Samples were stained as indicated. Yellow arrows point out areas where the staining for the TJ marker ZO-1 is disrupted. Note that cells with a moderate phenotype were more spread than control cells and therefore they appeared larger. Shown are epifluorescent images. Scale bar 10µm.

Regulation of RhoA is crucial during epithelial junction formation [60, 228]. Two of the GAPs identified regulate RhoA signalling. MYO9A has previously been published to associate with the junctional complex in Caco-2 cells [213]. OPHN1 also associates with the junctional complex as both endogenous and transfected OPHN1 were found to associate with cell-cell contacts in MDCK, Caco-2 and HCE cells (Figure 3.5, 3.6 and 3.7); and this staining was found to be specific as upon depletion of OPHN1, the junctional pool disappeared (Figure 3.7a), which was confirmed by immunoblotting (Figure 3.7b). OPHN1 has been shown to have GAP activity for RhoA, Rac and Cdc42 *in vitro* using a Rho GTPase and GST-tagged OPHN1 pulldown assays in order to measure GTP hydrolysis; however, its main function *in vivo* seems to be regulation of RhoA. This was suggested by OPHN1 deficient mice that show defects in endocytosis of synaptic vesicle endocytosis; a cellular function that is thought to lead to mental retardation in humans [183, 266].

Depletion of SH3BP1 caused one of the strongest phenotypes from all the GAPs screened. SH3BP1 had previously been discovered as an SH3 binding protein and ligand for the non receptor tyrosine kinase Abl and was shown to have GAP activity for Cdc42 and Rac *in vitro* [186, 187]. Given the strong phenotype of Cdc42 depletion, SH3BP1 was chosen to be analysed further in experiments described in the following chapters.

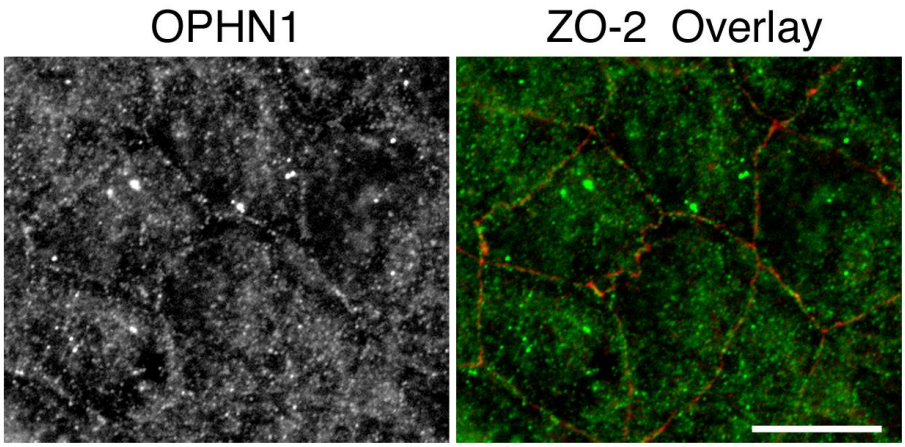

Figure 3.5 Endogenous OPHN1 localises to the AJC.

Caco-2 cells were fixed with methanol and stained for OPHN1 (green) and ZO-2 (red). Shown are epifluorescent images focusing on cell junctions and OPHN1. Scale bar 10µm.

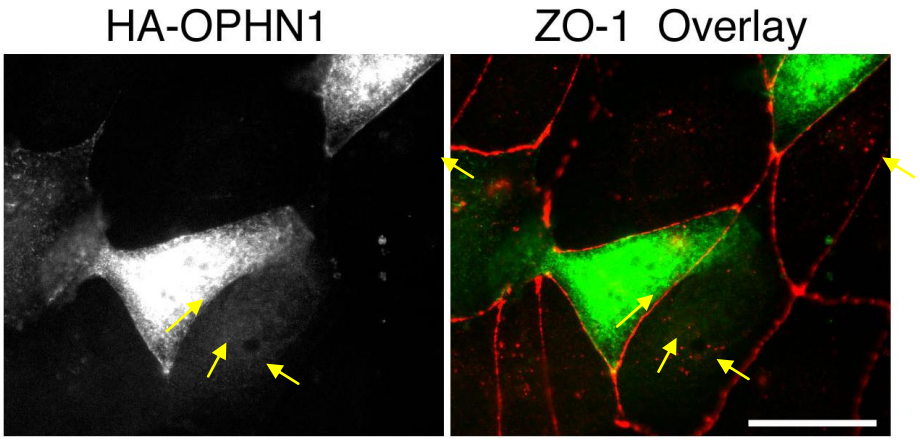

Figure 3.6 Transfected OPHN1 localises to the junctional complex.

MDCK cells were transfected with HA-tagged OPHN1. After 24 hours, the cells were fixed with methanol and stained for the HA tag (green) and ZO-1 (red). Scale bar 10µm.

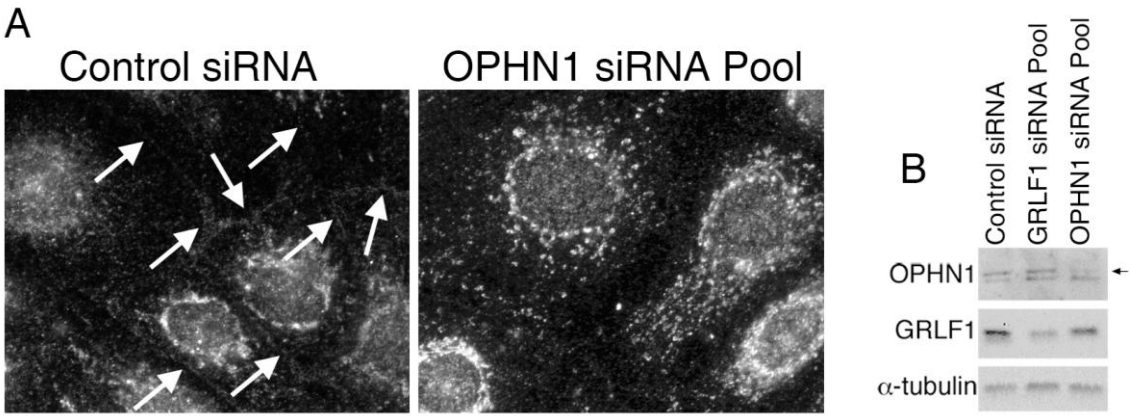

Figure 3.7 OPHN1 depletion reduces the junctional pool of the protein.

(A) HCE cells were transfected with either control siRNAs or a pool of OPHN1-specific siRNAs. Cells were stained for OPHN1. Shown are epifluorescent images. Arrows indicate junctional OPHN1 staining. (B) The levels of OPHN1 depletion were assessed by immunoblotting. Alpha-tubulin was used as a loading control. Arrow indicates correct band of OPHN1. Scale bar 10μm.

Chapter 3 - Discussion

In this part of the project, I wanted to identify Rho GTPases and GTPase Activating Proteins important for the maintenance of TJs and AJs in the intestinal epithelial cell line Caco-2. I employed a qualitative functional siRNA screen together with a library targeting Rho GTPases and GAPs.

From 71 candidates screened, 2 Rho GTPases, and 5 GAPs gave the strongest phenotypes. These positive hits had an effect on junction morphology, classified as either moderate or severe. The strongest candidates were naturally the Rho GTPases Cdc42 and RhoA. This was as expected as they have crucial roles in the formation of the AJC and cell polarity [11, 66, 223, 267]. However, it was surprising the weak effect of Rac1 depletion. Rac1 had previously been reported to be crucial for the formation of adherens junctions in other cell types than what was here analysed [223]. This weak phenotype might be due to a number of possibilities. Perhaps the most likely reason is that cells derived from different epithelial tissues might have different requirements for specific Rho GTPases. For example, many effectors are shared by Cdc42 and Rac1 [171, 268] and, hence, different tissues might rely on either Cdc42 or Rac1. On the other hand, it could also be that depletion of Rac1 was inefficient or occurred more slowly. However, even when the Rac1 depletion was repeated in separate experients, there was only a mild phenotype (Figure 3.3). This was also confirmed using a Rac1 specific inhibitor (NSC23766), which had also a mild effect on assembly of the AJC (data not shown). Finally, it could also be that the type of assay or proteins used to monitor assembly of the AJC affects the readout. For example, monitoring junction assembly during an assay that

involves proliferation of cells and dynamic formation of new cell borders might be different to one that is based on a calcium switch (i.e., cells plated in low calcium that are stimulated to form junctions by adding calcium). Hence, while our screening assay allowed us to identify proteins important for epithelial junction formation and polarisation, the lack of a phenotype in response to specific siRNAs such as those targeting Rac1 does not exclude that such proteins are of importance under different conditions or in other epithelial cell types. Therefore, the advantage of performing such a functional siRNA screen is the potential to identify multiple proteins involved in cell-cell adhesion in a short period of time. The disadvantage of the screen, however, is that negative results are not conclusive and may be due to inefficient depletion of a protein. Neverthess, the screen allowed us to identify candidate regulators of epithelial junction formation and differentiation that had not previously been identified; hence, the screen successfully delivered what it was designed for.

The Rho GAPs with the strongest phenotypes were the Cdc42/Rac1 GAP SH3BP1 and the RhoA GAPs OPHN1 and MYO9A. Some GAPs, which were expected to affect junction formation and polarity, such as the RhoA GAP p190 and the Cdc42 GAP Rich1 were found to have only a mild or normal phenotype. Rich1 was previously found to be important for the polarisation of MDCK cells [193]. Conversley, p190 was found to inactivate RhoA upon engagement of cadherins *in vivo* [269]. The lack of phenotype in our screen for GAPs such as Rich1 and p190 could be due to a few reasons as discussed above for Rac1.

The RhoA GAP OPHN1 has been shown *in vitro* to have also RhoGAP activity toward Cdc42 and Rac1, but has been shown to regulate RhoA *in vivo [266]*. OPHN1 depletion led to a disruption of TJ and AJ, and polarity markers were

disorganised. MYO9A is also a GAP for RhoA, and, similarly, depletion led to a defect in junction assembly. MYO9A also has an important role in epithelial differentiation, and MYO9A deficiency *in vivo* in mice results in an imbalance of homeostasis and fluid retention in the brain (hydrocephalus) [213]. The final Rho GAP whose depletion caused a phenotype, SH3BP1, had the strongest phenotypes of the GAPs in the siRNA screen and was an ideal candidate to study further. It caused a strong disruption of the TJ marker ZO-1 and the AJ marker beta-catenin. In the following chapters, I will describe experiments designed to elucidate the role of SH3BP1 in epithelial junction formation and differentiation.

Chapter 4

SH3BP1 Regulates Epithelial Junction Formation and Rho GTPase Activity

Chapter 4: SH3BP1 Regulates Epithelial Junction Formation and Rho GTPase Activity

Parts of this section were published in the J. Cell Biol. (2012), 198(4):677-93.

Introduction to chapter 4

This chapter focuses on the GTPase activating protein SH3BP1, a protein identified in a siRNA screen for Rho GTPases and GTPase activating proteins functionally relevant for the formation of epithelial junctions. SH3BP1 had initially been discovered in a cDNA library screen using the SH3 domain of the non-receptor tyrosine kinase Abl as a probe and had been shown to be a GAP for Rac1 and Cdc42 *in vitro* [186, 187]. Here, I describe data that demonstrate that different types of epithelial cells require SH3BP1 to form intercellular junctions, and that the GAP is required for normal organisation of the actin cytoskeleton. My data establish that SH3BP1 is a novel junction-associated inhibitor of Cdc42 and Rac1 activity, which aids in the formation of junctions, and that its membrane recruitment is stimulated by EGF signalling.

Results – Chapter 4

SH3BP1 depletion affects junctions in various epithelia

The siRNA screen in chapter 3 suggested that SH3BP1 is a regulator of junction assembly. To validate this phenotype, I first tested whether transfection of individual siRNAs also inhibited junction assembly and whether they indeed reduced expression of SH3BP1. Junction assembly was analysed by staining sets of TJ and AJ markers. Staining of TJ markers revealed that depletion of SH3BP1 led to flatter cells that did not assemble continuous junctions (Figure 4.0). Some markers were more strongly affected than others with, for example, ZO-1 still being recruited to cell-cell contacts and ZO-3 appearing completely dispersed. Staining for the AJ markers E-cadherin, alpha-catenin and p120 catenin in depleted cells resulted in a more disrupted and discontinuous junctional distribution, indicating that AJ assembly was also defective (Figure 4.0). I next stained for the actin cytoskeleton using fluorescent phalloidin for F-actin in Caco-2 cells and found that depletion resulted in a loss of the normal apical F-actin organisation and a thinning of perijunctional F-actin (Figure 4.1). This defect in actin organisation was confirmed by staining with antibodies against β–actin. There was also an increase in basal actin fibres that resembled stress fibres. Stress fibre formation is generally attributed to enhanced RhoA activation, but SH3BP1 is no effective GAP for RhoA [186, 187, 189]. However, It has been well documented that disassembly of junctions can result in activation of RhoA due to effects on p190RhoGAP and GEF-H1 [209, 270, 271]. It is thus likely that defects in junction assembly lead to enhanced stress fibre

formation. Moreover, stress fibres maybe more evident as the depleted cells become more spread, allowing easier visualization of the stress fibres in comparison to more compact cells.

Quantification of the junctional proteins and F-actin stains revealed significant differences between cells transfected with control and SH3BP1-targeting siRNAs (Figure 4.2). The efficiency of SH3BP1 protein depletion was validated by immunoblotting extracts derived from cells transfected with a pool as well as two individual siRNAs targeting SH3BP1 (Figures 4.1 and 4.2). Depletion was found to be very efficient with at least a 60% reduction in expression. These data thus indicate that SH3BP1 is important for the regulation of the actin cytoskeleton and the normal assembly of TJs and AJs.

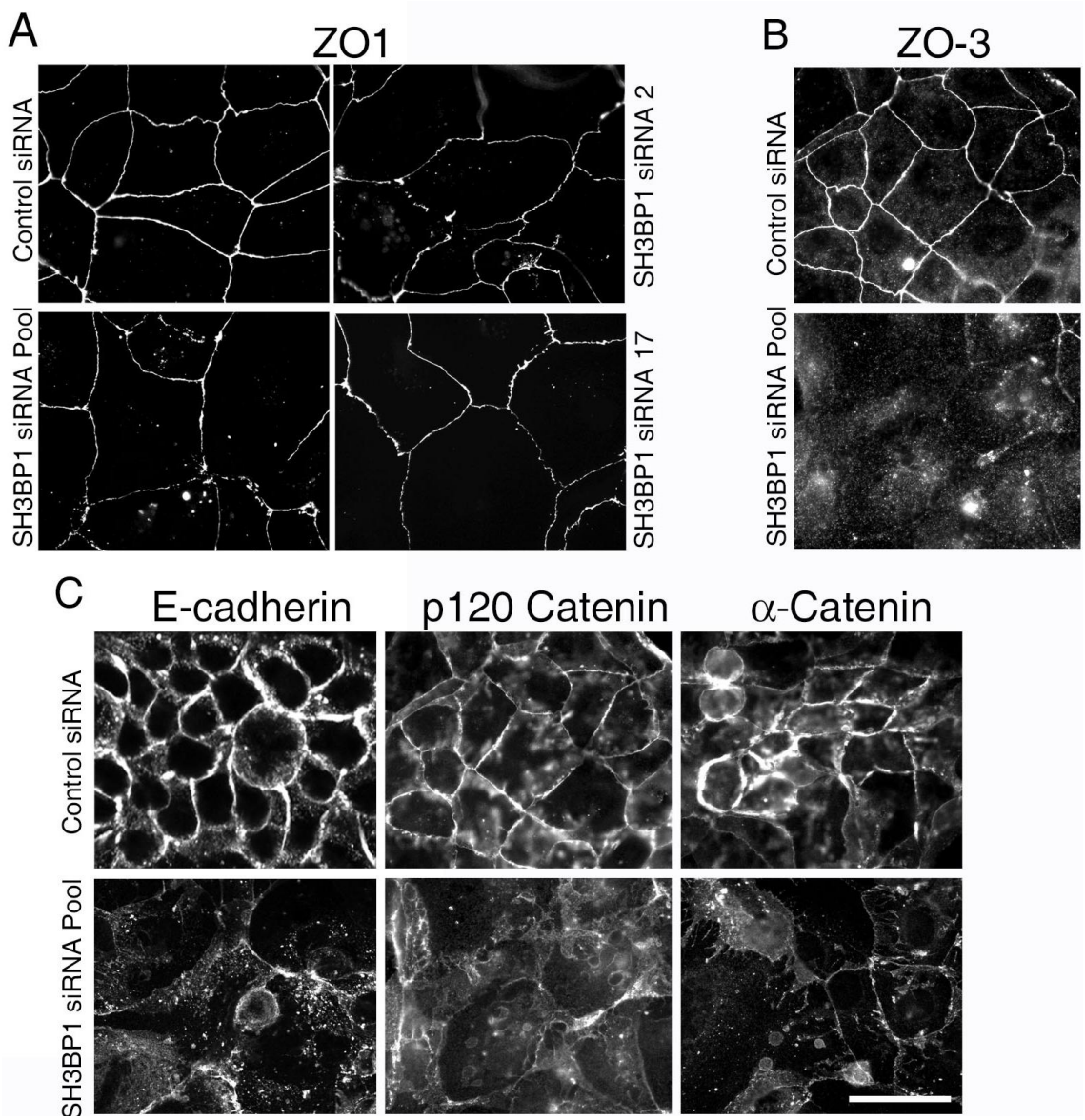

Figure 4.0 SH3BP1 depletion disrupts normal assembly of the apical junctional complex.

Caco-2 cells were transfected with either control siRNA or a pool of SH3BP1 specific siRNAs. After 96 hours, the cells were fixed with methanol. Coverslips were stained for TJ: (A) ZO-1, (B) ZO-3 or AJ: (C) E-cadherin, p120-Catenin or alpha-catenin. Shown are epifluorescence images of cell junction markers. Corresponding western blot can be seen in Figure 4.1. Scale bar 10μm.

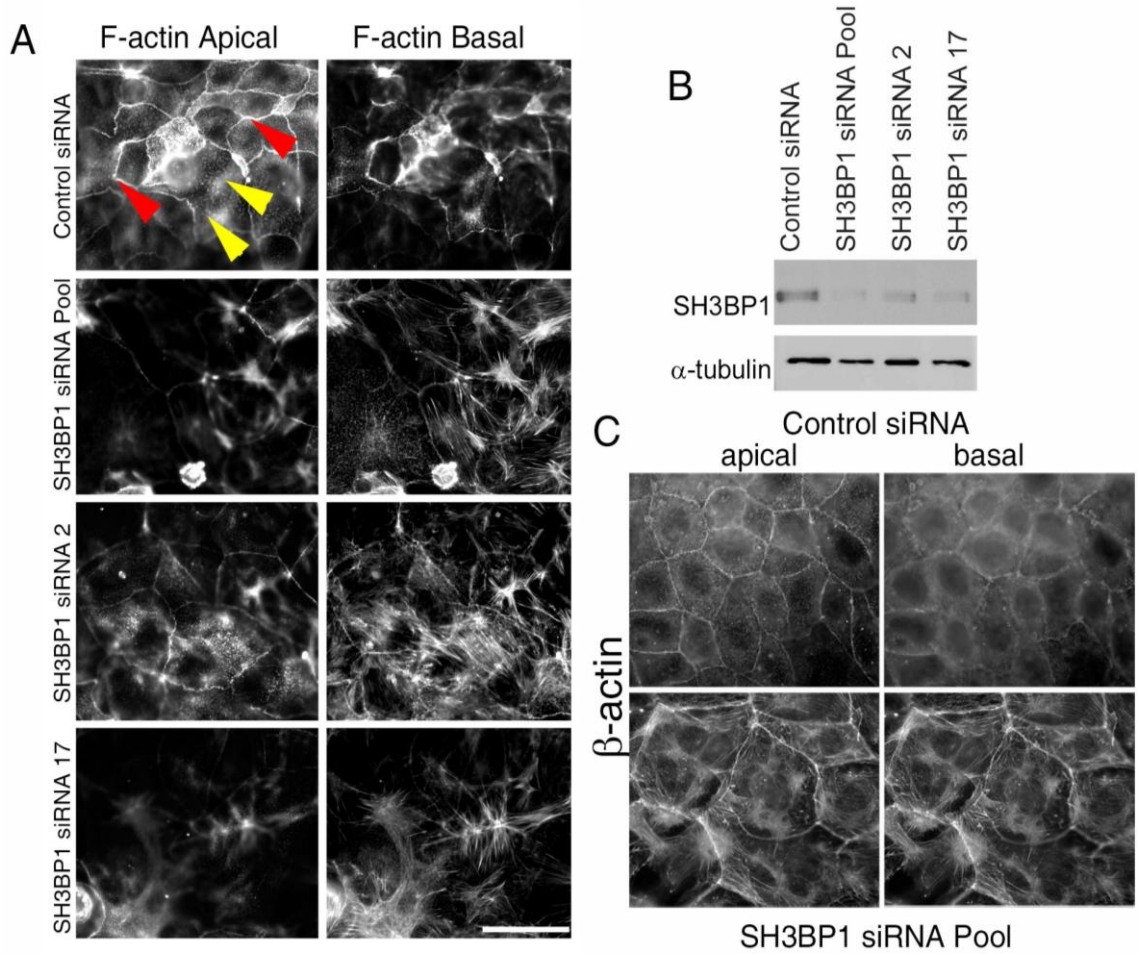

Figure 4.1 SH3BP1 depletion affects the actin cytoskeleton.

Caco-2 cells were transfected with either control siRNA, two different individual SH3BP1 specific siRNAs or a pool of SH3BP1 directed siRNAs. After 96 hours, the cells were either fixed with paraformaldehyde, permeabilised with Triton X-100 and stained for (A) F-actin or (B) lysed with sample buffer and processed for immunoblotting. Alpha-tubulin was used as a loading control. (C) For the beta-actin staining, the cells were fixed in methanol and labelled with antibodies specific for beta-actin. Shown are epifluorescence images. Cells were taken at same magnification. Yellow arrows denote apical F-actin, and red arrows denote perijunctional F-actin. Experiment was performed three times. Scale bar 10µm.

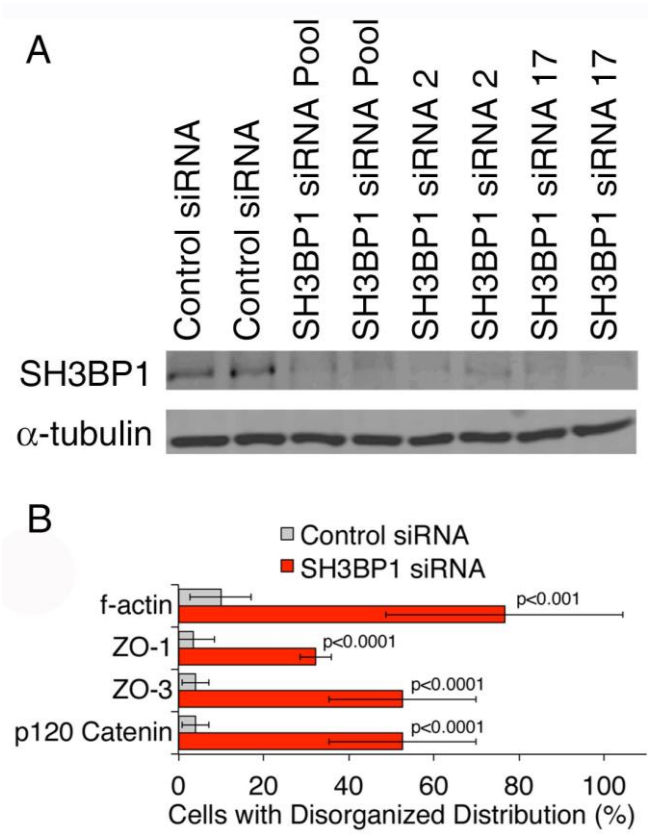

Figure 4.2 SH3BP1 siRNA efficiency and quantification of depletion-induced phenotypes.

(A) Caco-2 cells were transfected with either control siRNA, two different individual SH3BP1 specific siRNAs or a pool of SH3BP1 directed siRNAs. After 96 hours, extracts were collected and immunoblotted for SH3BP1. Alpha-tubulin was used as a loading control. (B) A quantification of the effect on the subcellular distribution of F-actin (counting cells with strongly induced basal F-actin; mean basal actin intensity increased by >60% in SH3BP1-depleted cells) and three junctional markers (counting cells with discontinuous, irregular junctional staining). Shown are means +/- 1 SD, representing the cells in at least five different fields per condition ($n \geq 5$). Note that assembly of tight and adherens junctions were affected, but different components are affected to different extents.

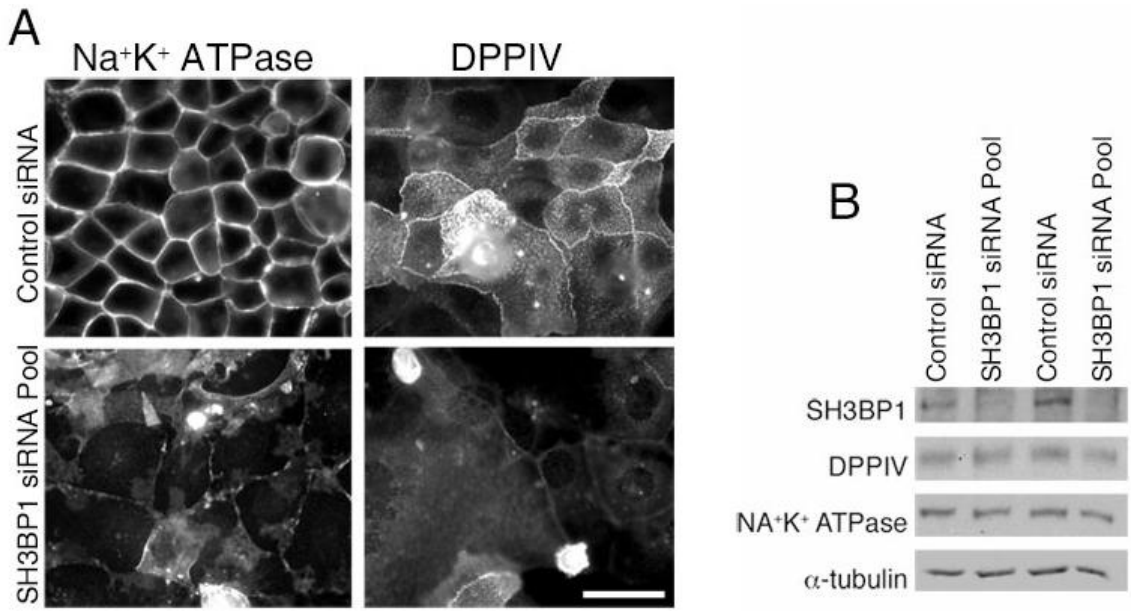

Figure 4.3 SH3BP1 depletion affects epithelial differentiation.

Caco-2 cells were transfected with either control siRNA or a pool of SH3BP1 directed siRNAs. After 96 hours, the cells were either fixed with paraformaldehyde or lysed with sample buffer and processed for immunoblotting. Coverslips were (A) stained for differentiation markers (Apical) DPPIV and (Basolateral) Na^+K^+ ATPase or (B) blotted for these and SH3BP1. Alpha-tubulin was used as a loading control. Shown are epifluorescence images (A) and protein expression (B) of polarisation markers. Experiment was performed three times. Scale bar 10µm.

In order to further clarify if the flattened cell phenotype seen upon SH3BP1 depletion was due to a loss of polarisation and differentiation, I decided to analyse the expression and distribution of cell surface markers in SH3BP1 depleted cells. The apical marker DPPIV and the basolateral marker Na^+K^+ ATPase were used. Apical staining of DPPIV was significantly reduced in depleted cells, and antibodies against Na^+K^+ ATPase resulted in a more disrupted and disorganised staining (Figure 4.3). Immunoblotting revealed the levels of expression of the cell surface markers were not affected. Confocal microscopy of samples stained for occludin and alpha-catenin further demonstrated that the depleted cells had lost their columnar appearance and were flatter and failed to assemble distinctive tight and adherens junctions (Figure 4.4). Thus, confirming that SH3BP1 is important for the differentiation of polarized epithelial cells.

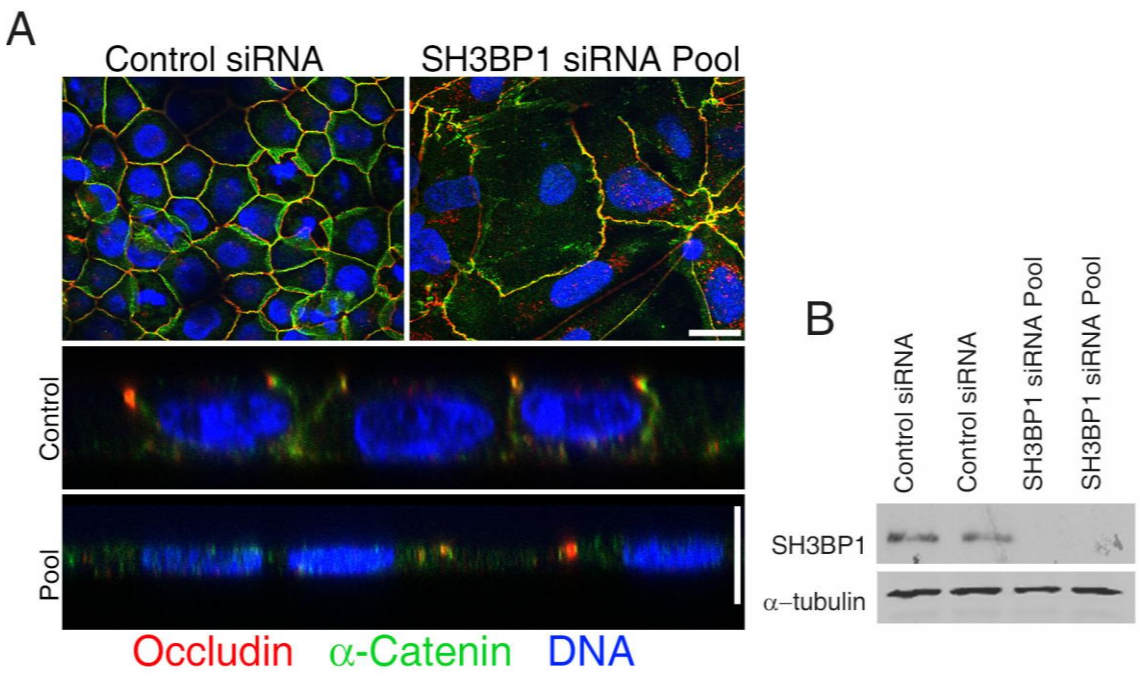

Figure 4.4 SH3BP1 depletion results in a loss of cell polarity.

Caco-2 cells were transfected with either control siRNA or a pool of SH3BP1 specific siRNAs. After 96 hours, the cells were either fixed with methanol for immunofluorescence or lysed with sample buffer and processed for immunoblotting. (A) The cells on coverslips were stained with antibodies against occludin (red) and alpha-catenin (green), and then analysed by confocal microscopy. Shown are sections representing the imaged areas and representative Z-line scans. (B) The levels of SH3BP1 depletion were assessed by blotting. Alpha-tubulin was used as a loading control. Experiment was performed twice. Scale bar 10µm**.**

Prior to analysing the molecular mechanism by which SH3BP1 regulates junction assembly, I wanted to test two aspects important to understand the biological significance of the defect in Caco-2 cells observed upon down-regulation of SH3BP1. Firstly, I wanted to know where it localises, as this would tell me whether the effect on junction assembly is likely to be direct, and, secondly, I wanted to test whether SH3BP1 is of functional relevance in different types of epithelial cells or whether its importance is restricted to intestinal epithelial cells.

Firstly, I analysed the subcellular distribution of SH3BP1. By indirect immunofluorescence, I found that anti-SH3BP1 antibodies stained both intercellular junctions as well as the cytoplasm. However, only the junctional staining disappeared following SH3BP1 depletion, suggesting that a part of the cytoplasmic staining is likely to reflect non-specific signal (Figure 4.5). These observations thus indicate that SH3BP1 can associate with epithelial intercellular junctions.

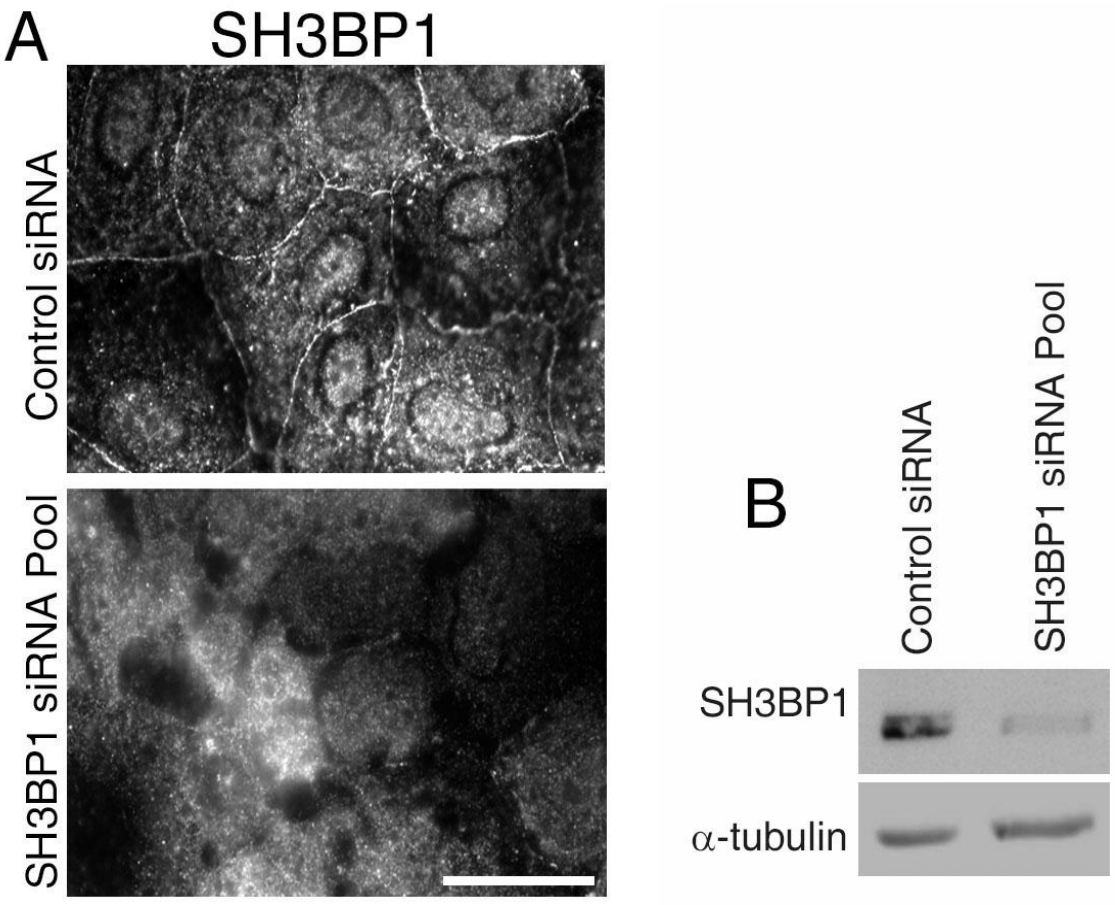

Figure 4.5 SH3BP1 associates with cell-cell contacts.

Caco-2 cells were transfected with either control siRNA or a pool of SH3BP1 directed siRNAs. After 96 hours, the cells were either extracted with Triton X-100 and then fixed with methanol for immunfluorescence or lysed with sample buffer and processed for immunoblotting. (A) Coverslips were stained for SH3BP1. Shown are epifluorescence images. (B) The levels of SH3BP1 depletion were assessed by blotting. Alpha-tubulin was used as a loading control. Experiment was performed 4 times. Scale bar 10µm.

Next I wanted to determine if the phenotype of SH3BP1 detected Caco-2 cells could be seen in other epithelial cells; so, I analysed Human Corneal Epithelial (HCE) cells. As above, the cells were transfected with control and SH3BP1-specific siRNAs and were then stained for TJ and AJ markers. The TJ marker ZO-1 was found to be significantly reduced from the junction although a faint junctional staining persisted as in Caco-2 cells. The AJ marker beta-catenin was disrupted with thin protrusions emitting from the membrane, resembling possible microspikes, filopodia or retraction fibres (Figure 4.6). The latter possibility is unlikely, however, as SH3BP1-depleted cells were flatter, more spread, and still in contact with their neighbours; it seems difficult to combine cell retraction with maintenance of cell-cell contact.

Further trying to explore the actin organisation defect observed in depleted SH3BP1 samples, I decided to use the epidermoid epithelial cell line A431, a keratinocyte-derived cell line. A431 cells overexpress EGF receptor and are known to form filopodia [272, 273]**.** F-actin staining indeed suggested the existence of short basal filopodia in control cells (Figure 4.7). Upon depletion of SH3BP1, the cells also started to spread out more and formed long F-actin-rich protrusions, suggesting that loss of SH3BP1 triggered increased growth of filopodia. As filopodia formation is stimulated by Cdc42 signalling, this suggests that depletion of SH3BP1 leads to deregulation of Cdc42 activation.

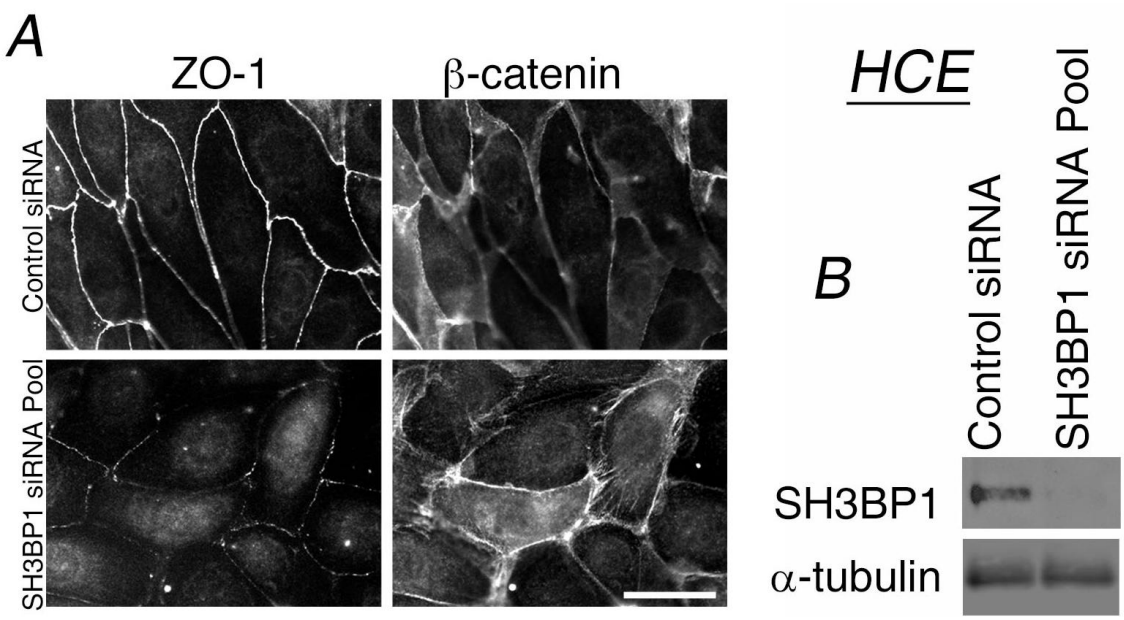

Figure 4.6 SH3BP1 depletion affects the apical junctional complex in HCE cells.

HCE cells were transfected with either control siRNA or a pool of SH3BP1 specific siRNAs. After 96 hours, the cells were either extracted with Triton X-100 and fixed with methanol for immunofluorescence or lysed with sample buffer and processed for immunoblotting. (A) Shown are epifluorescent images of cell junction markers ZO-1 (TJ) and beta-catenin (AJ). (B) The levels of SH3BP1 depletion were assessed by blotting. Alpha-tubulin was used as a loading control. Experiment was performed twice. Scale bar 10μm.

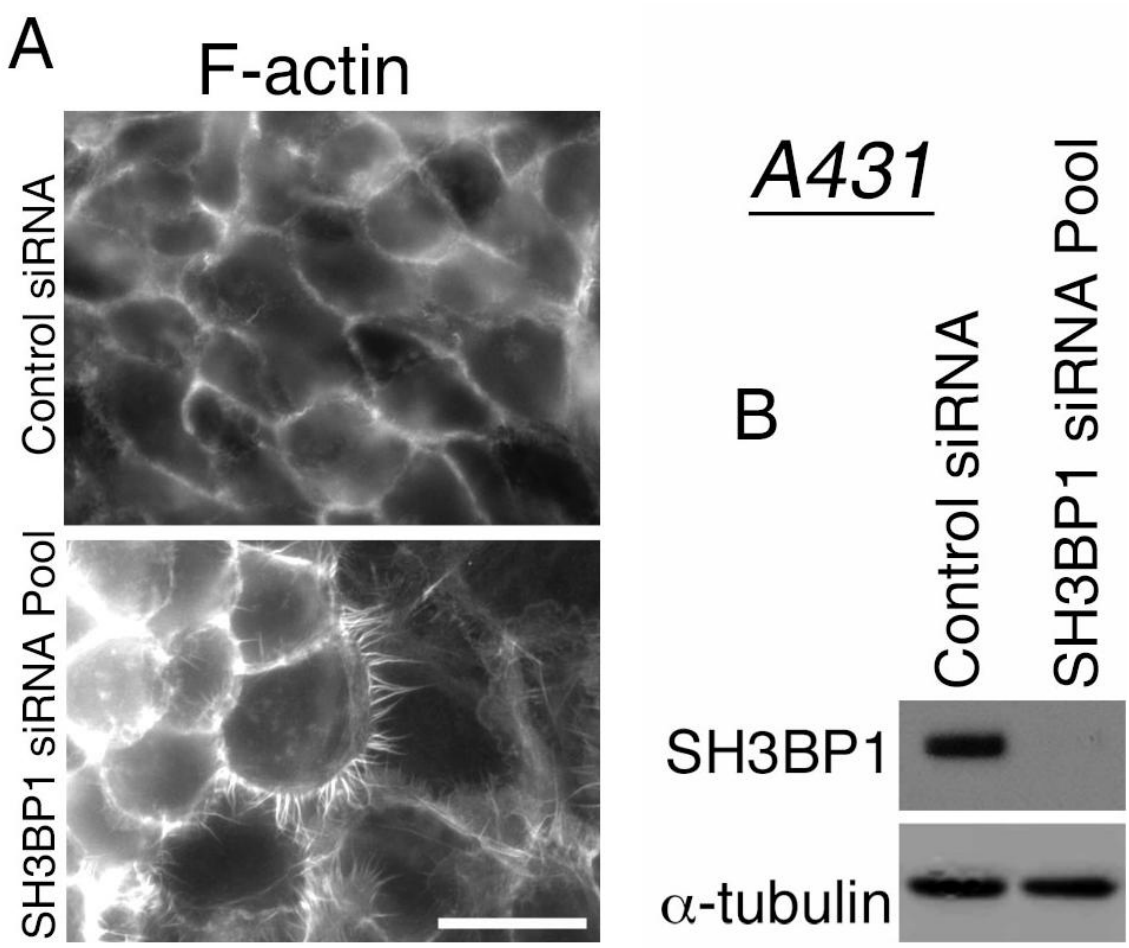

Figure 4.7 SH3BP1 depletion affects actin cytoskeleton in A431 cells.

A431 cells were transfected with either control siRNA or a pool of SH3BP1 specific siRNAs. After 96 hours, the cells were either fixed with paraformaldehyde and permeabilised with Triton X-100 for immunofluorescence or lysed with sample buffer and processed for immunoblotting. (A) Cells were stained for F-actin.(B) The levels of SH3BP1 depletion were assessed by blotting. Alpha-tubulin was used as a loading control. Shown are epifluorescence images. Experiment was performed three times. Scale bar 10μm.

SH3BP1 is important for the formation of functional epithelial junctions

Having established that SH3BP1 depletion results in the deregulation of epithelial junction assembly and differentiation, I next investigated whether the GAP was important for initial junction formation to further understand the molecular mechanism involved. To investigate *de novo* junction formation, a calcium switch assay was performed in Caco-2 cells depleted of SH3BP1. Transepithelial Electrical Resistance (TER), which measures ion conductance over an epithelial layer, was measured over a period of 48 hours in order to assess barrier formation. The levels of TER were clearly affected by depletion of SH3BP1, as depleted cells exhibited a reduction of 50% in TER after 48 hours in comparison to control cells. To assess the permeability further, two different size dextran tracers were used and found to diffuse more easily across the monolayers formed by SH3BP1 depleted cells. These data thus indicate that SH3BP1 depleted cells failed to form functional tight junctions (Figure 4.8).

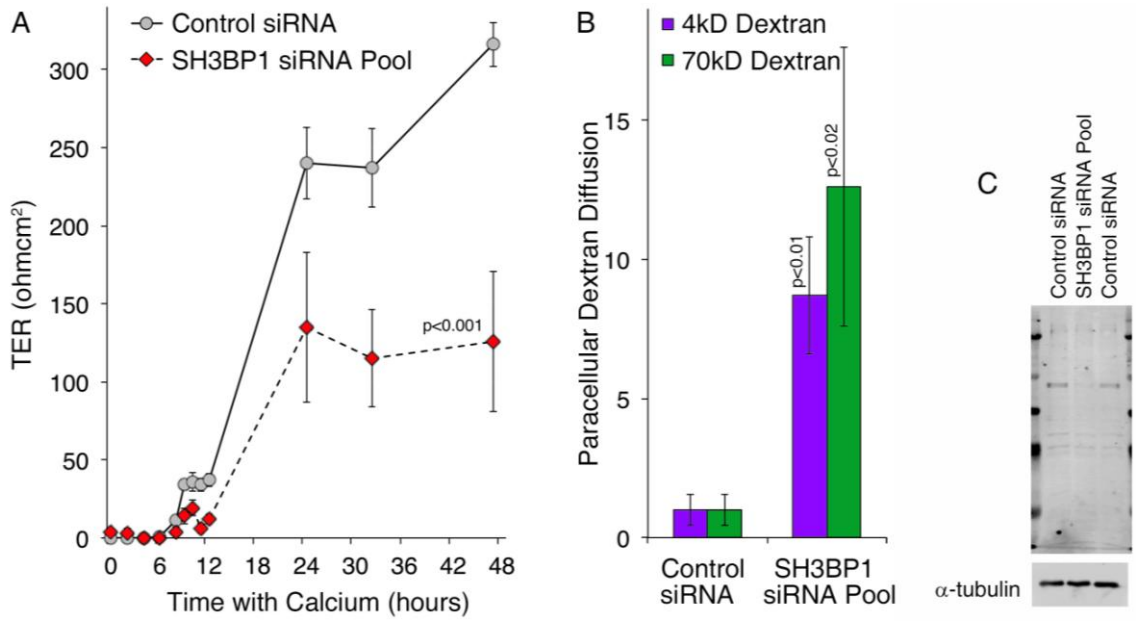

Figure 4.8 SH3BP1 regulates epithelial barrier formation.

Caco-2 cells were transfected with either control siRNA or a pool of SH3BP1 specific siRNAs, and were subsequently trypsinised and reseeded in low calcium medium on filters for 16 hours in order to prevent junction formation. Normal calcium medium was reintroduced and junction formation was followed during the next 48 hours by measuring transepithelial electrical resistance (TER) (A) and paracellular permeability (B). Paracellular permeability was assessed using two different fluorescently labelled dextrans. Data shown are the average and SD of triplicates. Bar graphs represent averages and the error bars 1 SD, n = 3. (C) Expression levels of SH3BP1 depletion were assessed at the end of experiments and alpha tubulin was used as a loading control.

In a morphological analysis of samples replenished with calcium and stained with the TJ marker ZO-1, I observed that junction formation was severely disrupted with a clear delay in TJ junction formation (Figure 4.9). This was also evident in samples labelled for the AJ markers E-cadherin and p120 catenin (Figure 4.10). As expected, the F-actin stain revealed a severe delay in the formation of the perijunctional actin ring with a disrupted and disorganised appearance upon SH3BP1 depletion (Figure 4.11).

Since it seems SH3BP1 is important for early junction formation, it was important to analyse how early SH3BP1 localised to the forming junctional complex. Analysis of SH3BP1 localization during a calcium switch revealed that SH3BP1 localizes early to cell-cell contacts, with junctional SH3BP1 being observed as early as 30 minutes with the initial stages of E-cadherin based junction formation (Figure 4.12).

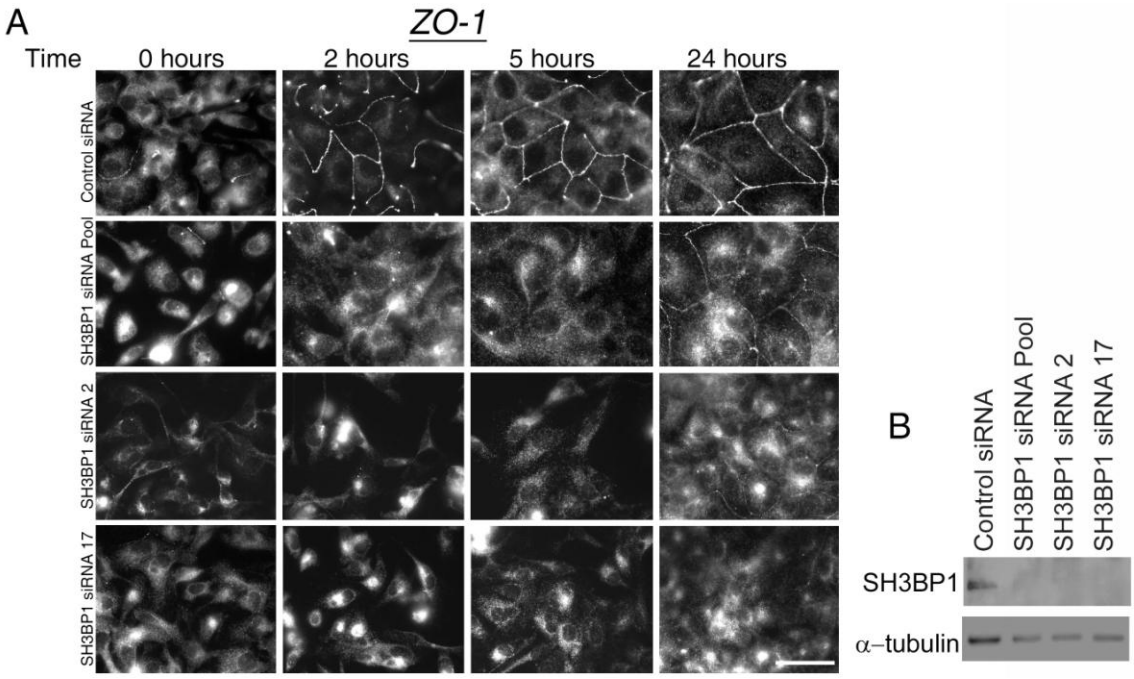

Figure 4.9 SH3BP1 is important for *de novo* TJ formation.

Caco-2 cells were transfected with control siRNA, two different individual SH3BP1-specific siRNAs or a pool of SH3BP1 directed siRNAs and were plated in low calcium medium. (A) Cells were fixed in methanol at the indicated timepoints after being transferred to calcium medium and immunostained for ZO-1. Shown are epifluorescent images. (B) Expression levels of SH3BP1 depletion were assessed at the end of the experiment and alpha tubulin was used as a loading control. Experiment was performed three times. Scale bar 10µm.

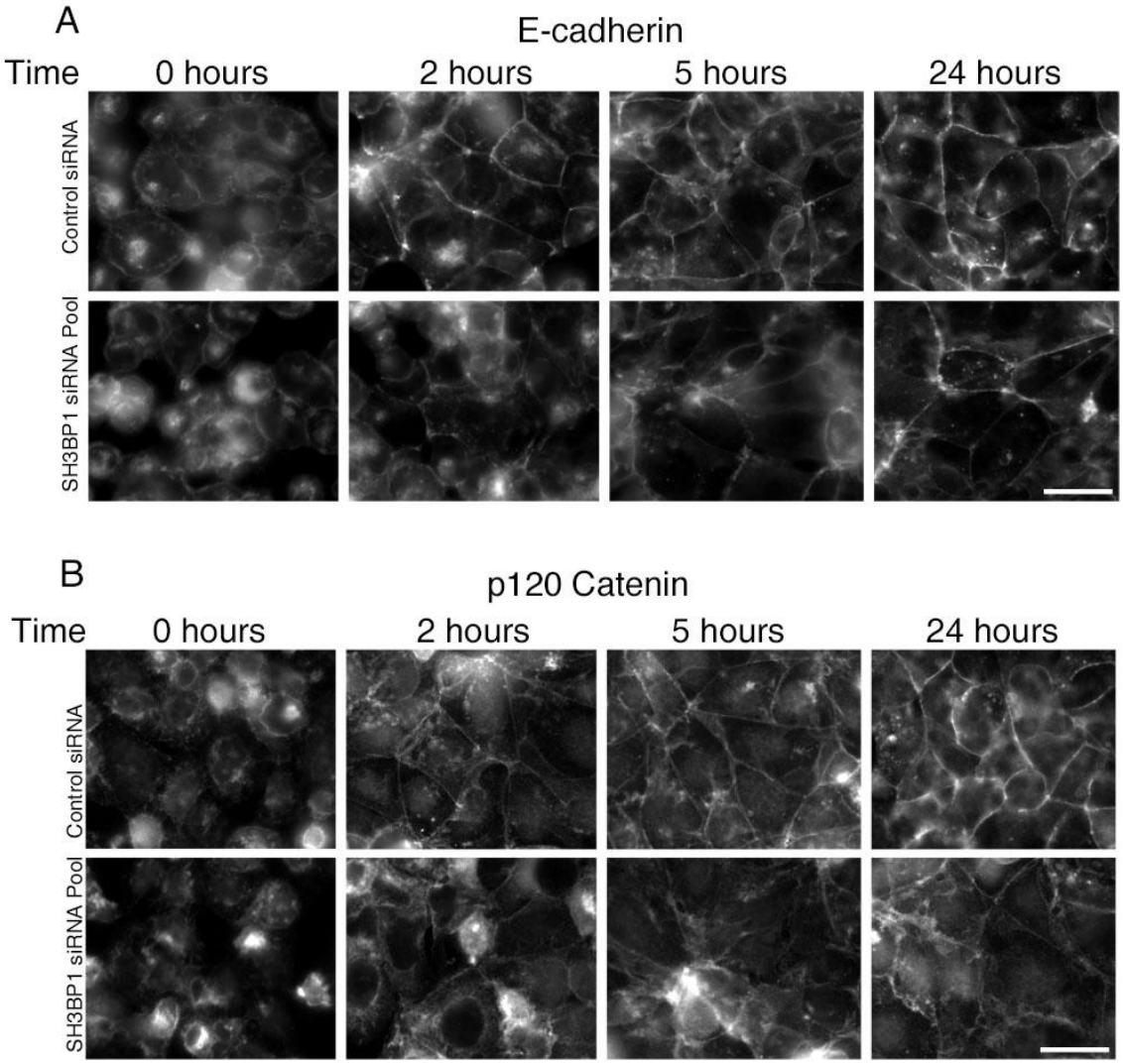

Figure 4.10 SH3BP1 is important for de novo AJ formation.

Caco-2 cells transfected with either control siRNA or a pool of SH3BP1-directed siRNAs were plated in low calcium medium. Cells were fixed in methanol at the indicated timepoints after being transferred to calcium medium and immunostained for (A) E-cadherin and (B) p120 catenin. Shown are epifluorescence images. Expression levels of SH3BP1 were assessed in figure 4.11. Experiment performed three times. Scale bar 10µm.

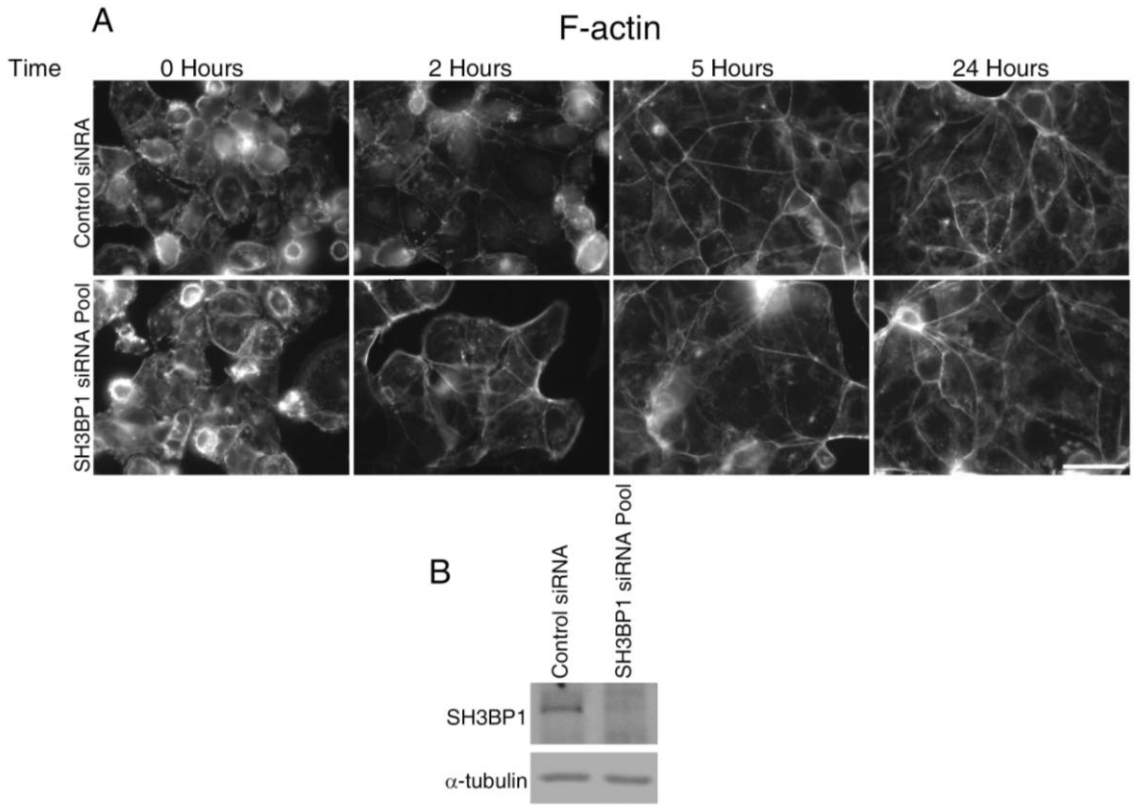

Figure 4.11 SH3BP1 is important for actin cytoskeleton organisation.

Caco-2 cells were transfected with either control siRNA or a pool of SH3BP1 specific siRNAs and were plated in low calcium medium. Cells were fixed in paraformaldehyde and permeabilised with Triton X-100 at the specified timepoints after reintroduction of calcium medium and were then (A) stained for F-actin. Shown are epifluorescent images. (B) Expression levels of SH3BP1 depletion were assessed at the end of the experiment and alpha-tubulin was used as a loading control. Experiment was performed twice. Scale bar 10µm.

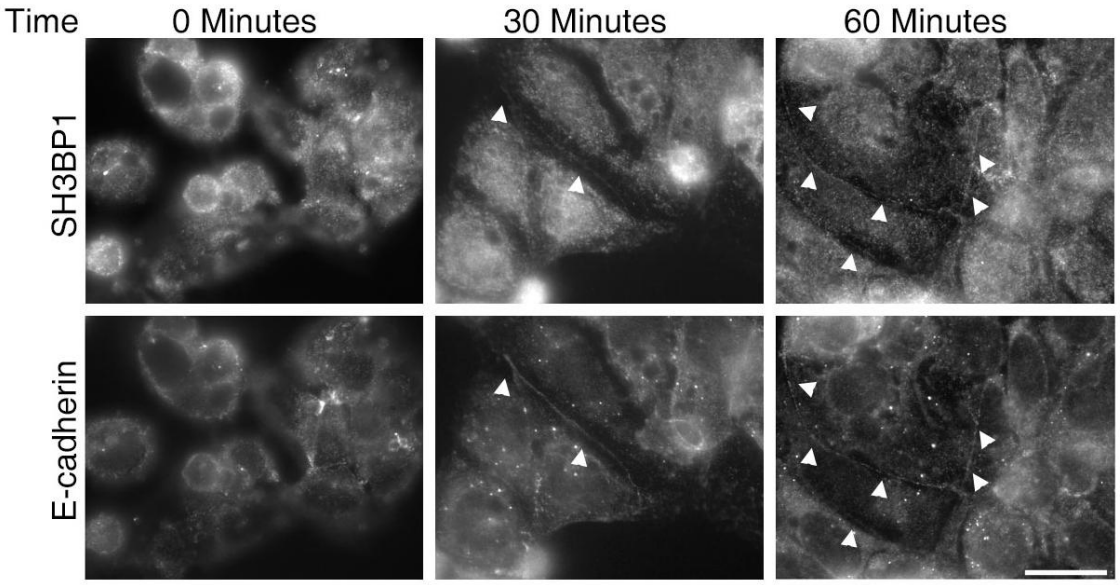

Figure 4.12 SH3BP1 localises early to the forming adherens junctions.

Caco-2 cells were plated in low calcium medium. Cells were extracted in Triton X-100 and fixed in methanol at the indicated timepoints after being transferred to calcium medium and immunostained for SH3BP1 and E-cadherin. Arrows represent areas in which SH3BP1 and E-cadherin localize to junctions. Shown are epifluorescence images. Experiment was performed three times. Scale bar 10µm.

Addition of calcium to A431 cells resulted in the formation of filopodia-like cell-cell contacts followed by AJ formation over the course of a few hours and resulted in continuous E-cadherin staining after 24 hours. In depleted cells, however, the rounded cells of early time points spread out normally and formed contacts, but they did not progress beyond the stage of forming intercalating filopodia-like protrusions. These protrusions were again seen upon staining of F-actin, suggesting that SH3BP1 depleted cells fail to form junctions upon initial contact formation (Figure 4.13). Thus, I conclude that SH3BP1 associates with intercellular junctions early during junction formation and seems to be required for the transformation of early cell-cell contacts to mature junctional complexes. The induction of protrusion formation during cell spreading and initiation of cell-cell contacts also seems difficult to reconcile with protrusions representing retraction fibres.

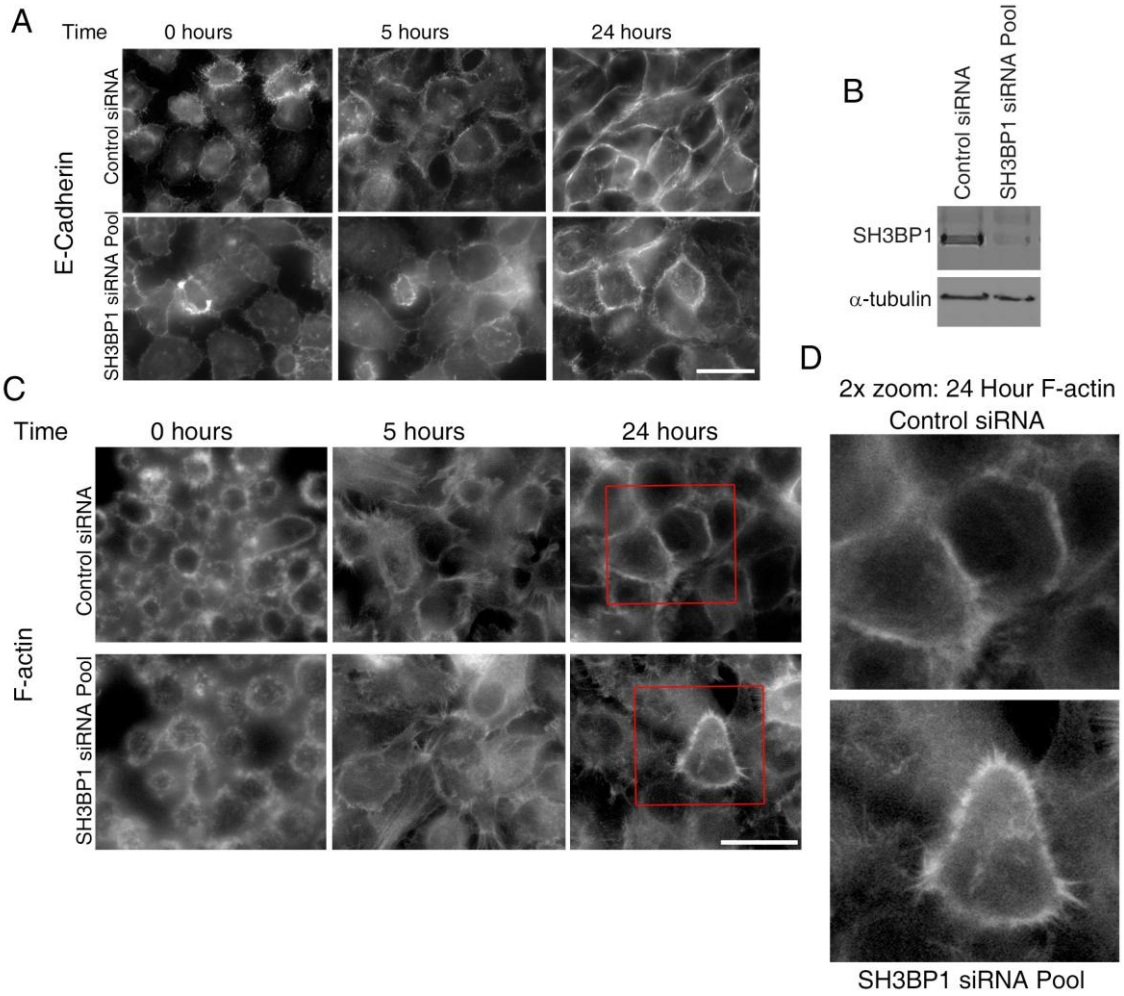

Figure 4.13 SH3BP1 depleted cells have a delay in adherens junction formation and display pronounced actin-based protrusions.

A431 cells were transfected with either control siRNA or a pool of SH3BP1-specific siRNAs and were plated in low calcium medium. Cells were fixed in paraformaldehyde and permeabilised with Triton X-100 at the timepoints of calcium reintroduction specified and were then stained for (A) E-cadherin and (C) F-actin. (B) Expression levels of SH3BP1 depletion were assessed at the end of the experiment and alpha-tubulin was used as a loading control. (D) Shows a 2x zoom of control and depleted F-actin staining clearly showing longer filopodia in SH3BP1 depleted conditions. Shown are epifluorescence images and zoomed basal images. Experiment was performed twice. Scale bar 10µm.

SH3BP1 localisation in different epithelia

I next investigated the subcellular localization of SH3BP1 in different epithelia more precisely to start to understand the mechanism by which it affects epithelial differentiation. In Caco-2 cells, SH3BP1 localizes to the AJC and its distribution overlaps with markers for TJs and AJs (Figure 4.14). Further analysis using confocal microscopy suggested that SH3BP1 localizes more toward the AJ than the TJ (Figure 4.15). However, its distribution did not precisely overlap with either of the two markers, indicating that it is not exclusively associated with a specific junction.

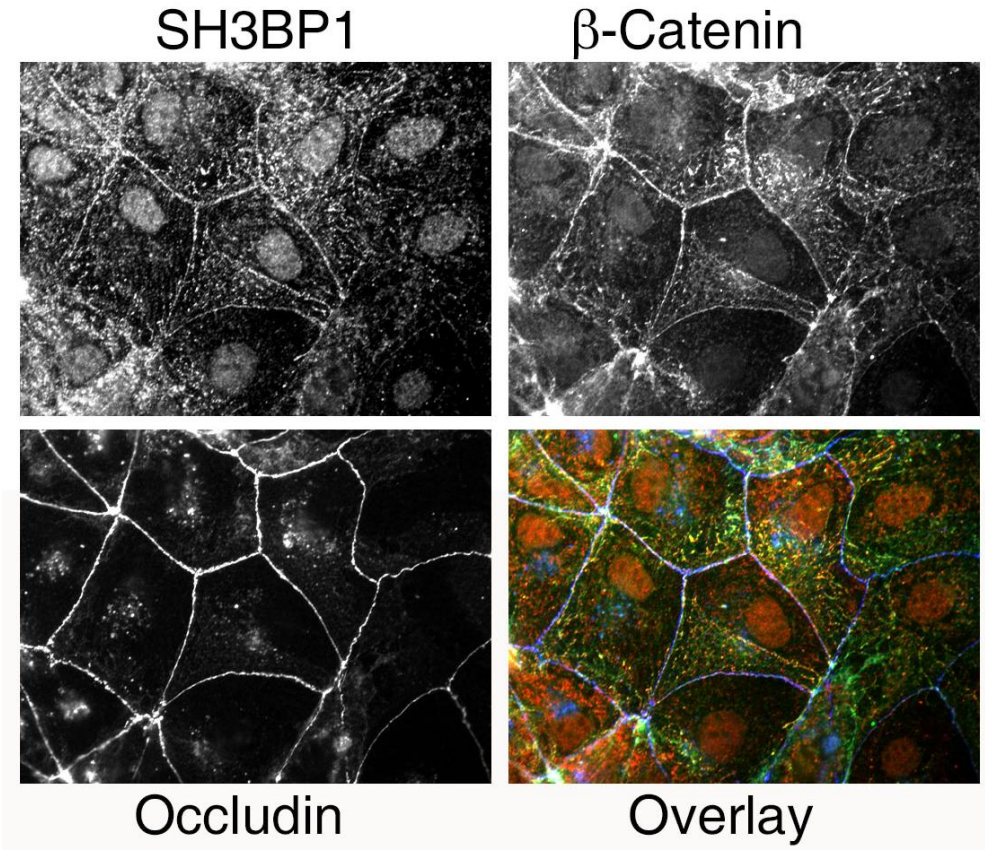

Figure 4.14 SH3BP1 is localized to the AJC in Caco-2 cells.

Caco-2 cells were immunostained with SH3BP1 (Red), occludin (Blue) and beta-catenin (Green) after being fixed with methanol. Shown are epifluorescence images. Experiment was performed three times. Scale bar 10µm.

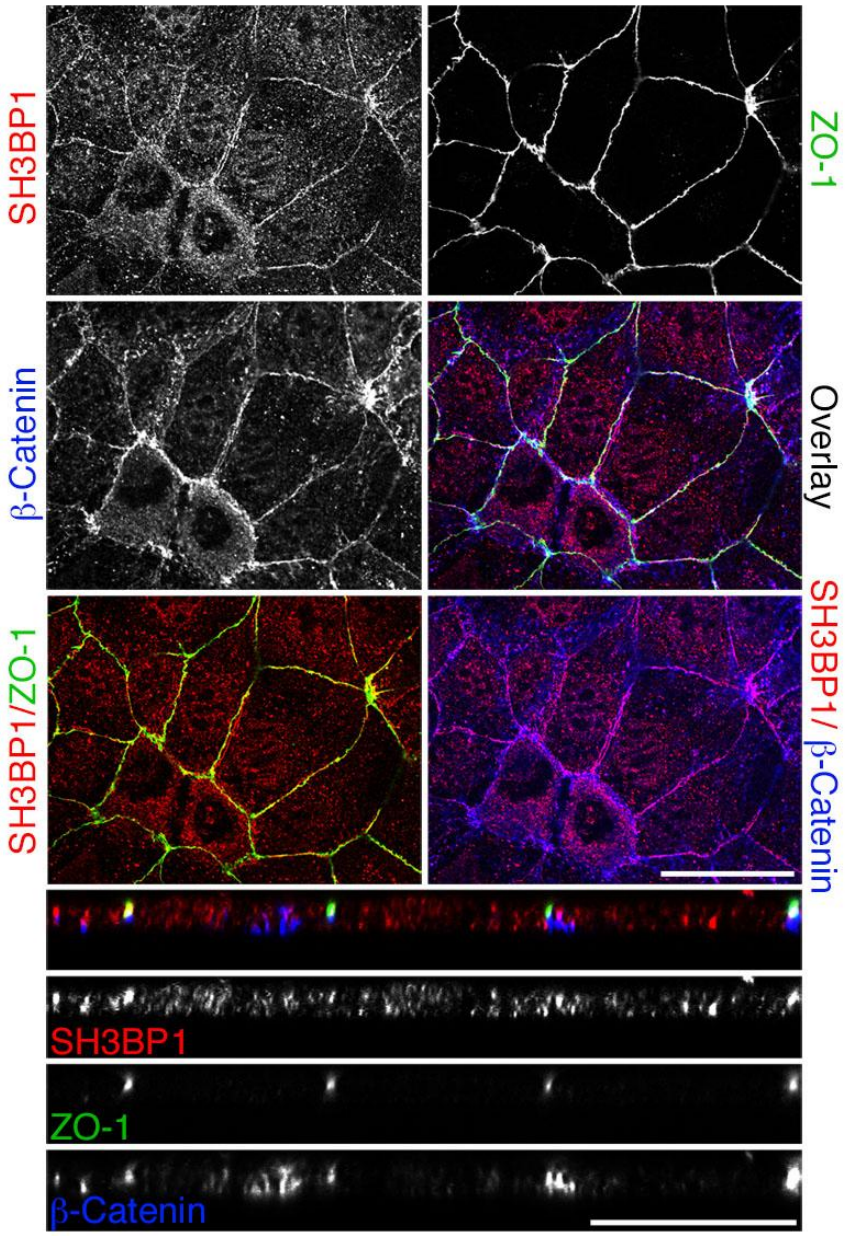

Figure 4.15 SH3BP1 is localized between the TJ and AJ in Caco-2 cells.

Caco-2 cells were fixed with methanol and stained with antibodies against SH3BP1 (red), ZO-1 (green), and beta-catenin (blue) and then analysed by confocal microscopy. Shown are sections representing the imaged areas and representative Z-line scans taken. Experiment was performed three times. Scale bar 10µm.

I next analysed the distribution of SH3BP1 in A431 cells as they allow the analysis of actin reorganisation and cell-cell junction formation in response to EGF receptor activation [274]. Therefore, analysis of junction formation can be studied in response to a physiological stimulus as opposed to manipulation of external calcium concentrations. In serum-starved A431 cells, ZO-1 is initially non-junctional but, upon EGF addition, is recruited to cell-cell junctions [274]. When this experimental protocol was applied to study SH3BP1, the GAP was recruited to dorsal ruffles within 5 minutes of EGF treatment. At dorsal ruffles, SH3BP1 co-localised with ZO-1 and F-actin; dorsal ruffle formation preceded junction formation (Figure 4.16). Given the role of EGF in the mobilisation of SH3BP1 from the cytosol to membranes, I next analysed whether EGF signalling could also stimulate junctional recruitment of SH3BP1 in Caco-2 cells. Serum-starved Caco-2 cells had only little SH3BP1 at junctions but recruitment was stimulated by the addition of EGF within 5 minutes (Figure 4.17). Conversely, if EGF receptor signalling was blocked in cells grown in standard serum-containing medium using the EGF receptor tyrosine kinase inhibitor PD153035 [275], the levels of junctional SH3BP1 were reduced in comparison to controls (Figure 4.17). These data indicate that growth factor signalling can stimulate SH3BP1 recruitment to sites of dynamic actin remodelling, such as dorsal ruffles, or that are enriched in F-actin, such as cell-cell junctions. Addition of EGF promotes a number of processes that involve Rho GTPases and stimulate actin dynamics [276]; hence, SH3BP1 maybe required for Rho GTPase regulation during such dynamic cellular processes.

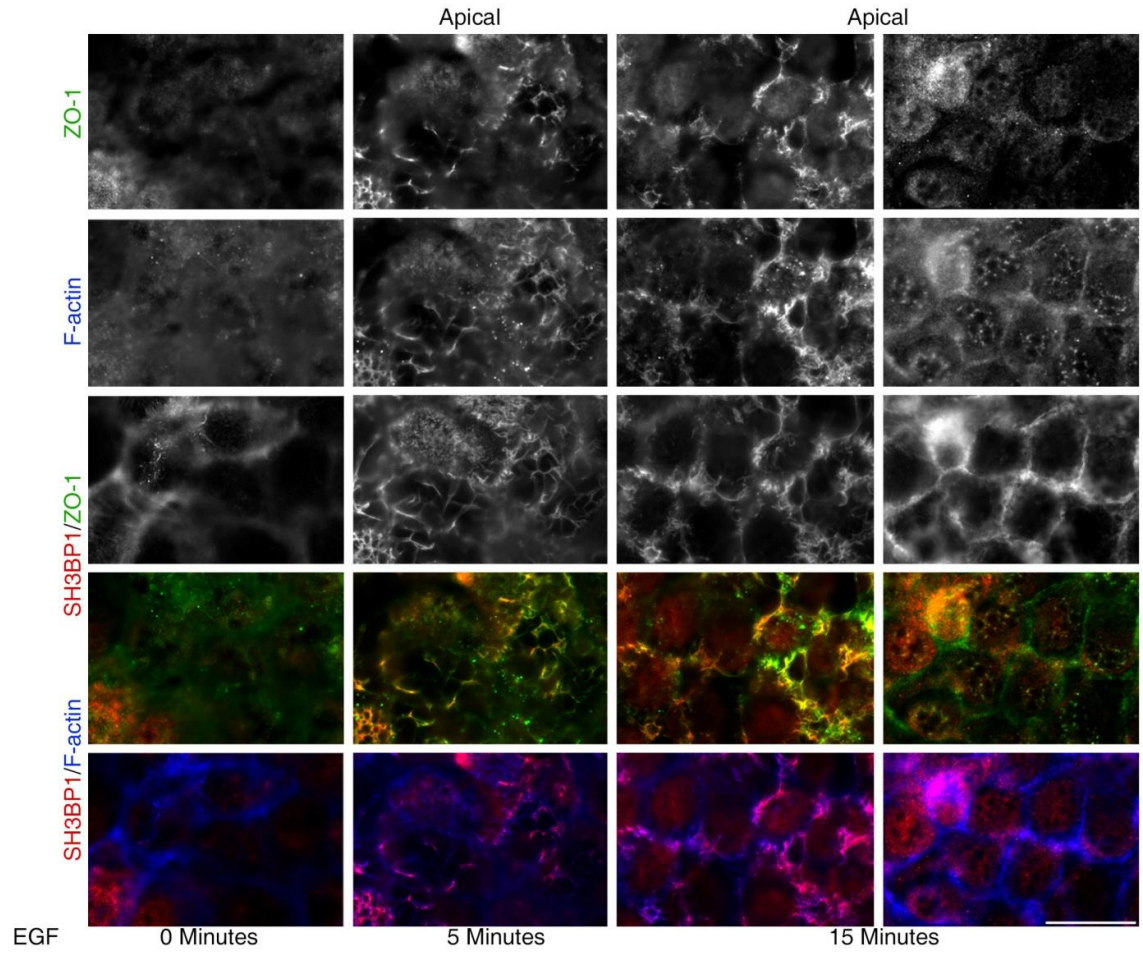

Figure 4.16 SH3BP1 is recruited to dorsal ruffles upon EGF stimulation of A431 cells.

Serum-starved A431 cells were stimulated with 100ng/ml EGF for specified timepoints, and immunostained with SH3BP1 (Red), F-actin (Blue) and ZO-1 (Green). Shown are epifluorescence images. Experiment was performed three times. Scale bar 10µm.

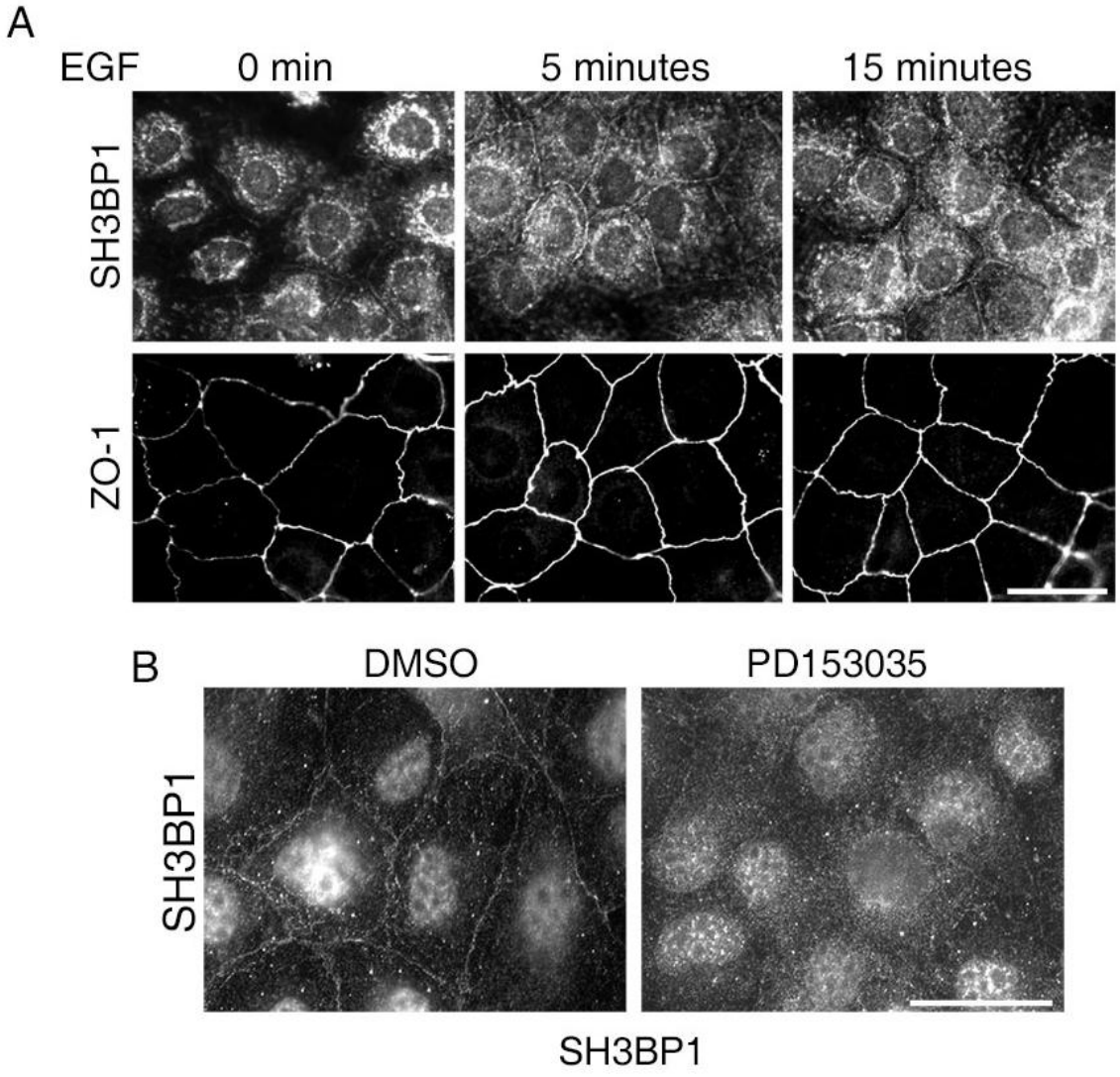

Figure 4.17 Regulation of SH3BP1 localisation by EGF signalling.

(A) Serum-starved Caco-2 cells were stimulated with 100ng/ml EGF for specified timepoints, and immunostained with antibodies against SH3BP1 and ZO-1. (B) Caco-2 cells were incubated with 3μM PD153035 for 24 hours or the same volume of DMSO used for the inhibitor as a control before fixation. The samples were subsequently immunostained for SH3BP1. Shown are epifluorescence images. Experiment was performed three times. Scale bar 10μm.

Given the role of EGF signalling in the localisation of SH3BP1, I next asked whether SH3BP1 plays a role in EGF-induced processes. As an experimental model, I employed A431 cells, as they lack ZO-1 at cell-cell junctions, and, if serum-depleted junctional ZO-1 can then be induced upon EGF stimulation [274, 277]. Upon depletion of SH3BP1, EGF stimulation did no longer lead to a continuous junctional distribution of ZO-1, but the junctional staining remained disrupted and discontinuous even at later timepoints (Figure 4.18). I also stained for the AJ marker beta-catenin. Unlike ZO-1, beta-catenin was present at junctions in unstimulated A431 cells. Nevertheless, depletion of SH3BP1 also led to disorganisation and discontinuous junctional distribution of beta-catenin with the peak of disruption occurring at the later timepoints of EGF stimulation (Figure 4.19).

I next analysed how depletion of SH3BP1 affects the actin cytoskeleton during EGF stimulation. A clear effect was observed in SH3BP1-depleted cells, as an increase in the number and length of the filopodia visualised by F-actin staining was observed (Figure 4.20). This was particularly striking after longer times of EGF stimulation, as basal filopodia seemed to grow in an uncontrolled manner. Uncontrolled filopodial growth correlated with the disruption of cell junctions. It is thus possible that the formation of cell junctions was defective because cells failed to control filopodial growth.

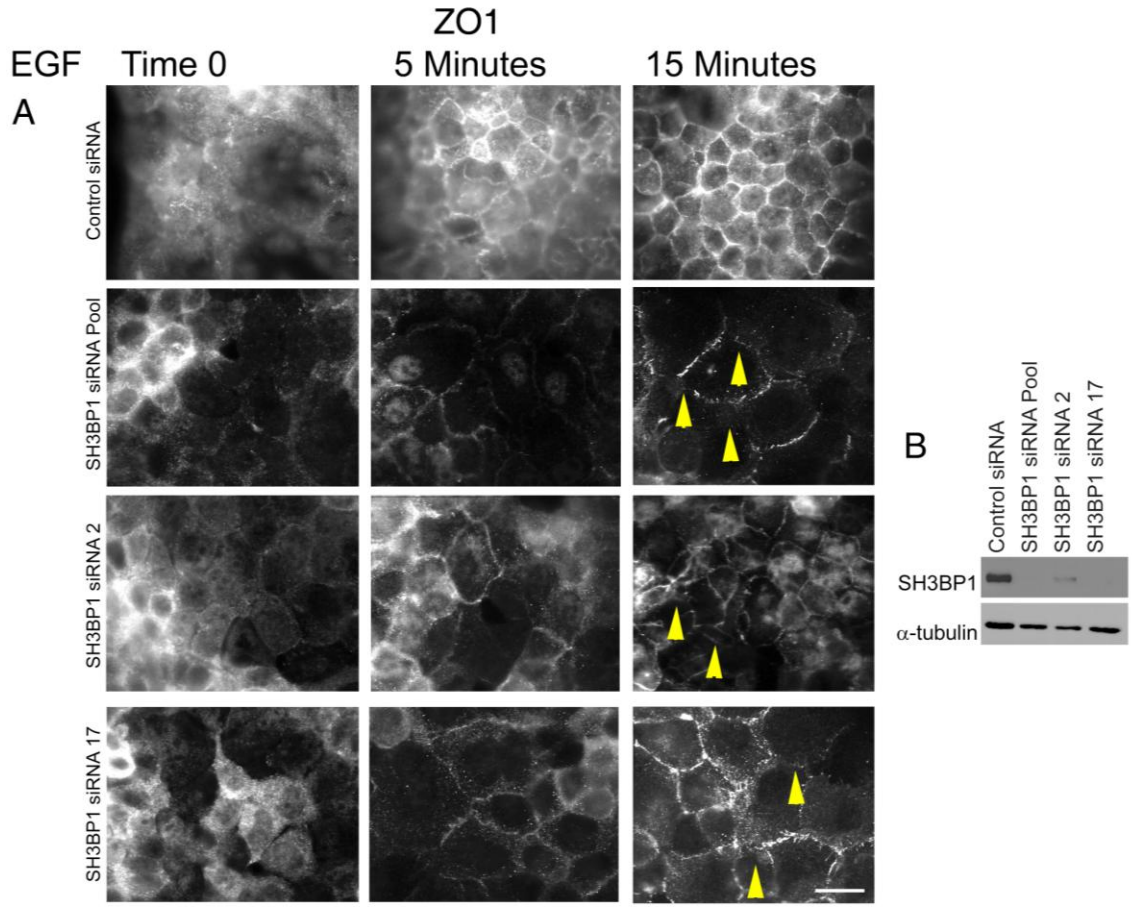

Figure 4.18 SH3BP1 depletion inhibits EGF-induced junctional recruitment of ZO-1 in A431 cells.

Serum-starved A431 cells that had been transfected with either control or SH3BP1-specific siRNAs were stimulated with 100ng/ml EGF as indicated. The cells were then either (A) fixed with paraformaldehyde and immunostained with ZO-1 antibodies, or (B) lysed with sample buffer and processed for immunoblotting. Arrows point to areas of junctional disruption. The levels of SH3BP1 depletion were assessed by blotting. Alpha-tubulin was used as a loading control. Shown are epifluorescence images. Experiment was performed three times. Scale bar 10µm.

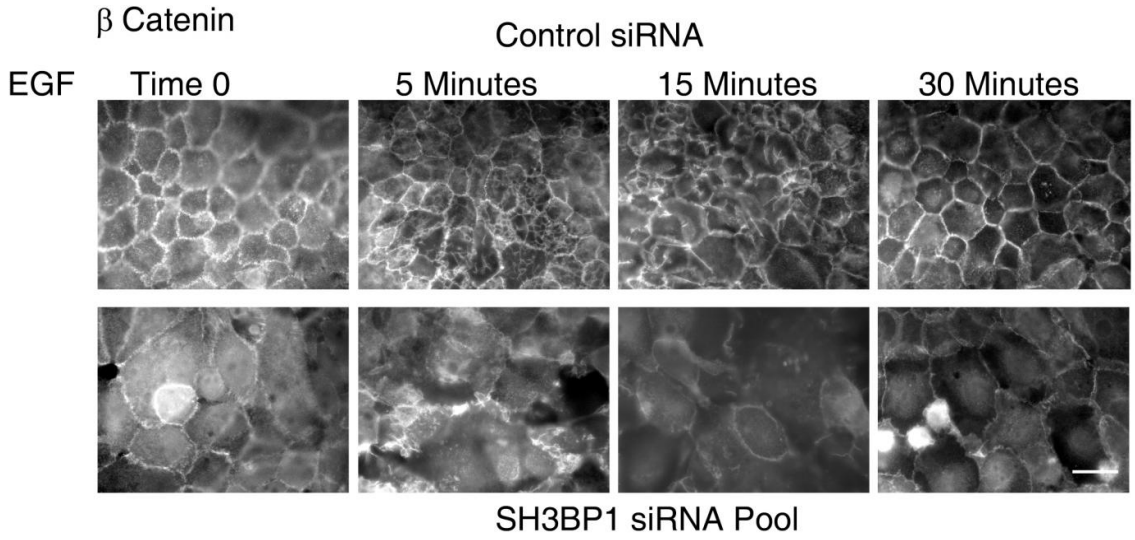

Figure 4.19 SH3BP1 depletion results in disruption of beta-catenin in A431 cells.

Serum-starved A431 cells that had been transfected with either control or SH3BP1-specific siRNAs were stimulated with 100ng/ml EGF as indicated. The cells were fixed with paraformaldehyde and immunostained for beta–catenin. Representative blot for SH3BP1 depletion can be seen in figure 4.18. Shown are epifluorescence images. Experiment was performed three times. Scale bar 10μm.

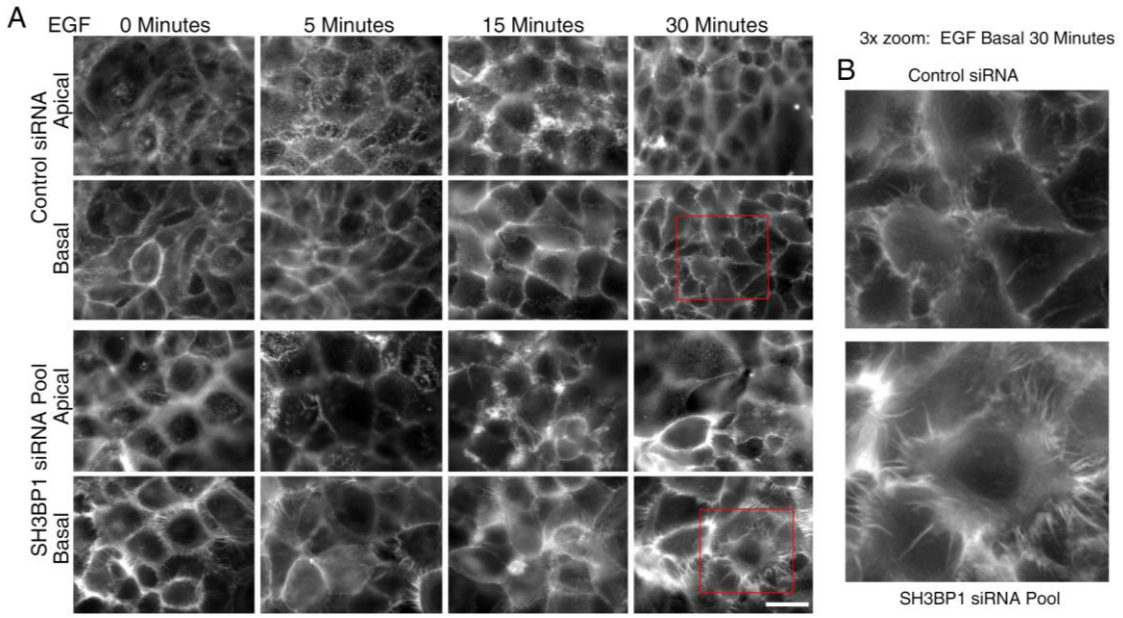

Figure 4.20 SH3BP1 depletion results in an increase in filopodial length.

Serum-starved A431 cells that had been transfected with either control or SH3BP1-specific siRNAs were stimulated with 100ng/ml EGF as indicated. (A) The cells were fixed with paraformaldehyde and stained with F-actin. Representative blot can be seen in figure 4.18. (B) Shown is a 3x zoom of control and depleted F-actin staining showing longer filopodia in SH3BP1 depleted cells. Shown are epifluorescence images. Experiment was performed three times. Scale bar 10µm.

In order to analyse further this increase in basal protrusions seen in fixed depleted samples, I made an EGFP-actin A431 cell line and recorded time lapse movies of depleted and control cells after EGF stimulation. As expected, actin dynamics was strongly influenced by SH3BP1 depletion. In control cells, EGF stimulation induced dorsal ruffling and led to the formation of a strong cortical perijunctional actin ring; in SH3BP1 depleted cells, however, actin dynamics was strongly reduced and did not extend beyond the extension of long filopodia (Figure 4.21 and Movies S1-S4). As with the original A431 cell line, GAP depleted cells were very flat and spread. Hence, expression of SH3PB1 seems to be required to maintain actin dynamics and support EGF-induced actin reorganisation.

Having observed a defect in junction formation, as well as a disruption and decrease in dorsal ruffle formation, I next assessed if depletion had an effect on ruffles containing cell-cell junction markers. Depletion indeed resulted in a decrease in recruitment of beta-catenin and ZO-1 to EGF-induced dorsal ruffles, suggesting that SH3BP1 affects membrane recruitment of junctional components (Figure 4.22).

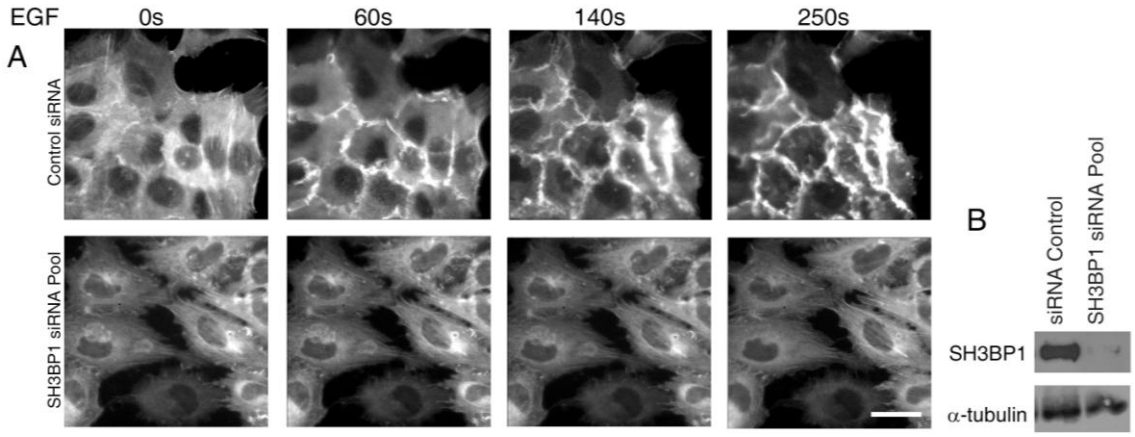

Figure 4.21 SH3BP1 depletion results in reduced actin dynamics and reorganisation.

(A) A431 cells expressing EGFP-actin that had been transfected for 96 hours with control or SH3BP1-specific siRNAs were stimulated with 100ng/ml EGF and a time-lapse movie was taken. Time is shown in seconds after EGF was added. (B) Expression levels of SH3BP1 depletion were assessed at the end of the experiment and alpha-tubulin was used as a loading control. Experiment was performed three times. Scale bar 10µm.

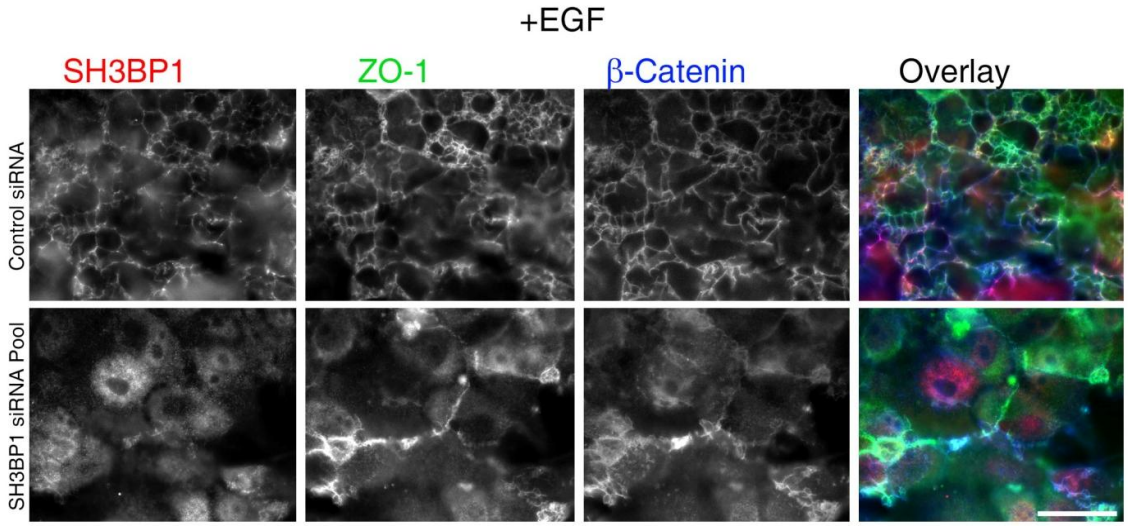

Figure 4.22 SH3BP1 depletion results in a decrease in dorsal ruffles.

Serum-starved A431 cells that had been transfected with either control or SH3BP1-specific siRNAs were stimulated with 100ng/ml EGF as indicated. The cells were fixed with paraformaldehyde and immunostained for SH3BP1 (Red), ZO-1 (Green) and beta-catenin (blue). Shown are epifluorescence images. Representative blot can be seen in figure 4.18. Experiment was performed three times. Scale bar 10µm.

Dorsal ruffles have been linked to EGF receptor internalisation [278]; hence, I next analysed EGF internalisation using fluorescently labelled growth factor. Stimulation led to the appearance of EGF positive dorsal ruffles within 3 minutes followed by internalisation and vesicular staining within 15 minutes. In SH3BP1 depleted cells, the dorsal labelling was disorganised, but the ligand was still internalised, although apparently more slowly (Figure 4.23). SH3BP1 expression was not required for EGF receptor signalling as such, as ERK was activated with similar kinetics in control and GAP depleted cells. This suggests that inhibition of EGF receptor signalling *per se* was not causing the lack of dorsal ruffling in SH3BP1 depleted cells (Figure 4.24).

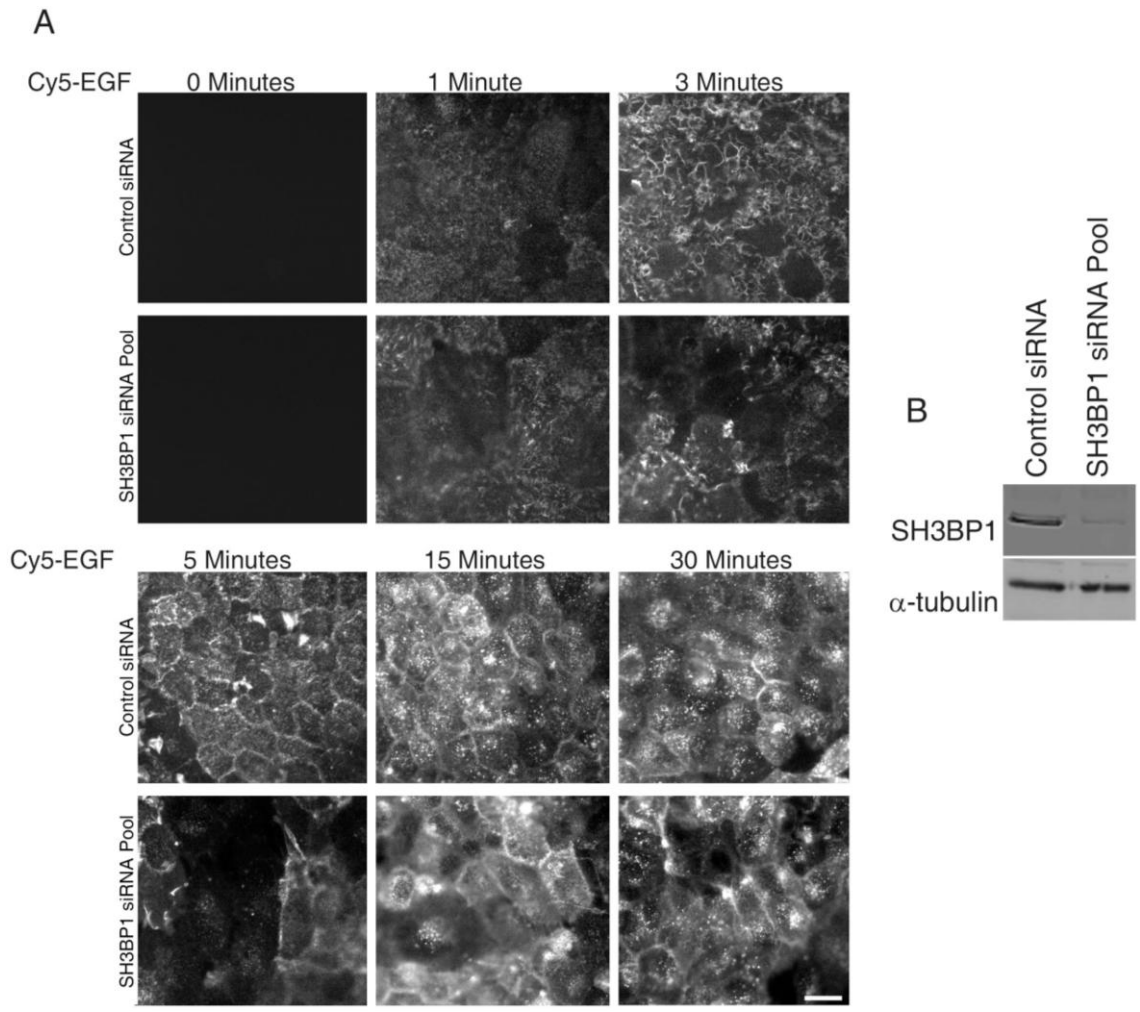

Figure 4.23 Effect of SH3BP1 depletion on EGF internalisation.

(A) Serum-starved A431 cells that had been transfected with either control or SH3BP1-specific siRNAs were stimulated with 100ng/ml EGF tagged with Cy5 as indicated. The cells cells were either fixed with paraformaldehyde or lysed with sample buffer and processed for immunoblotting. (B) The levels of depletion were assessed by blotting for SH3BP1. Alpha-tubulin was used as a loading control. Shown are epifluorescence images. Experiment was performed twice. Scale bar 10µm.

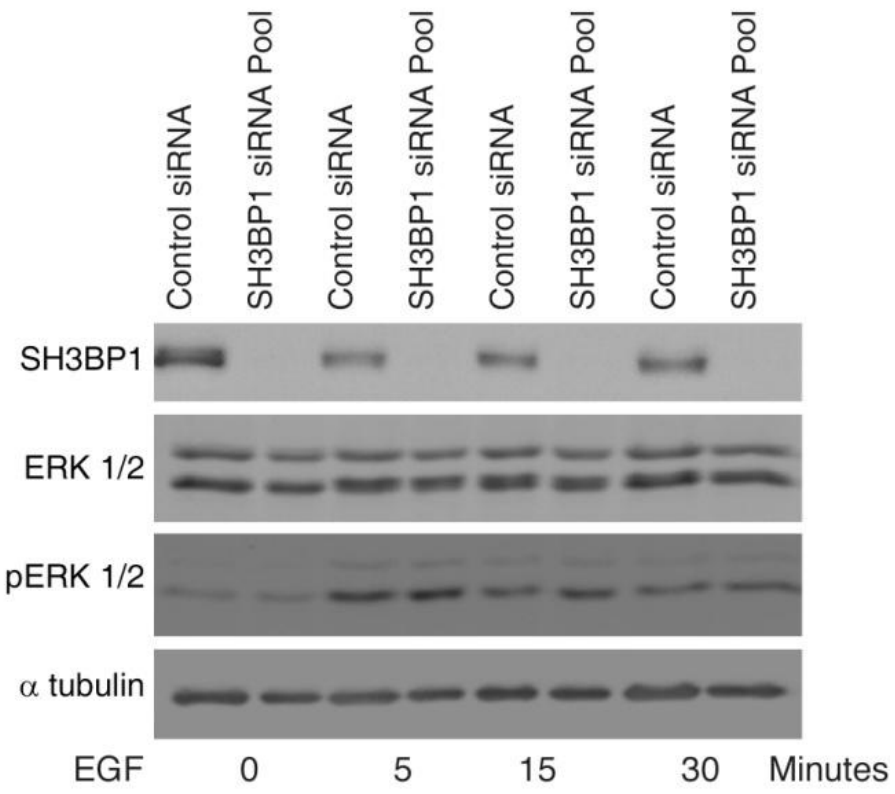

Figure 4.24 SH3BP1 depletion and ERK 1/2 activation.

Serum-starved A431 cells that had been transfected with either control or SH3BP1-specific siRNAs were stimulated with 100ng/ml EGF as indicated. Extracts were then collected and immunoblotted for SH3BP1, and total and phosphorylated ERK. Alpha-tubulin was used as a loading control. Experiment was performed twice.

SH3BP1 functions as a GAP for Cdc42 and Rac1

SH3BP1 is a known GAP that can stimulate GTP hydrolysis by Rac and Cdc42 *in vitro* [187]. In order to assess the levels of the main Rho GTPases, I performed a G-LISA assay, which measures global levels of active Rho GTPases. Using Caco-2 cells, I found that there was no apparent increase in any of the Rho GTPases, in depleted cells in comparison to control cells thus indicating that the GAP activity of SH3BP1 does not affect overall levels of Rho GTPases in this cell type (data not shown).

I next decided to use serum-starved A431 cells that were stimulated with EGF in order to assess the effect of SH3BP1 depletion on Rho GTPase activity in this model and to test whether the effect of the GAP activity of SH3BP1 may be transient. I found that EGF stimulation led to an increase in active Cdc42 within 15 minutes as expected (Figure 4.25). In SH3BP1 depleted cells, the levels of active Cdc42 was increased throughout all timepoints and gradually increased with increasing time of EGF stimulation, indicating that depletion of the GAP leads to enhanced Cdc42 activity. Increased Cdc42 activity thus corresponds with the increase of filopodial length described above. Upon depletion and measuring levels of active Rac1, only at 15 minutes of EGF stimulation a significant increase in active Rac1 was observed, suggesting that the effect on Rac1 is more modest (Figure 4.25). Previously, it was shown that upon EGF stimulation, Rac1 activation is transient, while Cdc42 activation is sustained, which may contribute to this difference between the two GTPases [256].

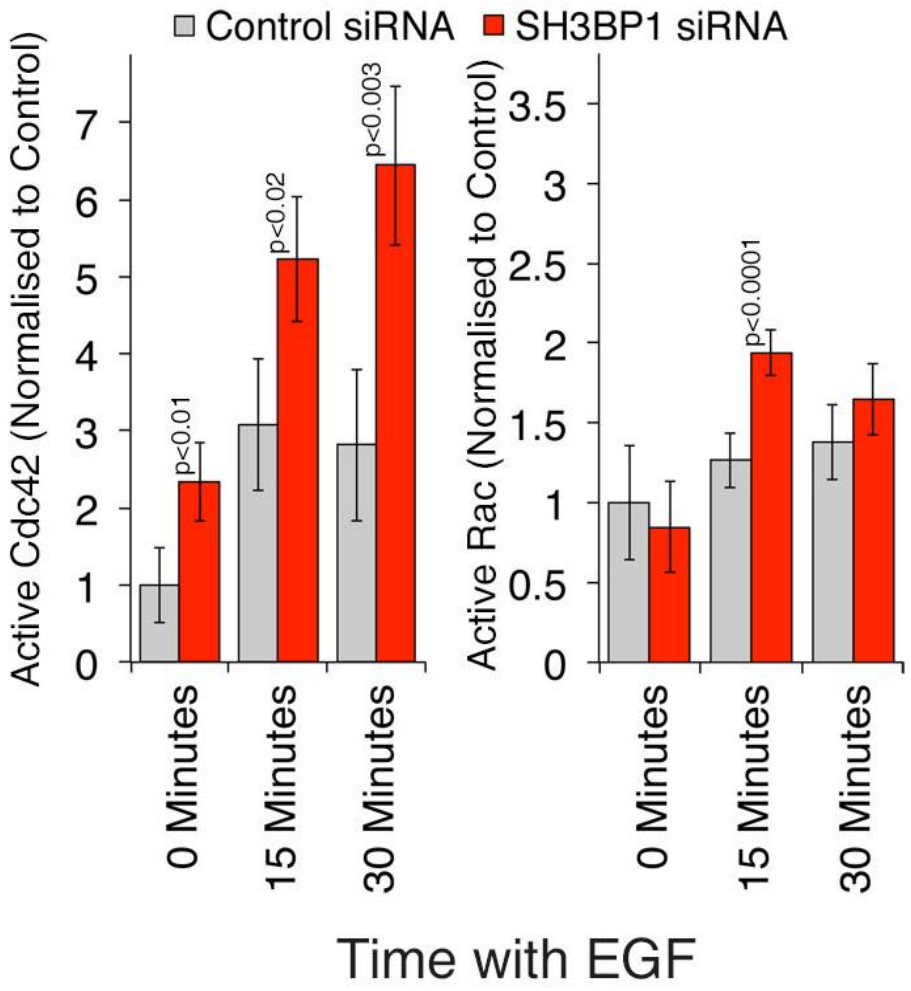

Figure 4.25 SH3BP1 depletion leads to enhanced Cdc42 and Rac1 activity.

A G-LISA assay was performed to assess active Rho GTPase levels in extracts from serum-starved or EGF stimulated (100ng/ml) A431 cells 96 hours after transfection with either control siRNA or a pool of SH3BP1 specific siRNAs. Levels of active (A) Cdc42 and (B) Rac1 are displayed normalized to control levels at time zero for the respective Rho GTPase. The bar graphs represent the average of three independent experiments, each using triplicate samples. Addition of recombinant Cdc42 as a positive control gives a value of 9.255 (Normalised to control). Addition of recombinant Rac1 as a positive control gave a value of 4.134 (Normalised to control). Error bars represent $\pm$ 1 SD.

Deregulation of Rho GTPase activity may not only involve altered total levels of activity but may lead to a spatial disorganisation. Therefore, I next determined whether depletion of SH3BP1 affected the subcellular localization of active Cdc42 and Rac1. Using an antibody raised against a GTP-bound form of Cdc42, we found that transfection of active Cdc42 GEFs stimulated increased fluorescent signals, indicating that the antibody indeed recognised active Cdc42 (Figure 4.26d and e). In Caco-2 cells, this antibody stained cell-cell junctions,and this signal disappeared when Cdc42 was depleted by transfecting siRNAs, indicating that it was due to junctional Cdc42 (Figure 4.26f). SH3BP1 depletion resulted in characteristically spread cells with a loss of the well-defined linear distribution of GTP-bound Cdc42 along cell junctions. Active Cdc42 appeared more diffuse and was spread away from the junction, suggesting that SH3BP1 is required to confine active Cdc42 at cell-cell contacts (Figure 4.26a).

Using the active Cdc42 antibody in EGF stimulated A431 cells, I found that Cdc42-GTP localized to dorsal ruffles within 5 minutes of stimulation; whereas in SH3BP1 depleted cells dorsal ruffles were disorganized and contained less GTP-bound Cdc42, and Cdc42-GTP was spread throughout the cells including filopodia (Figure 4.27). Moreover, stimulation with EGF led to clearly increased levels of staining. Active Rac1 also increased in response to EGF and was more prominent along the apical membrane of the cells, but did not accumulate in the large ruffles like in Cdc42. In depleted cells, active Rac1 often accumulated in perinuclear cup-like structures, indicating that the spatial organisation of Rac1 signalling was also disrupted (Figure 4.28). These observations thus indicate that SH3BP1 is required for the proper spatial

organisation of Cdc42 activity in A431 and Caco-2 cells. Whereas the GAP also regulates Rac1 in A431 cells, no effect on Rac1 activity was observed in Caco-2 cells (not shown).

I next assessed the levels of phosphorylated cofilin in depleted cell lysates, as this protein is important for the regulation of actin dynamics and it is regulated by phosphorylation in response to Rho GTPase activation [279]. Unstimulated and EGF stimulated SH3BP1 depleted A431 cells showed an increase in the levels of phosphorylated cofilin, confirming increased Rho GTPase activity (Figure 4.29). As the phosphorylated form of cofilin is inactive, cofilin inactivation may be at least one of the reasons why filopodia became so large and, as suggested by the videos of GFP-actin expressing cells, there seemed to be a general reduction in actin dynamics upon SH3BP1 depletion.

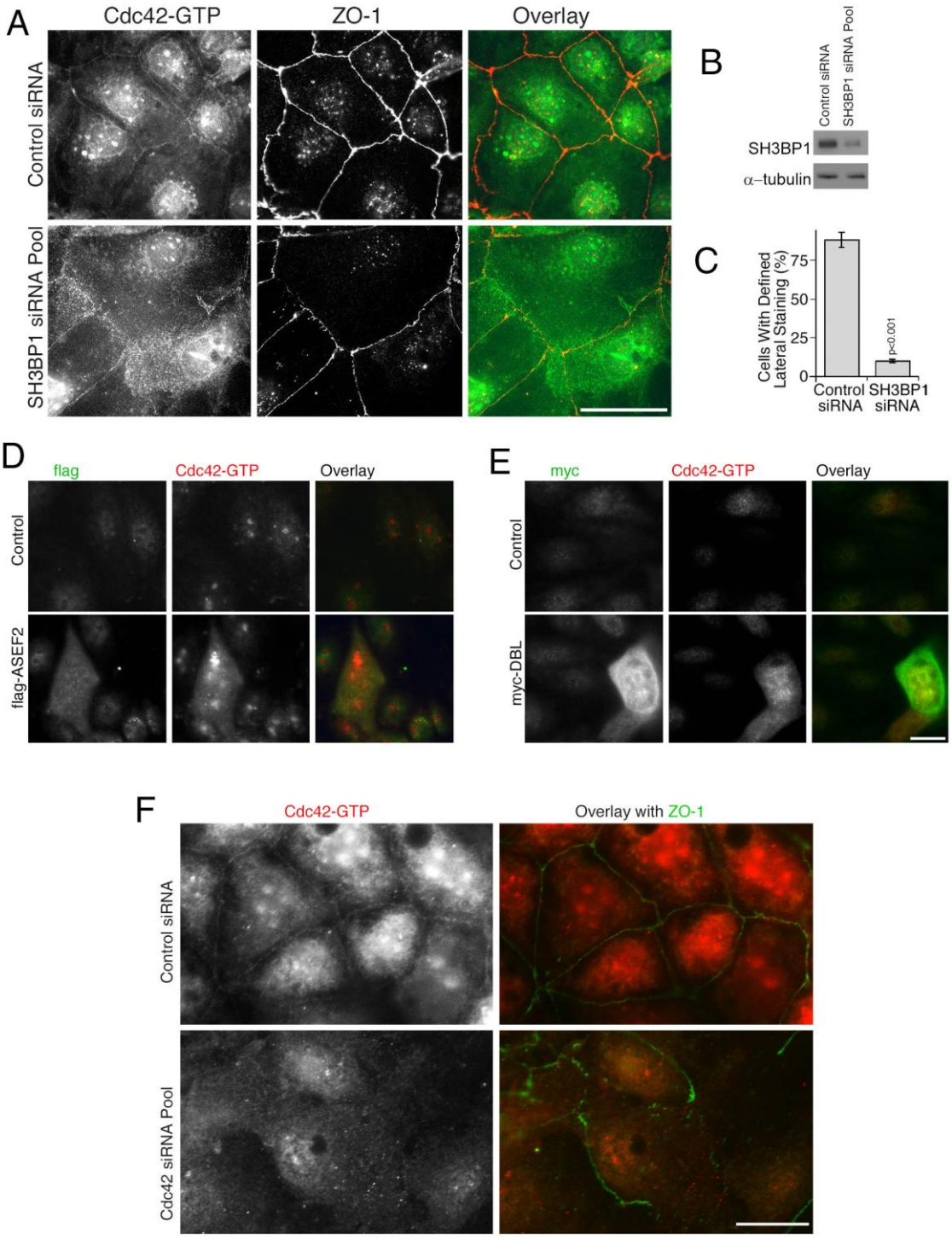
A
Cdc42-GTP
ZO-1
Overlay
Control siRNA
SH3BP1 siRNA Pool
B
Control siRNA
SH3BP1 siRNA Pool
SH3BP1
α–tubulin
C
Cells With Defined Lateral Staining (%)
75
50
25
0
p<0.001
Control siRNA
SH3BP1 siRNA
D
flag
Cdc42-GTP
Overlay
Control
flag-ASEF2
E
myc
Cdc42-GTP
Overlay
Control
myc-DBL
F
Cdc42-GTP
Overlay with ZO-1
Control siRNA
Cdc42 siRNA Pool

Figure 4.26 Loss of junctional confinement of active Cdc42 in SH3BP1 depleted cells.

Caco-2 cells were transfected with either control siRNA or a pool of SH3BP1 specific siRNAs. After 96 hours, the cells were either fixed with methanol and (A) immunostained with active Cdc42 (green) and ZO-1 (Red) or (B) lysed with sample buffer and processed for immunoblotting. The levels of depletion were assessed by blotting for SH3BP1. Alpha-tubulin was used as a loading control. (C) Levels of lateral staining in control and depleted samples were assessed. (D and E) HCE cells were transfected with either flag-tagged ASEF2 or myc-tagged DBL, two GEFs that stimulate Cdc42. The cells were then fixed with either methanol or PFA followed by processing for immunofluorescence with antibodies against the epitope tags and GTP-bound Cdc42. (F) For Cdc42 siRNA, Caco-2 cells were transfected with either control siRNA or a pool of Cdc42 specific siRNAs before fixation with methanol and staining with anti-GTP–bound Cdc42 and ZO-1 antibodies. Shown are epifluorescent images. Experiment was performed three times. Scale bar 10μm.

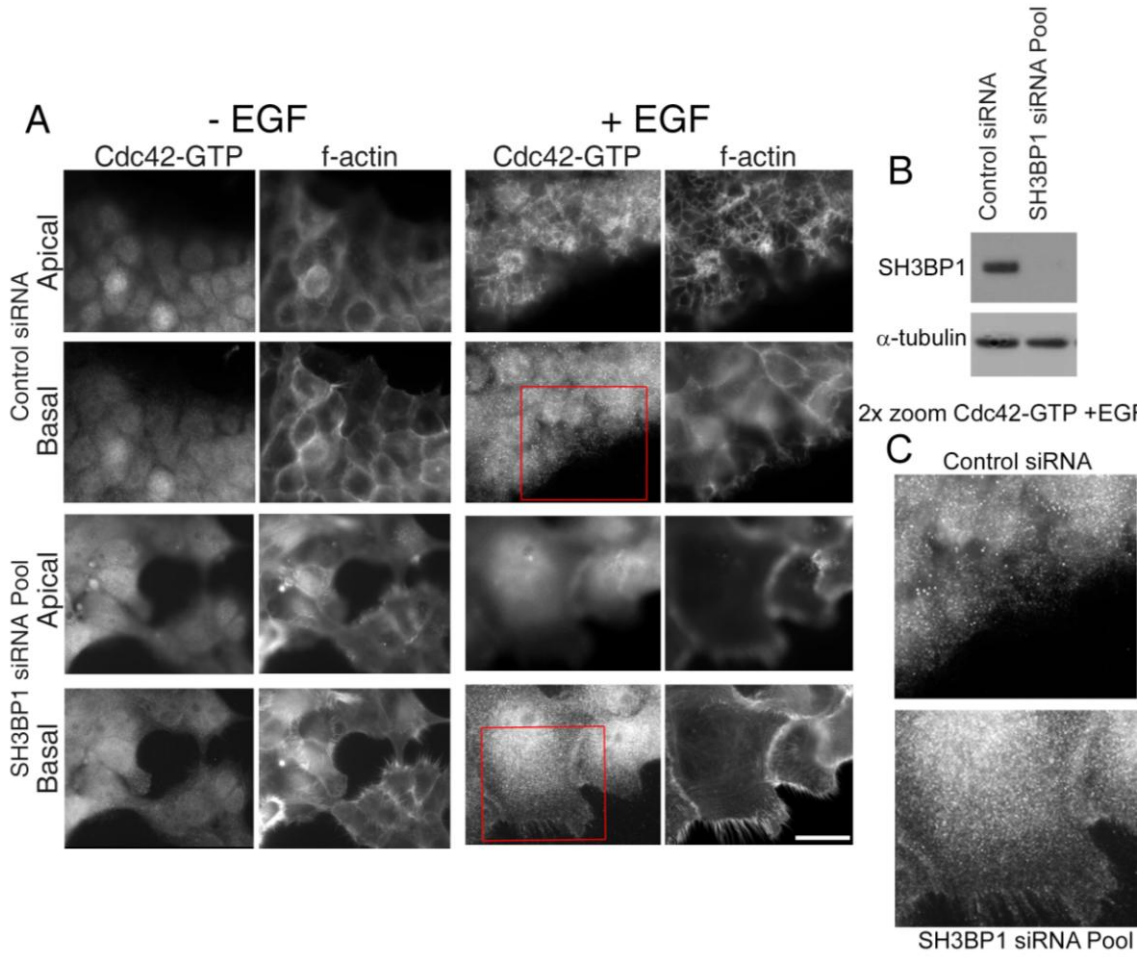

Figure 4.27 Dispersal of active Cdc42 in SH3BP1 depleted cells.

(A) Serum-starved A431 cells were stimulated with 100ng/ml EGF for specified timepoints after transfection with either control siRNA or a pool of SH3BP1 specific siRNAs. The cells were then fixed with paraformaldehyde and immunostained with the antibody against active Cdc42. (B) Depletion was assessed by blotting for SH3BP1. Alpha-tubulin was used as a loading control. (C) A 2x zoom of control and SH3BP1 depleted basal shots in EGF stimulated conditions is shown to emphasise the filopodia elongation induced by depletion. Shown are epifluorescent images. Experiment was performed three times. Scale bar 10µm.

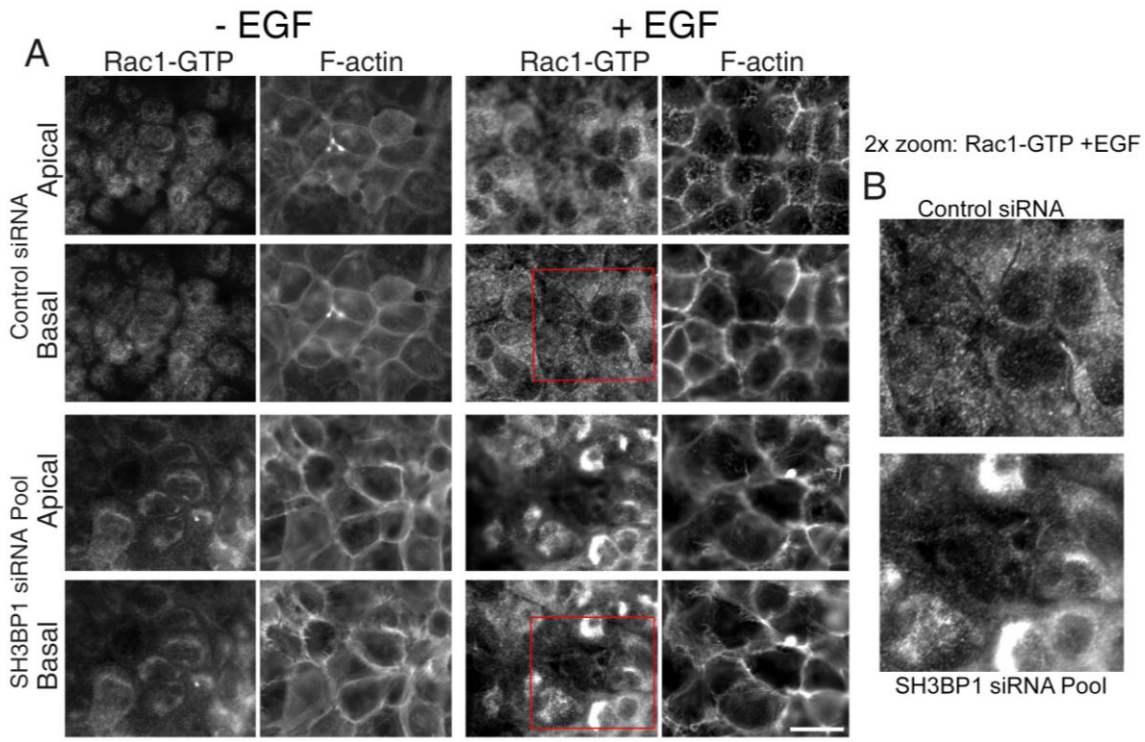

Figure 4.28 Active Rac1 is increased apically in SH3BP1 depleted cells.

Serum-starved A431 cells were stimulated with 100ng/ml EGF for specified timepoints after transfection with either control siRNA or a pool of SH3BP1 specific siRNAs. After 96 hours, the cells were fixed with paraformaldehyde and immunostained with the antibody against active Rac1. Depletion was assessed by blotting for SH3BP1. Alpha-tubulin was used as a loading control. Shown are epifluorescence images. Experiment was performed three times. Scale bar 10µm.

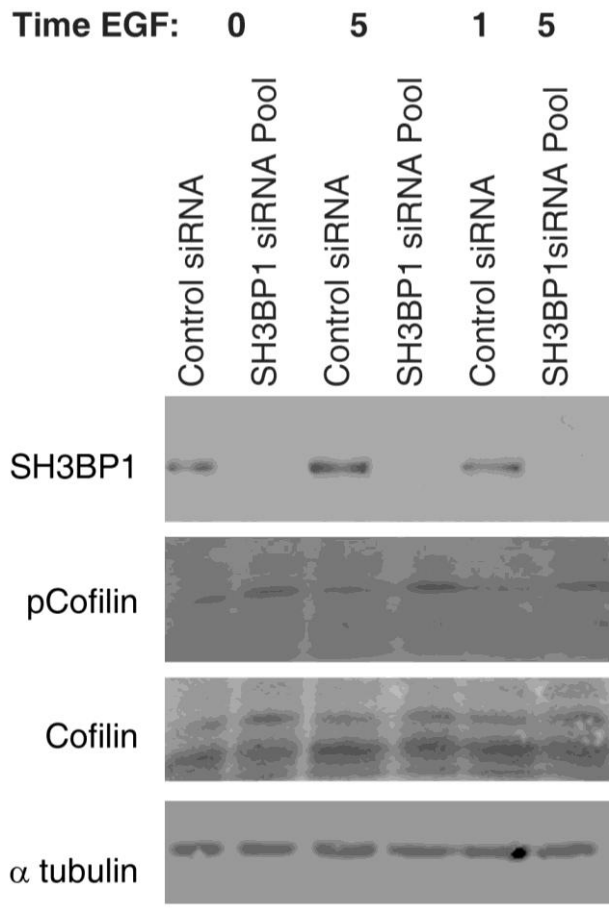

Figure 4.29 SH3BP1 depletion results in higher levels of cofilin and p-cofilin.

Whole cell lysates of A431 cells that had been transfected with either control siRNA or a pool of SH3BP1 specific siRNAs. After 72 hours extracts were serum-starved for 16 hours, before being stimulated with EGF, collected and immunoblotted for SH3BP1, cofilin and p-cofilin. Alpha tubulin was used as a loading control. The experiment was performed three times.

Finally, I assessed the effect SH3BP1 depletion on active Cdc42 in live cells using a FRET-based biosensor for Cdc42 [280]. In control Caco-2 cells, the FRET signal was enriched along cell-cell junctions and preferentially apical as opposed to basal; in depleted cells, the enrichment along cell-cell contacts was lost and the signal was more basal (Figure 4.30). In EGF-stimulated A431 cells, higher mean FRET activities were also measured along the apical surface than along the base of the cells and activity along cell-cell contacts was reduced upon depletion of SH3BP1 (Figure 4.31). As the transiently transfected FRET sensors are expressed at different levels in different cells, only the relative FRET levels were determined as the absolute levels are concentration dependent; hence, no conclusions about total levels of activity can be drawn. Taken together, these data suggest that SH3BP1 is a functionally important GAP for Cdc42 in two epithelial model cell lines and that depletion of the GAP results in a spatial disorganisation of Cdc42 signalling.

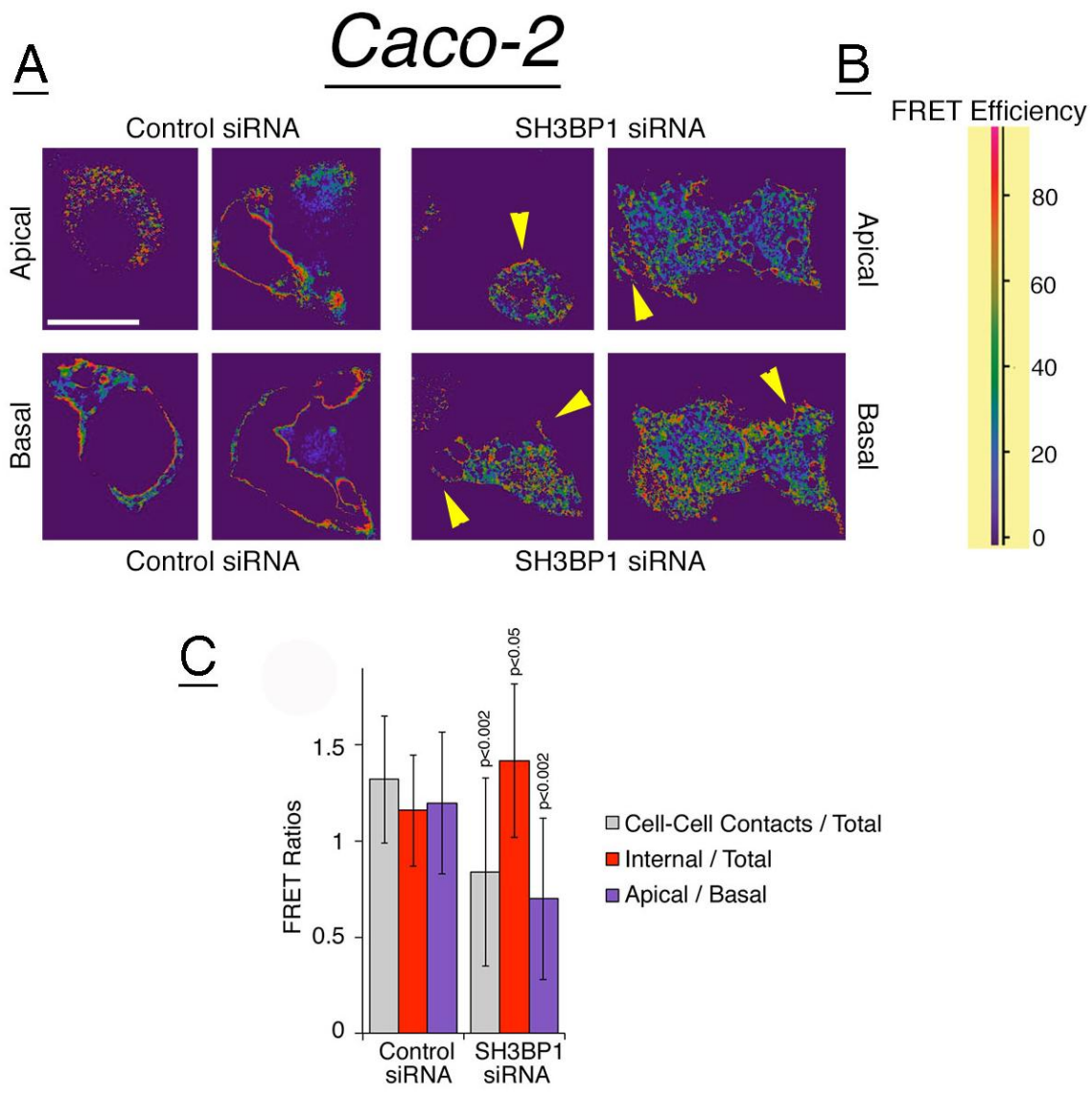
A
Caco-2
B
FRET Efficiency
Control siRNA
SH3BP1 siRNA
Apical
Basal
80
60
40
20
0
C
FRET Ratios
1.5
1
0.5
0
p<0.05
p<0.002
p<0.002
Control siRNA
SH3BP1 siRNA
Cell-Cell Contacts / Total
Internal / Total
Apical / Basal

Figure 4.30 SH3BP1 regulates the spatial distribution of active Cdc42 in Caco-2 cells.

(A) Caco-2 cells were transfected with either control siRNA or a pool of SH3BP1 directed siRNAs, and 48 hours later with a plasmid encoding the Cdc42 FRET biosensor. FRET was imaged by gain of donor fluorescence after acceptor bleaching. (B) Scale representing the colour coding of the FRET efficiency. Note, areas of highest FRET efficiency are encoded in red. (C) Quantification of images was prepared by normalizing FRET activity in specific cellular regions to the total FRET activity of quantified cells (cell-cell contacts, grey bars; internal cytoplasm, red bars; apical/basal ratio, purple bars). Yellow arrows represent areas of high FRET efficiency in GAP depleted cells as they are coloured in red (see FRET efficiency scale). Shown are means of different fields **+/-** 1 SD (n= 12). The experiment was performed three times. Scale bar 10µm.

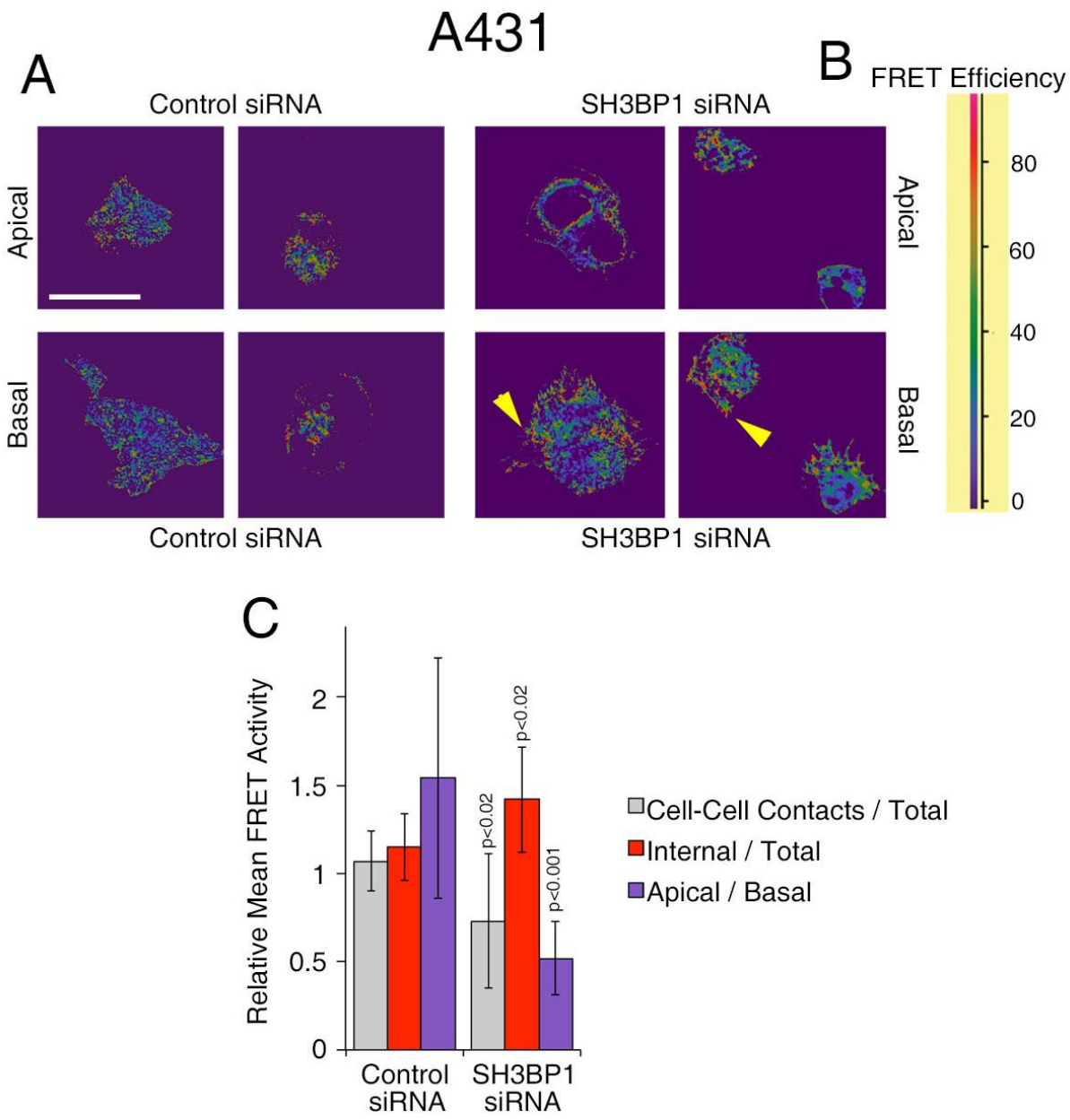
A431
A
Control siRNA
SH3BP1 siRNA
Apical
Basal
B
FRET Efficiency
80
60
40
20
0
C
Relative Mean FRET Activity
2
1.5
1
0.5
0
p<0.02
p<0.02
p<0.001
Control siRNA
SH3BP1 siRNA
Cell-Cell Contacts / Total
Internal / Total
Apical / Basal

Figure 4.31 SH3BP1 regulates the spatial distribution of active Cdc42 in A431 cells.

(A) A431 cells were transfected with either control siRNA or a pool of SH3BP1 directed siRNAs, and 48 hours later with a plasmid encoding the Cdc42 FRET biosensor. Cells were stimulated with 100ng/ml EGF. (B) Scale representing the colour coding of the FRET efficiency. (C) FRET was imaged and quantified as in figure 4.30. Yellow arrows point to areas of high and medium FRET efficiency, as they are coloured in red and green respectively (see FRET efficiency scale). Shown are means of 11 different fields +/- 1 SD (n= 11). The experiment was performed three times. Scale bar 10μm.

Effect of SH3BP1 overexpression on cell junctions

SH3BP1 is a 701 amino acid protein that contains three main domains. A Bin/Amphiphysin/Rvs(BAR) domain located near the N-terminus, a RhoGAP domain, and, finally, an SH3 binding domain found in the C-terminus (Figure 4.32). Using the full length cDNA as a template for PCR reactions, a full length HA-tagged cDNA was generated and inserted into an expression vector. An analogous construct was generated in which the catalytic activity of the GAP domain was inactivated by substituting an evolutionarily conserved catalytic arginine residue. This type of mutation has previously been shown to result in a GAP inactive construct [159, 189].

I first checked expression of the constructs by transfecting them in both Caco-2 and A431 cells. Immunoblotting with antibodies against the HA-epitope tag revealed that both constructs were expressed well and at comparable levels (Figure 4.32). Transfection of the wild-type protein did not have any obvious morphological consequences on the cells. However transfecting the mutant protein induced changes in the organisation of the actin cytoskeleton, such as filopodia-like structures (Figure 4.33), suggesting that this construct exerts a dominant-negative effect and that the GAP activity is required for the normal function of SH3BP1.

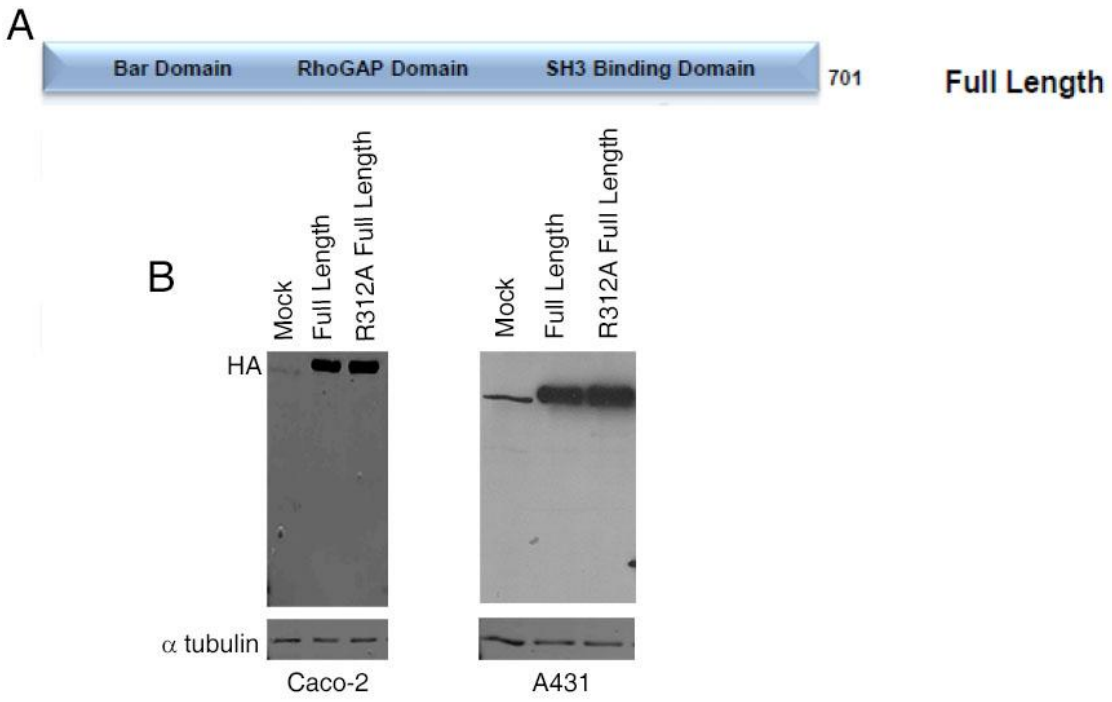

Figure 4.32 Expression of HA-tagged SH3BP1 cDNAs in Caco-2 and A431 cells.

(A) Diagram of structure of full length SH3BP1. (B) cDNAs encoding HA-tagged wild-type or GAP deficient SH3BP1 were overexpressed in Caco-2 and A431 cells for 24 hours before extracts were collected. Expression of SH3BP1 was analysed by immunoblotting with HA tag antibodies. Alpha-tubulin was used as a loading control. Experiment was performed three times.

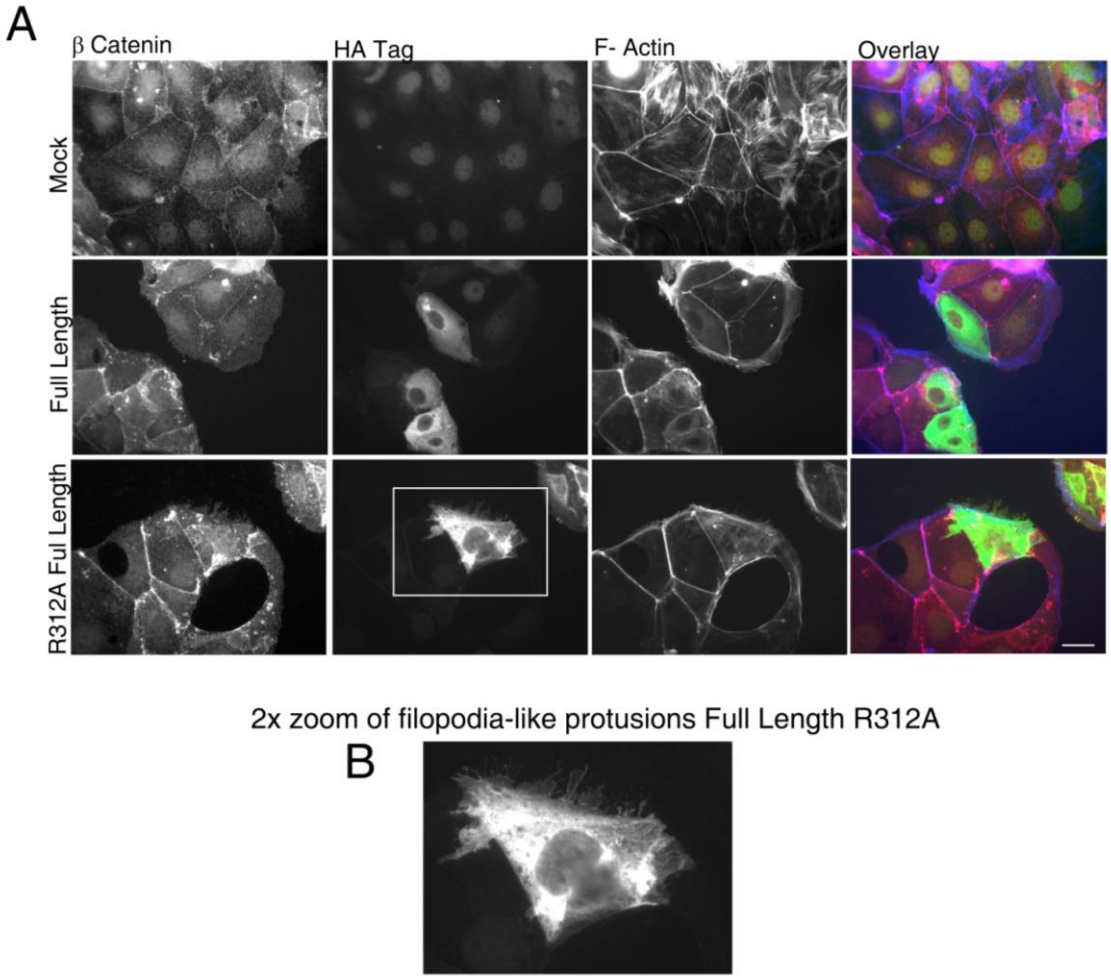

Figure 4.33 SH3BP1 R312A expression affects organisation of the actin cytoskeleton.

(A) cDNAs encoding HA-tagged wild-type or GAP deficient SH3BP1 were transiently expressed in Caco-2 cells for 24 hours before being fixed in paraformaldehyde and immunostained with HA tag (green), beta-catenin (red) and F-actin (blue). (B) 2x zoom of R312A mutant emphasising the filopodia-like protrusions produced. Shown are epifluorescent images. The experiment was performed twice. Scale bar 10μm.

As depletion of SH3BP1 caused activation of Cdc42 and defects in junction assembly, I next asked whether the two processes are indeed related using the GAP deficient mutant. Therefore, I generated a SH3BP1 cDNA resistant to one of the SH3BP1 siRNAs in order to perform complementation experiments. Three silent point mutations were required in order to generate this construct (see material and methods). I first assessed the efficiency of the rescue by transfecting the siRNA resistant cDNA into control and SH3BP1 depleted cells. This construct was expressed efficiently in the presence of control and SH3BP1 specific siRNAs (Figure 4.34b). I next overexpressed the wild type construct in serum-starved, EGF stimulated A431 cells, which are forming junctions. Overexpression indeed rescued the broken junctional ZO-1 distribution normally seen in depleted cells (Figure 4.34a). I next assessed the efficiency of the expression and rescue of the R312A siRNA resistant construct. This construct was also expressed independent of the siRNA transfected (4.35b). Strikingly, expression of the GAP deficient mutant failed to rescue junction formation (Figure 4.35a). Quantification suggested this to be significant (Figure 4.35c). Thus, these complementation assay results indicate that the GAP activity is crucial for SH3BP1's role in junction formation.

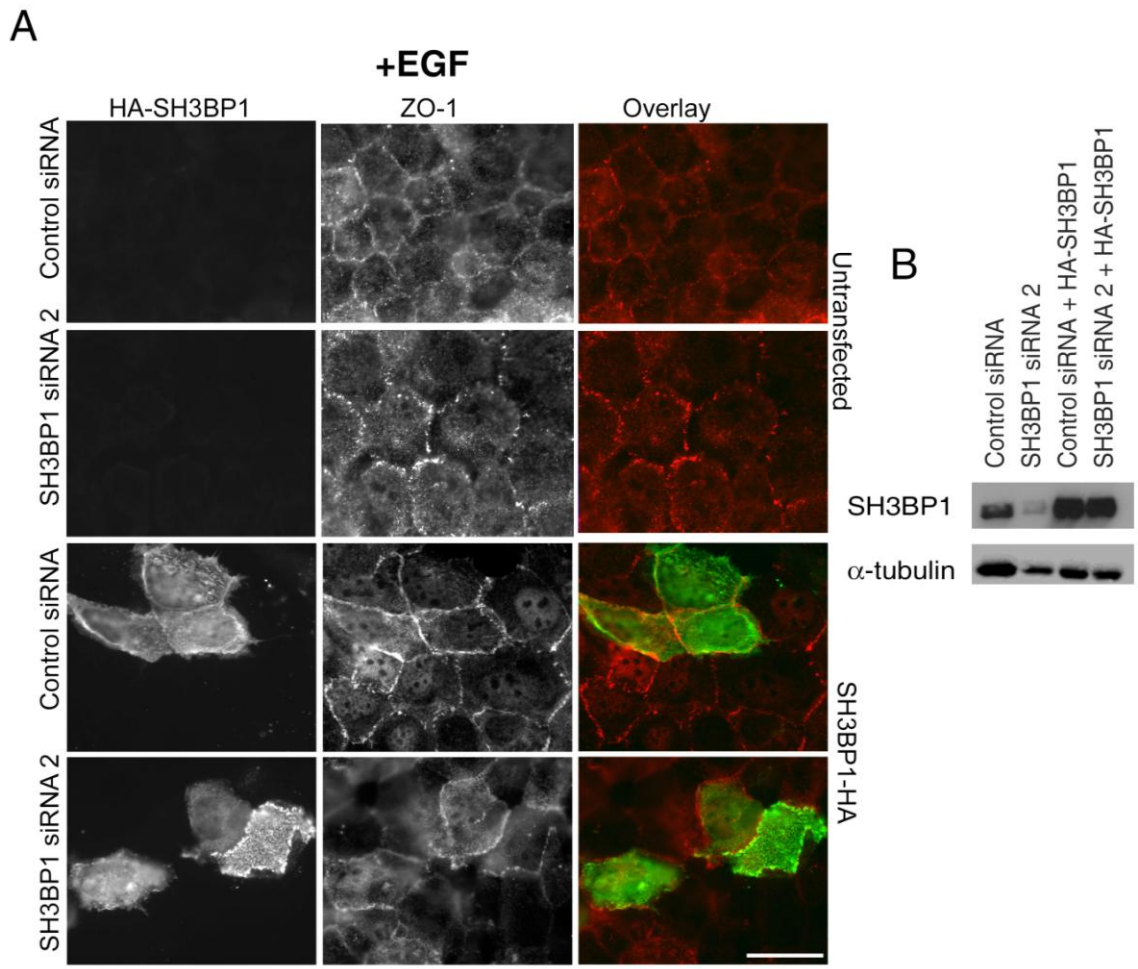

Figure 4.34 Junction formation is rescued by full length siRNA resistant mutant.

(A) Serum-starved A431 cells were stimulated with 100ng/ml EGF to allow junction formation, following transfection with an SH3BP1 specific siRNA or control siRNA, and transient expression of the siRNA resistant full length construct. The cells were then fixed with paraformaldehyde and immunostained with antibodies against ZO-1 (red) and the HA-epitope (green), or (B) lysed and analysed by immunoblotting. Experiment performed three times. Scale bar 10μm.

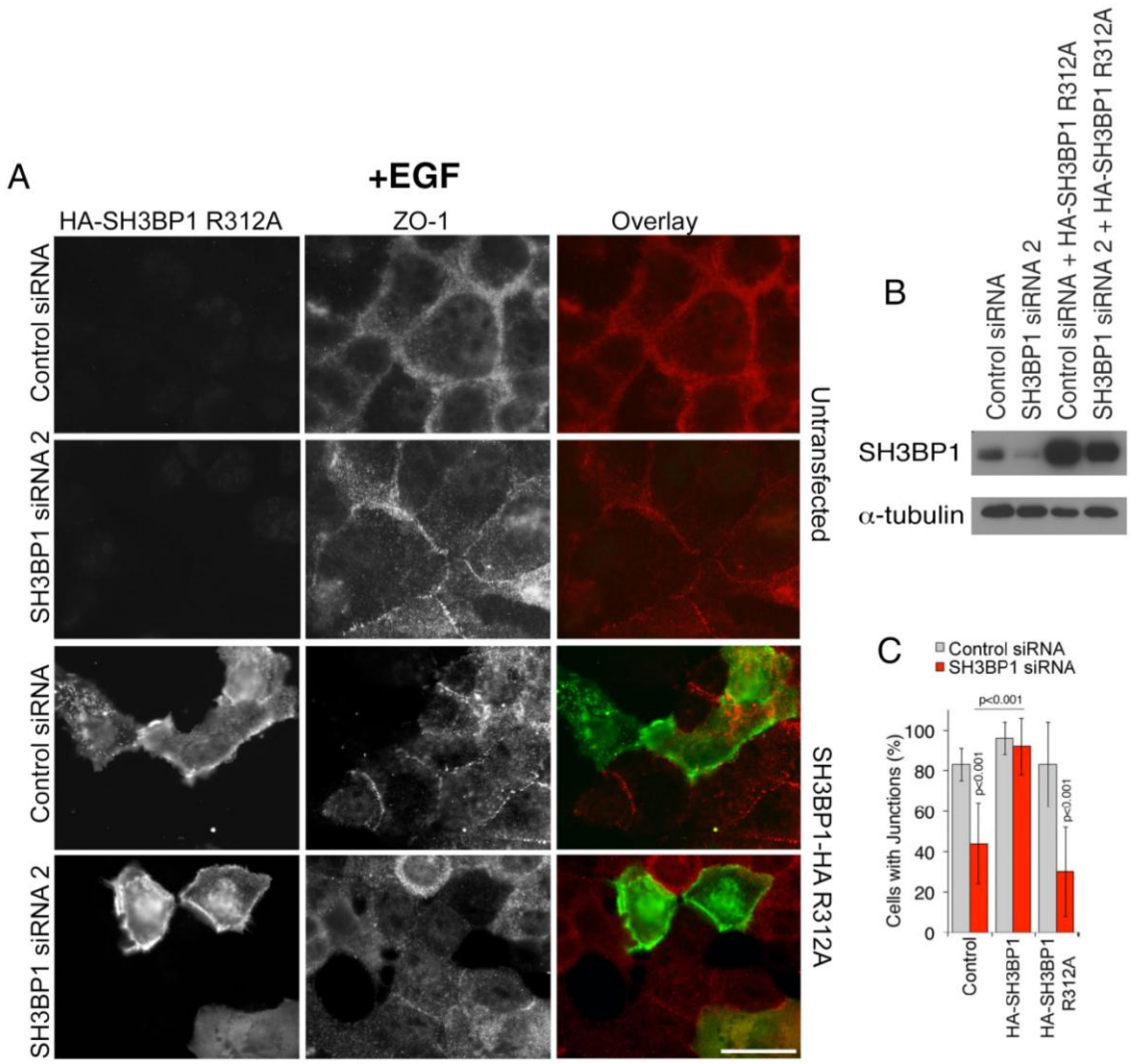

Figure 4.35 Junction formation is not rescued by GAP deficient SH3BP1.

(A) Serum-starved A431 cells were stimulated with 100ng/ml EGF to allow junction formation, following transfection with an SH3BP1 specific siRNA or control siRNA, and transient expression of the siRNA resistant and GAP deficient full length construct. The cells were then fixed with paraformaldehyde and immunostained with antibodies against ZO-1 (red) and the HA-epitope (green), or (B) lysed and analysed by immunoblotting. The experiments in this figure were performed at the same time as the ones in figure 4.36. (C) The experiments were quantified by analysing junctional ZO-1 staining. Shown are means ± 1 SD, representing the cells in at least seven different fields per condition (n≥ 7). Experiment performed three times. Scale bar 10µm.

Chapter 4 - Discussion

In this chapter, I have presented data that indicate that SH3BP1, a GAP that was identified with a functional siRNA library screen, regulates the formation of the AJC, epithelial differentiation and signalling by the Rho GTPases Cdc42 and, depending on the cellular model, Rac1.

Depletion of SH3BP1 compromised formation of both components of the AJC: tight and adherens junctions. This is supported by results from immunofluorescence and functional assays demonstrating loss of normal epithelial barrier properties. The severity of the effect depended on the protein analysed, suggesting that junction assembly occurs partially but that junctions don't fully form in the absence of SH3BP1. This might have two reasons. Firstly, it could be that initiation of junction formation occurs normally but that junctional maturation is blocked by the lack of SH3BP1. This is supported by my observations that initial cell spreading and cell-cell contact formation occurs normally during a calcium switch assay, but that then junctions don't seem to mature by SH3BP1 depletion. Secondly, it could also be that some junctional components are more sensitive to deregulation of Rho GTPase signalling. This possibility is supported by my observations that both the TJ protein cingulin and the AJ protein p120 catenin were more strongly affected and both proteins have previously been connected to Rho GTPase signalling mechanisms [270, 281, 282].

SH3BP1 does not only regulate junction assembly but also associates with the junctional complex. Similar to its effect on junction assembly, localisation of the protein overlaps with markers of AJs and TJs. Nevertheless, its distribution resembles more closely those of AJ proteins, suggesting that it may bind AJ components. Interestingly, a GAP with a similar structure, Rich1, has previously been linked to TJs and cell polarisation [193]. Although both proteins share a similar structure, they play two fundamentally different roles. SH3BP1 is recruited early to forming junctions, and is critical for the assembly of the AJC; while Rich1 has been found to be important for cellular polarisation once the AJC has been assembled and is not required for membrane dynamics or AJ assembly. This is supported by the screening results, as we could not detect a defect in junction formation upon Rich1 siRNA transfection in the siRNA screen that we performed (as it was a functional screen, depletion of targets was not assessed and, hence, the efficiency of Rich1 depletion is not known).

Depletion of SH3BP1 had striking effects on the organisation and dynamics of the actin cytoskeleton. Time-lapse recordings of EGFP-actin expressing and EGF stimulated A431 cells suggested that actin dynamics was dramatically reduced. Although long filopodia-like structures could still be seen, they grew slowly and no EGF-induced actin remodelling leading to dorsal ruffling and junction formation was observed in SH3BP1 depleted cells. This is compatible with the increase in cofilin phosphorylation, as active actin remodelling requires active cofilin.

In the absence of the GAP, A431 cells formed long filopodia-like structures at their basal side. A431 cells have previously been shown to form extensive filopodia [254]. As I found drastically increased Cdc42 activation in depleted

cells and filopodia are positively regulated by Cdc42 signalling [133, 283], it is thus likely that their growth is a direct consequence of Cdc42 deregulation. As I did not stain for filopodial markers, it could be that these filopodia-like structures are another type of finger-like actin-enriched membrane protrusion. One similarly shaped structure are retraction fibres [284]. However, SH3BP1 depleted cells did not retract but were more spread and still in contact with each other, which is incompatible with retraction fibres. Moreover, these filopodia-like structures were also seen during early stages of calcium-induced junction assembly in A431 cells, a phase of junction assembly when cells spread and approach each other that then persisted in GAP depleted cells. Hence, they were again associated with cell spreading and not retraction. I did also not detect any retracting cells in time lapse recordings of GFP-actin expressing cells; however, I could observe slowly growing protrusions. My observations are thus compatible with the conclusion that these protrusions are filopodia. Some authors differentiate between microspikes and filopodia; others treat them as the same. However, microspikes (in the stricter terminology) tend to be associated with leading edges of migrating cells and are thinner than what I observed. As Cdc42 was strongly activated in SH3BP1 depleted cells and this Rho GTPase drives filopodia formation, it seems thus most likely that the filopodia-like structures that I observed were indeed filopodia. This is also compatible with a previous report from Elaine Fuchs' laboratory reporting that filopodia can induce junction formation in keratinocytes *in vitro* and *in vivo* [106].

My experiments demonstrated that depletion of SH3BP1 strongly deregulated Cdc42 activity. Active Cdc42 was normally more closely associated with cell-cell junctions, but depletion of the GAP led to a loss of this spatial confinement. In

A431 cells, there was also a strong increase in the overall levels of Cdc42 activity. SH3BP1 can also function as a GAP for Rac1 and there was indeed an effect on Rac1-GTP levels and distribution in A431 cells [186, 187, 189]. In Caco-2 cells we could not detect an effect on Rac1 (not shown) and various attempts in the laboratory to identify a role for Rac in junction formation in Caco-2 cells failed (Karl Matter, personal communication). SH3BP1 depletion also led to an apparent increase in stress fibre formation, a process that has been linked to RhoA signalling. However, published attempts to demonstrate an effect of SH3BP1 on the GTP hydrolysis by RhoA did not reveal a clear effect on RhoA and it is thus generally assumed that SH3BP1 does not target RhoA. As junction formation is known to lead to a downregulation of RhoA signalling along the base of the cells and reduced stress fibre formation [198, 203], it thus seems more likely that the increase in stress fibres was caused indirectly by the defect in junction formation.

Junction formation is strongly regulated by Rho GTPase signalling [60, 195, 285]. It is thus not surprising that depletion of a junction-associated GAP led to a defect in junction assembly, and, as my complementation assay demonstrated, the GAP activity is essential for the cellular function of SH3BP1. In the case of Caco-2 cells, this seems to be mainly due to an effect on Cdc42, whereas there was also a minor effect on Rac1 in A431 cells. In fact, both GTPases have been linked to junction assembly in different experimental model systems. In some cases, the conditions under which junction assembly is analysed may even affect the role of a particular Rho GTPase, which might explain the contradictory reports on the role of Cdc42 in keratinocytes [204, 235]. Nevertheless, my data demonstrate that the GAP activity of SH3BP1 is

crucial for the regulation of junction formation in two different epithelial model cell lines.

In A431 cells, depletion of SH3BP1 inhibited the EGF-induced formation of dorsal ruffles that occurs prior to junction formation; most likely since the cells had lost their potential to reorganise the actin cytoskeleton, as suggested by the time-lapse movies of fluorescently labelled actin. Several junctional proteins were recruited to these ruffles including active Cdc42. It is unlikely this recruitment reflects an imaging artefact and that all proteins recruited to the apical membrane appear concentrated in these ruffles, as active Rac1, which also stained the apical membrane, was not enriched in the large ruffles. However, electron microscopy would be needed to clearly determine the relative concentrations of proteins in specific apical structures, as the folded double membrane of a ruffle cannot be resolved by epifluorescence and confocal microscopy. Moreover, there is currently no evidence for a direct role of dorsal ruffles in junction formation, as the observed kinetics of junctional protein recruitment might imply.

Based on my observations, I propose a model according to which SH3BP1 is recruited to forming cell-cell junctions to regulate Cdc42 and the remodelling of the actin cytoskeleton required for junctional maturation. In cell types in which junction formation is Rac1-dependent, this may also involve regulation of Rac; however, this has not been tested yet. Inactivation of Cdc42 is required for the remodelling of the actin cytoskeleton to allow cells to adapt to each other and assemble the typical junctional cytoskeletal network. In cells such as A431 cells that form pronounced filopodia, inactivation of Cdc42 is required for the morphological transition from interlocked neighbouring filopodia (i.e, the

adhesion zipper) to a continuous junctional actin belt. Other cells such as Caco-2, do not form such pronounced filopodia despite the deregulated Cdc42 activity (overall active Cdc42 levels did not increase in this model); However, their actin cytoskeleton was affected in a superficially similar manner by depletion of SH3BP1, as they failed to reorganise their actin cytoskeleton from the organisation required for cell spreading to the one supporting junctional maturation and polarisation.

Chapter 5

SH3BP1 is Part of a Multimeric Signalling Complex

Chapter 5: SH3BP1 is Part of a Multimeric Signalling Complex

Part of this chapter was published: J Cell Biol. 2012 Aug 20;198(4):677-93.

Introduction to chapter 5

Given the importance of SH3BP1 in the regulation of Cdc42 and epithelial junction assembly, I next wanted to determine how it is recruited to cell-cell junctions and whether it is part of a signalling module with different activities. Here, I will show that SH3BP1 is part of a novel complex that regulates junction formation. This complex comprises SH3BP1, JACOP (junction-associated coiled-coil protein)/paracingulin, CD2AP and CapZα1. The SH3BP1 complex is recruited to sites of actin remodelling and cell junctions, and depletion of any member of this complex affects the apical junctional complex. CapZα1 adds another activity to the complex that affects the actin cytoskeleton as it is a barbed end capping protein and is required for controlled actin remodelling. My data indicates that epithelial junction formation requires an SH3BP1-based dual activity complex that becomes recruited to sites of active membrane remodelling to guide Cdc42 signalling and actin dynamics.

Results – Chapter 5

SH3BP1 forms a complex with JACOP, CD2AP and CapZα1

SH3BP1 is important for junction formation and associates with cell-cell junctions; therefore, I decided to search for interaction partners that might mediate junctional recruitment. I first tested whether known TJ and AJ proteins co-immunoprecipitate with SH3BP1 in Caco-2 cells. Out of several TJ and AJ proteins tested, I found an interaction with the scaffold protein JACOP/paracingulin, a protein that can associate with both TJ and AJs (Figure 5.0) [61, 63]. As JACOP is a known to regulate Rho GTPase activity [63], it was an excellent candidate to analyse further. The interaction with JACOP also suggested that SH3BP1 might be recruited to cell-cell junctions by JACOP as I could not detect co-immunoprecipitation of SH3BP1 with any other of the TJ or AJ proteins tested.

Depletion of SH3BP1 results in elongated filopodia and failure of cell junctions to form correctly. Having identified a protein that may mediate junctional recruitment, I tested next proteins linked to the regulation of actin remodelling. I found that SH3BP1 was able to co-immunoprecipitate with the scaffold and actin capping regulator CD2AP, which has also been implicated in actin remodelling (Figure 5.1) [151, 286, 287]. Moreover, CD2AP also was found to co-immunoprecipitate with JACOP, suggesting that SH3BP1, JACOP and CD2AP form a tripartite complex.

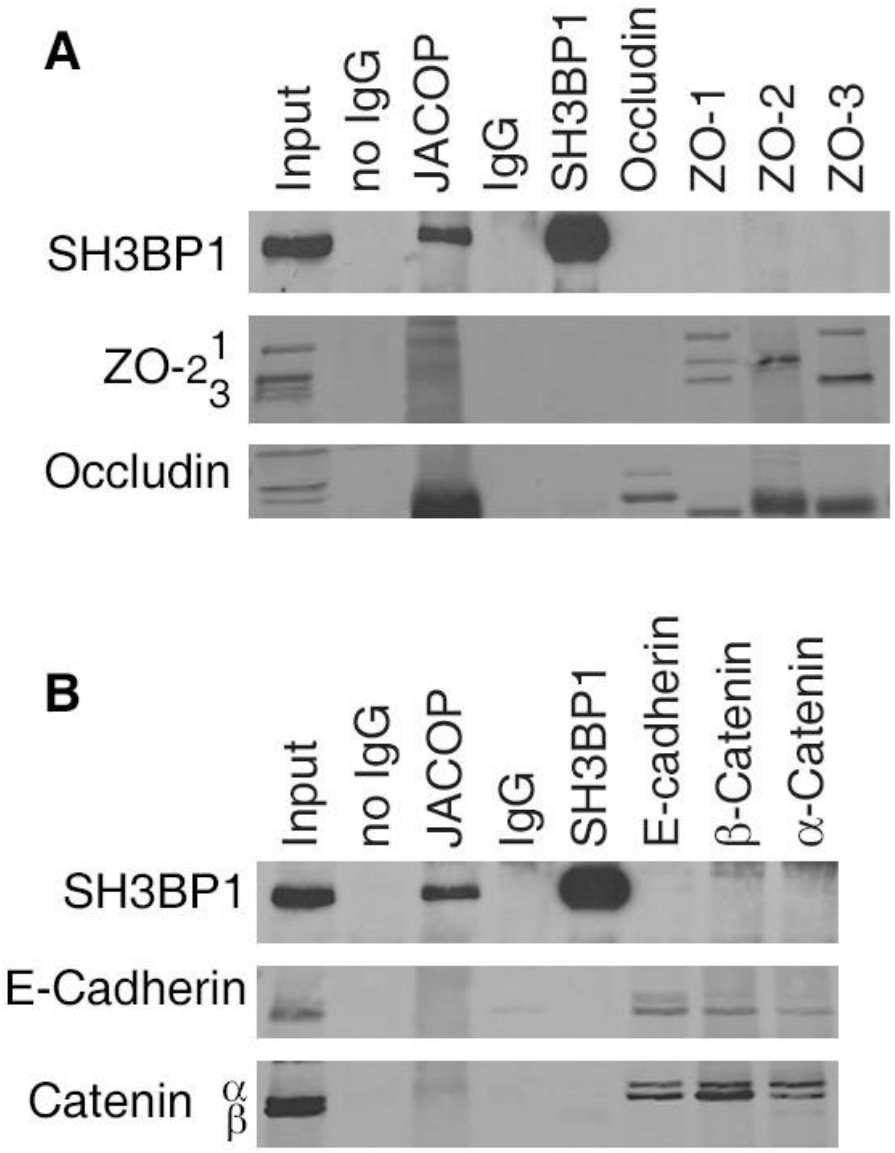

Figure 5.0 SH3BP1 interacts with the cell-cell junctional protein JACOP/paracingulin.

Caco-2 cell extracts were incubated with antibodies against the indicated proteins bound to beads**.** IgG refers to a sample with a non-specific rabbit IgG that was used as a negative control. Indicated proteins were analysed by immunoblotting. In panel A, TJ proteins were analysed and in panel B, AJ proteins. The experiment was performed three times.

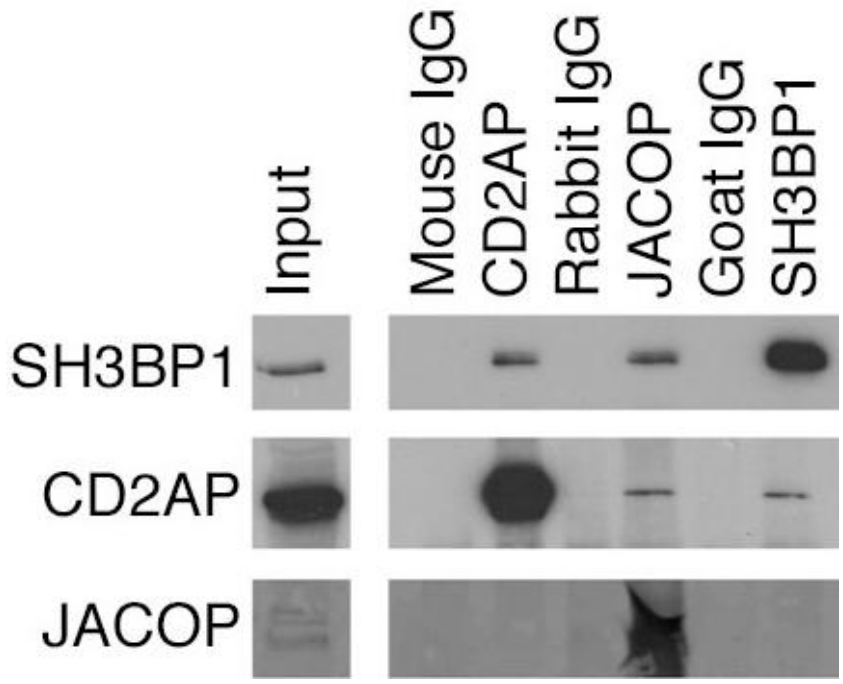

Figure 5.1 JACOP immunoprecipitates contain SH3BP1 and CD2AP.

Caco-2 cell extracts were subjected to immunoprecipitation using antibodies against the indicated proteins. As they were from three different species, respective control IgG were included as negative controls. The presence of the indicated proteins in immunoprecipitates was analysed by immunoblotting. Experiment was performed three times.

As I had found that the recruitment of SH3BP1 to sites of actin remodelling and cell-cell junctions is regulated by EGF signalling, I next used A431 cells to test whether the complex exists in these cells as well and, if yes, whether it was a constitutive complex or stimulated by EGF. Figure 5.2 shows that I could reproduce the same co-immunoprecipitations in A431 as in Caco-2 cells, suggesting that it is a complex common to different types of epithelial cells. Moreover, co-immunoprecipitation was not EGF-dependent, indicating that SH3BP1, JACOP and CD2AP form a constitutive protein complex (Figure 5.2). The observation that SH3BP1 or CD2AP IPs did not contain JACOP, may be due to the JACOP antibody not blotting efficiently, as if one is to observe the input levels of JACOP in comparison to SH3BP1 and CD2AP it can be seen as being considerably weaker. Taking into account the efficiency of, for example the CD2AP co-immunoprecipitations, then theoretically one would no longer see JACOP in the SH3BP1 immunoprecipitations.

To further corroborate the existence of a complex containing the three proteins, I next tested their subcellular distribution. Initial assessment indicated that they were all present along the AJC (Figure 5.3a). A more detailed analysis by confocal microscopy indicated that the three proteins co-localised at cell-cell junctions, with the majority of the overlap occurring with the AJ (Figure 5.3b).

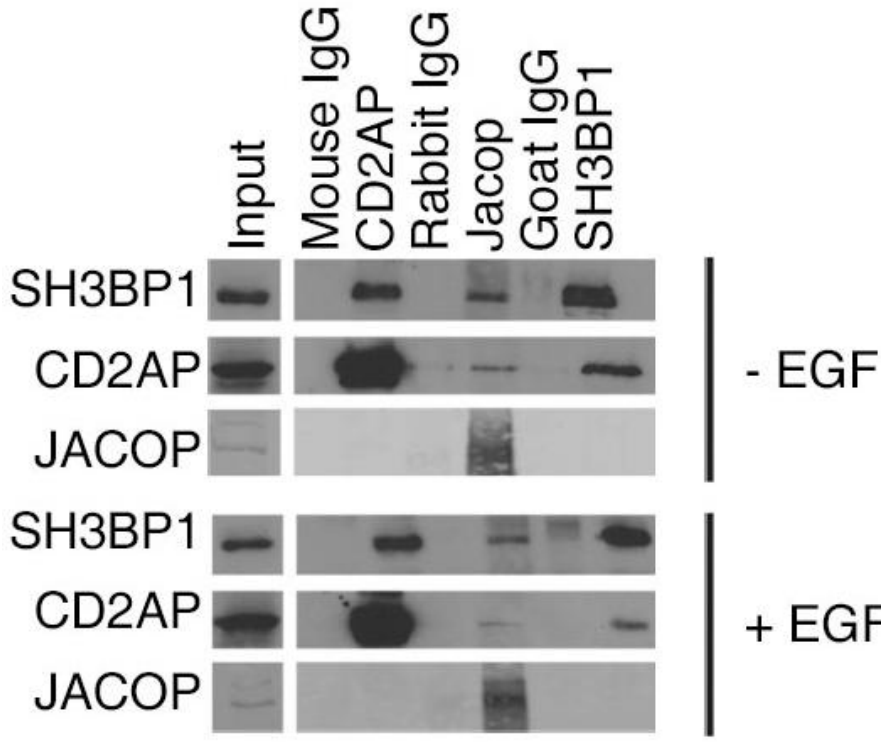

Figure 5.2 JACOP, SH3BP1 and CD2AP form a constitutive protein complex.

Cell extracts from serum starved or EGF-stimulated A431 cells were subjected to immunoprecipitation using the indicated antibodies. Mouse, goat and rabbit IgGs were used as negative controls. Proteins present in the precipitates were analysed by immunoblotting as indicated. Experiment was performed three times.

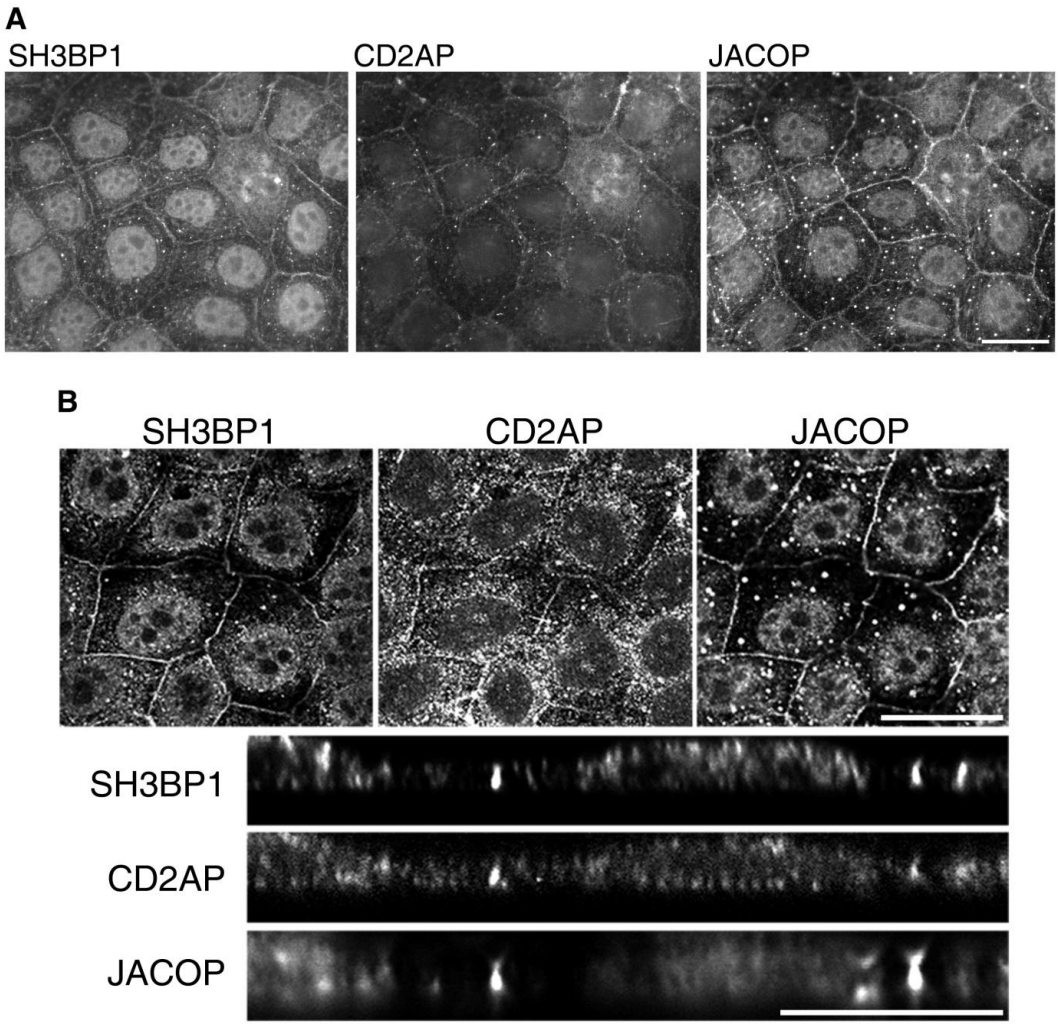

Figure 5.3 SH3BP1 co-localises with JACOP and CD2AP in Caco-2 cells.

Caco-2 cells were immunostained with antibodies against SH3BP1, JACOP and CD2AP after fixation with paraformaldehyde and permeabilisation with Triton X-100. Shown are: (A) epifluorescent and (B) confocal microscopy images with corresponding representative Z-line scans. Experiment was performed three times. Scale bar 10μm.

I next asked whether the three proteins also co-localised in A431 cells. As previously shown, SH3BP1 localised to apical dorsal ruffle structures within 5 minutes of EGF stimulation. Staining of JACOP or CD2AP, respectively, and F-actin along with SH3BP1 revealed co-localisation with SH3BP1 in dorsal structures (Figure 5.4), Therefore, the three proteins do not only form a biochemical complex, they also co-localise in the cells during actin remodelling and at cell junctions.

JACOP is a scaffold for SH3BP1 and CD2AP

The next question I addressed was whether the junctional adaptor JACOP was important for the junctional localization of SH3BP1 and CD2AP. Depletion of JACOP in Caco-2 cells indeed resulted in a strong decrease of junctional SH3BP1 and CD2AP staining (Figure 5.5). This suggests that JACOP may act as scaffold for both SH3BP1 and CD2AP that mediates junctional recruitment.

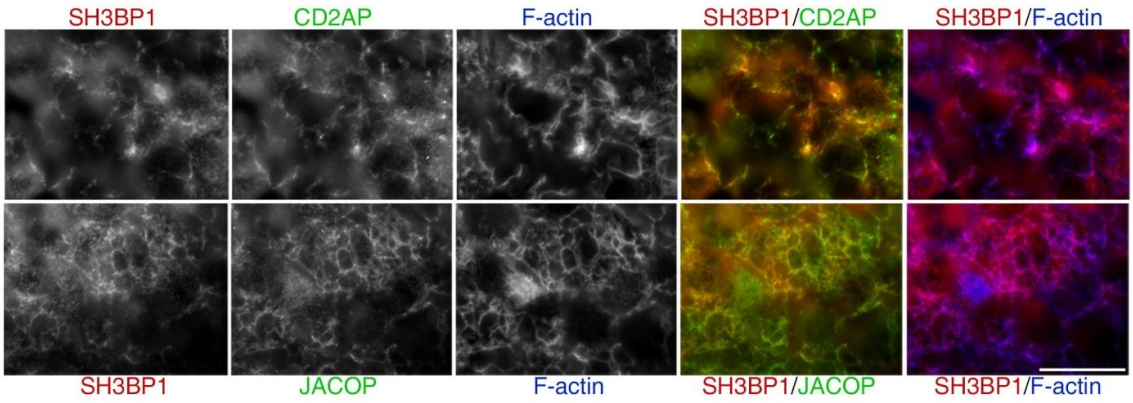

Figure 5.4 SH3BP1 co-localises with CD2AP and JACOP in EGF-stimulated A431 cells.

Serum starved A431 cells were stimulated for 5 minutes with 100ng/ml EGF and subsequently fixed and permeabilised before immunostaining with antibodies against SH3BP1 (red), F-actin (blue), and CD2AP or JACOP (green). Shown are epifluorescent images. Scale bar 10µm.

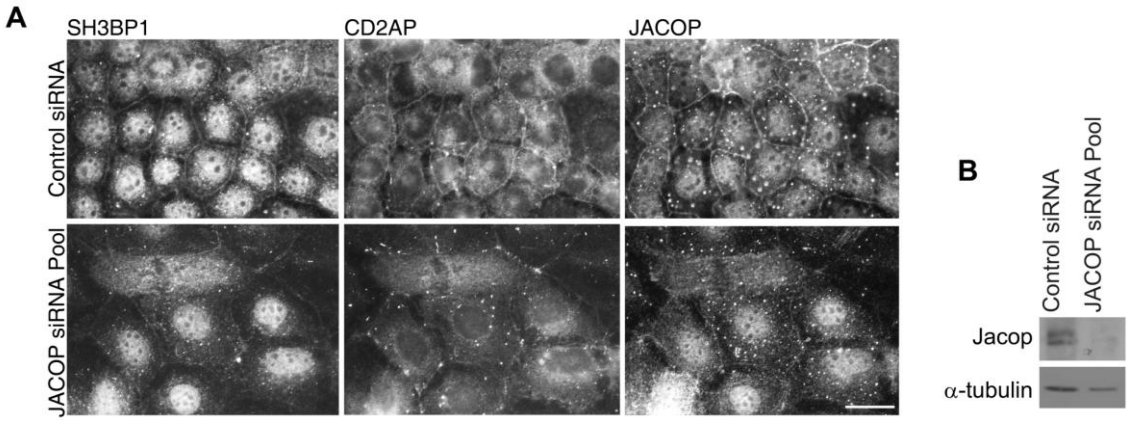

Figure 5.5 Depletion of JACOP affects SH3BP1 and CD2AP junctional localization.

Caco-2 cells were transfected with either control siRNA or a pool of JACOP directed siRNAs. After 96 hours, the cells were either (A) fixed with paraformaldehyde and permeabilised with Triton X-100 and immunostained for SH3BP1, CD2AP and JACOP; or (B) extracted and immunoblotted for JACOP. Alpha-tubulin was used as a loading control.The immunofluorescence images were taken with an epifluorescent microscope. Experiment was performed three times. Scale bar 10µm.

I next assessed if depletion of JACOP affected the expression levels of SH3BP1 and CD2AP by immunoblotting. Interestingly, depletion of JACOP led to a reduction in the expression levels of SH3BP1 but not CD2AP in both A431 and Caco-2 cells (Figure 5.6). This suggests that formation of a complex with JACOP may be important for SH3BP1 stabilisation.

I next tested the importance of JACOP for the junctional recruitment of SH3BP1 and CD2AP using an overexpresion approach. Overexpression of an HA-tagged JACOP construct in Caco-2 cells resulted in an increase in junctional CD2AP (Figure 5.7) and SH3BP1 (Figure 5.8), which further supports a model in which JACOP recruits SH3BP1 and CD2AP to cell-cell junctions.

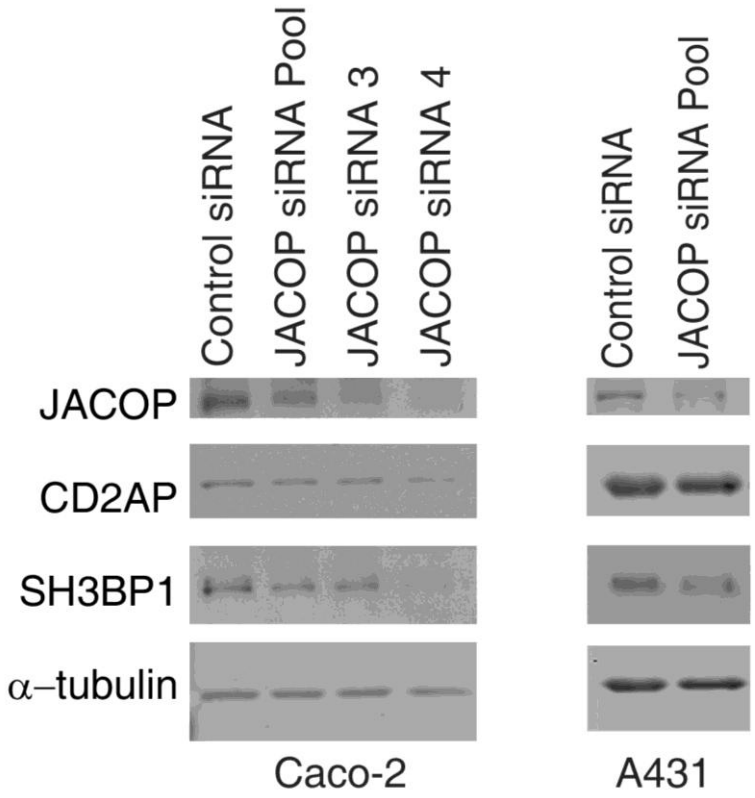

Figure 5.6 JACOP depletion affects SH3BP1 expression levels.

Caco-2 and A431 cells were transfected with siRNAs as indicated. After 96 hours, extracts were collected and immunoblotted for JACOP, CD2AP and SH3BP1. Experiment was performed three times. Alpha-tubulin was used as a loading control.

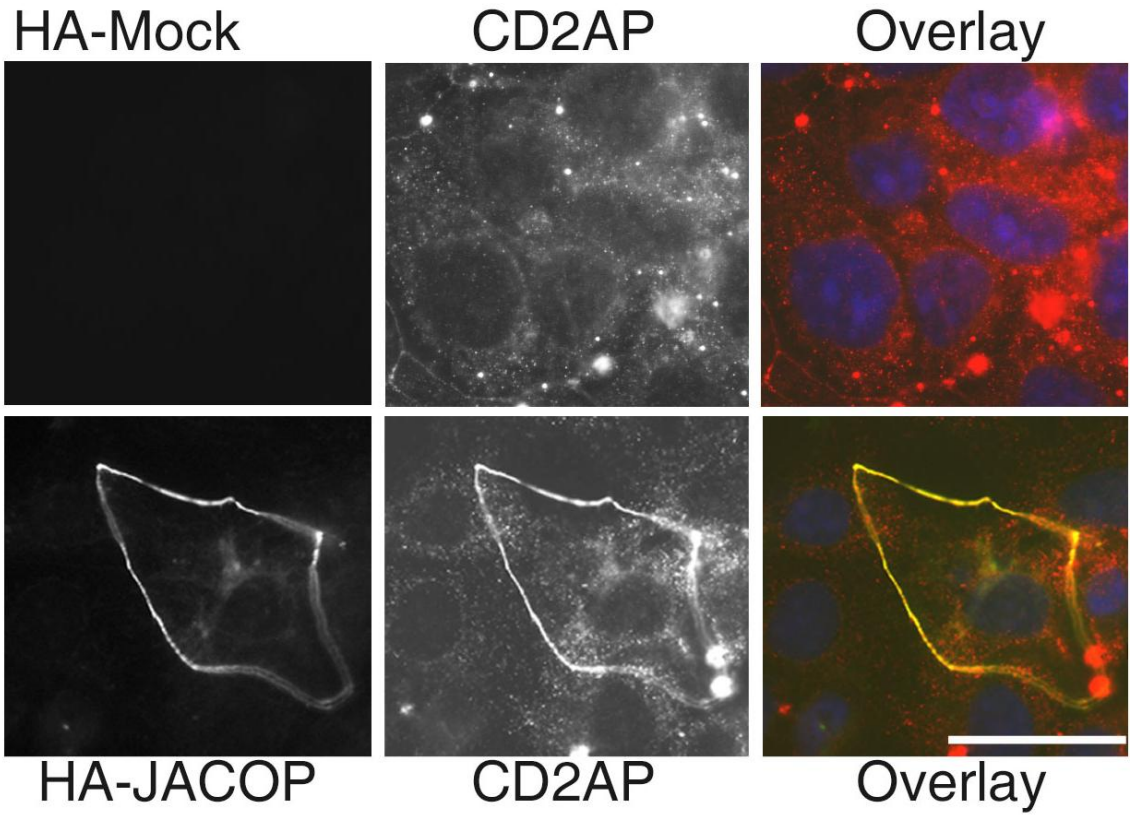

Figure 5.7 JACOP overexpression results in increased junctional staining for CD2AP.

Caco-2 cells were transfected with full length JACOP for 24 hours and then fixed with methanol. Cells were stained with antibodies against the HA-tag (green) and CD2AP (red).Shown are epifluorescent images. Experiment performed twice. Scale bar 10µm.

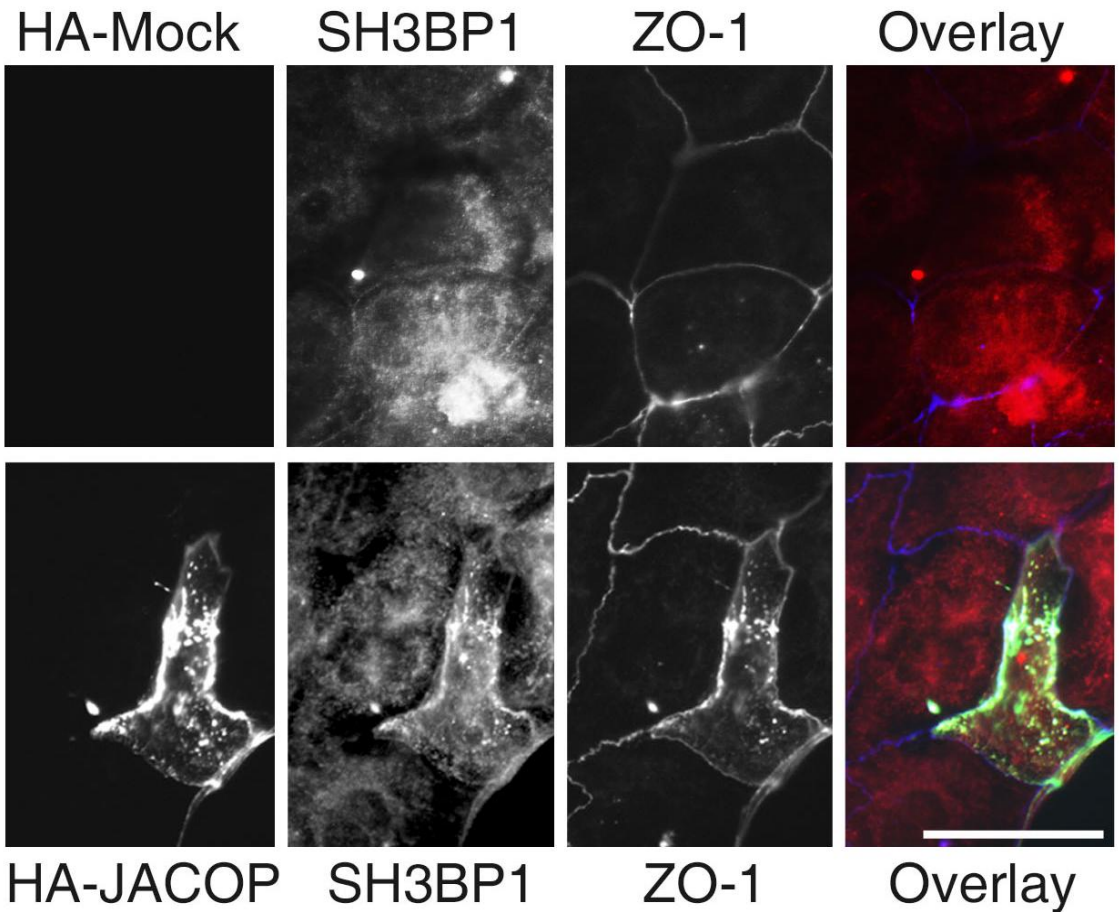

Figure 5.8 JACOP overexpression results in increased junctional staining for SH3BP1.

Caco-2 cells were transfected with full length JACOP for 24 hours and then fixed with methanol. Coverslips were stained with antibodies against the HA-tag (green), SH3BP1 (red) and ZO-1 (blue). Shown are epifluorescent images. Experiment was performed twice. Scale bar 10µm.

I next asked whether JACOP depletion affected assembly of the AJC. I firstly depleted JACOP in Caco-2 cells and noted that the continuous junctional distribution of ZO-1 was often disrupted. There was also apparently stronger staining for ZO-1 in some places, but this is likely to be due to the partial disassembly of junctions causing an unequal distribution of the protein. I also used individual siRNAs to confirm that the effect was not the result of off-target effects (Figure 5.9a and Figure 5.9b).

I next tested the role of JACOP in A431 cells. In EGF-stimulated A431 cells depletion of JACOP resulted in a disorganization of TJ formation based on the broken and diffuse appearance of ZO-1 in JACOP depleted cells (5.10). F-actin distribution was also affected, but this was less severe as when SH3BP1 was depleted and there was no increase in filopodial length (Figure 5.11). This lack in increased filopodial growth suggests that Cdc42 signalling is not increased in response to JACOP depletion.

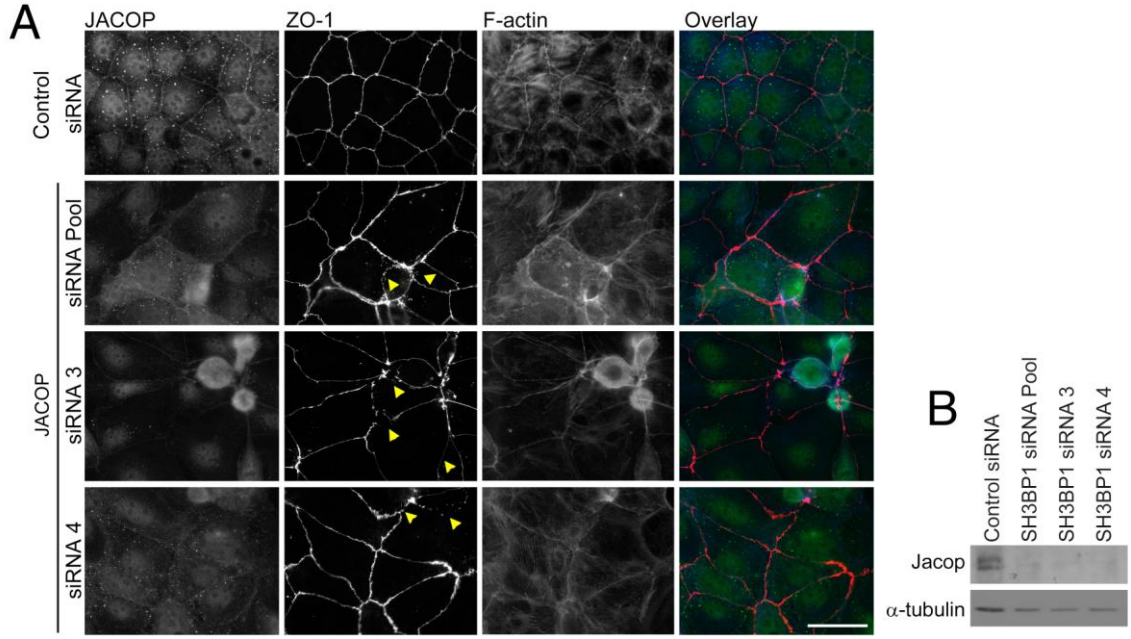

Figure 5.9 JACOP depletion effects TJ assembly and the actin cytoskeleton.

Caco-2 cells were transfected with siRNAs as indicated. After 96 hours, the cells were either (A) fixed with paraformaldehyde and permeabilised with Triton X-100, followed by staining for JACOP, ZO-1 and F-actin, or (B) collected and immunoblotted for JACOP. Alpha-tubulin was used as a loading control. The immunofluorescence were acquired with an epifluorescent microscope. Yellow arrows indicate areas of disruption. Experiment was performed three times. Scale bar 10µm.

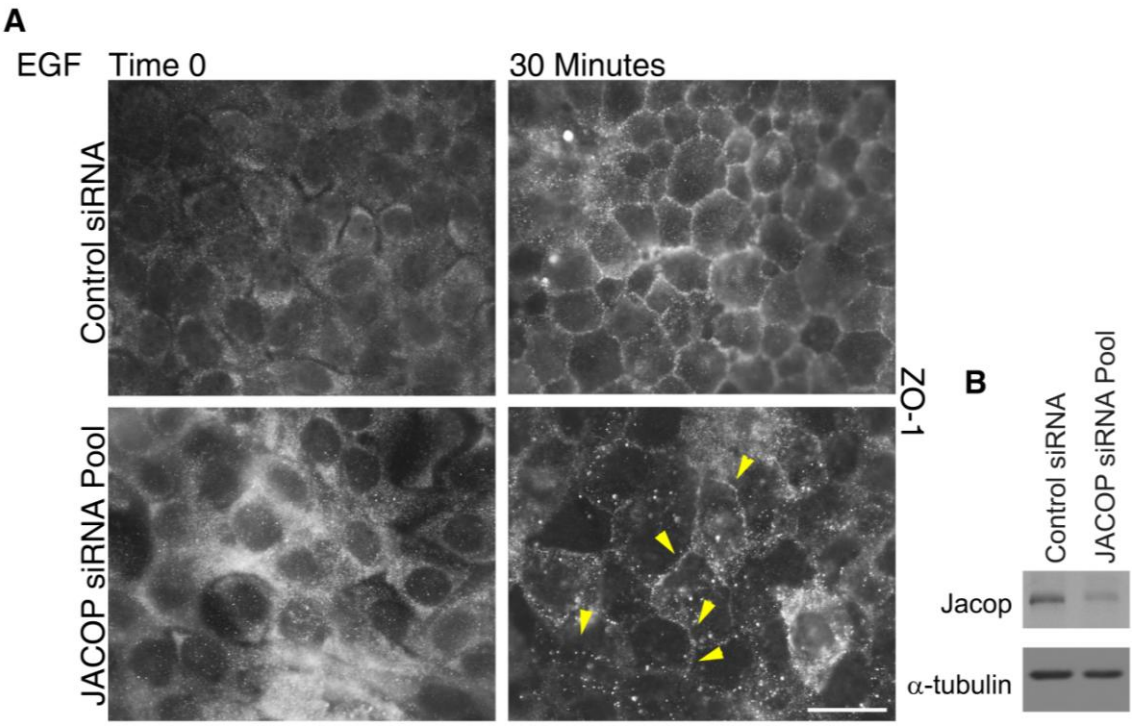

Figure 5.10 JACOP depletion affects the recruitment of ZO-1 to cell-cell junctions in EGF-stimulated A431 cells.

A431 cells were transfected with siRNAs as indicated. After 72 hours, the cells were serum-starved for 16 hours and subsequently stimulated with 100ng/ml EGF before being (A) fixed with paraformaldehyde and permeabilised with Triton X-100, or (B) collected and immunoblotted for JACOP expression. For the immunoblot, alpha-tubulin was used as a loading control. For the immunofluorescence, cells were stained for ZO-1. Yellow arrows show areas of ZO-1 disruption. Shown are epifluorescent images. Scale bar 10µm.

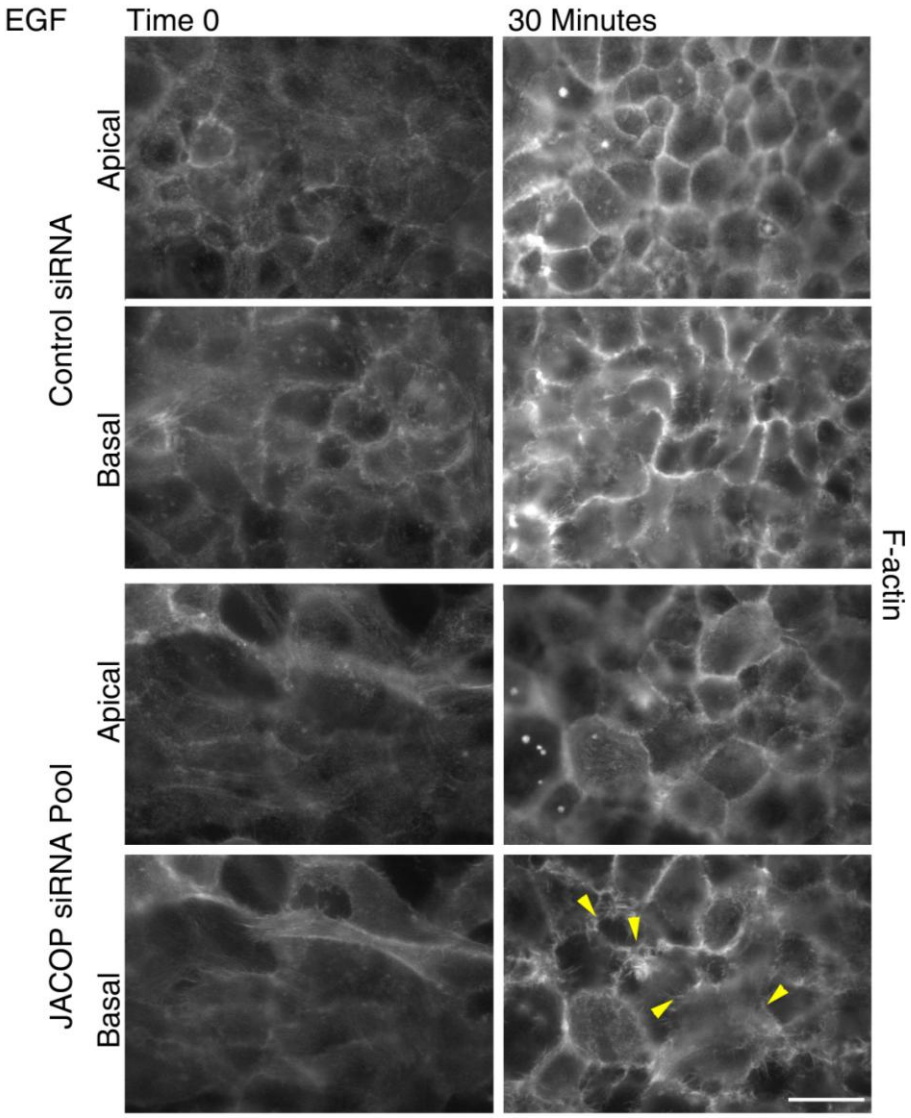

Figure 5.11 Effects of JACOP depletion on the actin cytoskeleton.

A431 cells were transfected with either control siRNAs or a pool of JACOP directed siRNAs. After 72 hours, the cells were serum starved for 16 hours and subsequently stimulated with 100ng/ml EGF, before being fixed with paraformaldehyde and permeabilised with Triton X-100. Cells were stained for F-actin using fluorescent phalloidin. Yellow arrows show areas of actin disruption. Shown are epifluorescent images. Representative blot is shown in figure 5.10. Experiment was performed twice. Scale bar 10µm.

JACOP depletion affected junctional recruitment and expression levels of SH3BP1, suggesting that it might lead to a deregulation of Cdc42 activation. Therefore, I measured the effect of depletion of JACOP on the levels of active Cdc42 using the G-LISA assay. Figure 5.12 shows that depletion of JACOP led to a decrease in active Cdc42 levels, indicating that reducing the expression of JACOP indeed leads to a deregulation of Cdc42 signalling. These data are in agreement with the observation that JACOP depletion did not lead to increase filopodial growth and suggest that SH3BP1 released from the complex may lead to uncontrolled Cdc42 inactivation throughout the cells.

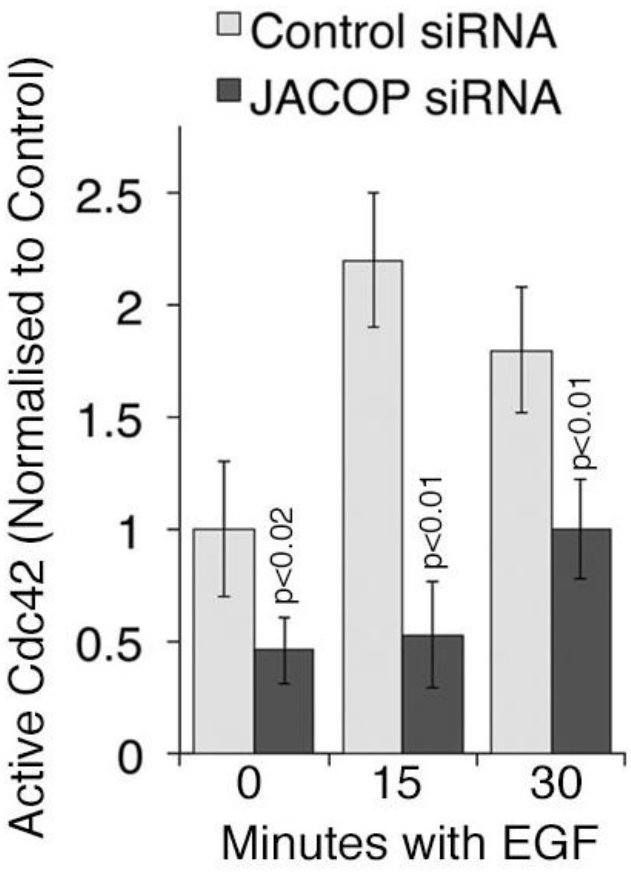

Figure 5.12 JACOP depletion in A431 cells results in lower levels of active Cdc42.

A G-LISA assay for active Cdc42 was performed using serum-starved and EGF-stimulated A431 cells 96 hours after transfection with either control siRNA or a pool of JACOP directed siRNAs. Levels of active Cdc42 are displayed normalized to control levels. The bar graphs represent the average of triplicate samples. Addition of recombinant Cdc42 as a positive control gave a value of 4.17 (Normalised to control). The experiment was performed three times. Error bars represent ± 1 SD.

CD2AP localization with JACOP is dependent on SH3BP1

The next question I addressed was how CD2AP and SH3BP1 interact with JACOP and whether one was dependent on the other. Depletion of SH3BP1 resulted in no change in the expression levels of both JACOP and CD2AP in both Caco-2 and A431 cells (Figure 5.13). If analysed by immunofluorescence, SH3BP1 depleted Caco-2 cells exhibited decreased junctional CD2AP staining but junctional JACOP did not seem to be decreased (Figure 5.14). Further evidence for the existence of a SH3BP1/CD2AP complex was obtained when cells overexpressing full length SH3BP1 were analysed and revealed a striking apparent upregulation and co-localization of CD2AP with the GAP (Figure 5.15).

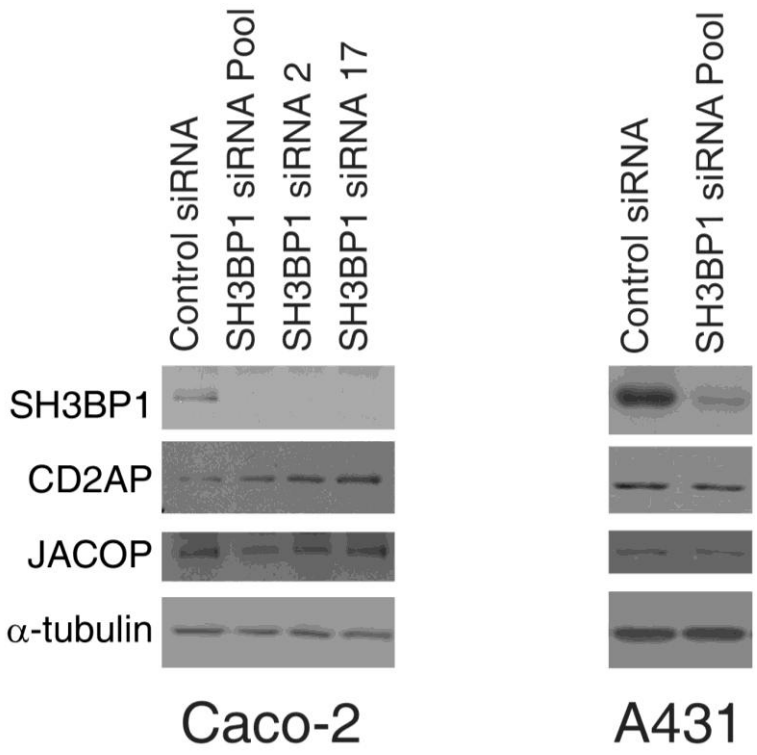

Figure 5.13 SH3BP1 depletion does not affect JACOP and CD2AP expression levels.

Caco-2 or A431 cells were transfected with siRNAs as indicated. After 96 hours extracts were collected and immunoblotted for JACOP, CD2AP and SH3BP1. Experiment was performed three times. Alpha-tubulin was used as a loading control.

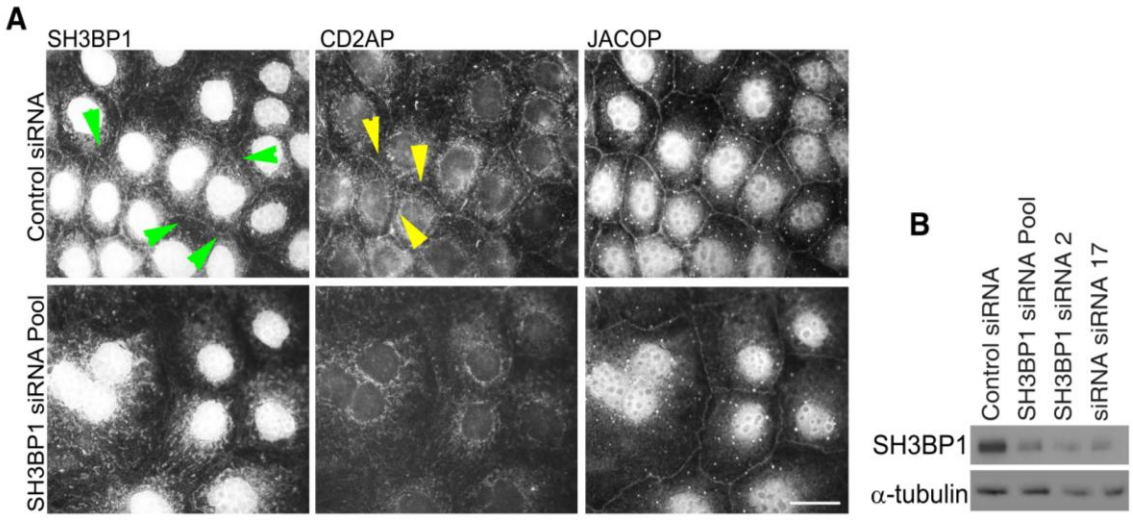

Figure 5.14 SH3BP1 depletion affects CD2AP localization.

Caco-2 cells were transfected siRNAs as indicated. After 96 hours, the cells were either (A) fixed with paraformaldehyde, permeabilised with Triton X-100, and immunostained for SH3BP1, CD2AP and JACOP; or (B) collected and immunoblotted for JACOP. Alpha-tubulin was used as a loading control. Panel A shows epifluorescent images. Note: this particular batch of SH3BP1 antibody resulted in increased non-specific staining of nuclei, which hindered the display of junctional staining because of its brightness. Yellow arrows denote CD2AP junctional staining, while green arrows denote SH3BP1 junctional staining. The experiment was performed three times. Scale bar 10µm.

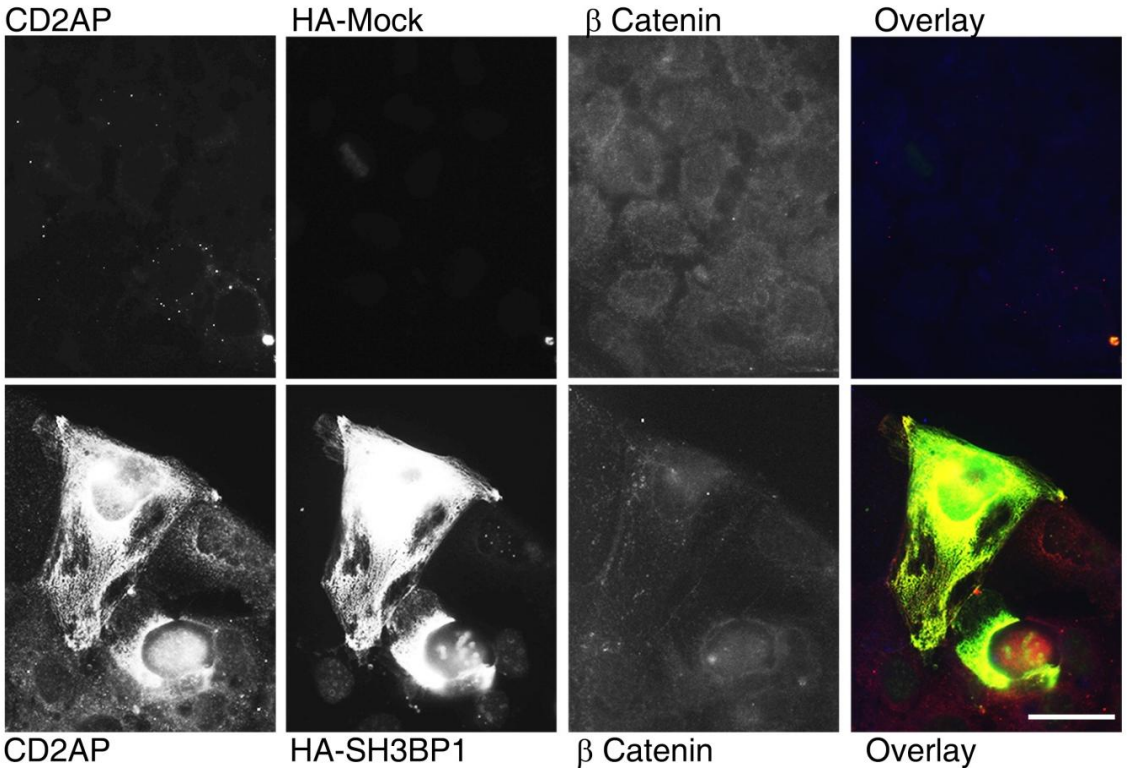

Figure 5.15 SH3BP1 overexpression results in increase CD2AP staining.

Caco-2 cells were transfected with full length HA-tagged SH3BP1 and fixed with methanol. Cells were stained for the HA tag (green), alpha-catenin (blue) and CD2AP (red). Shown are epifluorescent images. Scale bar 10µm.

I finally tested whether the interaction between CD2AP and JACOP was dependent on SH3BP1. So, I performed a co-immunoprecipitation experiment using A431 cells that were transfected with either control or SH3BP1-directed siRNAs. Figure 5.16 shows that JACOP antibodies precipitated SH3BP1 and CD2AP efficiently from control extracts but not from extracts of SH3BP1-depleted cells. This thus indicates that SH3BP1 is required for CD2AP to form complexes with JACOP.

I next addressed the role of CD2AP in the SH3BP1 complex and junction formation. As determined by immunoblotting, depletion of CD2AP affected the SH3BP1 expression levels in both A431 and Caco-2 cells, which seems to suggest that CD2AP may be required for SH3BP1 stabilisation (Figure 5.17).

Figure 5.16 SH3BP1 depletion prevents co-immunoprecipitation of CD2AP with JACOP.

A431 cells that had been transfected with control or SH3BP-directed siRNAs were extracted with PBS and 0.5% Triton X-100, and subjected to immunoprecipitation with anti-JACOP antibodies**.** The precipitates were then analysed by immunoblotting for the indicated proteins. The experiment was performed three times.

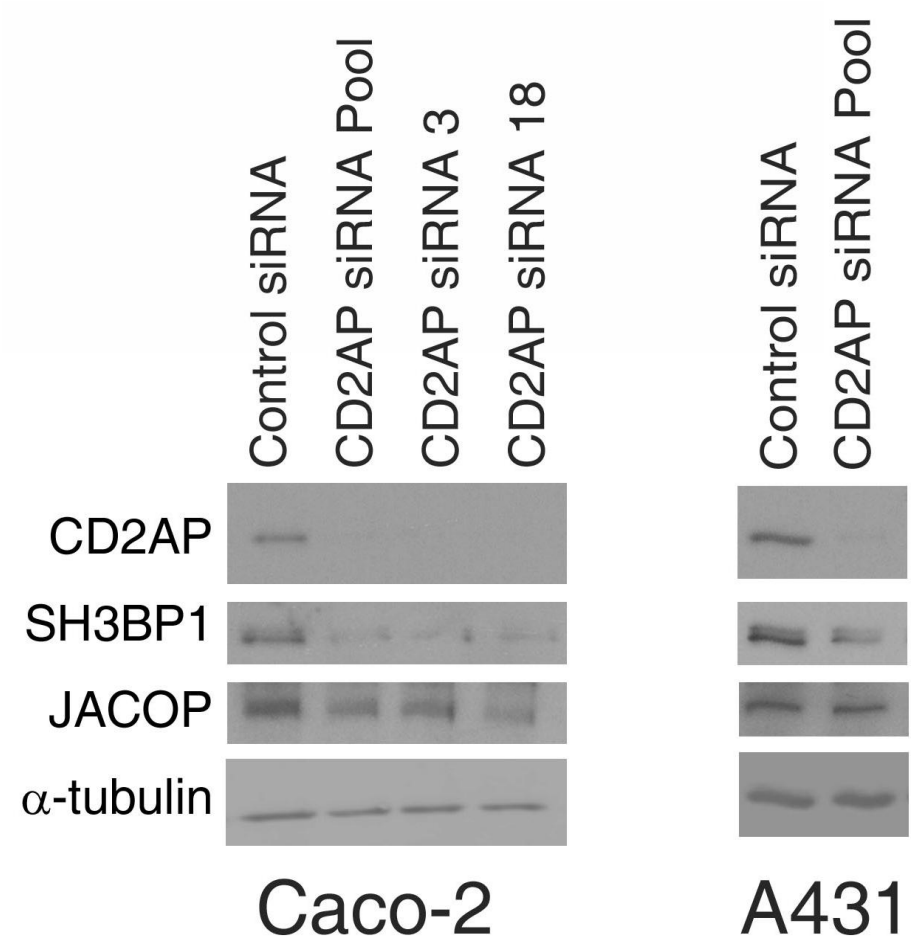

Figure 5.17 CD2AP depletion affects SH3BP1 expression levels.

Caco-2 or A431 cells were transfected with either two different individual CD2AP directed siRNAs or a pool of CD2AP directed siRNAs. After 96 hours cell extracts were collected and immunoblotted for JACOP, CD2AP and SH3BP1. Alpha-tubulin was used as a loading control.

I next asked whether CD2AP also affected the subcellular distribution of SH3BP1. Figure 5.18 shows that depletion of CD2AP in Caco-2 cells resulted in strongly reduced junctional SH3BP1 staining. However, the junctional association of JACOP was not visibly affected. As CD2AP depletion strongly affected the expression level of SH3BP1, it is not clear whether the reduced junctional staining is only due to the reduced expression or also to a redistribution of the GAP.

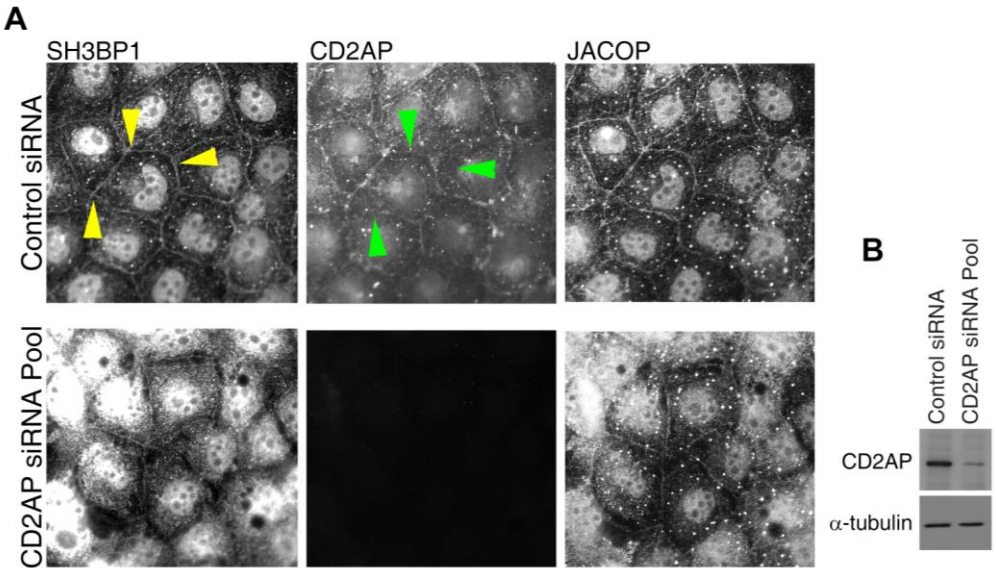

Figure 5.18 CD2AP depletion reduces junctional association of SH3BP1.

Caco-2 cells were transfected with control siRNA or a pool of CD2AP directed siRNAs. After 96 hours, the cells were (A) fixed with paraformaldehyde, permeabilised with Triton X-100, and stained with the indicated antibodies;or (B) collected and immunoblotted for JACOP (alpha-tubulin was used as a loading control). Shown are epifluorescent images. Note: junctional SH3BP1 is reduced, cytoplasmic staining is in part non-specific. The experiment was performed three times. Scale bar 10µm.

I next asked whether depletion of CD2AP had an effect on AJC assembly in Caco-2 and A431 cells. In Caco-2 cells depletion of CD2AP resulted in flatter cells and strongly irregular staining of the TJ protein ZO-1 (Figure 5.19). This effect was observed with a pool as well as individual siRNAs, supporting its specificity. Depletion of CD2AP in A431 cells also resulted in disruption of ZO-1, but the effect seemed to be weaker (Figure 5.20). There was also a disorganisation of F-actin evident particularly when cells had been treated with EGF (Figure 5.21). This thus indicates that CD2AP is functionally important for the regulation of junction assembly and EGF-induced actin reorganisation.

I next determined whether the interaction between SH3BP1 and JACOP was independent or dependent of CD2AP. Performing a co-immunoprecipitation with control and CD2AP-depleted lysates revealed decreased levels of SH3BP1 but no effect on the interaction between JACOP and SH3BP1 (Figure 5.22). As the remaining pool of expressed SH3BP1 still interacted with JACOP in CD2AP-depleted cells, the interaction between the two proteins is independent of CD2AP.

As depletion of CD2AP affects SH3BP1 expression, it may also affect the levels of active Cdc42. Therefore, I employed again the G-LISA assay to determine Cdc42 activity. Figure 5.23 shows that levels of active Cdc42 decreased with CD2AP depletion, thus indicating that reducing either of the two SH3BP1 binding partners affects Cdc42 activity (Figure 5.23).

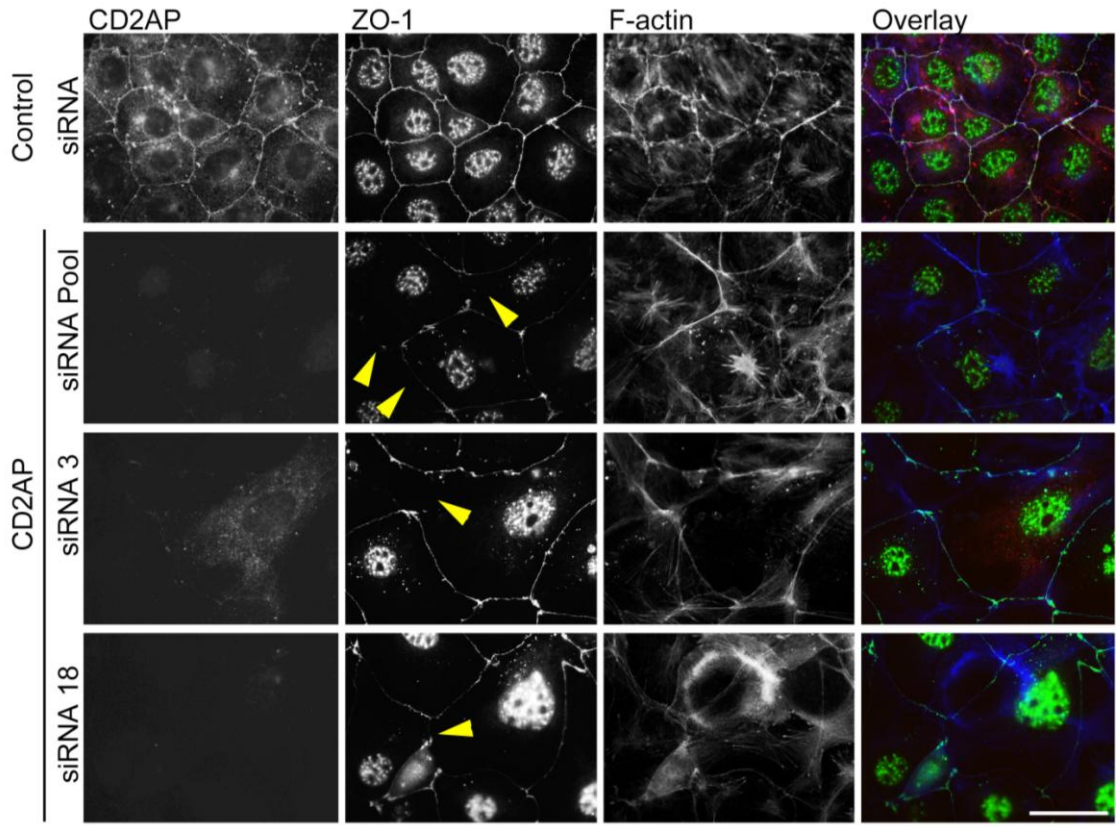

Figure 5.19 CD2AP depletion affects TJ and actin organisation.

Caco-2 cells were transfected with either control siRNA, individual CD2AP siRNAs or a pool of CD2AP directed siRNAs. After 96 hours, the cells were fixed with paraformaldehyde and permeabilised with Triton X-100. Cells were stained for JACOP (green), ZO-1 (red) and F-actin (blue). Yellow arrows show areas of ZO-1 disruption. Shown are epifluorescent images. Representative Caco-2 blot is shown in figure 5.17. Experiment was performed three times. Scale bar 10µm.

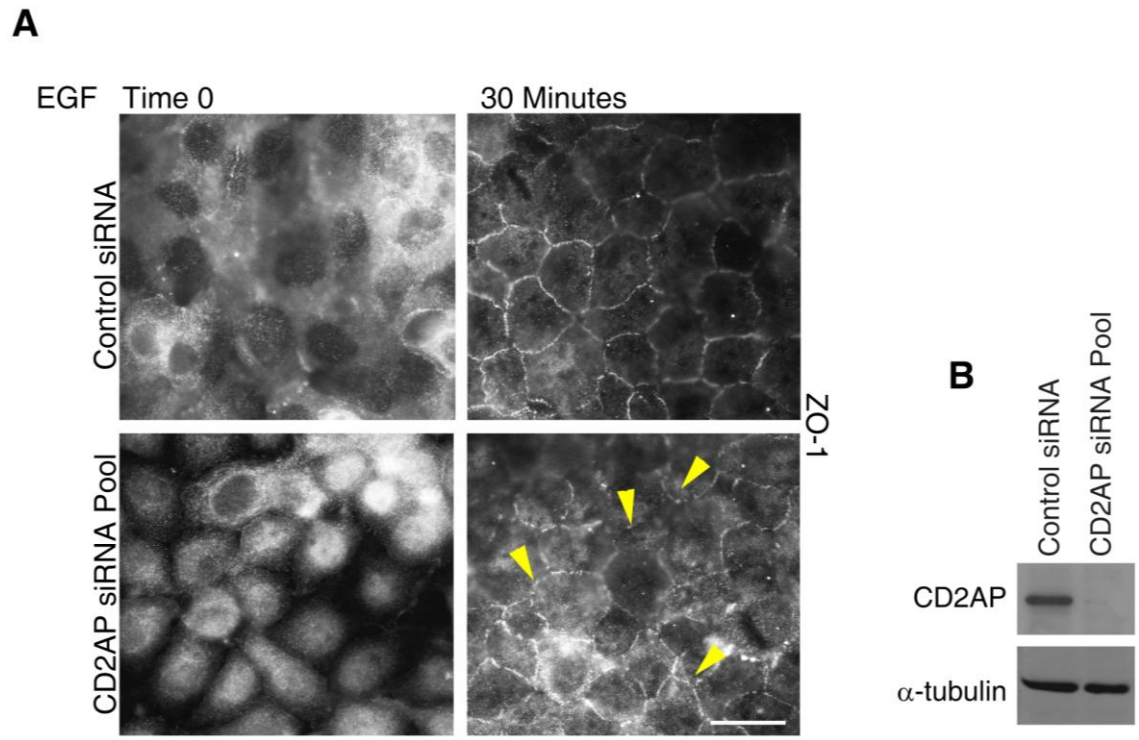

Figure 5.20 CD2AP depletion affects the junctional recruitment of ZO-1 in EGF-stimulated A431 cells.

A431 cells were transfected with either control siRNA or a pool of CD2AP directed siRNAs. After 72 hours, the cells were serum-starved for 16 hours and subsequently stimulated with 100ng/ml EGF before being (A) fixed with paraformaldehyde, permeabilised with Triton X-100, and stained for ZO-1; or (B) collected and immunoblotted for CD2AP. For the immunoblot, alpha-tubulin was used as a loading control. Panel A shows epifluorescent images. Yellow arrows denote areas of ZO-1 disruption. Experiment performed three times. Scale bar 10μm.

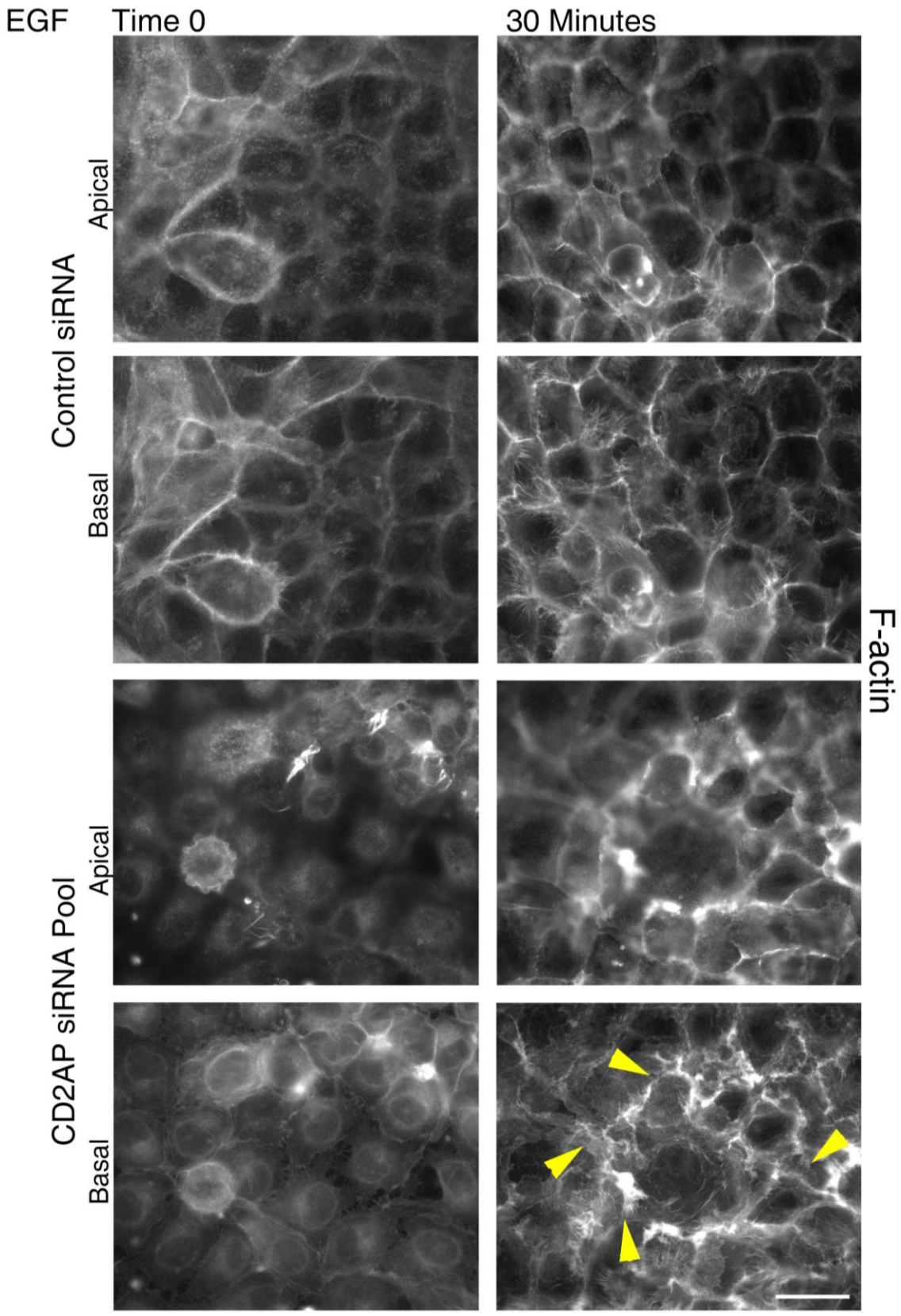
EGF
Time 0
30 Minutes
Control siRNA
Apical
Basal
CD2AP siRNA Pool
Apical
Basal
F-actin

Figure 5.21 Effect of CD2AP depletion on the actin cytoskeleton.

A431 cells were transfected with either control siRNA or a pool of CD2AP directed siRNAs. After 72 hours, the cells were serum starved for 16 hours and subsequently stimulated with 100ng/ml EGF, before being fixed with paraformaldehyde and permeabilised with Triton X-100. Cells were stained with fluorescent phalloidin to visualise F-actin. Yellow arrows denote disrupted actin. Shown are epifluorescent images. Scale bar 10μm.

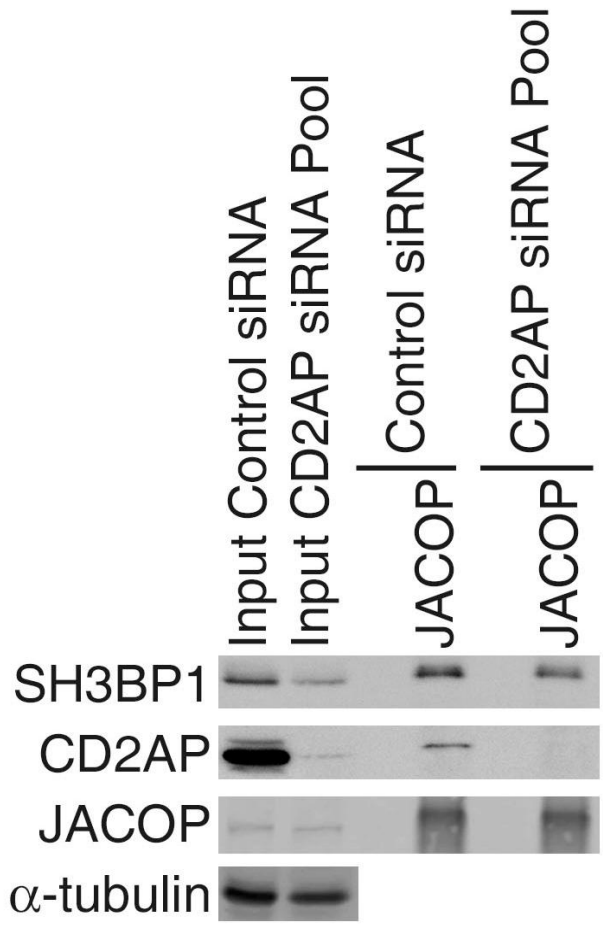

Figure 5.22 CD2AP depletion does not affect the interaction between SH3BP1 and JACOP.

A431 cells transfected with control siRNA or a pool of CD2AP directed siRNA were extracted in PBS and 0.5% Triton X-100. JACOP immunoprecipitates were analysed by immunoblotting for the indicated proteins. The experiment was performed twice.

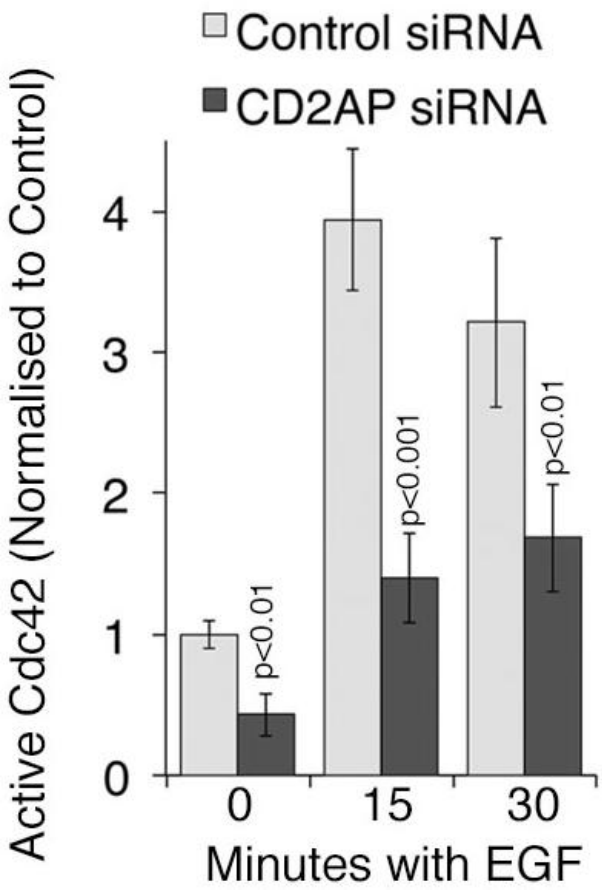

Figure 5.23 CD2AP depletion in A431 cells results in lower levels of active Cdc42.

A G-LISA assay was performed in serum starved and EGF-stimulated A431 cells 96 hours after transfection with either control siRNA or a pool of CD2AP directed siRNAs. Levels of active Cdc42 were normalised to control levels. The bar graphs represent the average of triplicates. The experiment was performed three times. Addition of recombinant Cdc42 as a positive control gave a value of 6 (Normalised to control). Error bars represent ± 1 SD.

The co-immunoprecipitation analysis suggested that SH3BP1 may form a bridge between JACOP and CD2AP as it was required for the two proteins to co-immunoprecipitate. Therefore, I next generated recombinant GST fusion proteins to map the interacting domains in SH3BP1 (Figure 5.24).

Recombinant full-length SH3BP1 as well as a fusion protein containing the C-terminal domain, which contains the SH3 binding domain, pulled down CD2AP (Figure 5.30). In contrast, JACOP was only pulled down by the N-terminal domain. The reason for the full-length protein not interacting with JACOP is not clear, but it could be due to the quality of the protein, which was found to be partially degraded. However, multiple attempts did not increase the quality of the fusion protein. However, JACOP binds to the N-terminal region, which is closer to GST, whereas CD2AP binds to the C-terminal domain, which is farther away from GST; as we used GST-bound to glutathione agarose, one would expect the pull-down of CD2AP to be affected and not the one of JACOP if protein degradation were a problem. It is thus more likely that full-length SH3BP1 is in a confirmation that does not allow efficient binding and that the protein may have to become activated for binding. As I had also degradation problems with the C-terminal domain construct, I cannot exclude that there is a second binding site for JACOP in that domain. Nevertheless, the construct was good enough to pull down CD2AP, indicating that it retained at least some activity. The pull-down data are compatible with the co-immunoprecipitation analysis and support a model according to which SH3BP1 functions as a bridge between CD2AP and JACOP.

Finally, I tested whether EGF signalling affects junctional recruitment of SH3BP1, CD2AP and JACOP the same way as they form a biochemical complex. Indeed, upon inhibition of EGFR, there was a strong reduction in the amount of junctional CD2AP and JACOP in Caco-2 cells in comparison to control cells (Figure 5.25). This correlates with the result with A431 cells described above that EGF stimulates recruitment of JACOP, CD2AP, and SH3BP1 to dorsal ruffles.

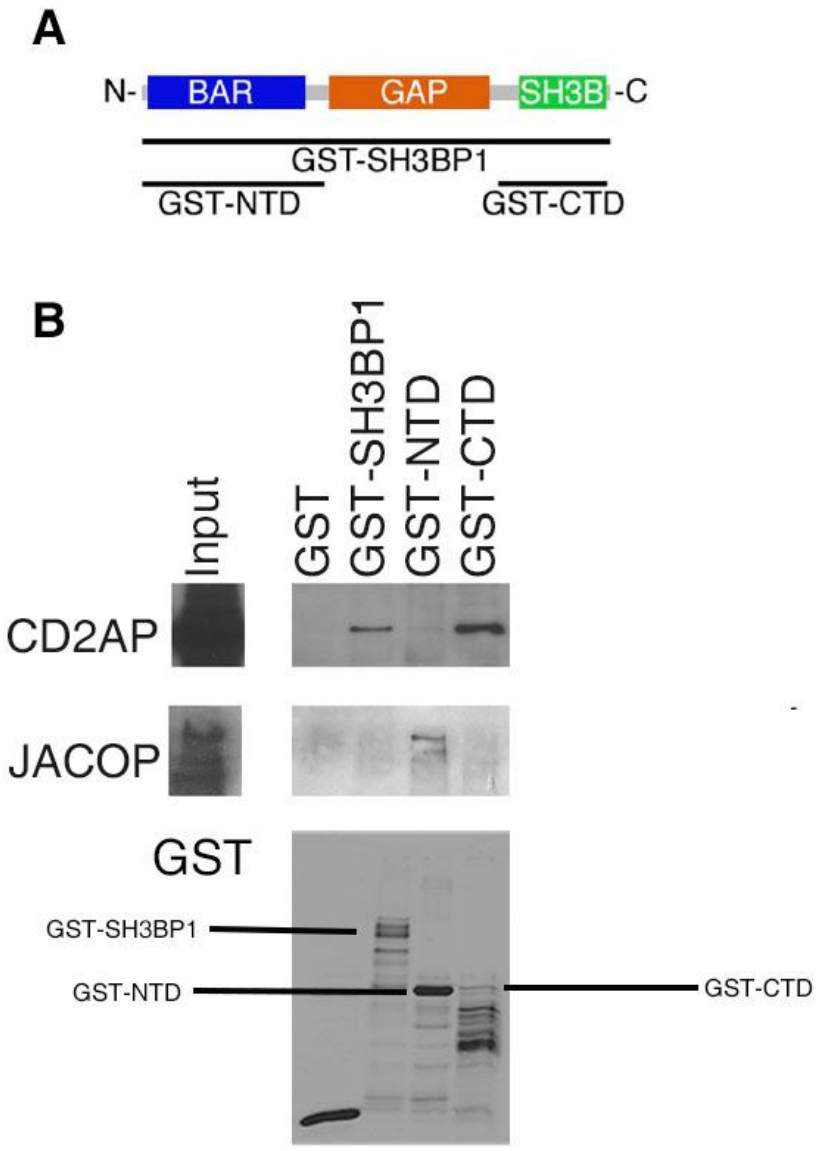

Figure 5.24 Recombinant GST fusion protein pull down assays.

(A) Diagram showing protein domains of SH3BP1 used for GST fusion proteins pull-down assays. (B) Fusion proteins were bound to beads and used in GST pull-down experiments using A431 cell extracts. The precipitates were analysed by immunoblotting for CD2AP, JACOP or GST. The experiment was performed twice.

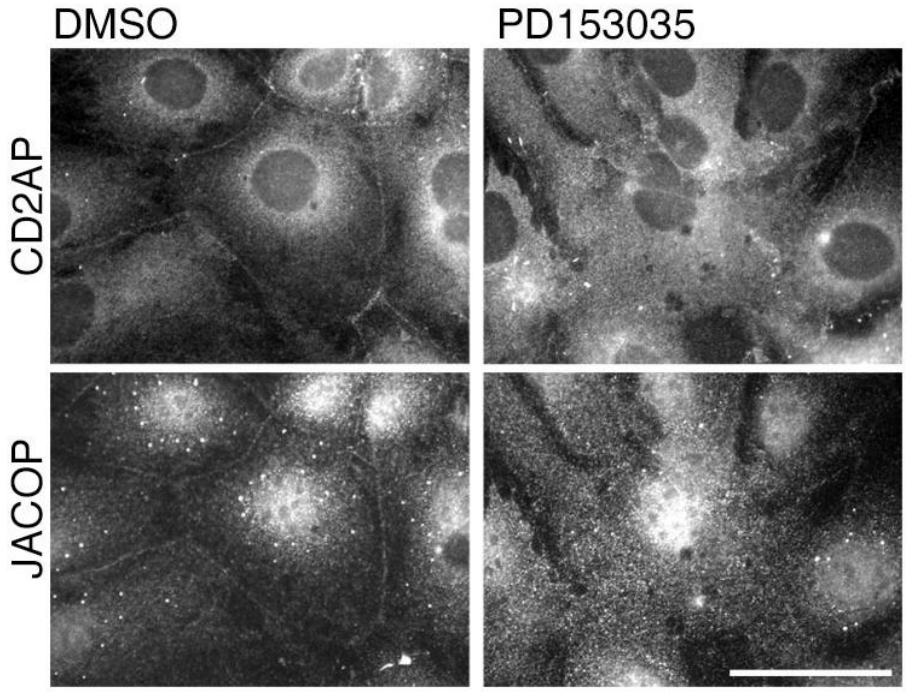

Figure 5.25 JACOP and CD2AP are relocalised upon EGFR inhibition.

Caco-2 cells were inhibited with 3μM PD153035 for 24 hours or a solvent control (DMSO) before being fixed with paraformaldehyde and permeabilised with Triton X-100. Samples were immunostained for JACOP and CD2AP. Shown are epifluorescent images. The experiment was performed twice. Scale bar 10μm.

The actin capping protein CapZα1 interacts with the SH3BP1 complex

Previous work had shown that CD2AP binds and modulates the activity of CapZα1, an F-actin capping protein that regulates filopodial growth [150, 286, 288]. Therefore, I tested whether the SH3BP1 complex also contained this protein and, hence, contains two activities that can regulate the actin cytoskeleton: a Cdc42 GAP and an actin filament capping protein.

Immunoblotting revealed that CapZα1 indeed co-immunoprecipitated with CD2AP, JACOP and SH3BP1 from extracts of A431 cells that had been stimulated with EGF for 30 minutes (Figure 5.26). It is intriguing to note that serum-starved unstimulated cells did not show co-immunoprecipitation of CapZα1, suggesting that the capping protein is recruited later to the complex. In SH3BP1 depleted samples, expression levels of CapZα1 were decreased in comparison to control cells, both by immunofluorescence (Figure 5.27a) and by immunoblotting (Figure 5.27b). This may imply that SH3BP1 may function in the stabilization of the capping protein. However, whether this is a direct effect of the complex or an indirect one via SH3BP's effect on the actin cytoskeleton is not known.

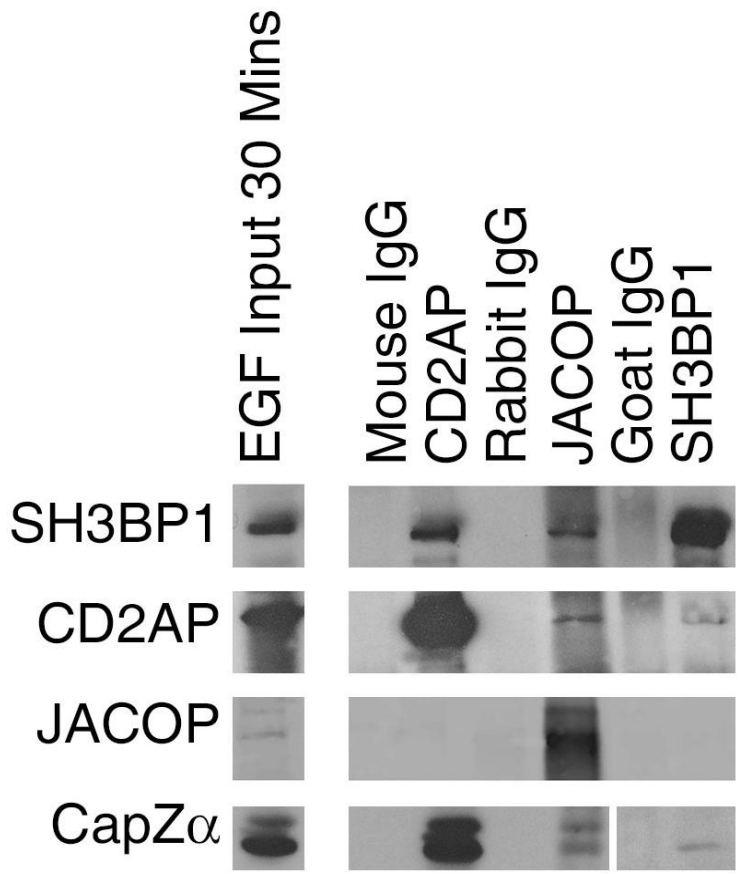

Figure 5.26 CapZα1 is part of the SH3BP1 complex in EGF-stimulated A431 cells.

Serum-starved, EGF-stimulated (30 minute EGF-stimulation) A431 whole cell lysates were extracted in PBS and 0.5% Triton X-100**.** Immunoprecipitates were performed with the antibodies indicated. Mouse, Goat and Rabbit IgG were used as negative controls. Co-immunoprecipitating proteins were analysed by immunoblotting as indicated.

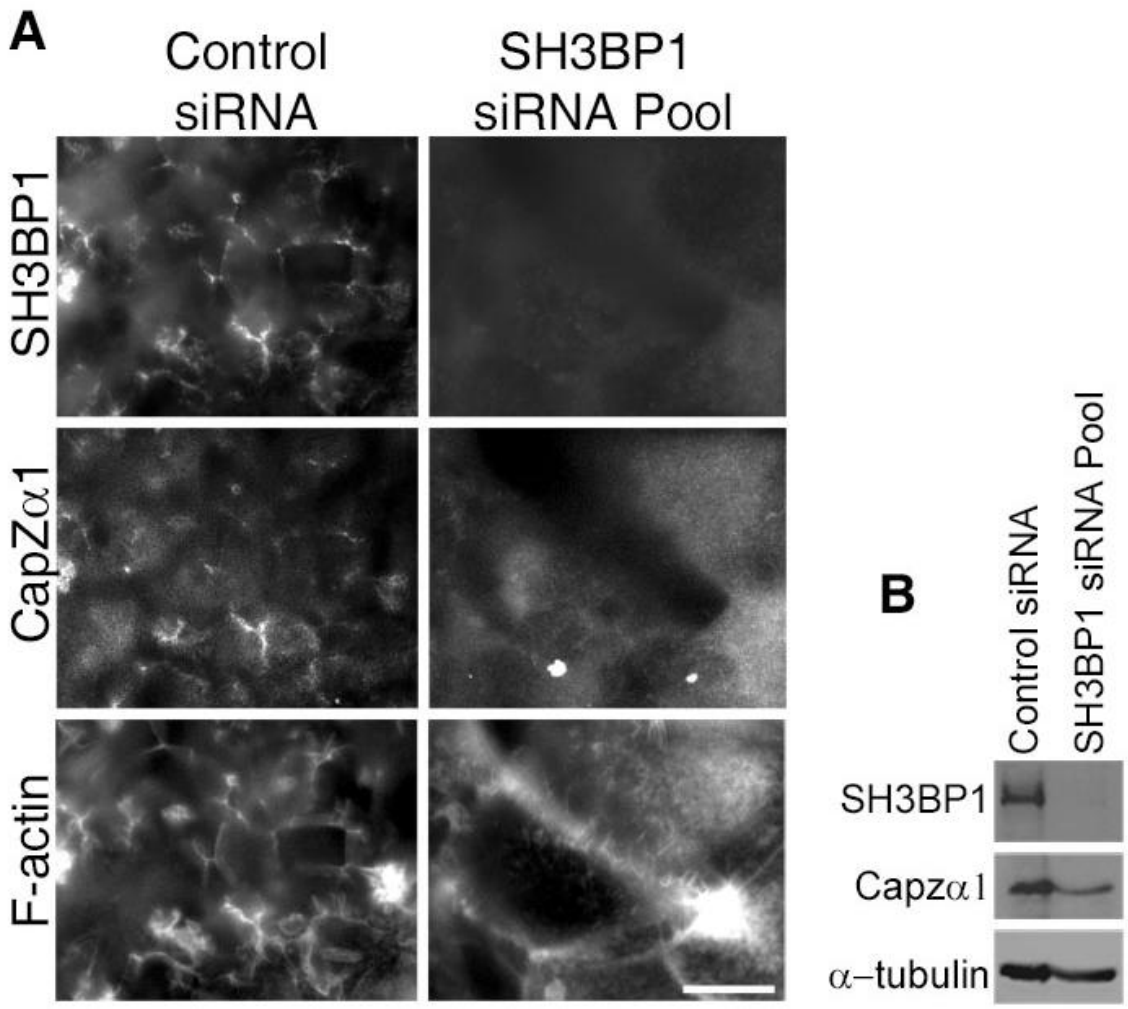

Figure 5.27 Effects of SH3BP1 depletion on CapZα1.

A431 cells were transfected with siRNAs as indicated. After 72 hours, the cells were serum-starved for 16 hours and subsequently stimulated with 100ng/ml EGF before being (A) fixed with paraformaldehyde and permeabilised with Triton X-100, or (B) collected and immunoblotted for SH3BP1 and CapZα1. For the immunoblot, alpha-tubulin was used as a loading control. (A) For the immunofluorescence, SH3BP1, CapZα1 and F-actin were stained. Shown are epifluorescent images. Scale bar 10μm.

Finally, I assessed whether knockdown of CapZα1 in A431 cells affects SH3BP1 expression and F-actin organisation. Depletion of CapZα1 in A431 cells resulted in an increase in filopodial length in a similar manner as SH3BP1 depletion (Figure 5.28a). By immunoblotting, depletion of CapZα1 had no effect on JACOP and CD2AP expression levels, while SH3BP1 levels were reduced, suggesting that SH3BP1 may also require CapZα1 for stabilization (Figure 5.28b).

My data thus indicate that the SH3BP1 complex contains two activities that regulate the actin cytoskeleton: the GAP SH3BP1 and the F-actin capping protein CapZ.

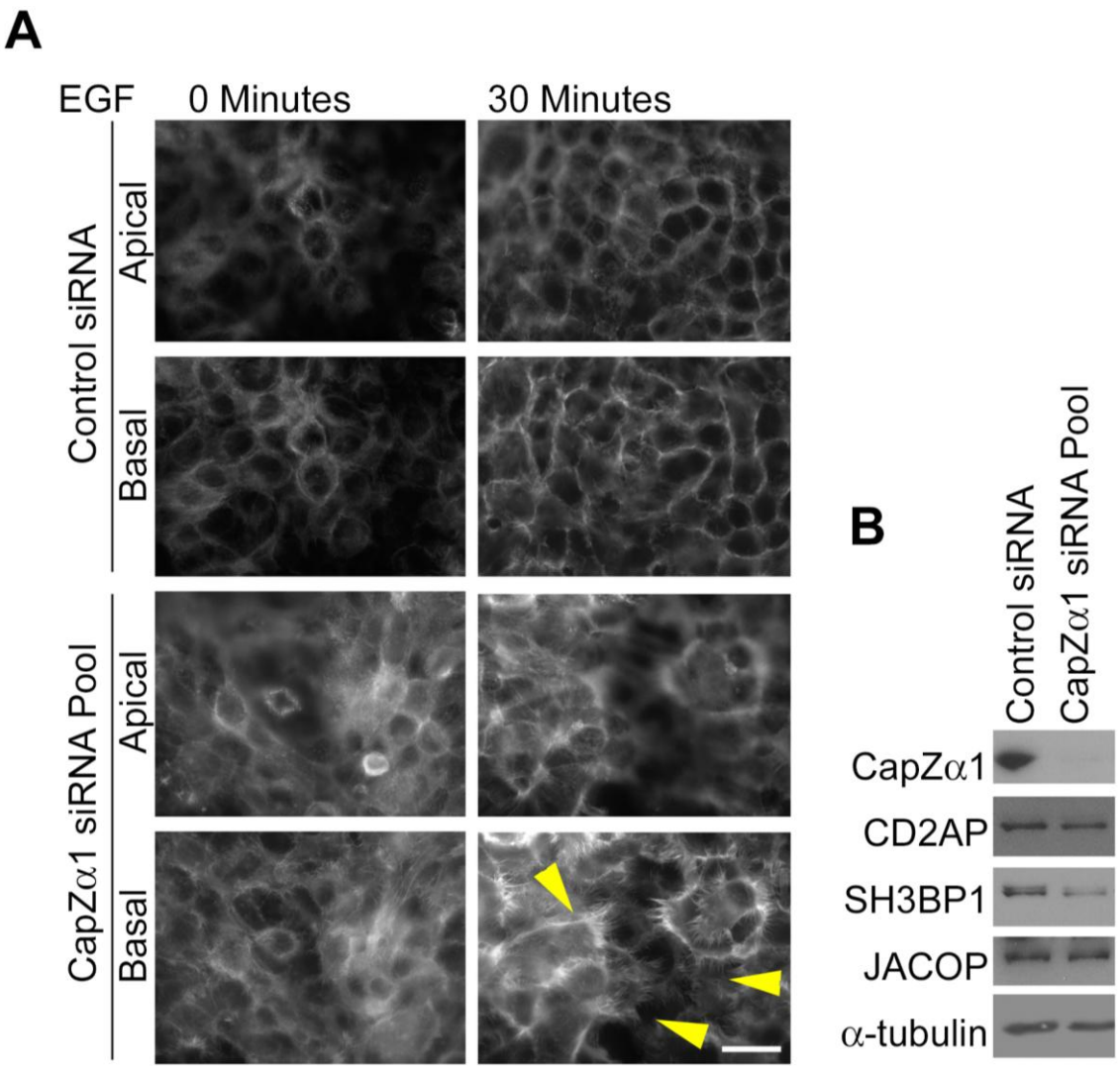

Figure 5.28 CapZα1 depletion phenocopies SH3BP1 depletion.

A431 cells were transfected with either control siRNA or a pool of CapZα1 directed siRNAs. After 72 hours, the cells were serum-starved for 16 hours and subsequently stimulated with 100ng/ml EGF, before either being (A) fixed with paraformaldehyde and permeabilised with Triton X-100, or (B) collected and immunoblotted for the indicated proteins. For the immunoblot, alpha-tubulin was used as a loading control. In panel A, F-actin was stained with fluorescent phalloidin. Yellow arrows denote filopodia. Shown are epifluorescent images. Scale bar 10µm.

Chapter 5 – Discussion

In this chapter, I have presented evidence that SH3BP1 forms a stable complex with the junctional adaptor JACOP/paracingulin, and the signalling scaffold CD2AP. If stimulated, this complex also recruits the actin capping protein CapZα1. Together with the results from chapter 4 indicating that SH3BP1 regulates Cdc42 signalling and junction assembly, these data demonstrate that SH3BP1 is part of a dual activity complex that regulates Rho GTPase activity and actin dynamics, and that the complex is recruited to sites of active actin remodelling and cell-cell junctions.

JACOP had been previously reported to be important for the regulation of the Rho GTPases RhoA and Rac1 in the canine kidney cell line MDCK [63]. Depletion of JACOP had an effect on the AJC and the actin cytoskeleton, although not as severe as depletion of SH3BP1. Upon assessment of global levels of active Cdc42, I found that JACOP depletion decreased levels of active Cdc42. This suggests that JACOP is required for the correct recruitment of SH3BP1 to sites of Rho GTPase induced dynamic actin remodelling and, if SH3BP1 is mislocalised, it maybe that upon depletion of JACOP, the GAP promotes uncontrolled inactivation of Cdc42. In MDCK cells, reduced Rac1 signalling upon JACOP depletion was attributed to reduce the junctional associated GEF for Rac, TIAM-1, although it was not possible to determine the distribution of endogenous TIAM-1 [63]. As SH3BP1 can also act on Rac1, it could be that it also contributes to Rac1 regulation downstream of JACOP in MDCK cells.

JACOP not only enhanced the junctional recruitment of SH3BP1 but also of CD2AP, a protein that requires SH3BP1 to form a complex with JACOP. In the AJC, the three proteins exhibit a promiscuous distribution as they neither localise specifically to the TJ or the AJ. It is interesting to note that already the first description of JACOP pointed out that, by immunofluorescence, this protein exhibits great plasticity in its localisation and, depending on the tissue analysed, can appear more closely associated with TJ or AJ, respectively [61]. Although my data suggest that JACOP mediates recruitment of the SH3BP1 complex, what determines the subjunctional distribution within the AJC remains to be identified.

The second SH3BP1 binding partner identified, CD2AP, was previously shown to be important for the regulation of the actin cytoskeleton, which may contribute to its role in podocytes and kidney function [289]. CD2AP had been proposed to function as an inhibitor of actin capping [286]; therefore, upon depletion of CD2AP, there was expected to be more capping and subsequently less actin dynamics. My observation that depletion of CD2AP interfers with junction assembly but did not lead to enhanced filopodial growth is thus in agreement with these data. Depletion of CD2AP also resulted in less global levels of active Cdc42, suggesting that regulates SH3BP1 activity. However, the molecular mechanism by which it regulates SH3BP1 remains to be determined as it also reduced the total expression levels of the GAP.

It is intriguing that the interaction between JACOP and CD2AP is dependent on SH3BP1, as upon depletion of the GAP, JACOP and CD2AP no longer co-immunoprecipitated. So, SH3BP1 seems to act as a bridge between JACOP and CD2AP (Figure 5.29). This model is supported by GST pull-down assays

that show that JACOP can bind to the BAR domain of SH3BP1 whereas CD2AP can interact with the SH3 binding domain of SH3BP1.

The fourth protein that I found in the SH3BP1 complex is CapZα1. CapZα1 is a subunit of a protein complex that regulates actin filament capping [290]. Because of lack of appropriate antibodies, I did not determine whether other subunits of this complex are also present in the SH3BP1 precipitates. As CapZ seems to form a stable complex, it is likely that the entire complex is present. Since CD2AP is thought to function as a CapZ inhibitor [291, 292], it would be feasible that the SH3BP1 complex regulates the function of CapZ by sequestration of one of its subunits.

Of the components of the SH3BP1 complex that I have identified, CapZα1 is the only one that was only associated with the complex in cells that had been stimulated. The molecular basis of the regulatory mechanisms that regulates this association is not known yet. CapZα1 is a known interaction partner of CD2AP, which is the reason why I investigated whether it is part of the SH3BP1 complex. It is not clear if and how this interaction is regulated. I have also not further investigated whether there are any other interactions between CapZ and SH3BP1 complex components. Based on the interactions known today, however, the complex seems to assembly as proposed in Figure 5.29, with SH3BP1 forming a bridge between JACOP and CD2AP, and the latter protein forming as a scaffold that recruits CapZ.

The components of the identified SH3BP1 complex thus seem to have concrete specific functions. JACOP is primarily responsible for the junctional recruitment of the complex; whereas SH3BP1 regulates the activity of the Rho GTPases Cdc42 and Rac, and serves as a structural linker to CD2AP. CD2AP then

recruits CapZ and, thereby regulates actin filament capping. The SH3BP1 complex thus regulates actin dynamics, membrane remodelling and junction formation via two mechanisms: regulation of Cdc42 and Rac, and regulation of actin filament dynamics.

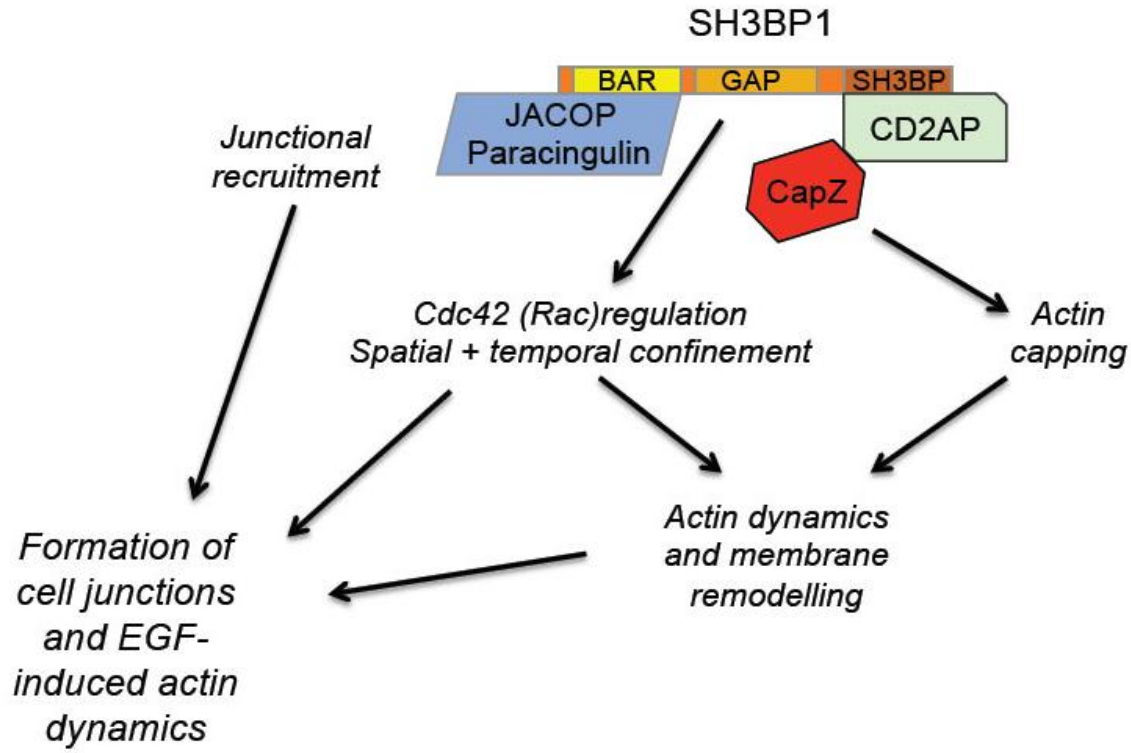

Figure 5.29 The SH3BP1 complex and regulation of junction formation.

The BAR domain-containing N-terminal domain of SH3BP1 binds to JACOP/paracingulin, a junctional adaptor, and the C-terminal domain to CD2AP, a scaffolding protein. The complex is required for normal Cdc42 signaling and junction formation. The filamentous actin-capping protein CapZ also associates with the SH3BP1 complex through binding to CD2AP and is required for the control of actin remodelling. Epithelial junction formation and morphogenesis thus require a dual activity complex that is recruited to sites of active membrane remodelling, containing SH3BP1 to guide Cdc42 signaling and CapZ to regulate cytoskeletal dynamics.

Chapter 6

SH3BP1 in Epithelial Morphogenesis

Chapter 6: The Role of SH3BP1 in Epithelial Morphogenesis

Part of this chapter was published: J Cell Biol. 2012 Aug 20;198(4):677-93.

Introduction to chapter 6

Given the importance of SH3BP1 in the regulation of junction assembly and epithelial differentiation, I next wanted to determine the importance of SH3BP1 in epithelial morphogenesis using three dimensional (3D) cultures. I will show in this chapter the effect of SH3BP1 during longer depletion and how upon depletion of SH3BP1, cysts development in 3D cultures become more disorganised and smaller suggesting that SH3BP1 is important for the development of normal cysts and epithelial morphogenesis.

Results – Chapter 6

SH3BP1 depletion results in disorganised epithelial cysts

Analysis of epithelial cyst formation by Caco-2 cells requires longer incubation times than the experiments in previous chapters. It was thus necessary to test first whether the siRNA-mediated depletion protocol was sufficient to suppress expression of SH3BP1 until the end of the experiment. Figure 6.0 shows that depletion even 120 hours after the siRNA transfection was still efficient, indicating that the depletion protocol could be used for the 3D morphogenesis studies.

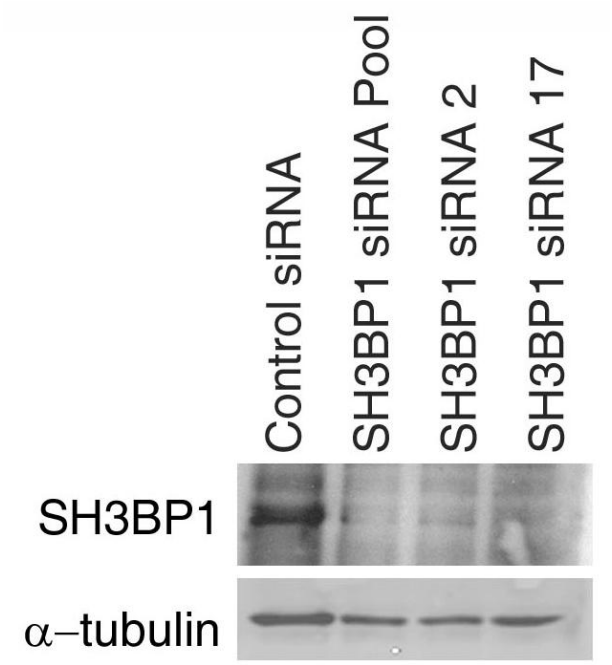

Figure 6.0 Long-term depletion of SH3BP1.

Caco-2 cells were transfected with either control siRNA, individual SH3BP1 directed siRNAs or a pool of SH3BP1 specific siRNAs. After 120 hours the cells were collected and immunoblotted for SH3BP1. Alpha-tubulin was used as a loading control.

Next, I performed the 3D morphogenesis experiments using the same depletion protocol. After the 120 hours of incubation, I first analyzed the phenotype by phase contrast before fixation in order to establish the primary phenotype. This revealed that SH3BP1-depleted samples formed smaller cysts, with evident disruption of the normal structure of cysts seen in control samples. The cysts did not exhibit their normal rounded shape and had a more disorganised structure. The lumen was not well-rounded as seen in the controls but was more warped with multiple lumens (Figure 6.1). These phase contrast images thus already indicate that SH3BP1 is required for normal cyst formation in 3D cultures.

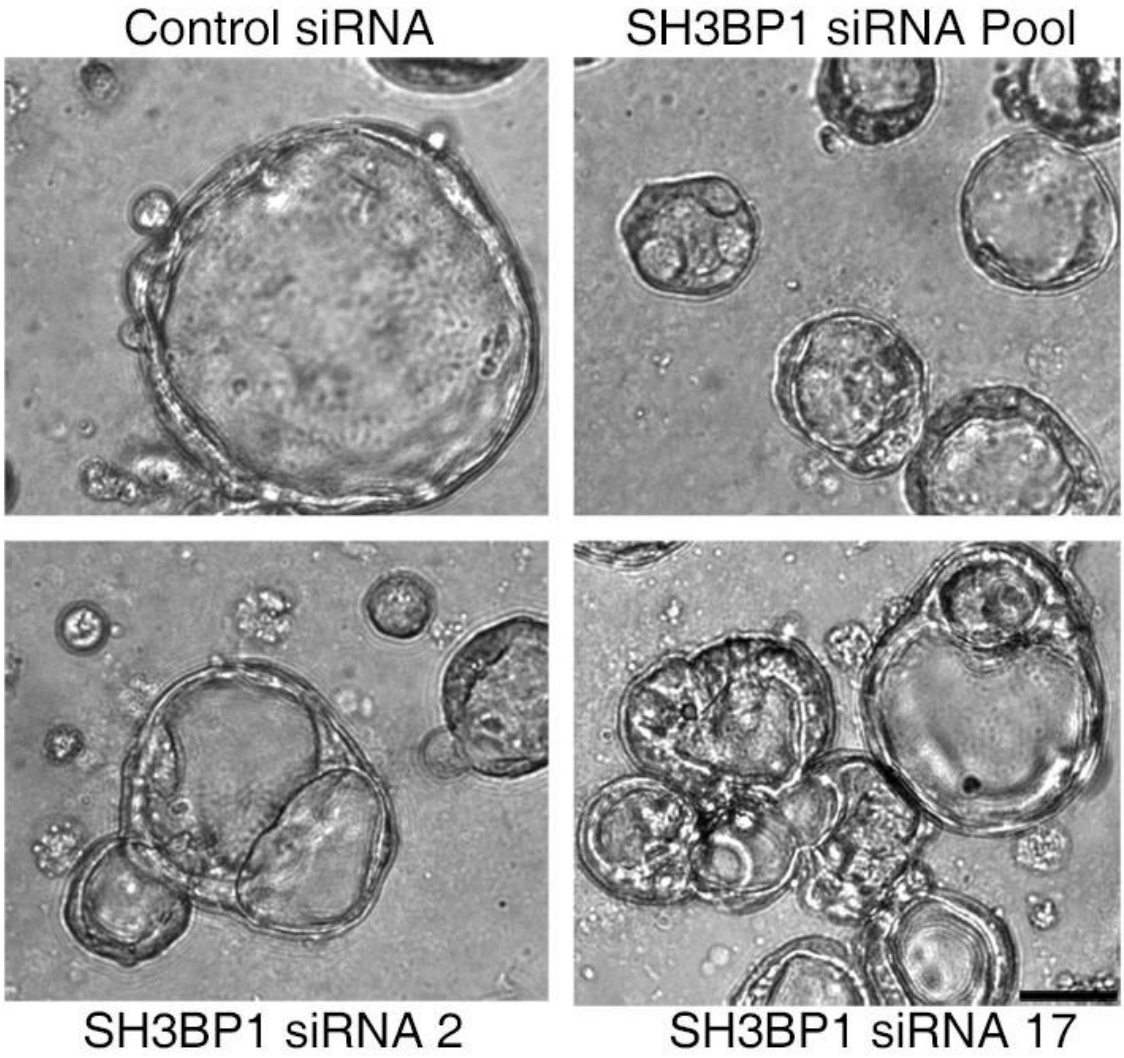

Figure 6.1 Depletion of SH3BP1 in 3D cultures interfers with normal cyst morphogenesis.

Caco-2 cells were transfected with either control siRNA, individual SH3BP1 directed siRNAs or a pool of SH3BP1 specific siRNAs. Every 48 hours cholera toxin (0.1ug/ml) was added in order to facilitate rapid lumen expansion. After 120 hours the cells were photographed using phase contrast with a 20x lens before being fixed. Scale bar 30µm.

I next stained the samples for F-actin using fluorescent phalloidin to visualise the outlines of the lumens, which are normally enriched in F-actin. Analysing the samples with a confocal microscope further displayed the extent of the phenotype. The F-actin staining highlighted two effects of the SH3BP1 depletion. Firstly, quantification revealed that the cysts were significantly smaller if SH3BP1 was depleted: the majority of the SH3BP1 depleted cysts were below 75μm in diameter whereas the majority of the cysts were above this size in control samples (Figures 6.2 and 6.3). Secondly, the cysts displayed a disrupted organisation and were not clearly defined. It was difficult to identify a ring of apical F-actin around a centralised lumen; there were often cells left within the lumen (Figure 6.3) [1]. I quantified these experiments by counting the number of lumens in cysts from images obtained from quadruplicate coverslips, performing two independent experiments (as the cyts from SH3BP1 depleted cells were smaller, only cysts that had a diameter of >30μm were considered; Figure 6.4). These observations thus demonstrate that SH3BP1 regulates cyst size as well as normal epithelial morphogenesis.

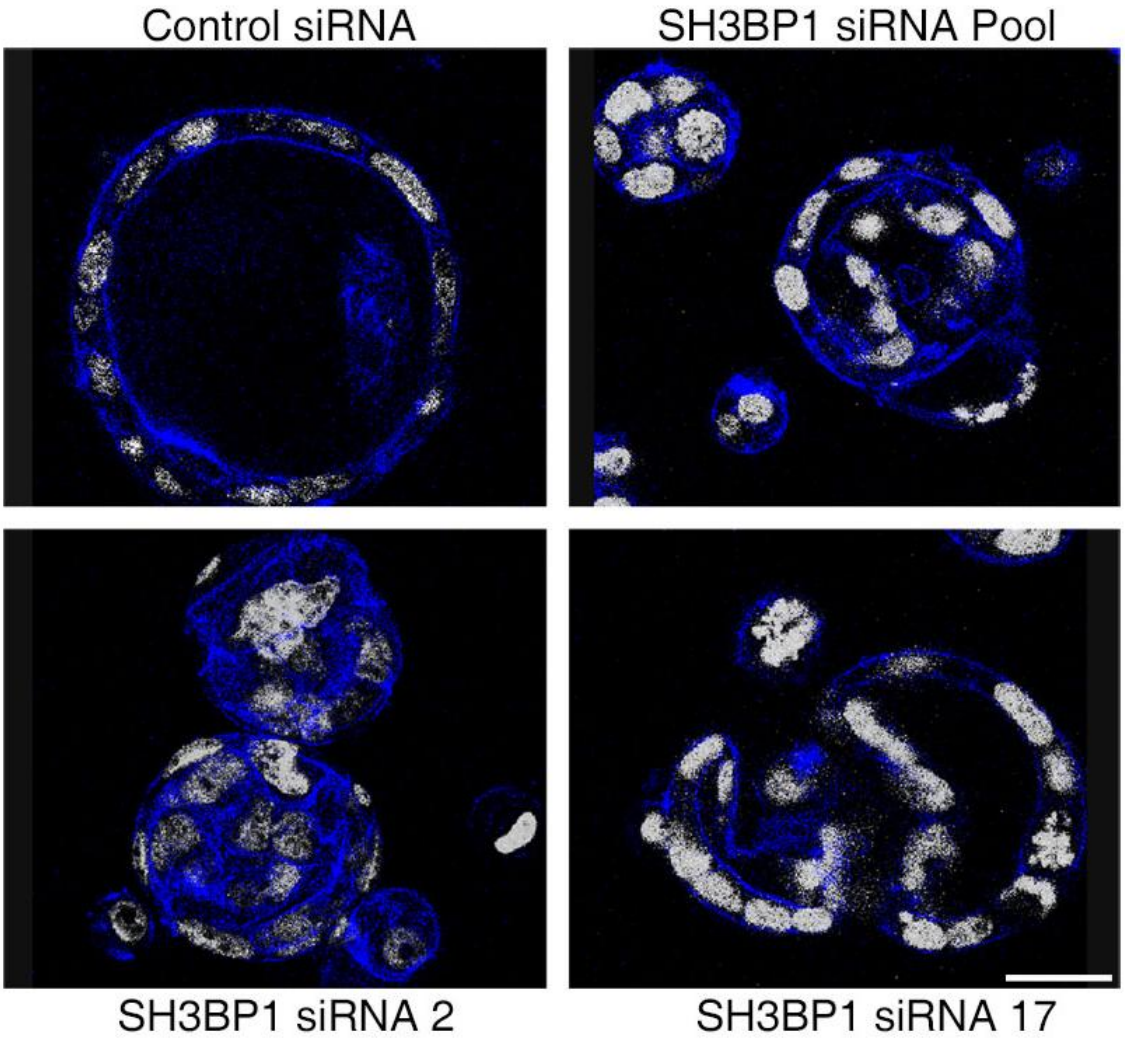

Figure 6.2 Depletion of SH3BP1 in 3D cultures results in disruption of normal F-actin organisation.

Caco-2 cells were transfected with either control siRNA, individual SH3BP1 directed siRNAs or a pool of SH3BP1 specific siRNAs. Every 48 hours cholera toxin (0.1ug/ml) was added in order to facilitate rapid lumen expansion. After 120 hours the cells were fixed with paraformaldehyde, and permeabilised with 1% Triton-X100/0.1% SDS. Cysts were stained for F-actin (Blue) and DNA (Grey). Shown are confocal images. Scale bar 10µm.

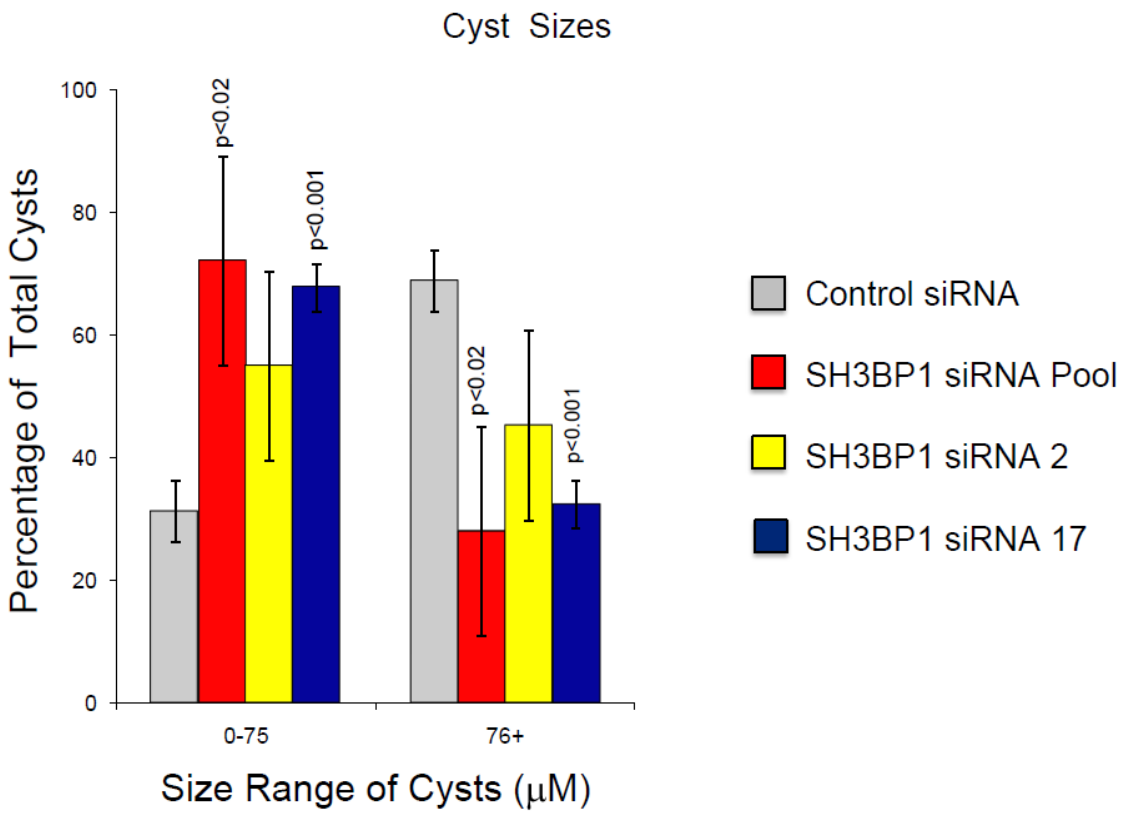

Figure 6.3 Quantification of cysts size.

Cysts were quantified from triplicate coverslips from two experiments. The diameters of the cysts were quantified using ImageJ as described in the materials and methods. Bars represent averages of 4 images per sample (Error bars ± 1 SD).

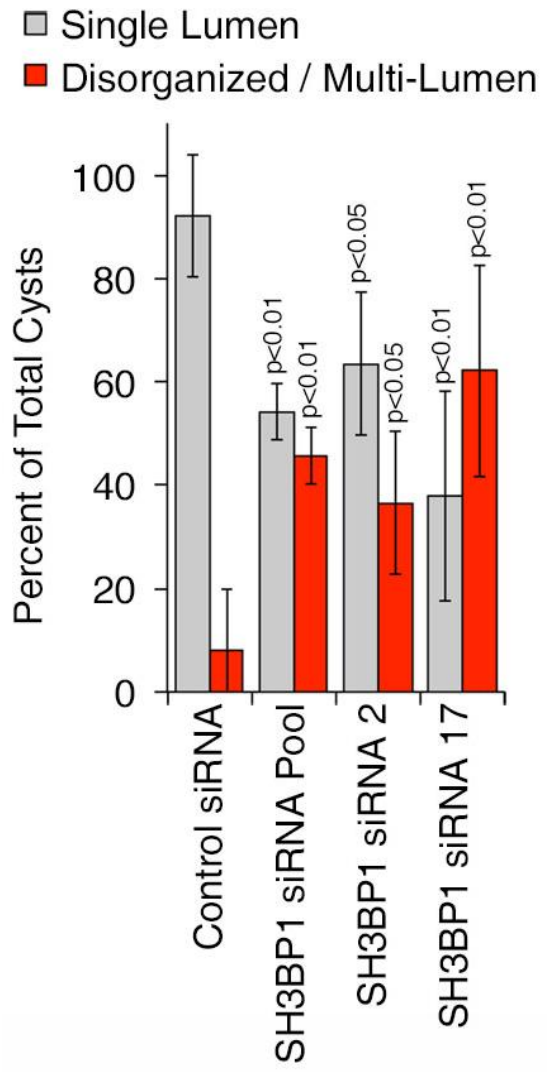

Figure 6.4 Quantification of lumen type.

Cysts were quantified from quadruplicate coverslips from two experiments. Cysts above 30μm in diameter were used to quantify lumen structures. Shown are averages ± 1 SD.

Chapter 6 - Discussion

In 3D extracelluar matrix cultures, epithelial cell lines such as Caco-2 cells develop cysts that resemble the normal organisation in tissues with a central lumen. My experiments show that SH3BP1 is also functionally important for epithelial morphogenesis and normal F-actin organisation in such organotypic cultures. Upon depletion of the GAP, there was a severe effect on the organisation of the cysts, with F-actin staining that was disrupted and dispersed, as well as cysts with either multiple or disorganised lumens and the remained lumen was smaller. This implies that SH3BP1, as with 2D cultures, is important for 3D epithelial morophogenesis.

SH3BP1 functions as a GAP for Cdc42 in Caco-2 cells and this Rho GTPase has been shown to be important for epithelial morphogenesis of this cell line, as it regulates the orientation of the spindle during mitosis [137]. This is a conserved mechanism as Cdc42 has also been shown to regulate the orientation of the spindle in early mouse oocytes and *C elegan* embryos [293, 294]. Regulation of Cdc42 is an important aspect of organogenesis as previously it was shown that the Cdc42 GEF tuba was important for spindle alignment [231]. Overactivation of Cdc42 due to SH3BP1 depletion may thus result in misorientation of the mitotic spindle. This would explain why there were more cells left inside the lumens and why the cells struggle to assemble a single apical lumen [116, 137]. It is further possible that the reason for the smaller cysts seen in SH3BP1 depleted cells is the misorientation of the spindle as the cell cycle may get retarded if the spindle is not oriented properly. Another possibility is that depletion of SH3BP1 results in a delay in proliferation and,

therefore, leads to smaller cysts. Rho GTPase signalling has been shown to be involved in cellular proliferation, with the GAP, Deleted in Liver Cancer 1 (DLC1) shown to surpress cell proliferation [295]. Conversley, IQGAP, an effector of Cdc42 was shown to regulate proliferation in conjunction with the serine/threonine kinase, mTOR [296, 297]. Although siRNA mediated depletion of SH3BP1 also leads to enhanced Rho GTPase signalling, it could be that it leads to a decrease in proliferation and thus smaller cysts due to deregulated Rho GTPase signalling.

Formation of lumens is an important aspect in organogenesis [118]. The formation of organs is due in part to a number of signals, which ultimately result in the correct formation of polarised structures and subsequently formation of an organ. Many of these pathways include Rho GTPases; hence, a protein that regulates Cdc42 activity and cell-cell adhesion was a likely candidate for a regulator of 3D morphogenesis. My experiments confirm this hypothesis and demonstrate that SH3BP1 is important for epithelial differentiation in 3D cultures.

Final Discussion

Rho GTPase regulation is an important component of a number of biological processes, including, crucially in the context of this project, regulation of the actin cytoskeleton. Rho GTPases had already been established as being part of several distinct signalling mechanisms that link the actin cytoskeleton to the AJC (Chapter 1). However, how they are regulated in the context of junction formation and function is not completely understood. Therefore, the initial question of my project was which negative regulators of Rho GTPases regulate epithelial differentiation and junction formation. Hence, we performed a functional siRNA screen to identify GAPs that play a role in junction assembly and epithelial differentiation in the columnar epithelial cell line Caco-2.

siRNA screen of GTPase activating proteins in Caco-2 cells

For the functional siRNA screen, we employed a library targeting all Rho GTPases and most known Rho GAPs. This screen revealed that siRNA mediated depletion of the Rho GTPases Cdc42 and RhoA had the strongest effects on the integrity of the AJC: depletion of either perturbed the morphology of the AJC considerably. From the GAPs screened, five had an effect on junction morphology that could be confirmed in a secondary screen, which used different sets of siRNAs that were chemically modified to enhance specificity (On-Target plus). These five hits were the Cdc42/Rac1 GAP SH3BP1, the RhoA GAPs OPHN1 and MYO9A, and two RasGAPs, PLXNA1 and PLXNB1

that function as Rho GTPase effectors. Of course, the screen does not rule out other GAPs important for epithelial differentiation as a few were missing from our library and we did not determine whether GAPs whose depletion did not affect junction formation were indeed depleted during the screen. Therefore, a more complete assessment of GAPs involved in junction formation in the future will need determinations of depletion efficiencies and, possibly, optimisation of the depletion protocol as different proteins may have different stability [298]. Of the GAPs identified, only two, SH3BP1 and MYO9A, have been analysed in detail. MYO9A also localises to the junctional complex and regulates junction formation and has recently been linked to the regulation of collective cell migration [213-215].

A possible future aim thus is to explore the other GAPs, which also provided a strong hit in the screen and characterize further how they regulate epithelial differentiation. However, due to time constraints, this was not possible during my thesis. Nevertheless, it is interesting that the screen generally led to the identification of junctional regulatory proteins. As SH3BP1 and MYO9A have now both been established as junctional components, and OPHN1, another positive hit from the screen, also associates with cell-cell contacts.

SH3BP1 is important for epithelial junction formation and Rho GTPase regulation

In the second experimental part of my thesis, I explored the function of SH3BP1 in junction formation in more detail. I made a number of key observations.

SH3BP1 was found to be an important regulator of Cdc42 and, to a lesser extent, Rac1, during epithelial junction formation in distinct epithelial cell lines. I also discovered that signalling induced by the growth factor EGF is important for the localization of SH3BP1 to the plasma membrane and the junctional complex. Depletion of SH3BP1 resulted in increased numbers and longer filopodia in ectodermal epithelial cell lines. As filopodia have been proposed to mediate initial cell-cell contact and thus represent an intermediate step in junction assembly, overactivation of Cdc42 seems to prevent the transition from early, immature cell-cell contacts to fully formed junctional complexes [299, 300]. Regulation of Rho GTPases is the central function of SH3BP1, as complementation experiments revealed that its GAP activity is required for normal junction formation. As active Cdc42 failed to localise normally in GAP depleted cells, I conclude that SH3BP1 represents an important regulator of Cdc42 signalling in epithelial cells and that it is a crucial regulator of epithelial junction formation by confining Cdc42 activity.

Two important aspects to investigate in future experiments are to elucidate how EGF receptor stimulation activates SH3BP1 and which mechanisms control SH3BP1 to regulate junction localisation and GAP activation. An obvious candidate maybe c-Abl. SH3BP1 was initially identified from a cDNA library screen, which used a c-Abl probe to identify potential binding partners to the protein [186]. Therefore, to understand whether and how manipulation of c-Abl could mimic some the SH3BP1 phenotypes or whether depletion of the GAP can affect some of the c-Abl described roles could be interesting future directions. Another possible mechanism to control SH3BP1 is ERK 1/2 [301]. SH3BP1 has five potential ERK binding sites and potential phosphorylation

sites, all predicted to be in the SH3 binding domain (Scansite), and the activation of the EGFR results in the stimulation of MAP kinase signalling, leading to phosphorylation and activation of ERK. Hence ERK may possibly represent an important regulator of SH3BP1, guiding its activation, localization to the junction and, subsequently, regulation of Cdc42 to control actin remodelling and formation of the AJC [302]. One particular potential phosphorylation site is conserved in all species and is a serine located at position S544 in the SH3 binding domain (ClustalW). Thus, it would be interesting to determine whether this residue is phosphorylated in response to EGFR activation and in an Erk-dependent manner, and if yes, to determine whether phosphorylation regulates activation by substituting the serine with either an alanine to prevent activation or a negatively charged amino acid to mimic constitutive phosphorylation.

SH3BP1 is part of a complex that regulates membrane remodelling and Cdc42

In the second part of my study of SH3BP1, I assessed mechanistic aspects of SH3BP1 in regard to the formation of the AJC and regulation of Rho GTPases. Several interesting observations were made. Firstly, SH3BP1 was found to interact with the junctional scaffold JACOP, which is important for the localization of SH3BP1 to the AJC. We also found that the actin capping inhibitor CD2AP is part of the complex, and, finally, the actin capping protein CapZα1 can also associate with the SH3BP1 complex. This suggests that the

complex can regulate two processes: Cdc42 signalling via the GAP activity of SH3BP1 and actin capping via the capping activity of CapZα1. Moreover, both JACOP and CD2AP are scaffolding proteins and can interact with other proteins. Hence, SH3BP1 may be part of a large multimeric complex with multiple activities that guides junction formation and morphogenesis. It would thus be interesting to use a proteomics approach to identify additional components and interactors of the SH3BP1 complex in the future.

SH3BP1 supports processes driven by Cdc42, demonstrating the importance of terminating the GTPase cycle for normal Rho GTPase signalling and cytoskeletal remodelling. Inactivation of the GAP did not prevent cells to initiate adhesion, but prevented them from assembling junctional complexes, underlining the importance of the temporal control of Cdc42 regulation for epithelial morphogenesis The SH3BP1 complex represents a dual activity feedback complex required for the coordination of actin-driven morphological processes that is recruited to sites of active membrane remodelling by the scaffolding components JACOP and CD2AP to terminate individual morphological steps, enabling activation of subsequent GTPase activated processes and junctional maturation. CapZα1 and SH3BP1 depletion resulted in the same actin disruption, and increase in filopodia. Therefore in possible future work, it would be interesting to determine how filopodia are disregulated and whether known regulators of filopodia are affected. A possible candidate is insulin-receptor substrate p53 (IRSp53). This protein has already been shown to interact with Cdc42, Rac1 and various actin-linked proteins. Therefore it is a likely candidate for a protein to be affected by disruption of the SH3BP1 complex [303-305].

SH3BP1 depletion in a 3D culture system

In the final part of my thesis, I assessed the importance of SH3BP1 in the formation of 3D epithelial structures. As such 3D culture systems are thought to represent conditions more similar to the situation in vivo than normal plastic substrates, it was important to test whether SH3BP1 also regulates differentiation in such organotypic cultures. I discovered that depletion of SH3BP1 led to an attenuation of normal cyst formation. Depletion affected two different aspects of epithelial morphogenesis: many cysts lost their normal organisation and developed into multilumen structures, and, generally, the cysts remained smaller in the absence of the GAP. Overactivation of Cdc42 had been shown to produce a misalignment of the mitotic spindle and affect cell polarity; therefore, it is likely that SH3BP1 importance for the formation of 3D cysts is because of its role in the confinement of Cdc42.

Another possible mechanism by which SH3BP1 may affect junction assembly is by affecting the function of polarity protein Par6, as it has previously been shown that deregulation of Cdc42 leads to delocalization of PAR6 in C.elegans embryos [306]. The interplay between polarity proteins and Rho GTPases is of general importance and occurs bidirectionally, as Par3 is known to regulate Rac activation by interacting with TIAM1 [113, 235, 307].

Further experiments could be performed in the future to characterise the role of SH3BP1 in cysts morphogenesis. For example, to deplete the other proteins associated in the complex, such as CD2AP, CapZα1or JACOP in order to assess what is their effect in cysts morphogenesis, if any; they have on the

correct formation of lumen and cyst structures. Other possible experiments would be to test whether SH3BP1 depleted cells have changes in cell proliferation, death and/or migration and if so, to analyse the cell cycle phase that is affected and at which extent such changes could correlated to the defect in cysts organisation.

Final summary

Rho GTPases are small G proteins that have an important role in a number of regulatory mechanisms linked to the assembly and function of the AJC. My thesis focused on how Rho GTPases are regulated during the control of actin reorganisation and junction formation. I approached this question by performing a screen of negative regulators of Rho GTPases known as GAPs and characterized one of them, SH3BP1. I demonstrated that SH3BP1 regulates the actin cytoskeleton and subsequent junction formation via the confinement of Cdc42 signalling. I also showed that SH3BP1 is part of a complex, which contains the scaffolds JACOP, and CD2AP as well as the actin capping protein CapZ□1. This novel complex regulates junction formation and filopodial dynamics. I finally showed that the effect of SH3BP1 depletion seen in 2D cultures also affected the epithelial morphogenesis potential in 3D culture system, supporting the physiological relevance of SH3BP1. As shown previously, membrane dynamics underlies initiation of cell contacts in various epithelial models; different types of epithelia can make use of different mechanisms of actin-driven processes. Some cells use filopodia and others rely

on lamellipodia [106, 107]. As for some cell types (e.g., keratinocytes), both mechanisms have been reported, it may even depend on the conditions analysed whether junction formation is initiated by filopodia or Lamellipodia [106, 204, 308, 309]**.** As filopodia are induced by Cdc42 whereas lamellipodia require Rac, different GTPases can initiate cell-cell contacts and, as they can both regulate polarity complexes, lead to successful epithelial differentiation [66, 310]. SH3BP1 was originally identified as a GAP with similar activities towards Cdc42 and Rac1 *in vitro* [187]. This was recently confirmed using cell-based assays for Cdc42 and Rac [189]. The latter paper also demonstrated that SH3BP1 regulates Rac at the front of migrating cells. Together with our data, this indicates that SH3BP1 can stimulate GTP hydrolysis by both Rac and Cdc42 *in vitro* and *in vivo*, and that the activities towards both GTPases are relevant for specific biological processes. Moreover, it could be that SH3BP1 regulates junction formation not only in epithelia that rely on filopodia but also of those that use lamellipodia. However, we could not detect clear morphological effects in response to expressing dominant-negative SH3BP1 in MDCK cells, suggesting that it is not of central importance in this cell type (data not shown). Nevertheless, it will be important to test the role of SH3BP1 in this cell line using a siRNA approach.

The observations that the GAP activity of SH3BP1 towards Rac and Cdc42 is differentially employed in specific cellular processes highlights the importance of the subcellular targeting of the GAP. While during migration SH3BP1 is targeted to the front of the cells and regulates Rac, which is active at the leading edge, it is targeted to cell-cell contacts during junction formation, and leads to deregulation of Cdc42, which is active at cell junctions. Targeting to subcellular sites that are enriched in the active form of either Cdc42 or Rac thus seems to

be a major determinant of the cellular GTPase selectivity of the GAP. Complex formation seems to play a fundamental role for junctional targeting of SH3BP1, as depletion of JACOP and, to a lesser extent; CD2AP resulted in loss of junctional SH3BP1.

The experiments I performed during my thesis thus led to the identification of a novel dual activity protein complex that regulates actin dynamics and junction formation. This complex contains SH3BP1 whose GAP activity is crucial for junction formation and Cdc42 regulation, and also functions as a structural linker between the junctional adaptor JACOP and the scaffold CD2AP, which binds and regulates the actin capping protein CapZ.

Acknowledgements

I wish to thank Karl Matter and Maria Balda for all the help and support over the years with the project and for being great supervisors. **I especially would like to thank Elisa Vitiello and Kasia Anton for being great friends and for being there to share the problems, results, and trips to the market, lunches and coffee and for the activities we always do. I'm glad I got to know you two great ladies and hope we still have a good moan over a coffee when we have our own labs, and of course providing their listening ears and patience when I constantly told my bad jokes. Thanks guys. :)** I also would like to thank Ceniz Zihni for the ideas and advice he gave me during the project. Steve Terry for all the help and advice he gave me in the early days. Finally I want to thank the rest of our gang, Ingrid, Clare, Cristian, Tom, Katharina, Zanetta, Joana, Apostalos, Mafalda, Emily Steed, Simon, James, Jenny Williams and anyone else I have forgotten. Thanks for making activities and lunch fun. I also want to thank Aida for all her help. Finally I wish to thank my family for everything.

'**Nobody trips over mountains. It is the small pebble that causes you to stumble. Pass all the pebbles in your path and you will find you have crossed the mountain'. ~Author Unknown**

Bibliography

1. Bryant, D.M. and K.E. Mostov, *From cells to organs: building polarized tissue.* Nat Rev Mol Cell Biol, 2008. **9**(11): p. 887-901.

2. Mostov, K.E., *Epithelial polarity and morphogenesis.* Methods, 2003. **30**(3): p. 189-90.

3. Eaton, S. and K. Simons, *Apical, basal, and lateral cues for epithelial polarization.* Cell, 1995. **82**(1): p. 5-8.

4. Ikenouchi, J., et al., *Requirement of ZO-1 for the formation of belt-like adherens junctions during epithelial cell polarization.* J Cell Biol, 2007. **176**(6): p. 779-86.

5. Lodish, H.F., *Molecular cell biology*. 5th ed. ed. 2003, New York: W. H. Freeman ; Basingstoke : [Palgrave]. xxxiii, 973 , [79] p.

6. Yamada, S. and W.J. Nelson, *Synapses: sites of cell recognition, adhesion, and functional specification.* Annu Rev Biochem, 2007. **76**: p. 267-94.

7. Wang, Q. and B. Margolis, *Apical junctional complexes and cell polarity.* Kidney Int, 2007. **72**(12): p. 1448-58.

8. Steed, E., M.S. Balda, and K. Matter, *Dynamics and functions of tight junctions.* Trends Cell Biol. **20**(3): p. 142-9.

9. Braga, V.M., *Cell-cell adhesion and signalling.* Curr. Opin. Cell Biol., 2002. **14**(5): p. 546-56.

10. Terry, S., et al., *Rho signaling and tight junction functions.* Physiology (Bethesda). **25**(1): p. 16-26.

11. Citi, S., et al., *Regulation of small GTPases at epithelial cell-cell junctions.* Mol Membr Biol. **28**(7-8): p. 427-44.

12. Hartsock, A. and W.J. Nelson, *Adherens and tight junctions: structure, function and connections to the actin cytoskeleton.* Biochim Biophys Acta, 2008. **1778**(3): p. 660-9.

13. Miyoshi, J. and Y. Takai, *Molecular perspective on tight-junction assembly and epithelial polarity.* Adv Drug Deliv Rev, 2005. **57**(6): p. 815-55.

14. Farquhar, M.G. and G.E. Palade, *Junctional complexes in various epithelia.* J. Cell Biol., 1963. **17**: p. 375-412.

15. Chiba, H., et al., *Transmembrane proteins of tight junctions.* Biochim Biophys Acta, 2008. **1778**(3): p. 588-600.

16. Schneeberger, E.E. and R.D. Lynch, *The tight junction: a multifunctional complex.* Am. J. Physiol., 2004. **286**(6): p. C1213-28.

17. Gonzalez-Mariscal, L., et al., *Tight junction proteins.* Prog. Biophys. Mol. Biol., 2003. **81**(1): p. 1-44.

18. Russ, P.K., et al., *Bves modulates tight junction associated signaling.* PLoS One. **6**(1): p. e14563.

19. Steed, E., et al., *Identification of MarvelD3 as a tight junction-associated transmembrane protein of the occludin family.* BMC Cell Biol, 2009. **10**: p. 95.

20. Gonzalez-Mariscal, L., et al., *Tight junction proteins.* Prog Biophys Mol Biol, 2003. **81**(1): p. 1-44.

21. Guillemot, L., et al., *The cytoplasmic plaque of tight junctions: a scaffolding and signalling center.* Biochim Biophys Acta, 2008. **1778**(3): p. 601-13.

22. Shin, K., V.C. Fogg, and B. Margolis, *Tight junctions and cell polarity.* Annu Rev Cell Dev Biol, 2006. **22**: p. 207-35.

23. Balda, M.S., M.D. Garrett, and K. Matter, *The ZO-1 associated Y-box factor ZONAB regulates epithelial cell proliferation and cell density.* J. Cell Biol., 2003. **160**: p. 423-432.

24. Balda, M.S. and K. Matter, *Tight junctions at a glance.* J Cell Sci, 2008. **121**(Pt 22): p. 3677-82.

25. Saitou, M., et al., *Occludin-deficient embryonic stem cells can differentiate into polarized epithelial cells bearing tight junctions.* J. Cell Biol., 1998. **141**(2): p. 397-408.

26. Tsukita, S., M. Furuse, and M. Itoh, *Multifunctional strands in tight junctions.* Nat. Rev. Mol. Cell Biol., 2001. **2**: p. 286-293.

27. Saitou, M., et al., *Complex phenotype of mice lacking occludin, a component of tight junction strands.* Mol Biol Cell, 2000. **11**(12): p. 4131-42.

28. Raleigh, D.R., et al., *Tight junction-associated MARVEL proteins marveld3, tricellulin, and occludin have distinct but overlapping functions.* Mol Biol Cell. **21**(7): p. 1200-13.

29. Wittchen, E.S., J. Haskins, and B.R. Stevenson, *Protein interactions at the tight junction. Actin has multiple binding partners, and ZO-1 forms independent complexes with ZO-2 and ZO-3.* J. Biol. Chem., 1999. **274**(49): p. 35179-85.

30. Barrios-Rodiles, M., et al., *High-throughput mapping of a dynamic signaling network in mammalian cells.* Science, 2005. **307**(5715): p. 1621-5.

31. Yu, A.S., et al., *Knockdown of occludin expression leads to diverse phenotypic alterations in epithelial cells.* Am J Physiol Cell Physiol, 2005. **288**(6): p. C1231-41.

32. Murata, M., et al., *Down-regulation of survival signaling through MAPK and Akt in occludin-deficient mouse hepatocytes in vitro.* Exp Cell Res, 2005. **310**(1): p. 140-51.

33. Du, D., et al., *The tight junction protein, occludin, regulates the directional migration of epithelial cells.* Dev Cell. **18**(1): p. 52-63.

34. Furuse, M., et al., *Claudin-1 and -2: novel integral membrane proteins localizing at tight junctions with no sequence similarity to occludin.* J. Cell Biol., 1998. **141**: p. 1539-1550.

35. Krause, G., et al., *Structure and function of claudins.* Biochim Biophys Acta, 2008. **1778**(3): p. 631-45.

36. Kiuchi-Saishin, Y., et al., *Differential expression patterns of claudins, tight junction membrane proteins, in mouse nephron segments.* J. Am. So.c Nephrol., 2002. **13**(4): p. 875-86.

37. Martinez-Estrada, O.M., et al., *The transcription factors Slug and Snail act as repressors of Claudin-1 expression in epithelial cells.* Biochem J, 2006. **394**(Pt 2): p. 449-57.

38. Ikenouchi, J., et al., *Regulation of tight junctions during the epithelium-mesenchyme transition: direct repression of the gene expression of claudins/occludin by Snail.* J Cell Sci, 2003. **116**(Pt 10): p. 1959-67.

39. Batlle, E., et al., *The transcription factor snail is a repressor of E-cadherin gene expression in epithelial tumour cells.* Nat Cell Biol, 2000. **2**(2): p. 84-9.

40. Usami, Y., et al., *Snail-associated epithelial-mesenchymal transition promotes oesophageal squamous cell carcinoma motility and progression.* J Pathol, 2008. **215**(3): p. 330-9.

41. Paris, L., et al., *Structural organization of the tight junctions.* Biochim Biophys Acta, 2008. **1778**(3): p. 646-59.

42. Kojima, T., et al., *Downregulation of tight junction-associated MARVEL protein marvelD3 during epithelial-mesenchymal transition in human pancreatic cancer cells.* Exp Cell Res.

43. Ikenouchi, J., et al., *Tricellulin constitutes a novel barrier at tricellular contacts of epithelial cells.* J Cell Biol, 2005. **171**(6): p. 939-45.

44. Ikenouchi, J., et al., *Loss of occludin affects tricellular localization of tricellulin.* Mol Biol Cell, 2008. **19**(11): p. 4687-93.

45. Bazzoni, G., *The JAM family of junctional adhesion molecules.* Curr. Opin. Cell Biol., 2003. **15**(5): p. 525-30.

46. Itoh, M., et al., *Junctional adhesion molecule (JAM) binds to PAR-3: a possible mechanism for the recruitment of PAR-3 to tight junctions.* J Cell Biol, 2001. **154**(3): p. 491-7.

47. Mandell, K.J., I.C. McCall, and C.A. Parkos, *Involvement of the junctional adhesion molecule-1 (JAM1) homodimer interface in regulation of epithelial barrier function.* J Biol Chem, 2004. **279**(16): p. 16254-62.

48. Severson, E.A. and C.A. Parkos, *Mechanisms of outside-in signaling at the tight junction by junctional adhesion molecule A.* Ann N Y Acad Sci, 2009. **1165**: p. 10-8.

49. Rehder, D., et al., *Junctional adhesion molecule-a participates in the formation of apico-basal polarity through different domains.* Exp Cell Res, 2006. **312**(17): p. 3389-403.

50. Cohen, C.J., et al., *The coxsackievirus and adenovirus receptor is a transmembrane component of the tight junction.* Proc Natl Acad Sci U S A, 2001. **98**(26): p. 15191-6.

51. Bradfield, P.F., et al., *JAM family and related proteins in leukocyte migration (Vestweber series).* Arterioscler Thromb Vasc Biol, 2007. **27**(10): p. 2104-12.

52. Weber, C., L. Fraemohs, and E. Dejana, *The role of junctional adhesion molecules in vascular inflammation.* Nat Rev Immunol, 2007. **7**(6): p. 467-77.

53. Willott, E., et al., *The tight junction protein ZO-1 is homologous to the Drosophila discs-large tumor suppressor protein of septate junctions.* Proc. Natl. Acad. Sci. USA, 1993. **90**: p. 7834-7838.

54. Fanning, A.S., T.Y. Ma, and J.M. Anderson, *Isolation and functional characterization of the actin binding region in the tight junction protein ZO-1.* FASEB J, 2002. **16**(13): p. 1835-7.

55. Balda, M.S. and K. Matter, *The tight junction protein ZO-1 and an interacting transcription factor regulate ErbB-2 expression.* EMBO J., 2000. **19**(9): p. 2024-2033.

56. Matter, K. and M.S. Balda, *Tight junctions, gene expression and nucleo-junctinal interplay.* J. Cell Sci., 2007. **120**: p. 1505-1511.

57. Cordenonsi, M., et al., *Cingulin contains globular and coiled-coil domains and interacts with ZO-1, ZO-2, ZO-3, and myosin.* J. Cell Biol., 1999. **147**(7): p. 1569-82.

58. Citi, S., et al., *Cingulin, a new peripheral component of tight junctions.* Nature, 1988. **333**(6170): p. 272-6.

59. Aijaz, S., et al., *Binding of GEF-H1 to the tight junction-associated adaptor cingulin results in inhibition of Rho signaling and G1/S phase transition.* Dev. Cell, 2005. **8**: p. 777-786.

60. Terry, S.J., et al., *Spatially restricted activation of RhoA signalling at epithelial junctions by p114RhoGEF drives junction formation and morphogenesis.* Nat Cell Biol. **13**(2): p. 159-66.

61. Ohnishi, H., et al., *JACOP, a novel plaque protein localizing at the apical junctional complex with sequence similarity to cingulin.* J. Biol. Chem., 2004. **279**(44): p. 46014-22.

62. Pulimeno, P., S. Paschoud, and S. Citi, *A role for ZO-1 and PLEKHA7 in recruiting paracingulin to tight and adherens junctions of epithelial cells.* J Biol Chem. **286**(19): p. 16743-50.

63. Guillemot, L., et al., *Paracingulin regulates the activity of Rac1 and RhoA GTPases by recruiting Tiam1 and GEF-H1 to epithelial junctions.* Mol Biol Cell, 2008. **19**(10): p. 4442-53.

64. Furuse, M., *Molecular basis of the core structure of tight junctions.* Cold Spring Harb Perspect Biol. **2**(1): p. a002907.

65. Sourisseau, T., et al., *Regulation of PCNA and cyclin D1 expression and epithelial morphogenesis by the ZO-1-regulated transcription factor ZONAB/DbpA.* Mol Cell Biol, 2006. **26**(6): p. 2387-98.

66. Matter, K. and M.S. Balda, *Signalling to and from tight junctions.* Nat. Rev. Mol. Cell Biol., 2003. **4**(3): p. 225-36.

67. Traweger, A., et al., *The tight junction protein ZO-2 localizes to the nucleus and interacts with the heterogeneous nuclear ribonucleoprotein scaffold attachment factor-B.* J Biol Chem, 2003. **278**(4): p. 2692-700.

68. Baum, B. and M. Georgiou, *Dynamics of adherens junctions in epithelial establishment, maintenance, and remodeling.* J Cell Biol. **192**(6): p. 907-17.

69. Niessen, C.M. and C.J. Gottardi, *Molecular components of the adherens junction.* Biochim Biophys Acta, 2008. **1778**(3): p. 562-71.

70. Gooding, J.M., K.L. Yap, and M. Ikura, *The cadherin-catenin complex as a focal point of cell adhesion and signalling: new insights from three-dimensional structures.* Bioessays, 2004. **26**(5): p. 497-511.

71. Halbleib, J.M. and W.J. Nelson, *Cadherins in development: cell adhesion, sorting, and tissue morphogenesis.* Genes Dev, 2006. **20**(23): p. 3199-214.

72. Perez-Moreno, M. and E. Fuchs, *Catenins: keeping cells from getting their signals crossed.* Dev Cell, 2006. **11**(5): p. 601-12.

73. Adams, C.L., et al., *Mechanisms of epithelial cell-cell adhesion and cell compaction revealed by high-resolution tracking of E-cadherin-green fluorescent protein.* J Cell Biol, 1998. **142**(4): p. 1105-19.

74. Cavey, M. and T. Lecuit, *Molecular bases of cell-cell junctions stability and dynamics.* Cold Spring Harb Perspect Biol, 2009. **1**(5): p. a002998.

75. van Roy, F. and G. Berx, *The cell-cell adhesion molecule E-cadherin.* Cell Mol Life Sci, 2008. **65**(23): p. 3756-88.

76. Yap, A.S., C.M. Niessen, and B.M. Gumbiner, *The juxtamembrane region of the cadherin cytoplasmic tail supports lateral clustering, adhesive strengthening, and interaction with p120ctn.* J Cell Biol, 1998. **141**(3): p. 779-89.

77. Aberle, H., et al., *Assembly of the cadherin-catenin complex in vitro with recombinant proteins.* J Cell Sci, 1994. **107 (Pt 12)**: p. 3655-63.

78. Alema, S. and A.M. Salvatore, *p120 catenin and phosphorylation: Mechanisms and traits of an unresolved issue.* Biochim Biophys Acta, 2007. **1773**(1): p. 47-58.

79. Reynolds, A.B., et al., *Transformation-specific tyrosine phosphorylation of a novel cellular protein in chicken cells expressing oncogenic variants of the avian cellular src gene.* Mol Cell Biol, 1989. **9**(2): p. 629-38.

80. Reynolds, A.B., et al., *p120, a novel substrate of protein tyrosine kinase receptors and of p60v-src, is related to cadherin-binding factors beta-catenin, plakoglobin and armadillo.* Oncogene, 1992. **7**(12): p. 2439-45.

81. Huber, A.H. and W.I. Weis, *The structure of the beta-catenin/E-cadherin complex and the molecular basis of diverse ligand recognition by beta-catenin.* Cell, 2001. **105**(3): p. 391-402.

82. Yamada, S., et al., *Deconstructing the cadherin-catenin-actin complex.* Cell, 2005. **123**(5): p. 889-901.

83. Takai, Y. and H. Nakanishi, *Nectin and afadin: novel organizers of intercellular junctions.* J Cell Sci, 2003. **116**(Pt 1): p. 17-27.

84. Takai, Y., et al., *Nectins and nectin-like molecules: roles in cell adhesion, migration, and polarization.* Cancer Sci, 2003. **94**(8): p. 655-67.

85. Irie, K., et al., *Roles and modes of action of nectins in cell-cell adhesion.* Semin. Cell Dev. Biol., 2004. **15**(6): p. 643-56.

86. Ikeda, W., et al., *Afadin: A key molecule essential for structural organization of cell- cell junctions of polarized epithelia during embryogenesis.* J. Cell Biol., 1999. **146**(5): p. 1117-32.

87. Takai, Y., et al., *Nectins and nectin-like molecules: roles in contact inhibition of cell movement and proliferation.* Nat Rev Mol Cell Biol, 2008. **9**(8): p. 603-15.

88. Chen, X. and B.M. Gumbiner, *Crosstalk between different adhesion molecules.* Curr Opin Cell Biol, 2006. **18**(5): p. 572-8.

89. Yokoyama, S., et al., *alpha-catenin-independent recruitment of ZO-1 to nectin-based cell-cell adhesion sites through afadin.* Mol. Biol. Cell, 2001. **12**(6): p. 1595-609.

90. Rajasekaran, A.K., et al., *Catenins and zonula occludens-1 form a complex during early stages in the assembly of tight junctions.* J. Cell Biol., 1996. **132**(3): p. 451-463.

91. Huber, O., *Structure and function of desmosomal proteins and their role in development and disease.* Cell Mol Life Sci, 2003. **60**(9): p. 1872-90.

92. Al-Amoudi, A. and A.S. Frangakis, *Structural studies on desmosomes.* Biochem Soc Trans, 2008. **36**(Pt 2): p. 181-7.

93. Getsios, S., A.C. Huen, and K.J. Green, *Working out the strength and flexibility of desmosomes.* Nat Rev Mol Cell Biol, 2004. **5**(4): p. 271-81.

94. Tomschy, A., et al., *Homophilic adhesion of E-cadherin occurs by a co-operative two-step interaction of N-terminal domains.* EMBO J, 1996. **15**(14): p. 3507-14.

95. Garrod, D. and M. Chidgey, *Desmosome structure, composition and function.* Biochim Biophys Acta, 2008. **1778**(3): p. 572-87.

96. Yeaman, C., K.K. Grindstaff, and W.J. Nelson, *New perspectives on mechanisms involved in generating epithelial cell polarity.* Physiol. Rev., 1999. **79**(1): p. 73-98.

97. Kass, L., et al., *Mammary epithelial cell: influence of extracellular matrix composition and organization during development and tumorigenesis.* Int J Biochem Cell Biol, 2007. **39**(11): p. 1987-94.

98. Lopez, J.I., J.K. Mouw, and V.M. Weaver, *Biomechanical regulation of cell orientation and fate.* Oncogene, 2008. **27**(55): p. 6981-93.

99. Hynes, R.O., *Integrins: Versatility, modulation, and signaling in cell adhesion.* Cell, 1992. **69**: p. 11-25.

100. Mellman, I. and W.J. Nelson, *Coordinated protein sorting, targeting and distribution in polarized cells.* Nat Rev Mol Cell Biol, 2008. **9**(11): p. 833-45.

101. Iden, S. and J.G. Collard, *Crosstalk between small GTPases and polarity proteins in cell polarization.* Nat Rev Mol Cell Biol, 2008. **9**(11): p. 846-59.

102. Rikitake, Y., K. Mandai, and Y. Takai, *The role of nectins in different types of cell-cell adhesion.* J Cell Sci. **125**(Pt 16): p. 3713-22.

103. Balda, M.S., et al., *Assembly of tight junctions: the role of diacylglycerol.* J. Cell Biol., 1993. **123**: p. 293-302.

104. Balda, M.S. and K. Matter, *Tight junctions.* J Cell Sci, 1998. **111 (Pt 5)**: p. 541-7.

105. Nose, A., A. Nagafuchi, and M. Takeichi, *Expressed recombinant cadherins mediate cell sorting in model systems.* Cell, 1988. **54**(7): p. 993-1001.

106. Vasioukhin, V., et al., *Directed actin polymerization is the driving force for epithelial cell-cell adhesion.* Cell, 2000. **100**(2): p. 209-19.

107. Ehrlich, J.S., M.D. Hansen, and W.J. Nelson, *Spatio-temporal regulation of Rac1 localization and lamellipodia dynamics during epithelial cell-cell adhesion.* Dev Cell, 2002. **3**(2): p. 259-70.

108. Johnston, S.A., et al., *Arp2/3 complex activity in filopodia of spreading cells.* BMC Cell Biol, 2008. **9**: p. 65.

109. Zigmond, S.H., *Beginning and ending an actin filament: control at the barbed end.* Curr Top Dev Biol, 2004. **63**: p. 145-88.

110. Scott, J.A., et al., *Ena/VASP proteins can regulate distinct modes of actin organization at cadherin-adhesive contacts.* Mol Biol Cell, 2006. **17**(3): p. 1085-95.

111. Kobielak, A., H.A. Pasolli, and E. Fuchs, *Mammalian formin-1 participates in adherens junctions and polymerization of linear actin cables.* Nat Cell Biol, 2004. **6**(1): p. 21-30.

112. Ebnet, K., et al., *The cell polarity protein ASIP/PAR-3 directly associates with junctional adhesion molecule (JAM).* EMBO J., 2001. **20**(14): p. 3738-48.

113. Chen, X. and I.G. Macara, *Par-3 controls tight junction assembly through the Rac exchange factor Tiam1.* Nat. Cell Biol., 2005. **7**(3): p. 262-9.

114. Suzuki, A., et al., *aPKC acts upstream of PAR-1b in both the establishment and maintenance of mammalian epithelial polarity.* Curr. Biol., 2004. **14**(16): p. 1425-35.

115. Suzuki, A., et al., *aPKC kinase activity is required for the asymmetric differentiation of the premature junctional complex during epithelial cell polarization.* J. Cell Sci., 2002. **115**(Pt 18): p. 3565-73.

116. Zegers, M.M., et al., *Epithelial polarity and tubulogenesis in vitro.* Trends Cell Biol., 2003. **13**(4): p. 169-76.

117. Kroschewski, R., *Molecular mechanisms of epithelial polarity: about shapes, forces, and orientation problems.* News Physiol Sci, 2004. **19**: p. 61-6.

118. Martin-Belmonte, F., et al., *Cell-polarity dynamics controls the mechanism of lumen formation in epithelial morphogenesis.* Curr Biol, 2008. **18**(7): p. 507-13.

119. Debnath, J., *Detachment-induced autophagy during anoikis and lumen formation in epithelial acini.* Autophagy, 2008. **4**(3): p. 351-3.

120. Mailleux, A.A., M. Overholtzer, and J.S. Brugge, *Lumen formation during mammary epithelial morphogenesis: insights from in vitro and in vivo models.* Cell Cycle, 2008. **7**(1): p. 57-62.

121. Martin-Belmonte, F., et al., *PTEN-mediated apical segregation of phosphoinositides controls epithelial morphogenesis through Cdc42.* Cell, 2007. **128**(2): p. 383-97.

122. Gassama-Diagne, A., et al., *Phosphatidylinositol-3,4,5-trisphosphate regulates the formation of the basolateral plasma membrane in epithelial cells.* Nat Cell Biol, 2006. **8**(9): p. 963-70.

123. Takahama, S., T. Hirose, and S. Ohno, *aPKC restricts the basolateral determinant PtdIns(3,4,5)P3 to the basal region.* Biochem Biophys Res Commun, 2008. **368**(2): p. 249-55.

124. von Stein, W., et al., *Direct association of Bazooka/PAR-3 with the lipid phosphatase PTEN reveals a link between the PAR/aPKC complex and phosphoinositide signaling.* Development, 2005. **132**(7): p. 1675-86.

125. Pinal, N., et al., *Regulated and polarized PtdIns(3,4,5)P3 accumulation is essential for apical membrane morphogenesis in photoreceptor epithelial cells.* Curr Biol, 2006. **16**(2): p. 140-9.

126. Yamanaka, T., et al., *PAR-6 regulates aPKC activity in a novel way and mediates cell-cell contact-induced formation of the epithelial junctional complex.* Genes Cells, 2001. **6**(8): p. 721-31.

127. Iden, S., et al., *aPKC phosphorylates JAM-A at Ser285 to promote cell contact maturation and tight junction formation.* J Cell Biol. **196**(5): p. 623-39.

128. Nagai-Tamai, Y., et al., *Regulated protein-protein interaction between aPKC and PAR-3 plays an essential role in the polarization of epithelial cells.* Genes Cells, 2002. **7**(11): p. 1161-71.

129. Boulter, E., et al., *Off the beaten paths: alternative and crosstalk regulation of Rho GTPases.* FASEB J. **26**(2): p. 469-79.

130. Aspenstrom, P., A. Ruusala, and D. Pacholsky, *Taking Rho GTPases to the next level: the cellular functions of atypical Rho GTPases.* Exp Cell Res, 2007. **313**(17): p. 3673-9.

131. Espinosa, E.J., et al., *RhoBTB3: a Rho GTPase-family ATPase required for endosome to Golgi transport.* Cell, 2009. **137**(5): p. 938-48.

132. Allen, W.E., et al., *Rho, Rac and Cdc42 regulate actin organization and cell adhesion in macrophages.* J Cell Sci, 1997. **110 (Pt 6)**: p. 707-20.

133. Nobes, C.D. and A. Hall, *Rho, rac, and cdc42 GTPases regulate the assembly of multimolecular focal complexes associated with actin stress fibers, lamellipodia, and filopodia.* Cell, 1995. **81**(1): p. 53-62.

134. Bender, A. and J.R. Pringle, *Multicopy suppression of the cdc24 budding defect in yeast by CDC42 and three newly identified genes including the ras-related gene RSR1.* Proc Natl Acad Sci U S A, 1989. **86**(24): p. 9976-80.

135. Heasman, S.J. and A.J. Ridley, *Mammalian Rho GTPases: new insights into their functions from in vivo studies.* Nat Rev Mol Cell Biol, 2008. **9**(9): p. 690-701.

136. Goldstein, B. and I.G. Macara, *The PAR proteins: fundamental players in animal cell polarization.* Dev Cell, 2007. **13**(5): p. 609-22.

137. Jaffe, A.B., et al., *Cdc42 controls spindle orientation to position the apical surface during epithelial morphogenesis.* J Cell Biol, 2008. **183**(4): p. 625-33.

138. Sells, M.A., et al., *Human p21-activated kinase (Pak1) regulates actin organization in mammalian cells.* Curr Biol, 1997. **7**(3): p. 202-10.

139. Delorme, V., et al., *Cofilin activity downstream of Pak1 regulates cell protrusion efficiency by organizing lamellipodium and lamella actin networks.* Dev Cell, 2007. **13**(5): p. 646-62.

140. Fukata, M., et al., *Rac1 and Cdc42 capture microtubules through IQGAP1 and CLIP-170.* Cell, 2002. **109**(7): p. 873-85.

141. Suetsugu, S. and A. Gautreau, *Synergistic BAR-NPF interactions in actin-driven membrane remodeling.* Trends Cell Biol. **22**(3): p. 141-50.

142. Ahmed, S., W.I. Goh, and W. Bu, *I-BAR domains, IRSp53 and filopodium formation.* Semin Cell Dev Biol. **21**(4): p. 350-6.

143. Scita, G., et al., *IRSp53: crossing the road of membrane and actin dynamics in the formation of membrane protrusions.* Trends Cell Biol, 2008. **18**(2): p. 52-60.

144. Deeks, M.J. and P.J. Hussey, *Arp2/3 and 'the shape of things to come'.* Curr Opin Plant Biol, 2003. **6**(6): p. 561-7.

145. Snapper, S.B., et al., *N-WASP deficiency reveals distinct pathways for cell surface projections and microbial actin-based motility.* Nat Cell Biol, 2001. **3**(10): p. 897-904.

146. Steffen, A., et al., *Filopodia formation in the absence of functional WAVE- and Arp2/3-complexes.* Mol Biol Cell, 2006. **17**(6): p. 2581-91.

147. Schirenbeck, A., et al., *Formins and VASPs may co-operate in the formation of filopodia.* Biochem Soc Trans, 2005. **33**(Pt 6): p. 1256-9.

148. Ridley, A.J., *Life at the leading edge.* Cell. **145**(7): p. 1012-22.

149. Xu, J., J.F. Casella, and T.D. Pollard, *Effect of capping protein, CapZ, on the length of actin filaments and mechanical properties of actin filament networks.* Cell Motil Cytoskeleton, 1999. **42**(1): p. 73-81.

150. Mejillano, M.R., et al., *Lamellipodial versus filopodial mode of the actin nanomachinery: pivotal role of the filament barbed end.* Cell, 2004. **118**(3): p. 363-73.

151. van Duijn, T.J., et al., *Rac1 recruits the adapter protein CMS/CD2AP to cell-cell contacts.* J Biol Chem. **285**(26): p. 20137-46.

152. Jaffe, A.B. and A. Hall, *Rho GTPases: biochemistry and biology.* Annu Rev Cell Dev Biol, 2005. **21**: p. 247-69.

153. Derivery, E. and A. Gautreau, *Generation of branched actin networks: assembly and regulation of the N-WASP and WAVE molecular machines.* Bioessays. **32**(2): p. 119-31.

154. Ellenbroek, S.I. and J.G. Collard, *Rho GTPases: functions and association with cancer.* Clin Exp Metastasis, 2007. **24**(8): p. 657-72.

155. Aktories, K. and A. Hall, *Botulinum ADP-ribosyltransferase C3: a new tool to study low molecular weight GTP-binding proteins.* Trends Pharmacol Sci, 1989. **10**(10): p. 415-8.

156. Narumiya, S., T. Ishizaki, and N. Watanabe, *Rho effectors and reorganization of actin cytoskeleton.* FEBS Lett, 1997. **410**(1): p. 68-72.

157. Ridley, A.J. and A. Hall, *The small GTP-binding protein rho regulates the assembly of focal adhesions and actin stress fibers in response to growth factors.* Cell, 1992. **70**(3): p. 389-99.

158. Pertz, O., *Spatio-temporal Rho GTPase signaling - where are we now?* J Cell Sci. **123**(Pt 11): p. 1841-50.

159. Bos, J.L., H. Rehmann, and A. Wittinghofer, *GEFs and GAPs: critical elements in the control of small G proteins.* Cell, 2007. **129**(5): p. 865-77.

160. Rossman, K.L., C.J. Der, and J. Sondek, *GEF means go: turning on RHO GTPases with guanine nucleotide-exchange factors.* Nat Rev Mol Cell Biol, 2005. **6**(2): p. 167-80.

161. DerMardirossian, C. and G.M. Bokoch, *GDIs: central regulatory molecules in Rho GTPase activation.* Trends Cell Biol, 2005. **15**(7): p. 356-63.

162. Eva, A., et al., *The predicted DBL oncogene product defines a distinct class of transforming proteins.* Proc Natl Acad Sci U S A, 1988. **85**(7): p. 2061-5.

163. Hart, M.J., et al., *Catalysis of guanine nucleotide exchange on the CDC42Hs protein by the dbl oncogene product.* Nature, 1991. **354**(6351): p. 311-4.

164. Baumeister, M.A., et al., *The Dbs PH domain contributes independently to membrane targeting and regulation of guanine nucleotide-exchange activity.* Biochem J, 2006. **400**(3): p. 563-72.

165. Chhatriwala, M.K., et al., *The DH and PH domains of Trio coordinately engage Rho GTPases for their efficient activation.* J Mol Biol, 2007. **368**(5): p. 1307-20.

166. Garcia-Mata, R. and K. Burridge, *Catching a GEF by its tail.* Trends Cell Biol, 2007. **17**(1): p. 36-43.

167. Garrett, M.D., et al., *Identification of distinct cytoplasmic targets for ras/R-ras and rho regulatory proteins.* J Biol Chem, 1989. **264**(1): p. 10-3.

168. Diekmann, D., et al., *Bcr encodes a GTPase-activating protein for p21rac.* Nature, 1991. **351**(6325): p. 400-2.

169. Moon, S.Y. and Y. Zheng, *Rho GTPase-activating proteins in cell regulation.* Trends Cell Biol, 2003. **13**(1): p. 13-22.

170. Van Aelst, L. and C. D'Souza-Schorey, *Rho GTPases and signaling networks.* Genes Dev, 1997. **11**(18): p. 2295-322.

171. Bishop, A.L. and A. Hall, *Rho GTPases and their effector proteins.* Biochem J., 2000. **348**(2): p. 241-255.

172. Liu, H., et al., *Physical and functional interaction of Fyn tyrosine kinase with a brain-enriched Rho GTPase-activating protein TCGAP.* J Biol Chem, 2006. **281**(33): p. 23611-9.

173. Tcherkezian, J., et al., *The human orthologue of CdGAP is a phosphoprotein and a GTPase-activating protein for Cdc42 and Rac1 but not RhoA.* Biol Cell, 2006. **98**(8): p. 445-56.

174. Caloca, M.J., et al., *Phorbol esters and related analogs regulate the subcellular localization of beta 2-chimaerin, a non-protein kinase C phorbol ester receptor.* J Biol Chem, 2001. **276**(21): p. 18303-12.

175. Caloca, M.J., et al., *Beta2-chimaerin is a high affinity receptor for the phorbol ester tumor promoters.* J Biol Chem, 1997. **272**(42): p. 26488-96.

176. Jenna, S., et al., *The activity of the GTPase-activating protein CdGAP is regulated by the endocytic protein intersectin.* J Biol Chem, 2002. **277**(8): p. 6366-73.

177. Zimmerberg, J. and S. McLaughlin, *Membrane curvature: how BAR domains bend bilayers.* Curr Biol, 2004. **14**(6): p. R250-2.

178. Saarikangas, J., et al., *Molecular mechanisms of membrane deformation by I-BAR domain proteins.* Curr Biol, 2009. **19**(2): p. 95-107.

179. Habermann, B., *The BAR-domain family of proteins: a case of bending and binding?* EMBO Rep, 2004. **5**(3): p. 250-5.

180. Fricke, R., C. Gohl, and S. Bogdan, *The F-BAR protein family Actin' on the membrane.* Commun Integr Biol. **3**(2): p. 89-94.

181. Ahmed, S., et al., *F-BAR domain proteins: Families and function.* Commun Integr Biol. **3**(2): p. 116-21.

182. Blood, P.D. and G.A. Voth, *Direct observation of Bin/amphiphysin/Rvs (BAR) domain-induced membrane curvature by means of molecular dynamics simulations.* Proc Natl Acad Sci U S A, 2006. **103**(41): p. 15068-72.

183. Billuart, P., et al., *Oligophrenin-1 encodes a rhoGAP protein involved in X-linked mental retardation.* Nature, 1998. **392**(6679): p. 923-6.

184. Borkhardt, A., et al., *The human GRAF gene is fused to MLL in a unique t(5;11)(q31;q23) and both alleles are disrupted in three cases of myelodysplastic syndrome/acute myeloid leukemia with a deletion 5q.* Proc Natl Acad Sci U S A, 2000. **97**(16): p. 9168-73.

185. Eberth, A., et al., *A BAR domain-mediated autoinhibitory mechanism for RhoGAPs of the GRAF family.* Biochem J, 2009. **417**(1): p. 371-7.

186. Cicchetti, P., et al., *Identification of a protein that binds to the SH3 domain region of Abl and is similar to Bcr and GAP-rho.* Science, 1992. **257**: p. 803-806.

187. Cicchetti, P., et al., *3BP-1, an SH3 domain binding protein, has GAP activity for Rac and inhibits growth factor-induced membrane ruffling in fibroblasts.* Embo J, 1995. **14**(13): p. 3127-35.

188. Zhang, B. and Y. Zheng, *Regulation of RhoA GTP hydrolysis by the GTPase-activating proteins p190, p50RhoGAP, Bcr, and 3BP-1.* Biochemistry, 1998. **37**(15): p. 5249-57.

189. Parrini, M.C., et al., *SH3BP1, an exocyst-associated RhoGAP, inactivates Rac1 at the front to drive cell motility.* Mol Cell. **42**(5): p. 650-61.

190. Richnau, N. and P. Aspenstrom, *Rich, a rho GTPase-activating protein domain-containing protein involved in signaling by Cdc42 and Rac1.* J Biol Chem, 2001. **276**(37): p. 35060-70.

191. Harada, A., et al., *Nadrin, a novel neuron-specific GTPase-activating protein involved in regulated exocytosis.* J Biol Chem, 2000. **275**(47): p. 36885-91.

192. Furuta, B., et al., *Identification and functional characterization of nadrin variants, a novel family of GTPase activating protein for rho GTPases.* J Neurochem, 2002. **82**(5): p. 1018-28.

193. Wells, C.D., et al., *A Rich1/Amot complex regulates the Cdc42 GTPase and apical-polarity proteins in epithelial cells.* Cell, 2006. **125**(3): p. 535-48.

194. Yi, C., et al., *A tight junction-associated Merlin-angiomotin complex mediates Merlin's regulation of mitogenic signaling and tumor suppressive functions.* Cancer Cell. **19**(4): p. 527-40.

195. Bruewer, M., et al., *RhoA, Rac1, and Cdc42 exert distinct effects on epithelial barrier via selective structural and biochemical modulation of junctional proteins and F-actin.* Am J Physiol Cell Physiol, 2004. **287**(2): p. C327-35.

196. Kroschewski, R., A. Hall, and I. Mellman, *Cdc42 controls secretory and endocytic transport to the basolateral plasma membrane of MDCK cells.* Nat Cell Biol, 1999. **1**(1): p. 8-13.

197. Rojas, R., et al., *Cdc42-dependent modulation of tight junctions and membrane protein traffic in polarized Madin-Darby canine kidney cells.* Mol Biol Cell, 2001. **12**(8): p. 2257-74.

198. Nakagawa, M., et al., *Recruitment and activation of Rac1 by the formation of E-cadherin- mediated cell-cell adhesion sites.* J. Cell Sci., 2001. **114**(Pt 10): p. 1829-38.

199. Noren, N.K., et al., *Cadherin engagement regulates Rho family GTPases.* J Biol Chem, 2001. **276**(36): p. 33305-8.

200. Betson, M., et al., *Rac activation upon cell-cell contact formation is dependent on signaling from the epidermal growth factor receptor.* J Biol Chem, 2002. **277**(40): p. 36962-9.

201. Yamada, S. and W.J. Nelson, *Localized zones of Rho and Rac activities drive initiation and expansion of epithelial cell-cell adhesion.* J Cell Biol, 2007. **178**(3): p. 517-27.

202. Kovacs, E.M., et al., *E-cadherin homophilic ligation directly signals through Rac and phosphatidylinositol 3-kinase to regulate adhesive contacts.* J Biol Chem, 2002. **277**(8): p. 6708-18.

203. Kim, S.H., Z. Li, and D.B. Sacks, *E-cadherin-mediated cell-cell attachment activates Cdc42.* J Biol Chem, 2000. **275**(47): p. 36999-7005.

204. Erasmus, J., et al., *Newly formed E-cadherin contacts do not activate Cdc42 or induce filopodia protrusion in human keratinocytes.* Biol Cell. **102**(1): p. 13-24.

205. Kawakatsu, T., et al., *Trans-interactions of nectins induce formation of Filopodia and Lamellipodia through the respective activation of Cdc42 and Rac small G proteins.* J. Biol. Chem., 2002. **11**: p. 11.

206. Sahai, E. and C.J. Marshall, *ROCK and Dia have opposing effects on adherens junctions downstream of Rho.* Nat. Cell Biol., 2002. **4**(6): p. 408-15.

207. Itoh, M., et al., *Rho GTP exchange factor ARHGEF11 regulates the integrity of epithelial junctions by connecting ZO-1 and RhoA-myosin II signaling.* Proc Natl Acad Sci U S A. **109**(25): p. 9905-10.

208. Benais-Pont, G., et al., *Identification of a tight junction-associated guanine nucleotide exchange factor that activates Rho and regulates paracellular permeability.* J. Cell Biol., 2003. **160**: p. 729-740.

209. Wildenberg, G.A., et al., *p120-catenin and p190RhoGAP regulate cell-cell adhesion by coordinating antagonism between Rac and Rho.* Cell, 2006. **127**(5): p. 1027-39.

210. Ratheesh, A., et al., *Centralspindlin and alpha-catenin regulate Rho signalling at the epithelial zonula adherens.* Nat Cell Biol. **14**(8): p. 818-28.

211. Liu, X.F., et al., *Nucleotide exchange factor ECT2 interacts with the polarity protein complex Par6/Par3/protein kinase Czeta (PKCzeta) and regulates PKCzeta activity.* Mol. Cell Biol., 2004. **24**(15): p. 6665-75.

212. Sousa, S., et al., *ARHGAP10 is necessary for alpha-catenin recruitment at adherens junctions and for Listeria invasion.* Nat Cell Biol, 2005. **7**(10): p. 954-60.

213. Abouhamed, M., et al., *Myosin IXa regulates epithelial differentiation and its deficiency results in hydrocephalus.* Mol Biol Cell, 2009. **20**(24): p. 5074-85.

214. Omelchenko, T. and A. Hall, *Myosin-IXA regulates collective epithelial cell migration by targeting RhoGAP activity to cell-cell junctions.* Curr Biol. **22**(4): p. 278-88.

215. Chandhoke, S.K. and M.S. Mooseker, *A role for myosin IXb, a motor-RhoGAP chimera, in epithelial wound healing and tight junction regulation.* Mol Biol Cell. **23**(13): p. 2468-80.

216. Tatsumoto, T., et al., *Human ECT2 is an exchange factor for Rho GTPases, phosphorylated in G2/M phases, and involved in cytokinesis.* J Cell Biol, 1999. **147**(5): p. 921-8.

217. Matthews, H.K., et al., *Changes in Ect2 localization couple actomyosin-dependent cell shape changes to mitotic progression.* Dev Cell. **23**(2): p. 371-83.

218. Chang, Y.C., et al., *GEF-H1 Couples Nocodazole-induced Microtubule Disassembly to Cell Contractility via RhoA.* Mol Biol Cell, 2008.

219. Rogers, S.L., et al., *Drosophila RhoGEF2 associates with microtubule plus ends in an EB1-dependent manner.* Curr Biol, 2004. **14**(20): p. 1827-33.

220. Jou, T.S., E.E. Schneeberger, and W.J. Nelson, *Structural and functional regulation of tight junctions by RhoA and Rac1 small GTPases.* J. Cell Biol., 1998. **142**(1): p. 101-15.

221. Jou, T.S. and W.J. Nelson, *Effects of regulated expression of mutant RhoA and Rac1 small GTPases on the development of epithelial (MDCK) cell polarity.* J. Cell Biol., 1998. **142**(1): p. 85-100.

222. Takaishi, K., et al., *Regulation of cell-cell adhesion by rac and rho small G proteins in MDCK cells.* J. Cell Biol., 1997. **139**(4): p. 1047-59.

223. Braga, V.M., et al., *The small GTPases Rho and Rac are required for the establishment of cadherin-dependent cell-cell contacts.* J. Cell Biol., 1997. **137**(6): p. 1421-31.

224. Braga, V.M., et al., *Activation of the small GTPase Rac is sufficient to disrupt cadherin-dependent cell-cell adhesion in normal human keratinocytes.* Mol Biol Cell, 2000. **11**(11): p. 3703-21.

225. Wallace, S.W., et al., *Cdc42 regulates apical junction formation in human bronchial epithelial cells through PAK4 and Par6B.* Mol Biol Cell. **21**(17): p. 2996-3006.

226. Du, D., et al., *Cdc42 is crucial for the maturation of primordial cell junctions in keratinocytes independent of Rac1.* Exp Cell Res, 2009. **315**(8): p. 1480-9.

227. Perez, T.D., et al., *Immediate-early signaling induced by E-cadherin engagement and adhesion.* J Biol Chem, 2008. **283**(8): p. 5014-22.

228. Braga, V.M. and A.S. Yap, *The challenges of abundance: epithelial junctions and small GTPase signalling.* Curr Opin Cell Biol, 2005. **17**(5): p. 466-74.

229. Otani, T., et al., *Cdc42 GEF Tuba regulates the junctional configuration of simple epithelial cells.* J Cell Biol, 2006. **175**(1): p. 135-46.

230. Bryant, D.M., et al., *A molecular network for de novo generation of the apical surface and lumen.* Nat Cell Biol. **12**(11): p. 1035-45.

231. Qin, Y., et al., *Tuba, a Cdc42 GEF, is required for polarized spindle orientation during epithelial cyst formation.* J Cell Biol. **189**(4): p. 661-9.

232. Kovacs, E.M., et al., *Tuba and N-WASP function cooperatively to position the central lumen during epithelial cyst morphogenesis.* Cell Adh Migr. **5**(4): p. 344-50.

233. Rodriguez-Fraticelli, A.E., et al., *The Cdc42 GEF Intersectin 2 controls mitotic spindle orientation to form the lumen during epithelial morphogenesis.* J Cell Biol. **189**(4): p. 725-38.

234. Hordijk, P.L., et al., *Inhibition of invasion of epithelial cells by Tiam1-Rac signaling.* Science, 1997. **278**(5342): p. 1464-6.

235. Mertens, A.E., et al., *The Rac activator Tiam1 controls tight junction biogenesis in keratinocytes through binding to and activation of the Par polarity complex.* J Cell Biol, 2005. **170**(7): p. 1029-37.

236. Yano, T., et al., *Tara up-regulates E-cadherin transcription by binding to the Trio RhoGEF and inhibiting Rac signaling.* J Cell Biol. **193**(2): p. 319-32.

237. Nola, S., et al., *Ajuba is required for Rac activation and maintenance of E-cadherin adhesion.* J Cell Biol. **195**(5): p. 855-71.

238. Matsuda, M., et al., *Identification of adherens junction-associated GTPase activating proteins by the fluorescence localization-based expression cloning.* Exp Cell Res, 2008. **314**(5): p. 939-49.

239. Gentile, A., et al., *Met-driven invasive growth involves transcriptional regulation of Arhgap12.* Oncogene, 2008. **27**(42): p. 5590-8.

240. Lozano, E., et al., *PAK is required for the disruption of E-cadherin adhesion by the small GTPase Rac.* J Cell Sci, 2008. **121**(Pt 7): p. 933-8.

241. Wells, A., *EGF receptor.* Int J Biochem Cell Biol, 1999. **31**(6): p. 637-43.

242. Sherrill, J.M. and J. Kyte, *Activation of epidermal growth factor receptor by epidermal growth factor.* Biochemistry, 1996. **35**(18): p. 5705-18.

243. Gschwind, A., et al., *Cell communication networks: epidermal growth factor receptor transactivation as the paradigm for interreceptor signal transmission.* Oncogene, 2001. **20**(13): p. 1594-600.

244. Fujishiro, S.H., et al., *ERK1/2 phosphorylate GEF-H1 to enhance its guanine nucleotide exchange activity toward RhoA.* Biochem Biophys Res Commun, 2008. **368**(1): p. 162-7.

245. Huveneers, S. and E.H. Danen, *Adhesion signaling - crosstalk between integrins, Src and Rho.* J Cell Sci, 2009. **122**(Pt 8): p. 1059-69.

246. Van Itallie, C.M., M.S. Balda, and J.M. Anderson, *Epidermal growth factor induces tyrosine phosphorylation and reorganization of the tight junction protein ZO-1 in A431 cells.* J. Cell Sci., 1995. **108 (Pt 4)**: p. 1735-42.

247. Terakado, M., et al., *The Rac1/JNK pathway is critical for EGFR-dependent barrier formation in human airway epithelial cells.* Am. J. Physiol., 2011. **300**(1): p. L56-63.

248. Flores-Benitez, D., et al., *Control of tight junctional sealing: role of epidermal growth factor.* Am. J. Physiol., 2007. **292**(2): p. F828-36.

249. Singh, A.B. and R.C. Harris, *Epidermal growth factor receptor activation differentially regulates claudin expression and enhances transepithelial resistance in Madin-Darby canine kidney cells.* J. Biol. Chem., 2004. **279**(5): p. 3543-52.

250. Brown, K.E., A. Baonza, and M. Freeman, *Epithelial cell adhesion in the developing Drosophila retina is regulated by Atonal and the EGF receptor pathway.* Dev. Biol. , 2006. **300**(2): p. 710-21.

251. Al Moustafa, A.E., A. Achkhar, and A. Yasmeen, *EGF-receptor signaling and epithelial-mesenchymal transition in human carcinomas.* Front. Biosci., 2012. **4**: p. 671-84.

252. Schneider, C.P., et al., *Epidermal growth factor receptor-related tumor markers and clinical outcomes with erlotinib in non-small cell lung cancer: an analysis of patients from german centers in the TRUST study.* J Thorac Oncol, 2008. **3**(12): p. 1446-53.

253. Frasa, M.A., et al., *Armus is a Rac1 effector that inactivates Rab7 and regulates E-cadherin degradation.* Curr Biol. **20**(3): p. 198-208.

254. Hu, J., A. Mukhopadhyay, and A.W. Craig, *Transducer of Cdc42-dependent actin assembly promotes epidermal growth factor-induced cell motility and invasiveness.* J Biol Chem. **286**(3): p. 2261-72.

255. El-Sibai, M., et al., *Cdc42 is required for EGF-stimulated protrusion and motility in MTLn3 carcinoma cells.* J Cell Sci, 2007. **120**(Pt 19): p. 3465-74.

256. Kurokawa, K., et al., *Coactivation of Rac1 and Cdc42 at lamellipodia and membrane ruffles induced by epidermal growth factor.* Mol Biol Cell, 2004. **15**(3): p. 1003-10.

257. Kurokawa, K., et al., *Mechanism and role of localized activation of Rho-family GTPases in growth factor-stimulated fibroblasts and neuronal cells.* Biochem Soc Trans, 2005. **33**(Pt 4): p. 631-4.

258. Van Itallie, C.M., M.S. Balda, and J.M. Anderson, *Epidermal growth factor induce tyrosine phosphorylation and reorganization of tight junction protein ZO-1 in A431 cells.* J. Cell Sci., 1995. **108**: p. 1735-1742.

259. Sharma, S.V., et al., *Epidermal growth factor receptor mutations in lung cancer.* Nat Rev Cancer, 2007. **7**(3): p. 169-81.

260. Sweeney, W.E., et al., *Treatment of polycystic kidney disease with a novel tyrosine kinase inhibitor.* Kidney Int, 2000. **57**(1): p. 33-40.

261. Terry, S.J., et al., *Spatially restricted activation of RhoA signalling at epithelial junctions by p114RhoGEF drives junction formation and morphogenesis.* Nat. Cell Biol., 2011. **13**(2): p. 159-66.

262. Itoh, R.E., et al., *Activation of rac and cdc42 video imaged by fluorescent resonance energy transfer-based single-molecule probes in the membrane of living cells.* Mol. Cell Biol., 2002. **22**(18): p. 6582-91.

263. Adams, A.E., et al., *CDC42 and CDC43, two additional genes involved in budding and the establishment of cell polarity in the yeast Saccharomyces cerevisiae.* J Cell Biol, 1990. **111**(1): p. 131-42.

264. Turner, L.J., S. Nicholls, and A. Hall, *The activity of the plexin-A1 receptor is regulated by Rac.* J Biol Chem, 2004. **279**(32): p. 33199-205.

265. Perrot, V., J. Vazquez-Prado, and J.S. Gutkind, *Plexin B regulates Rho through the guanine nucleotide exchange factors leukemia-associated Rho GEF (LARG) and PDZ-RhoGEF.* J Biol Chem, 2002. **277**(45): p. 43115-20.

266. Khelfaoui, M., et al., *Inhibition of RhoA pathway rescues the endocytosis defects in Oligophrenin1 mouse model of mental retardation.* Hum Mol Genet, 2009. **18**(14): p. 2575-83.

267. Braga, V.M., et al., *Regulation of cadherin function by Rho and Rac: modulation by junction maturation and cellular context.* Mol. Biol. Cell, 1999. **10**(1): p. 9-22.

268. Cotteret, S. and J. Chernoff, *The evolutionary history of effectors downstream of Cdc42 and Rac.* Genome Biol, 2002. **3**(2): p. REVIEWS0002.

269. Noren, N.K., W.T. Arthur, and K. Burridge, *Cadherin engagement inhibits RhoA via p190RhoGAP.* J. Biol. Chem., 2003. **278**(16): p. 13615-8.

270. Aijaz, S., et al., *Binding of GEF-H1 to the tight junction-associated adaptor cingulin results in inhibition of Rho signaling and G1/S phase transition.* Dev Cell, 2005. **8**(5): p. 777-86.

271. Noren, N.K., W.T. Arthur, and K. Burridge, *Cadherin engagement inhibits RhoA via p190RhoGAP.* J Biol Chem, 2003. **278**(16): p. 13615-8.

272. Lichtner, R.B., et al., *Rapid effects of EGF on cytoskeletal structures and adhesive properties of highly metastatic rat mammary adenocarcinoma cells.* Clin Exp Metastasis, 1993. **11**(1): p. 113-25.

273. Rabinovitz, I., A. Toker, and A.M. Mercurio, *Protein kinase C-dependent mobilization of the alpha6beta4 integrin from hemidesmosomes and its association with actin-rich cell protrusions drive the chemotactic migration of carcinoma cells.* J Cell Biol, 1999. **146**(5): p. 1147-60.

274. Van Itallie, C.M., M.S. Balda, and J.M. Anderson, *Epidermal growth factor induces tyrosine phosphorylation and reorganization of the tight junction protein ZO-1 in A431 cells.* J Cell Sci, 1995. **108 (Pt 4)**: p. 1735-42.

275. Bos, M., et al., *PD153035, a tyrosine kinase inhibitor, prevents epidermal growth factor receptor activation and inhibits growth of cancer cells in a receptor number-dependent manner.* Clin Cancer Res, 1997. **3**(11): p. 2099-106.

276. Chen, W.S., et al., *Requirement for intrinsic protein tyrosine kinase in the immediate and late actions of the EGF receptor.* Nature, 1987. **328**(6133): p. 820-3.

277. Hunter, T. and J.A. Cooper, *Epidermal growth factor induces rapid tyrosine phosphorylation of proteins in A431 human tumor cells.* Cell, 1981. **24**(3): p. 741-52.

278. Buccione, R., J.D. Orth, and M.A. McNiven, *Foot and mouth: podosomes, invadopodia and circular dorsal ruffles.* Nat Rev Mol Cell Biol, 2004. **5**(8): p. 647-57.

279. Pavlov, D., et al., *Actin filament severing by cofilin.* J Mol Biol, 2007. **365**(5): p. 1350-8.

280. Graham, D.L., P.N. Lowe, and P.A. Chalk, *A method to measure the interaction of Rac/Cdc42 with their binding partners using fluorescence resonance energy transfer between mutants of green fluorescent protein.* Anal Biochem, 2001. **296**(2): p. 208-17.

281. Guillemot, L. and S. Citi, *Cingulin regulates claudin-2 expression and cell proliferation through the small GTPase RhoA.* Mol Biol Cell, 2006. **17**(8): p. 3569-77.

282. Anastasiadis, P.Z., et al., *Inhibition of RhoA by p120 catenin.* Nat Cell Biol, 2000. **2**(9): p. 637-44.

283. Kozma, R., et al., *The Ras-related protein Cdc42Hs and bradykinin promote formation of peripheral actin microspikes and filopodia in Swiss 3T3 fibroblasts.* Mol Cell Biol, 1995. **15**(4): p. 1942-52.

284. Mitchison, T.J., *Actin based motility on retraction fibers in mitotic PtK2 cells.* Cell Motil Cytoskeleton, 1992. **22**(2): p. 135-51.

285. Noren, N.K., et al., *Cadherin engagement regulates Rho family GTPases.* J. Biol. Chem., 2001. **276**(36): p. 33305-8.

286. Bruck, S., et al., *Identification of a novel inhibitory actin-capping protein binding motif in CD2-associated protein.* J Biol Chem, 2006. **281**(28): p. 19196-203.

287. Roldan, J.L., et al., *Solution structure, dynamics and thermodynamics of the three SH3 domains of CD2AP.* J Biomol NMR. **50**(2): p. 103-17.

288. Hutchings, N.J., et al., *Linking the T cell surface protein CD2 to the actin-capping protein CAPZ via CMS and CIN85.* J Biol Chem, 2003. **278**(25): p. 22396-403.

289. Wolf, G. and R.A. Stahl, *CD2-associated protein and glomerular disease.* Lancet, 2003. **362**(9397): p. 1746-8.

290. Krause, M., et al., *Ena/VASP proteins: regulators of the actin cytoskeleton and cell migration.* Annu Rev Cell Dev Biol, 2003. **19**: p. 541-64.

291. Schafer, D.A. and J.A. Cooper, *Control of actin assembly at filament ends.* Annu Rev Cell Dev Biol, 1995. **11**: p. 497-518.

292. Menna, E., et al., *From filopodia to synapses: the role of actin-capping and anti-capping proteins.* Eur J Neurosci. **34**(10): p. 1655-62.

293. Gotta, M., M.C. Abraham, and J. Ahringer, *CDC-42 controls early cell polarity and spindle orientation in C. elegans.* Curr Biol, 2001. **11**(7): p. 482-8.

294. Gotta, M. and J. Ahringer, *Axis determination in C. elegans: initiating and transducing polarity.* Curr Opin Genet Dev, 2001. **11**(4): p. 367-73.

295. Wong, C.M., et al., *Rho GTPase-activating protein deleted in liver cancer suppresses cell proliferation and invasion in hepatocellular carcinoma.* Cancer Res, 2005. **65**(19): p. 8861-8.

296. Wang, J.B., et al., *IQGAP1 regulates cell proliferation through a novel CDC42-mTOR pathway.* J Cell Sci, 2009. **122**(Pt 12): p. 2024-33.

297. Meyer, R.D., D.B. Sacks, and N. Rahimi, *IQGAP1-dependent signaling pathway regulates endothelial cell proliferation and angiogenesis.* PLoS One, 2008. **3**(12): p. e3848.

298. Chiu, Y.L. and T.M. Rana, *siRNA function in RNAi: a chemical modification analysis.* RNA, 2003. **9**(9): p. 1034-48.

299. Vasioukhin, V. and E. Fuchs, *Actin dynamics and cell-cell adhesion in epithelia.* Curr Opin Cell Biol, 2001. **13**(1): p. 76-84.

300. Yang, L., L. Wang, and Y. Zheng, *Gene targeting of Cdc42 and Cdc42GAP affirms the critical involvement of Cdc42 in filopodia induction, directed migration, and proliferation in primary mouse embryonic fibroblasts.* Mol Biol Cell, 2006. **17**(11): p. 4675-85.

301. Boulton, T.G. and M.H. Cobb, *Identification of multiple extracellular signal-regulated kinases (ERKs) with antipeptide antibodies.* Cell Regul, 1991. **2**(5): p. 357-71.

302. Roudabush, F.L., et al., *Transactivation of the EGF receptor mediates IGF-1-stimulated shc phosphorylation and ERK1/2 activation in COS-7 cells.* J Biol Chem, 2000. **275**(29): p. 22583-9.

303. Lim, K.B., et al., *The Cdc42 effector IRSp53 generates filopodia by coupling membrane protrusion with actin dynamics.* J Biol Chem, 2008. **283**(29): p. 20454-72.

304. Krugmann, S., et al., *Cdc42 induces filopodia by promoting the formation of an IRSp53:Mena complex.* Curr Biol, 2001. **11**(21): p. 1645-55.

305. Disanza, A., et al., *Regulation of cell shape by Cdc42 is mediated by the synergic actin-bundling activity of the Eps8-IRSp53 complex.* Nat Cell Biol, 2006. **8**(12): p. 1337-47.

306. Anderson, D.C., et al., *Polarization of the C. elegans embryo by RhoGAP-mediated exclusion of PAR-6 from cell contacts.* Science, 2008. **320**(5884): p. 1771-4.

307. Georgiou, M. and B. Baum, *Polarity proteins and Rho GTPases cooperate to spatially organise epithelial actin-based protrusions.* J Cell Sci. **123**(Pt 7): p. 1089-98.

308. Has, C., et al., *Kindlin-1 Is required for RhoGTPase-mediated lamellipodia formation in keratinocytes.* Am J Pathol, 2009. **175**(4): p. 1442-52.

309. Schafer, C., et al., *One step ahead: role of filopodia in adhesion formation during cell migration of keratinocytes.* Exp Cell Res, 2009. **315**(7): p. 1212-24.

310. Nelson, W.J., *Remodeling epithelial cell organization: transitions between front-rear and apical-basal polarity.* Cold Spring Harbor Perspec. Biol., 2009. **1**(1): p. a000513.